

A Field Guide to Experimental Designs

The Latin Square design

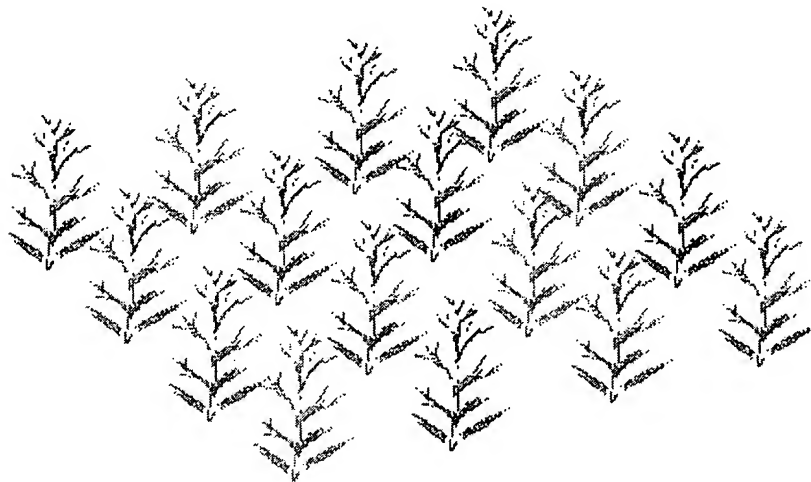
The Latin square design is used where the researcher desires to control the variation in an experiment that is related to rows and columns in the field.

Field marks:

- Treatments are assigned at random within rows and columns, with each treatment once per row and once per column.
- There are equal numbers of rows, columns, and treatments.
- Useful where the experimenter desires to control variation in two different directions

Sample layout:

Different colors represent different treatments. There are 4 treatments (A-D) assigned to 4 rows (I-IV) and 4 columns (1-4).



Row I	A	B	C	D
Row II	C	D	A	B
Row III	D	C	B	A
Row IV	B	A	D	C
Column	1	2	3	4

ANOVA table format:

--	--	--	--	--

Source of variation	Degrees of freedom ^a	Sums of squares (SSQ)	Mean square (MS)	F
Rows (R)	$r-1$	SSQ_R	$SSQ_R/(r-1)$	MS_R/MS_E
Columns (C)	$r-1$	SSQ_C	$SSQ_C/(r-1)$	MS_C/MS_E
Treatments (Tr)	$r-1$	SSQ_{Tr}	$SSQ_{Tr}/(r-1)$	MS_{Tr}/MS_E
Error (E)	$(r-1)(r-2)$	SSQ_E	$SSQ_E/((r-1)(r-2))$	
Total (Tot)	r^2-1	SSQ_{Tot}		

^awhere r =number of treatments, rows, and columns.

Sample ANOVA table:

Source of variation	Degrees of freedom	Sums of squares (SSQ)	Mean square (MS)	F
Rows	3	40.77	13.59	5.91 ^a
Columns	3	125.39	41.80	18.16 ^a
Treatments	3	160.57	53.52	23.26 ^a
Error	6	13.81	2.30	
Total	15	340.54		

^aF test with 3,6 degrees of freedom at $P=0.05$ is 4.76

Sample SAS GLM statements:

```
PROC GLM;
  CLASS ROWS COLUMNS TREATS;
  MODEL WHATEVER = ROWS COLUMNS TREATS;
RUN;
```

Compare with:

- Randomized Complete Block (RCB): treatments are repeated once per block in only one direction

Return to index

Washington State University
Tree Fruit Research and Extension Center
1100 N. Western Ave.
Wenatchee WA 98801

phone: 509-663-8181
fax: 509-662-8714

Copyright © Washington State University Disclaimer
WSU Electronic Publishing and Appropriate Use Policy

Comments concerning this page to webservant@tfrec.wsu.edu

Wednesday, August 16, 2000

The cardiac transcription factors Nkx2-5 and GATA-4 are mutual cofactors

Daniel Durocher¹, Frédéric Charron¹,
René Warren¹, Robert J. Schwartz² and
Mona Nemer^{1,3,4}

¹Laboratoire de Développement et Différenciation Cardiaques, Institut de Recherches Cliniques de Montréal, 110 des Pins Ouest, Montréal Québec, Canada H2W 1R7 and Department of Medicine, Division of Experimental Medicine, McGill University, Montréal Québec, Canada, ²Department of Cell Biology, Baylor College of Medicine, Houston, TX, USA and ³Département de Pharmacologie, Université de Montréal, Canada

⁴Corresponding author
e-mail: nemer@ircm.umontreal.ca

The tissue-restricted GATA-4 transcription factor and Nkx2-5 homeodomain protein are two early markers of precardiac cells. Both are essential for heart formation, but neither can initiate cardiogenesis. Over-expression of GATA-4 or Nkx2-5 enhances cardiac development in committed precursors, suggesting each interacts with a cardiac cofactor. We tested whether GATA-4 and Nkx2-5 are cofactors for each other by using transcription and binding assays with the cardiac atrial natriuretic factor (ANF) promoter—the only known target for Nkx2-5. Co-expression of GATA-4 and Nkx2-5 resulted in synergistic activation of the ANF promoter in heterologous cells. The synergy involves physical Nkx2-5–GATA-4 interaction, seen *in vitro* and *in vivo*, which maps to the C-terminal zinc finger of GATA-4 and a C-terminus extension; similarly, a C-terminally extended homeodomain of Nkx2-5 is required for GATA-4 binding. Structure/function studies suggest that binding of GATA-4 to the C-terminus autorepressive domain of Nkx2-5 may induce a conformational change that unmasks Nkx2-5 activation domains. GATA-6 cannot substitute for GATA-4 for interaction with Nkx2-5. This interaction may impart functional specificity to GATA factors and provide cooperative crosstalk between two pathways critical for early cardiogenesis. Given the co-expression of GATA proteins and NK2 class members in other tissues, the GATA/Nkx partnership may represent a paradigm for transcription factor interaction during organogenesis.

Keywords: ANF/cardiogenesis/GATA factors/homeodomain/transcription

Introduction

The GATA family of transcription factors are key developmental regulators that have been conserved throughout evolution (Fu and Marzluf, 1990; Spieth *et al.*, 1991; Winick *et al.*, 1993; Stanbrough *et al.*, 1995; Coffman *et al.*, 1996; Platt *et al.*, 1996). Various family members

have been shown to alter transcription of target genes via binding to the consensus WGATAR sequence through a DNA-binding domain consisting of two adjacent zinc-fingers of the C2/C2 family. Sequence-specific DNA-binding requires the C-terminal zinc-finger and the N-terminal finger may stabilize the DNA–protein complex via electrostatic interactions with the phosphate backbone (Whyatt *et al.*, 1993). This DNA-binding domain is the highest conserved region among the various GATA proteins. In vertebrates, six members have been identified so far and they can be divided into two subgroups based on sequence homology and tissue distribution. The first subgroup, which includes GATA-1, -2 and -3, is largely restricted to the hematopoietic system where all three GATA factors have been shown to play essential, non-redundant functions (Tsai *et al.*, 1994; Pandolfi *et al.*, 1995; Fujiwara *et al.*, 1996; Ting *et al.*, 1996). Remarkably, arrested proerythroblasts lacking GATA-1 express several GATA-1 target genes although they are unable to achieve terminal erythroid differentiation (Weiss *et al.*, 1994), raising the possibility that GATA-2—which is co-expressed with GATA-1 in proerythroblasts—may partially substitute for GATA-1. Consistent with this, GATA factors appear to be functionally interchangeable in some (Blobel *et al.*, 1995; Visvader *et al.*, 1995) but not all (Briegel *et al.*, 1993; Weiss *et al.*, 1994) *in vitro* assays. Taken together with the *in vivo* data, these results suggest that functional specificity of GATA proteins likely involves interactions with other cell-restricted cofactors. Consistent with this hypothesis, GATA-1 was found to interact with the erythroid-specific LIM protein RBTN2 and to be present in complexes containing RBTN2 and the hematopoietic basic helix-loop-helix protein SCL/TAL1 (Osada *et al.*, 1995). GATA-1 was also shown to cooperate with the ubiquitous SP1 protein and with two other erythroid factors, the basic leucine zipper NFE-2 (Walters and Martin, 1992; Gong and Dean, 1993) and the zinc finger EKLF (Merika and Orkin, 1995; Gregory *et al.*, 1996) for transcriptional activation of erythroid promoters/enhancers. At least, in the case of SP1 and EKLF, the interaction was also observed with GATA-2 and involved direct contact through the DNA-binding domains (Merika and Orkin, 1995). Thus, the identity of the proteins that serve as cofactor(s) to impart functional specificity of GATA proteins in the hematopoietic system remains essentially unknown.

The other subclass of vertebrate GATA factors includes GATA-4, -5 and -6 whose expression is restricted to the heart and gut (Arceci *et al.*, 1993; Kelley *et al.*, 1993; Grépin *et al.*, 1994; Laverriere *et al.*, 1994; Jiang and Evans, 1996). All three genes are transcribed at very early stages of *Xenopus*, avian and mouse cardiac development (Kelley *et al.*, 1993; Heikinheimo *et al.*, 1994; Laverriere *et al.*, 1994; Jiang and Evans, 1996; Morrisey *et al.*, 1996).

Within the heart, transcripts for GATA-4, -5 and -6 are found in distinct cell types with GATA-5 mRNA predominantly found in endocardial cells while GATA-4 and -6 are present in the myocardium (Kelley *et al.*, 1993; Grépin *et al.*, 1994; Morrisey *et al.*, 1996). The spatial and temporal expression of GATA-4 together with various functional studies are consistent with an important role of this GATA family member in cardiogenesis. Thus, GATA-4 was found to be a potent transactivator of several cardiac-specific promoters (Grépin *et al.*, 1994; Ip *et al.*, 1994; Molkentin *et al.*, 1994); inhibition of GATA-4 expression in an *in vitro* model of cardiogenesis altered survival of precardiac cells and inhibited terminal cardiomyocyte differentiation (Grépin *et al.*, 1995, 1997). Moreover, targeted inactivation of the GATA-4 gene blocks formation of the primitive heart tube, indicating a crucial role for GATA-4 in heart development (Kuo *et al.*, 1997; Molkentin *et al.*, 1997). However, ectopic expression of GATA-4 is not sufficient to initiate cardiac differentiation or to activate the cardiac genetic program, although it markedly potentiates cardiogenesis (Jiang and Evans, 1996; Grépin *et al.*, 1997) suggesting cooperative interaction between GATA-4 and other cardiac transcription factors.

Genetic studies in *Drosophila melanogaster* have identified the gene *Tinman* as a key regulator of heart differentiation. In *tin* embryos, flies lack the dorsal vessel, the fly structure homologous to the heart, as a result of defects in late mesoderm specification (Bodmer *et al.*, 1990; Azpiazu and Frasch, 1993; Bodmer, 1993). Presumptive homologues of *Tinman* have been cloned in vertebrates (Nkx2-3, Nkx2-5 and Nkx2-7) and are expressed in the myocardium (reviewed in Harvey, 1996; see also Lints *et al.*, 1993; Tonissen *et al.*, 1994; Evans *et al.*, 1995; Schultheiss *et al.*, 1995; Buchberger *et al.*, 1996; Chen and Fishman, 1996; Lee *et al.*, 1996). Targeted disruption of the Nkx2-5 gene in mice leads to embryonic death due to cardiac morphogenetic defects (Lyons *et al.*, 1995). However, gain-of-function studies in zebrafish *Danio rerio* and *Xenopus laevis* indicate that ectopic expression of Nkx2-5 results in enhanced myocyte recruitment but is not sufficient to initiate cardiac gene expression or differentiation (Chen and Fishman, 1996; Cleaver *et al.*, 1996), suggesting that Nkx2-5 acts in concert with other transcription factors to specify the cardiac phenotype.

Since the cardiac-specific atrial natriuretic factor (ANF) promoter is a transcriptional target for both GATA-4 and Nkx2-5 (Grépin *et al.*, 1994; Durocher *et al.*, 1996), we used it to investigate functional cooperation between Nkx2-5 and GATA-4 in the heart. We present data showing that Nkx2-5 and GATA-4 specifically cooperate in activating ANF and other cardiac promoters, and physically interact both *in vitro* and *in vivo*. This molecular interaction provides the interesting possibility that instead of being part of the same epistatic group, the two pathways collaborate in the early events of cardiogenesis.

Results

GATA-4 and Nkx2-5 synergistically activate cardiac transcription

Recent studies from our laboratory have demonstrated that two cardiac-specific transcriptional pathways converge on the ANF promoter (Grépin *et al.*, 1994; Durocher

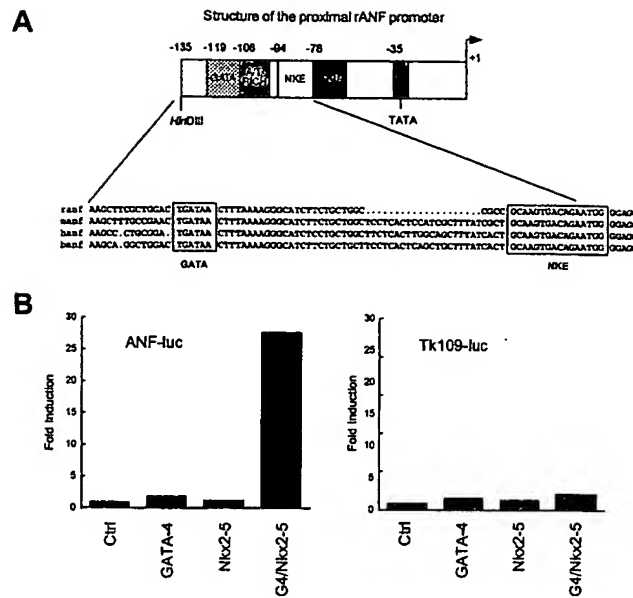


Fig. 1. Nkx2-5 and GATA-4 can cooperate transcriptionally. **(A)** Structural organization of the proximal ANF promoter. Regulatory elements of the ANF promoter are boxed, and their location relative to the transcription start are indicated. The PERE corresponds to the phenylephrine response element (Ardati and Nemer, 1993), the NKE to the NK2 response element (Durocher *et al.*, 1996). The Nkx2-5 binding site and the GATA elements of the ANF promoter are conserved among species (rat, human, bovine and mouse promoters) and their spacing is conserved (20 bp, two turns of the DNA double helix). **(B)** GATA-4 and Nkx2-5 synergistically activate the ANF promoter. HeLa cells were transiently co-transfected as described in Materials and methods using CMV-driven expression vectors for GATA-4 and Nkx2-5 or the backbone vector as control (pCGN) in conjunction with either ANF-luciferase or Tk109-luciferase reporters. The results, expressed as fold induction of reporter constructs, are from one representative experiment (out of at least four) and represent the mean of a duplicate.

et al., 1996), ANF being the major secretory product of embryonic and postnatal cardiomyocytes. The region of the ANF promoter which is essential for high basal cardiac activity (Argentin *et al.*, 1994) harbors a GATA element located at -120 bp in the rat promoter which binds with high affinity all the members of the cardiac GATA subfamily (F.Charron *et al.*, manuscript in preparation), and the NKE which binds Nkx2-5 and is required for ANF promoter and enhancer function (Durocher *et al.*, 1996). As seen in Figure 1A, the nucleotide composition of these elements as well as their phasing are conserved across species, suggesting an evolutionary pressure to maintain important regulatory pathways. This led us to investigate whether GATA proteins and Nkx2-5 could functionally interact at the level of the ANF promoter. We tested this hypothesis by co-transfected GATA-4 and Nkx2-5 expression vectors in non-cardiac cells (HeLa cells) at limiting DNA concentrations (Grépin *et al.*, 1994; Durocher *et al.*, 1996) in order to avoid squelching. Under these conditions, GATA-4 and Nkx2-5 were able to activate synergistically the ANF promoter but not control promoters lacking GATA and NKE sites such as TK109 (Figure 1B). This cooperative response was not caused by transactivation of the CMV promoter which drives Nkx2-5 and GATA-4 expression since the co-expression of both vectors does not alter the level of either Nkx2-5 or GATA-4 protein (see Figure 6B).

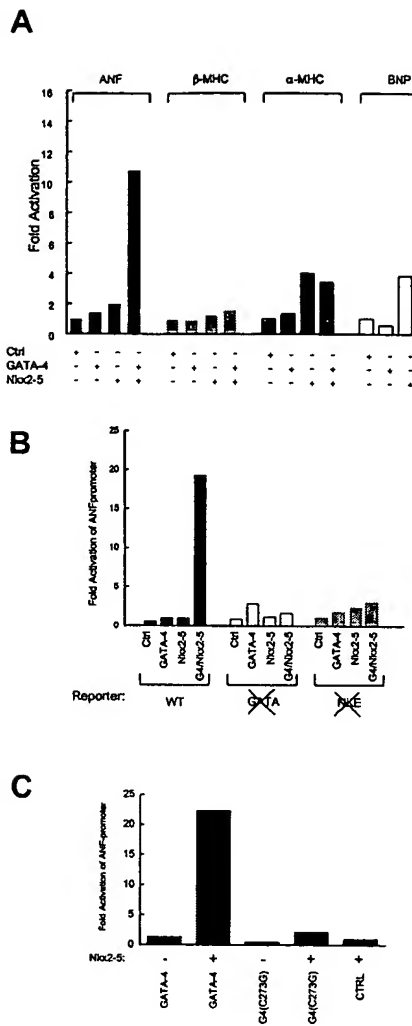


Fig. 2. A subset of cardiac promoters are synergistically activated by the Nkx2-5-GATA-4 combination. (A) HeLa cells were transiently co-transfected as described in Figure 1 using various cardiac promoters linked to the luciferase reporter. ANF represents the rat ANF -135 construct; β -MHC, the rat -667 bp promoter; α -MHC, the rat -613 bp promoter whereas BNP represents the rat -2 kbp promoter. (B) The synergy between GATA-4 and Nkx2-5 requires both binding sites in the context of the ANF promoter. Transient co-transfections in HeLa cells were carried out as described in the previous figures and the promoter described represents either the -135 bp promoter (WT), the Δ -106/-135 bp promoter which removes the GATA element and the Δ -57/-106 bp promoter which removes the NKE site. (C) GATA-4 binding to DNA is required for synergy. A point mutant of GATA-4 (C273G) which does not bind DNA *in vitro* and which cannot activate GATA-dependent promoters was used in a co-transfection assay with or without Nkx2-5.

The relevance of this synergy to cardiac transcription was further assessed by co-transfecting Nkx2-5 and GATA-4 with other cardiac promoters including ANF, β -MHC, α -MHC and the B-type natriuretic peptide (BNP) reporters. Under the conditions used in Figure 1, a subset of promoters that contain both NKE and GATA elements could be synergistically activated by the combination of Nkx2-5 and GATA-4 (Figure 2A). Thus, BNP promoter which is a GATA-4 target (Argentin *et al.*, 1994) responds synergistically to Nkx2-5 and GATA-4. Interestingly, sequences with high homology to the NKE are present around -385 and -437 bp and are conserved across species;

promoter fragments lacking these putative NKEs are no longer responsive to Nkx2-5/GATA synergy (data not shown). On the other hand, neither additive nor synergistic effects were observed on the α -MHC and the β -MHC promoters in response to Nkx2-5 and GATA-4 at all different DNA concentrations tested (Figure 2A and data not shown). These data suggest that only a subgroup of cardiac genes are targeted by both transcription factors and that both NKE and GATA sites are required for synergy. This hypothesis was further tested using ANF promoter mutants deleted of either the GATA or the NKE elements. As shown in Figure 2B, there appears to be an absolute requirement for both elements to achieve synergy. The same results were obtained using BNP promoters containing only GATA sites or heterologous promoters with multimerized GATA elements (data not shown). This suggests that, in natural promoters, both proteins have to be recruited at the promoter or require a conformational change induced upon DNA-binding. Indeed, a GATA-4 mutant that no longer binds DNA because one of the zinc-coordinating cysteines in the carboxy-terminal zinc finger was mutated, no longer supports Nkx2-5 synergy (Figure 2C).

Since multiple GATA and homeobox proteins are expressed in the heart, we investigated the specificity of the synergy. In co-transfection assays using the proximal -135 bp ANF promoter as reporter, we found that Nkx2-5 was able cooperatively to activate transcription of the ANF reporter only with GATA-4 and GATA-5 (Figure 3A). No synergy was observed with either GATA-1 or GATA-6. Since GATA-6 is as potent as GATA-4 in transactivating the ANF promoter (our unpublished data), the results suggest that transcriptional cooperativity between Nkx2-5 and GATA proteins requires specific molecular/structural determinants on the GATA-4 and -5 proteins. The same approach was used to identify homeoproteins that could cooperate with GATA-4, including other NK2 proteins (TTF-1/Nkx2-1; Guazzi *et al.*, 1990; Lints *et al.*, 1993), Hox proteins (HoxB3), Pou proteins (Oct1; Sturm *et al.*, 1988) or *bicoid*-related homeoboxes (Ptx1; Lammonerie *et al.*, 1996). Transcriptional cooperativity was observed with the members of the *Antp* superfamily Nkx2-5, TTF-1 and HoxB3, but not with Oct1 and Ptx1 (Figure 3B). These results suggest that the *Antp*-type homeodomain plays an important role in the specificity of the synergy.

We then used deletion mutants of both Nkx2-5 and GATA-4 to map the domains involved in synergy over the ANF promoter. All mutant proteins were tested for expression level and nuclear localization (data not shown). The analyses revealed that, in addition to the DNA-binding domain (Figure 2C), two GATA-4 domains are required for the synergy, one located within the N-terminal 119 amino acids of the protein, and the second in the C-terminal 121 amino acids (Figure 4). Both domains contain GATA-4 activation domains although the presence of either domain is sufficient for transactivation of GATA-dependent promoters in heterologous cells (Figure 4B). The observation that both domains are required for cooperative interaction with Nkx2-5, suggests that synergistic interaction between these two domains may be required for Nkx2-5-induced transcriptional activation of the ANF promoter or that each domain fulfills a distinct function. Mutational analysis

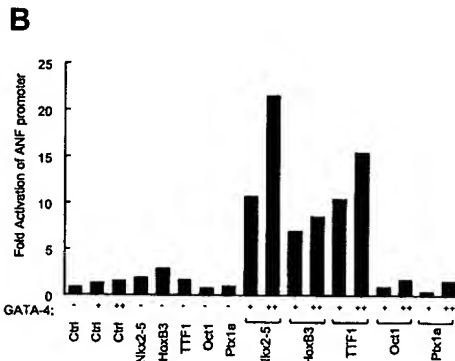
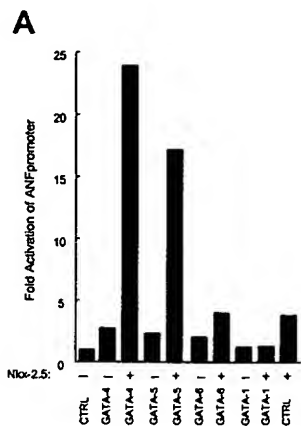


Fig. 3. The synergy is specific for a subset of cardiac GATA proteins and *Antp*-type homeoproteins. (A) Co-transfection assays in HeLa cells using various GATA expression vectors were done in presence (+) or absence (-) of the Nkx2-5 expression vector. Ctrl represents the backbone vector for most of the GATA constructs (pCGN). (B) Co-transfection assays in HeLa cells were performed in the presence of various homeodomain protein expression vectors in absence (-) or in presence (+) of GATA-4 (+, 0.1 µg; ++, 0.25 µg).

of Nkx2-5 showed that, while the homeodomain is critical for Nkx-GATA synergy, domains outside the homeobox, particularly sequences C-terminus of the homeodomain, are also important (Figure 5A). Thus, neither the homeodomain (122–203), nor in fusion with the N-terminal regions of Nkx2-5 (1–203) is able to stimulate GATA-4 activity. Deletion of the entire C-terminal region totally impairs the ability of Nkx2-5 to stimulate GATA-4 transcription while partial deletions of the C-terminus (1–246 and Δ204–246) reduce consistently the extent of synergy observed without completely abolishing it. This result suggests that these two regions of the C-terminus are only partially redundant or that the functional interaction between Nkx2-5 and GATA-4 requires an ‘extended’ homeodomain in the C-terminus. The C-terminus is not known as a transcriptional activation domain, in fact; it appears to be an autorepression domain since its deletion leads to superactivation (Figure 5B). Thus, the requirement for the C-terminus suggests that GATA-4 physically interacts with Nkx2-5 to cause a conformational change and derepress (or unmask) Nkx2-5 activation domains.

GATA-4 and Nkx2-5 physically interact *in vitro* and *in vivo*

We first assessed possible physical interaction between Nkx2-5 and GATA-4 using pull-down assays with

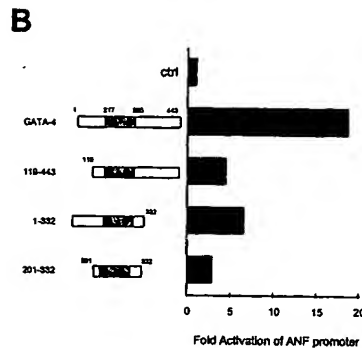
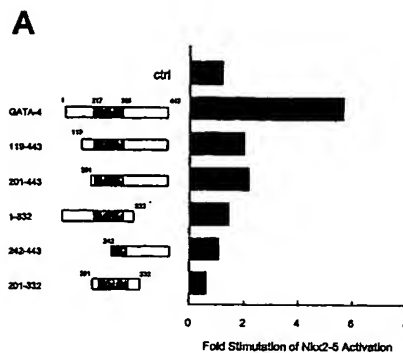


Fig. 4. The synergy requires both activation domains of GATA-4. (A) GATA-4 vectors (50 ng/35 mm dish) expressing truncated GATA-4 proteins able to translocate to the nucleus were used in co-transfection assays with or without the Nkx2-5 expression vector. ctrl represents the backbone vector. The results are expressed as fold stimulation of Nkx2-5 activation (equivalent to fold synergy where the value of 1 represents no synergy, i.e. the ratio between the activity of the reporter in the presence of the GATA deletion mutant plus Nkx2-5 over the activity of the reporter only in the presence of the GATA deletion mutant). (B) GATA-4 activation domains are located both at the C- and N-termini. GATA-4 vectors were transfected in HeLa cells at the dose of 0.2 µg/dish with the ANF –135 bp luciferase reporter.

immobilized MBP-Nkx2-5 and *in vitro*-translated, ³⁵S-labeled GATA-4 (Figure 6A). MBP-Nkx2-5 was able to retain GATA-4 specifically while a MBP-LacZ control fusion could not retain GATA-4 on the column and the immobilized Nkx2-5 could not interact with labeled control luciferase (Figure 6A). The interaction between GATA-4 and Nkx2-5 was also observed in the presence of ethidium bromide, suggesting that this interaction occurs without DNA bridging (data not shown). In order to ascertain the *in vivo* relevance of this interaction, co-immunoprecipitations were performed on nuclear extracts from 293 cells transfected with expression vectors for wild-type GATA-4 or HA-tagged Nkx2-5 alone or in combination. Nuclear extracts from these transfected cells were then incubated with the monoclonal antibody 12CA5 which recognizes the HA epitope. Immunocomplexes were separated on SDS-PAGE, subjected to Western blotting and visualized with the anti-GATA-4 antibody. As seen in Figure 6B, GATA-4 protein was precipitated by the 12CA5 mAb solely when both proteins were expressed, implying either a direct or indirect contact with Nkx2-5.

Next, deletion mutants of GATA-4 were generated in order to map the region(s) of GATA-4 protein involved in physical interaction with Nkx2-5. Figure 7A displays

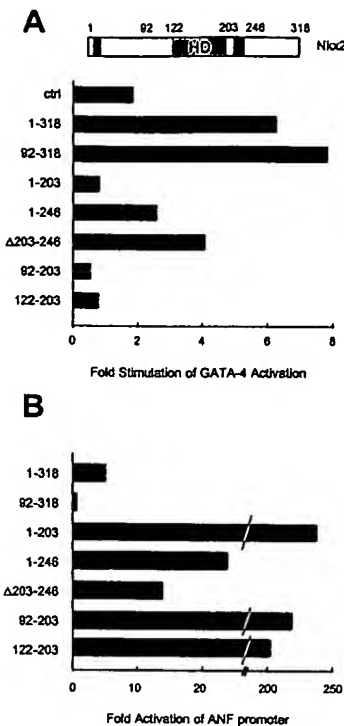


Fig. 5. The synergy requires the C-terminus of Nkx2-5. (A) CMV-driven vectors, expressing various deletions of Nkx2-5, were used in co-transfection assays as described in Figure 4A, where Nkx2-5 concentration was kept at 0.5 μ g/35 mm dish. ctrl represents the backbone vector without insert. The data are expressed as fold stimulation of GATA-4 activation which is calculated by the ratio of the reporter activation when GATA-4 and Nkx2-5 expression vectors are present over the reporter activation when GATA-4 alone is present. (B) The C-terminus domain of Nkx2-5 is an auto-inhibitory domain that masks an activation domain located N-terminal of the homeodomain. Co-transfections in HeLa cells were carried out with an optimal dose of pCGN-Nkx2-5 constructs (2 μ g/dish) on the ANF -135 bp promoter. The results depict the mean of six independent experiments.

the results of the binding studies and the left panel of Figure 8A shows the structure of the deletion mutants and summarizes their behavior in pull-down and transfection assays. The Nkx2-5 interaction domain seems to map to the second zinc-finger and a C-terminal basic region that is not part of any known activation domain of GATA-4. This localization is consistent with the observation that the physical interaction requires zinc ions, since pull-down assays in the presence of chelating agents (EDTA and phenanthroline) abolish the interaction (data not shown). Unfortunately the requirement of the Nkx2-5 binding domain for the synergy could not be assessed since it is part of a basic region essential for the nuclear targeting of GATA-4 (F.Charron *et al.*, unpublished results). Interestingly, neither GATA-1 nor GATA-6, which do not transcriptionally synergize with Nkx2-5, could be retained on the MBP-Nkx2-5 column, suggesting that physical interaction is required for functional cooperativity.

The same approach was also used to map the GATA-4 interaction domain on Nkx2-5. A series of Nkx2-5 deletion mutants were bacterially produced in fusion with MBP, quantified and assayed for their ability to interact with 35 S-labeled GATA-4. The results of these binding assays revealed that both the homeodomain and its C-terminal

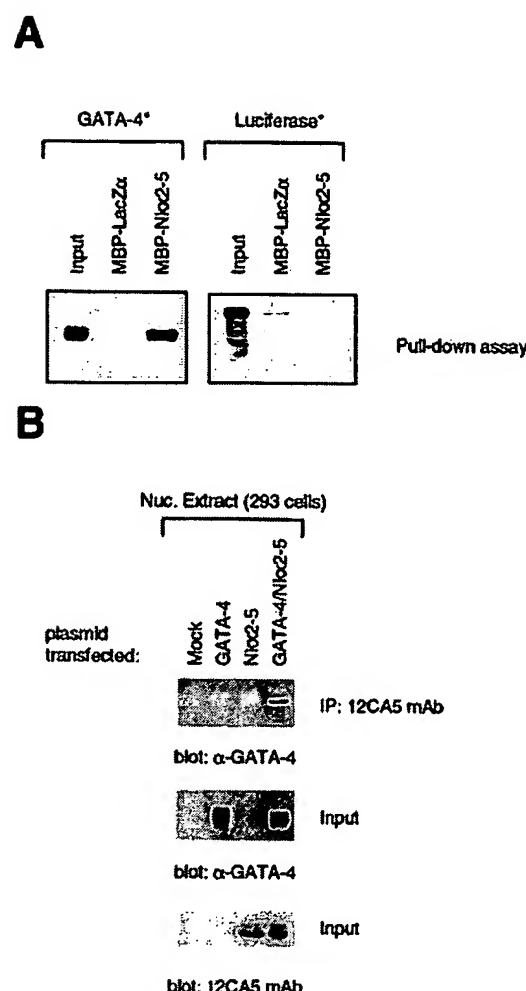


Fig. 6. GATA-4 and Nkx2-5 physically interact *in vitro* and *in vivo*. (A) GATA-4 and Nkx2-5 interact *in vitro*. Pull-down protein-protein binding assays were performed using immobilized, bacterially produced MBP fusions (MBP-Nkx2-5 and MBP-LacZ as control) and either 35 S-labeled GATA-4 or luciferase protein. After incubation, the protein complexes were spun, extensively washed and separated on a 10% SDS-PAGE. Labeled proteins were visualized and quantified by autoradiography on phosphor plates. (B) GATA-4 and Nkx2-5 interact *in vivo*. Nuclear extracts from the simian kidney cell line 293 transfected with either the backbone vectors (mock), GATA-4 expression vector alone (GATA-4), HA-tagged Nkx2-5 (Nkx2-5), or a combination of GATA-4 and HA-Nkx2-5 (GATA-4/Nkx2-5) were used for immunoprecipitation. 60 μ g of nuclear extract were incubated with the mAb 12CA5 and precipitated with protein-G-agarose. The top panel represents the immunocomplex separated by electrophoresis and blotted with an anti-GATA-4 polyclonal antibody. The bottom two panels represent Western blots on the transfected nuclear extracts (20 μ g) using either the anti-GATA-4 Ab (middle panel) or the anti-HA (12CA5) mAb. The white ghost bands are produced by the immunoglobulin heavy chains that co-migrate with GATA-4 on SDS-PAGE.

region are required for physical interaction (Figures 7B and 8A). The homeodomain by itself (122-203) or extended to contain the N-terminal domain (1-203) were insufficient for physical interaction. However, when the homeodomain was fused to parts of the C-terminal (1-246 and Δ 204-246) the fusion proteins regained the ability to bind GATA-4, suggesting that the C-terminal extension provided an essential docking site for the GATA protein or was required for the proper folding of the homeodomain.

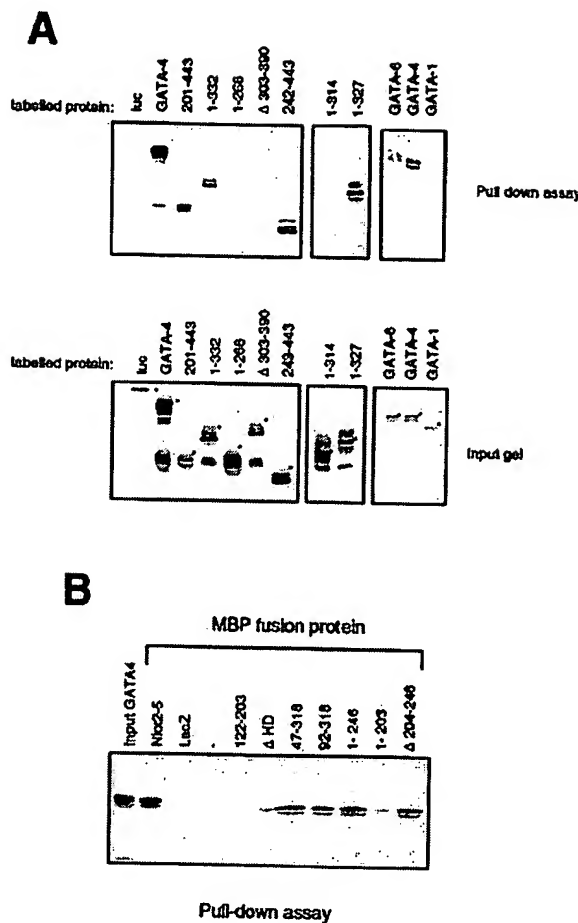


Fig. 7. The physical interaction maps near the C-terminal zinc-finger of GATA-4 and to the C-terminally extended homeodomain of Nkx2-5. (A) Luciferase (luc) or deletion mutants of GATA-4 were translated and labeled with [³⁵S]methionine to be subsequently used in pull-down assays with full-length MBP-Nkx2-5 as described in Figure 6. (B) A series of immobilized deletion mutants of Nkx2-5, in fusion with the maltose binding protein (MBP), were produced in bacteria, quantified on gel, and used in pull-down assays with *in vitro* translated GATA-4. ΔHD represents Nkx2-5 Δ122-203. Protein complexes were separated by electrophoresis and GATA-4 protein was visualized by autoradiography on phosphor plates.

It is noteworthy that these results are in complete agreement with the transfection data and indicate that the determinants of Nkx2-5 and GATA-4 interaction reside mostly in the homeodomain and a C-terminal extension. Collectively, the results also suggest that functional synergy between Nkx2-5 and GATA-4 requires physical interactions of the two proteins.

Discussion

Transcription factors GATA-4 and Nkx2-5 are two of the earliest markers of precardiac cells and, as evidenced by gene inactivation studies (Lyons *et al.*, 1995; Kuo *et al.*, 1997; Molkentin *et al.*, 1997), both play critical roles in cardiogenesis. The data presented here show that GATA-4 and Nkx2-5 interact physically and synergistically to activate cardiac transcription, suggesting functional convergence of two critical cardiac pathways.

Modulation of Nkx2-5 activity by GATA-4

Members of the GATA family of transcription factors (GATA-1, -2 and -3) have been shown to interact with other classes of nuclear proteins containing Lim domain (Osada *et al.*, 1995), zinc finger (Merika and Orkin, 1995; Gregory *et al.*, 1996), and basic leucine zipper (Walters and Martin, 1992; Gong and Dean, 1993; Kawana *et al.*, 1995) motifs. The present work demonstrates that GATA factors are also able to interact with homeodomain-containing proteins of the NK2 and *Antp* type. This GATA-Nkx interaction is so far the first example of zinc finger-homeodomain interaction in vertebrates. The only other known zinc finger-homeodomain cooperation is in *Drosophila*, where it was recently shown that the orphan nuclear receptor αFtz-F1 is a cofactor for the homeo-domain protein Ftz (Guichet *et al.*, 1997; Yu *et al.*, 1997); in this case, the physical association between αFtz-F1 and Ftz is thought to enhance the binding of the Ftz to its lower-affinity target sequences (Guichet *et al.*, 1997; Yu *et al.*, 1997), much in the same way that Extradenticle and Pbx modulate the DNA binding activity of Hox proteins (Phelan *et al.*, 1995; Lu and Kamps, 1996; Peltenburg and Murre, 1997). The interaction of GATA-4 with Nkx2-5 does not appear to result in cooperative DNA binding since neither protein appears to alter the affinity or sequence specificity of the other; moreover, the presence of both GATA and NKE sites does not enhance either GATA-4 or Nkx2-5 binding to their sites, as evidenced by gel shift assays using nuclear extracts containing both proteins or each one separate (data not shown). Instead, the data suggest that GATA-4 interaction with Nkx2-5 serves to unmask the activation domains of Nkx2-5 as illustrated in Figure 8B; this would be reminiscent of the Extradenticle-induced conformational change, that switches Hox proteins from repressors to activators (Chan *et al.*, 1996; Peltenburg and Murre, 1997).

The region of GATA-4 that contacts Nkx2-5 spans the second zinc finger and a ~40 amino acid C-terminal extension (Figure 8A, left panel). This represents a highly conserved segment among the cardiac GATA-4, -5 and -6 proteins with an overall 85–95% homology; notable differences between GATA-4 and -6 (but not GATA-4 and -5) that may account for the differential interaction with Nkx2-5 are found in the hinge region (aa 243–270) preceding the second zinc finger and three non-conservative changes that affect phosphorylatable residues (H244S, N250S, S262P). The differential interaction of GATA proteins with Nkx2-5 reveals for the first time differences between GATA proteins in an *in vitro* assay.

Is Nkx2-5 a specificity cofactor for GATA-4?

Two GATA proteins, GATA-4 and -6, are present in the myocardium and both are potent activators of cardiac transcription. However, inactivation of the GATA-4 gene arrests cardiac development at a very early stage, despite marked up-regulation of GATA-6 arguing for specificity of GATA-4 and -6 function (Kuo *et al.*, 1997; Molkentin *et al.*, 1997). The up-regulation of GATA-6 might, at least partially, account for ANF expression in presumed cardiogenic cells of the GATA-4^{-/-} embryos (Molkentin *et al.*, 1997), much like up-regulation of GATA-2 in GATA-1^{-/-} pre-erythroblasts might explain globin gene expression in the absence of GATA-1. However, it should

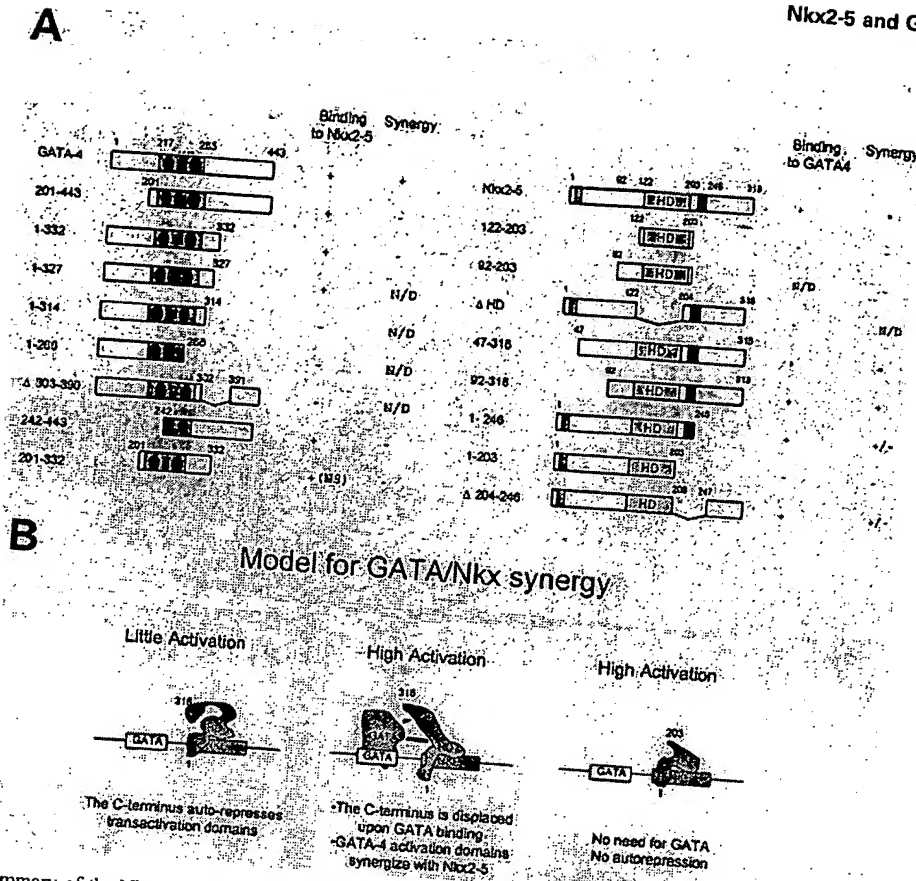


Fig. 8. (A) Schematic summary of the Nkx2-5-GATA-4 interaction. The left panel represents the activity of GATA-4 deletions both in transfection experiments and in pull-down assays. N/D represents constructs that were not tested. Constructs deleting the 266-332 region cannot be used in co-transfections since they do not translocate into the nucleus. The right panel summarizes the activities of Nkx2-5 deletion mutants in co-transfections with GATA-4 or in pull-down assays. The asterisks (*) on the GATA-4 molecule represents the amino acids that are conserved between GATA-4 and -5 but not in GATA-6, they are: H244S, N250D, L261V, S262P where the second amino acid represents the residue present on GATA-6 at the equivalent position. (B) Model of Nkx/GATA synergy. Synergistic interactions between Nkx2-5 and GATA-4 require the binding of GATA-4 and Nkx2-5 to their cognate binding sites. GATA-4 displaces the C-terminal auto-inhibitory region of Nkx2-5 and liberates the Nkx2-5 activation domain. The GATA-4 activation domains can then synergize with Nkx2-5 activation domains.

be pointed out that ANF transcription is controlled by multiple pathways in complex spatiotemporal manner (Argentin *et al.*, 1994; Durocher *et al.*, 1996); thus, the presence of ANF transcripts in GATA-4^{-/-} cells may reflect activation or maintenance of more complex compensatory pathways; moreover, GATA-5—which can also cooperate with Nkx2-5 in the heart—does not seem to be restricted to the endocardial cells before the primitive heart tube stage (Morrisey *et al.*, 1997). The exact reason for which GATA-4 is obviously essential for primitive heart development must await further biochemical and genetic studies. Nevertheless, the available evidence clearly indicates that GATA-6 is unable to substitute fully for GATA-4 with respect to cardiogenesis. Similarly, despite their seemingly interchangeable role in some *in vitro* assays (Blobel *et al.*, 1995; Visvader *et al.*, 1995), the hematopoietic members of the GATA family are clearly non-redundant (Tsai *et al.*, 1994; Pandolfi *et al.*, 1995; Fujiwara *et al.*, 1996; Ting *et al.*, 1996). Unfortunately, the molecular basis for GATA factor specificity has yet to be unraveled. The data presented suggest that interaction of GATA proteins with other tissue-restricted transcription factors might be the underlying mechanism for functional specificity of the GATA family members. Thus, Nkx2-5 may be the specific cofactor for GATA-4 while other homeodomain pro-

teins of the NK2 or *antennapedia* class may fulfill a similar function for GATA-6 in the myocardium.

The presence of a cofactor for GATA proteins is likely the case for the hematopoietic system. Indeed, in a recent publication, Weiss *et al.* demonstrated that the presence of the GATA-1 zinc fingers was essential for erythroid differentiation. Interestingly, the homologous region of GATA-3 (which is not co-expressed with GATA-1) but not the entire GATA-2 (which is up-regulated in GATA-1^{-/-} pre-erythroblasts) could functionally substitute for GATA-1 zinc fingers, suggesting that interaction of zinc fingers with an as yet unidentified nuclear factor may be an important determinant for definitive erythropoiesis (Weiss *et al.*, 1997). Since GATA proteins and other members of the NK2 family are also co-expressed in other tissues such as spleen (GATA-5 and Nkx2-5) and gut (GATA-5, -6 and Xbp) (Lints *et al.*, 1993; Morrisey *et al.*, 1996, 1997; Newman *et al.*, 1997), it is tempting to speculate whether the GATA-Nkx partnership may represent a paradigm for transcription factor interaction during cell fate determination.

It is noteworthy that, at least in cardiac muscle, such paradigm appears to have been evolutionarily conserved. Indeed, in *Drosophila*, the cardiac promoter of the transcription factor D-mef which is a target for Tinman,

Table I. Evolutionary conservation of the GATA-NK2 interaction on muscle promoters

Gene	Species	Promoter sequence	GATA	NK2	Reference
ANF	vertebrates	TGATAACTT (N₂₀) CGCCGCAAGTG	GATA-4	Nkx2-5	this study
Myo-2	<i>C.elegans</i>	TAAAGTGGTTGTGTGGATAA	elt-2 (?)	Ceh-22	Okkema and Fire (1994)
D-Mef	<i>Drosophila</i>	GGATAAGGGGCTCAAGTGG CACTTGAGACCGGGGCTCGCTATCG	pannier (?)	Timman	Gajewski et al. (1997)

Conserved GATA or NKE motifs are depicted in bold letters.

contains juxtaposed GATA and NKE sites (Table I); while the NKEs are necessary, they are not sufficient for cardiac expression, thus raising the possibility of an interaction with other factors (Gajewski et al., 1997). Moreover, in *Caenorhabditis elegans*, two members of the GATA family have been described (elt-1 and -2; Spieth et al., 1991; Hawkins and McGhee, 1995) whose expression is found in gut and perhaps pharyngeal muscles, and GATA elements are necessary for tissue-specific transcription in those tissues (Okkema and Fire, 1994; Egan et al., 1995). Moreover, at least one member of the NK2 family, CEH-22, is also expressed in *C.elegans* pharyngeal muscle and has been implicated in activation of the muscle-specific myosin heavy chain (Myo-2) enhancer (Okkema and Fire, 1994). Interestingly, the Myo-2 enhancer requires the closely linked GATA and NKE sites (Table I) for muscle expression (Okkema and Fire, 1994). Thus, at least in muscle cells the GATA and Nkx interactions appear to have been evolutionarily conserved.

Materials and methods

Cell cultures and transfections

HeLa and 293 cells were grown in Dulbecco's modified Eagle's medium (DMEM) supplemented with 10% fetal calf serum. Transfections were carried out using calcium phosphate precipitation 24 h after plating. At 36 h post-transfection, cells were harvested and luciferase activity was assayed with an LKB luminometer and the data were recorded automatically. In all experiments, RSV-hGH was used as internal control and the amount of reporter was kept at 3 μ g per dish; the total amount of DNA was kept constant (usually 8 μ g). Unless otherwise stated, the results reported were obtained from at least four independent experiments with at least two different DNA preparations for each plasmid. Primary cardiocyte cultures were prepared from 1- or 4-day-old Sprague-Dawley rats and kept in serum-free medium as described previously (Argentin et al., 1994).

Plasmids

ANF-luciferase promoter constructs were cloned in the PXP-2 vector as described previously (Argentin et al., 1994; Durocher et al., 1996). The construction of the various pCG-GATA-4 vectors was based on the original rat GATA-4 cDNA described by Grépin et al. (1994). The position of the mutation/deletion is indicated on the figures. All constructs were sequenced and functionally tested for nuclear translocation and DNA-binding activity following transfection in L cells as previously described (Grépin et al., 1994). pRSET-GATA-4 derivatives for *in vitro* translation were constructed by insertion of the *Xba*I-BamHI fragment of the corresponding pCG-GATA-4 construct into the *Nhe*I-BamHI sites or *Nhe*I-BglII sites of pRSETA (Invitrogen Corp.). MBP-Nkx2-5 (Δ 203-246) was obtained by the insertion of an oligonucleotide corresponding to aa 198-203 in the *Pst*MI-SacII sites of Nkx2-5. The *Sph*I-SacII fragment corresponding to the deletion was then transferred in MBP-Nkx2-5. The other MBP-Nkx2-5 deletions were described by Chen and Schwartz (1995).

Recombinant protein production

After transformation of BL21(DE3) *Escherichia coli* strain with the MBP fusion vectors derived from pMalc-2 (New England Biolabs), individual colonies were picked and grown in 50 ml 2XYT up to an

OD of 0.6 at 600 nm. Induction of the recombinant proteins and their purification were carried out as previously described (Durocher et al., 1996). *In vitro* translation of GATA-4 and Nkx2-5 derivatives were performed with rabbit reticulocyte lysates using the TNT-coupled *in vitro* transcription/translation system (Promega Corp., Madison, WI)

Protein-protein binding assays

In vitro binding studies were performed with MBP-Nkx2-5 derivatives purified from bacteria and coupled to amylose-Sepharose beads (New England Biolabs). GATA-4 derivatives were labeled with [³⁵S]methionine during *in vitro* translation and typically 2-8 μ l of labeled GATA proteins were incubated in the presence of 300 ng of immobilized Nkx2-5 fusion proteins in 400 μ l of 1X binding buffer (150 mM NaCl, 50 mM Tris-Cl, pH 7.5, 0.3% Nonidet P-40, 10 mM ZnCl₂, 1 mM dithiothreitol, 0.5 mM phenylmethylsulfonyl fluoride, 0.25% BSA) for 2 h at 4°C with agitation and then centrifuged for 2 min at 13 000 r.p.m. at room temperature. Beads were washed three times by vortexing in 500 ml of binding buffer at room temperature, the protein complexes were released after boiling in Laemmli buffer and resolved by SDS-PAGE. Labeled proteins were visualized and quantified by autoradiography on phosphor storage plates (PhosphorImager, Molecular Dynamics).

Immunoprecipitations and immunoblots

Immunoprecipitations on nuclear extracts of transfected 293 cells were done using 60 μ g of nuclear extract. Extracts were pre-cleared with 20 μ l of normal rabbit serum and 15 μ l of agarose-protein G beads (Sigma Chemicals) for 2 h at 4°C. Binding reactions were carried out with 40 μ l of 12CA5 antibody in 500 μ l of 1X binding buffer without BSA as described in the protein-protein binding assays paragraph for 2 h at 4°C, with agitation without protein G beads and for an additional 2 h with 15 μ l of protein G beads. Bound immunocomplexes were washed four times in 1X binding buffer and were resuspended in 20 μ l of 1X Laemmli buffer, boiled and subjected to SDS-PAGE electrophoresis. Proteins were transferred on Hybond-PVDF membrane and subjected to immunoblotting. GATA-4 antibody (Santa-Cruz Biotechnology) was used at a dilution of 1/1000 and was revealed with biotinylated anti-goat antibody (dilution 1/12 000) and avidin-biotinylated horseradish peroxidase (HRP) complex (Vectastain). The 12CA5 (anti-Ha) antibody was used at a dilution of 1/500 and was a generous gift of Benoit Grondin and Muriel Aubry (Grondin et al., 1996). The secondary antibody was anti-mouse-HRP and the antigens were visualized with chemiluminescence (Kodak).

Acknowledgements

We are grateful to Michel Chamberland for oligonucleotide synthesis, to Lise Laroche for secretarial assistance and to members of the Nemer laboratory for discussions and critical reading of this manuscript. This work was supported by grants from the Canadian Medical Research Council (MRC) and the National Institutes of Health (RO150422). D.D. is a recipient of the Canada 1967 fellowship from the Natural Sciences and Engineering Research Council of Canada (NSERC), F.C. holds a studentship from the Heart and Stroke Foundation of Canada (HSFC) and M.N. is a MRC Scientist.

References

- Arceci, R.J., King, A.A., Simon, M.C., Orkin, S.H. and Wilson, D.B. (1993) Mouse GATA-4: a retinoic acid-inducible GATA-binding transcription factor expressed in endodermally derived tissues and heart. *Mol. Cell. Biol.*, 13, 2235-2246.
- Ardati, A. and Nemer, M. (1993) A nuclear pathway for α_1 -adrenergic receptor signaling in cardiac cells. *EMBO J.*, 12, 5131-5139.

Argentin,S., Ardati,A., Tremblay,S., Lahrmann,I., Robitaille,L., Drouin,J. and Nemer,M. (1994) Developmental stage-specific regulation of atrial natriuretic factor gene transcription in cardiac cells. *Mol. Cell. Biol.*, **14**, 777–790.

Azpiazu,N. and Frasch,M. (1993) *tinman* and *bagpipe*: two homeo box genes that determine cell fates in the dorsal mesoderm of *Drosophila*. *Genes Dev.*, **7**, 1325–1340.

Blobel,G.A., Simon,M.C. and Orkin,S.H. (1995) Rescue of GATA-1-deficient embryonic stem cells by heterologous GATA-binding proteins. *Mol. Cell. Biol.*, **15**, 626–633.

Bodmer,R. (1993) The gene *tinman* is required for specification of the heart and visceral muscles in *Drosophila*. *Development*, **118**, 719–729.

Bodmer,R., Jan,L.Y. and Jan,Y.N. (1990) A new homeobox-containing gene, *msh-2*, is transiently expressed early during mesoderm formation of *Drosophila*. *Development*, **110**, 661–669.

Briegel,K., Limi,K.C., Plank,C., Beug,H., Engel,J.D. and Zenke,M. (1993) Ectopic expression of a conditional GATA-2/estrogen receptor chimera arrests erythroid differentiation in a hormone-dependent manner. *Genes Dev.*, **7**, 1097–1109.

Buchberger,A., Pabst,O., Brandl,T., Seidl,K. and Arnold,H.H. (1996) Chick Nkx-2.3 represents a novel family member of vertebrate homologues to the *Drosophila* homeobox gene *tinman* – differential expression of CNkx-2.3 and CNkx-2.5 during heart and gut development. *Mech. Dev.*, **56**, 151–163.

Chan,S.K., Popperl,H., Krumlauf,R. and Mann,R.S. (1996) An extradenticle-induced conformational change in a HOX protein overcomes an inhibitory function of the conserved hexapeptide motif. *EMBO J.*, **15**, 2476–2487.

Chen,C.Y. and Schwartz,R.J. (1995) Identification of novel DNA binding targets and regulatory domains of a murine *tinman* homeodomain factor, *nkx-2.5*. *J. Biol. Chem.*, **270**, 15628–15633.

Chen,J.N. and Fishman,M.C. (1996) Zebrafish *tinman* homolog demarcates the heart field and initiates myocardial differentiation. *Development*, **122**, 3809–3816.

Cleaver,O.B., Patterson,K.D. and Krieg,P.A. (1996) Overexpression of the *tinman*-related genes XNKX-2.5 and XNKX-2.3 in *Xenopus* embryos results in myocardial hyperplasia. *Development*, **122**, 3549–3556.

Coffman,J.A., Rai,R., Cunningham,T., Svetlov,V. and Cooper,T.G. (1996) *Gat1p*, a GATA family protein whose production is sensitive to nitrogen catabolite repression, participates in transcriptional activation of nitrogen-catabolic genes in *Saccharomyces cerevisiae*. *Mol. Cell. Biol.*, **16**, 847–858.

Durocher,D., Chen,C.Y., Ardati,A., Schwartz,R.J. and Nemer,M. (1996) The ANF promoter is a downstream target for Nkx-2.5 in the myocardium. *Mol. Biol. Cell*, **16**, 4648–4655.

Egan,C.R., Chung,M.A., Allen,F.L., Heschl,M.F., Van Buskirk,C.L. and McGhee,J.D. (1995) A gut-to-pharynx/tail switch in embryonic expression of the *Caenorhabditis elegans* ges-1 gene centers on two GATA sequences. *Dev. Biol.*, **170**, 397–419.

Evans,S.M., Yan,W., Murillo,M.J., Ponce,J. and Papalopulu,N. (1995) *Tinman*, a *Drosophila* homeobox gene required for heart and visceral mesoderm specification, may be represented by a family of genes in vertebrates – *xnkx-2.3*, a second vertebrate homologue of *tinman*. *Development*, **121**, 3889–3899.

Fu,Y.H. and Marzluf,G.A. (1990) *nit-2*, the major nitrogen regulatory gene of *Neurospora crassa*, encodes a protein with a putative zinc finger DNA-binding domain. *Mol. Cell. Biol.*, **10**, 1056–1065.

Fujiwara,Y., Browne,C.P., Cunniff,K., Goff,S.C. and Orkin,S.H. (1996) Arrested development of embryonic red cell precursors in mouse embryos lacking transcription factor GATA-1. *Proc. Natl Acad. Sci. USA*, **93**, 12355–12358.

Gajewski,K., Kim,Y., Lee,Y.M., Olson,E.N. and Schulz,R.A. (1997) D-mef2 is a target for *Tinman* activation during *Drosophila* heart development. *EMBO J.*, **16**, 515–522.

Gong,Q. and Dean,A. (1993) Enhancer-dependent transcription of the epsilon-globin promoter requires promoter-bound GATA-1 and enhancer-bound AP-1/NF-E2. *Mol. Cell. Biol.*, **13**, 911–917.

Gregory,R.C., Taxman,D.J., Seshasayee,D., Kensinger,M.H., Bieker,J.J. and Wojchowski,D.M. (1996) Functional interaction of GATA1 with erythroid Kruppel-like factor and Sp1 at defined erythroid promoters. *Blood*, **87**, 1793–1801.

Grépin,C., Dagnino,L., Robitaille,L., Haberstroh,L., Antakly,T. and Nemer,M. (1994) A hormone-encoding gene identifies a pathway for cardiac but not skeletal muscle gene transcription. *Mol. Cell. Biol.*, **14**, 3115–3129.

Grépin,C., Robitaille,L., Antakly,T. and Nemer,M. (1995) Inhibition of transcription factor GATA-4 expression blocks *in vitro* cardiac muscle differentiation. *Mol. Cell. Biol.*, **15**, 4095–4102.

Grépin,C., Nemer,G. and Nemer,M. (1997) Enhanced cardiogenesis in embryonic stem cells overexpressing the GATA-4 transcription factor. *Development*, **124**, 2387–2395.

Grondin,B., Bazinet,M. and Aubry,M. (1996) The KRAB zinc finger gene ZNF74 encodes an RNA-binding protein tightly associated with the nuclear matrix. *J. Biol. Chem.*, **271**, 15458–15467.

Guazzi,S., Price,M., De Felice,M., Damante,G., Mattei,M.G. and Di Lauro,R. (1990) Thyroid nuclear factor 1 (TTF-1) contains a homeodomain and displays a novel DNA binding specificity. *EMBO J.*, **9**, 3631–3639.

Guichet,A. et al. (1997) The nuclear receptor homologue Ftz-F1 and the homeodomain protein Ftz are mutually dependent cofactors. *Nature*, **385**, 548–552.

Harvey,R.P. (1996) NK-2 homeobox genes and heart development. *Dev. Biol.*, **178**, 203–216.

Hawkins,M.G. and McGhee,J.D. (1995) *elt-2*, a second GATA factor from the nematode *Caenorhabditis elegans*. *J. Biol. Chem.*, **270**, 14666–14671.

Heikinheimo,M., Scandrett,J.M. and Wilson,D.B. (1994) Localization of transcription factor GATA-4 to regions of the mouse embryo involved in cardiac development. *Dev. Biol.*, **164**, 361–373.

Ip,H.S., Wilson,D.B., Heikinheimo,M., Tang,Z., Ting,C.N., Simon,M.C., Leiden,J.M. and Parmacek,M.S. (1994) The GATA-4 transcription factor transactivates the cardiac muscle-specific troponin C promoter-enhancer in nonmuscle cells. *Mol. Cell. Biol.*, **14**, 7517–7526.

Jiang,Y.M. and Evans,T. (1996) The *Xenopus* GATA-4/5/6 genes are associated with cardiac specification and can regulate cardiac-specific transcription during embryogenesis. *Dev. Biol.*, **174**, 258–270.

Kawana,M., Lee,M.E., Quertermous,E.E. and Quertermous,T. (1995) Cooperative interaction of gata-2 and ap1 regulates transcription of the endothelin-1 gene. *Mol. Cell. Biol.*, **15**, 4225–4231.

Kelley,C., Blumberg,H., Zon,L.I. and Evans,T. (1993) GATA-4 is a novel transcription factor expressed in endocardium of the developing heart. *Development*, **118**, 817–827.

Kuo,C.T., Morrissey,E.E., Anandappa,R., Sigrist,K., Lu,M.M., Parmacek,M.S., Soudais,C. and Leiden,J.M. (1997) GATA4 transcription factor is required for ventral morphogenesis and heart tube formation. *Genes Dev.*, **11**, 1048–1060.

Lamonterie,T., Tremblay,J.J., Lanctôt,C., Therrien,M., Gauthier,Y. and Drouin,J. (1996) *PTX1*, a *bicoid*-related homeobox transcription factor involved in transcription of pro-opiomelanocortin (POMC) gene. *Genes Dev.*, **10**, 1284–1295.

Laverriere,A.C., MacNeill,C., Mueller,C., Poelmann,R.E., Burch,J.B. and Evans,T. (1994) GATA-4/5/6, a subfamily of three transcription factors transcribed in developing heart and gut. *J. Biol. Chem.*, **269**, 23177–23184.

Lee,K.H., Xu,Q. and Breitbart,R.E. (1996) A new *tinman*-related gene, *nkx2.7*, anticipates the expression of *nkx2.5* and *nkx2.3* in Zebrafish heart and pharyngeal endoderm. *Dev. Biol.*, **180**, 722–731.

Lints,T.J., Parsons,L.M., Hartley,L., Lyons,I. and Harvey,R.P. (1993) Nkx-2.5: a novel murine homeobox gene expressed in early heart progenitor cells and their myogenic descendants. *Development*, **119**, 419–431.

Lu,Q. and Kamps,M.P. (1996) Structural determinants within Pbx1 that mediate cooperative DNA binding with pentapeptide-containing Hox proteins: proposal for a model of a Pbx1-Hox-DNA complex. *Mol. Cell. Biol.*, **16**, 1632–1640.

Lyons,I., Parsons,L.M., Hartley,L., Li,R., Andrews,J.E., Robb,L. and Harvey,R.P. (1995) Myogenic and morphogenetic defects in the heart tubes of murine embryos lacking the homeo box gene Nkx2-5. *Genes Dev.*, **9**, 1654–1666.

Merika,M. and Orkin,S.H. (1995) Functional synergy and physical interactions of the erythroid transcription factor gata-1 with the kruppel family proteins spl and eklf. *Mol. Cell. Biol.*, **15**, 2437–2447.

Molkentin,J.D., Kalvakanu,D.V. and Markham,B.E. (1994) Transcription factor GATA-4 regulates cardiac muscle-specific expression of the α -myosin heavy-chain gene. *Mol. Cell. Biol.*, **14**, 4947–4957.

Molkentin,J.D., Lin,Q., Duncan,S.A. and Olson,E.N. (1997) Requirement of the transcription factor GATA4 for heart tube formation and ventral morphogenesis. *Genes Dev.*, **11**, 1061–1072.

Morrissey,E.E., Ip,H.S., Lu,M.M. and Parmacek,M.S. (1996) GATA-6 – a zinc finger transcription factor that is expressed in multiple cell lineages derived from lateral mesoderm. *Dev. Biol.*, **177**, 309–322.

Morrisey,E.E., Ip,H.S., Tang,Z.H., Lu,M.M. and Parmacek,M.S. (1997) GATA-5 – a transcriptional activator expressed in a novel temporally and spatially-restricted pattern during embryonic development. *Dev. Biol.*, **183**, 21–36.

Newman,C.S., Grow,M.W., Cleaver,O., Chia,F. and Krieg,P. (1997) Xbp, a vertebrate gene related to bagpipe, is expressed in developing craniofacial structures and in anterior gut muscle. *Dev. Biol.*, **181**, 223–233.

Okkema,P.G. and Fire,A. (1994) The *Caenorhabditis elegans* NK-2 class homeoprotein CEH-22 is involved in combinatorial activation of gene expression in pharyngeal muscle. *Development*, **120**, 2175–2186.

Osada,H., Grutz,G., Axelson,H., Forster,A. and Rabbitts,T.H. (1995) Association of erythroid transcription factors: complexes involving the lim protein rbtm2 and the zinc-finger protein gata1. *Proc. Natl Acad. Sci. USA*, **92**, 9585–9589.

Pandolfi,P.P., Roth,M.E., Karis,A., Leonard,M.W., Dzierzak,E., Grosfeld,F.G., Engel,J.D. and Lindenbaum,M.H. (1995) Targeted disruption of the GATA3 gene causes severe abnormalities in the nervous system and in fetal liver haematopoiesis [see comments]. *Nature Genet.*, **11**, 40–44.

Peltenburg,L.T.C. and Murre,C. (1997) Specific residues in the PBX homeodomain differentially modulate the DNA-binding activity of Hox and engrailed proteins. *Development*, **124**, 1089–1098.

Phelan,M.L., Rambaldi,I. and Featherstone,M.S. (1995) Cooperative interactions between HOX and PBX proteins mediated by a conserved peptide motif. *Mol. Cell. Biol.*, **15**, 3989–3997.

Platt,A., Langdon,T., Arst,H.N.J., Kirk,D., Tollervey,D., Sanchez,J.M. and Caddick,M.X. (1996) Nitrogen metabolite signalling involves the C-terminus and the GATA domain of the *Aspergillus* transcription factor AREA and the 3' untranslated region of its mRNA. *EMBO J.*, **15**, 2791–2801.

Schultheiss,T.M., Xydas,S. and Lassar,A.B. (1995) Induction of avian cardiac myogenesis by anterior endoderm. *Development*, **121**, 4203–4214.

Spieth,J., Shim,Y.H., Lea,K., Conrad,R. and Blumenthal,T. (1991) elt-1, an embryonically expressed *Caenorhabditis elegans* gene homologous to the GATA transcription factor family. *Mol. Cell. Biol.*, **11**, 4651–4659.

Stanbrough,M., Rowen,D.W. and Magasanik,B. (1995) Role of the GATA factors Gln3p and Nil1p of *Saccharomyces cerevisiae* in the expression of nitrogen-regulated genes. *Proc. Natl Acad. Sci. USA*, **92**, 9450–9454.

Sturm,R.A., Das,G. and Herr,W. (1988) The ubiquitous octamer-binding protein Oct-1 contains a POU domain with a homeo box subdomain. *Genes Dev.*, **2**, 1582–1599.

Ting,C.N., Olson,M.C., Barton,K.P. and Leiden,J.M. (1996) Transcription factor GATA-3 is required for development of the T-cell lineage. *Nature*, **384**, 474–478.

Tonissen,K.F., Drysdale,T.A., Lints,T.J., Harvey,R.P. and Krieg,P.A. (1994) XNkx-2.5, a *Xenopus* gene related to Nkx-2.5 and tinman: evidence for a conserved role in cardiac development. *Dev. Biol.*, **162**, 325–328.

Tsai,F.Y., Keller,G., Kuo,F.C., Weiss,M., Chen,J., Rosenblatt,M., Alt,F.W. and Orkin,S.H. (1994) An early haematopoietic defect in mice lacking the transcription factor GATA-2. *Nature*, **371**, 221–226.

Visvader,J.E., Crossley,M., Hill,J., Orkin,S.H. and Adams,J.M. (1995) The C-terminal zinc finger of GATA-1 or GATA-2 is sufficient to induce megakaryocytic differentiation of an early myeloid cell line. *Mol. Cell. Biol.*, **15**, 634–641.

Walters,M. and Martin,D.I. (1992) Functional erythroid promoters created by interaction of the transcription factor GATA-1 with CACCC and AP-1/NFE-2 elements. *Proc. Natl Acad. Sci. USA*, **89**, 10444–10448.

Weiss,M.J., Keller,G. and Orkin,S.H. (1994) Novel insights into erythroid development revealed through *in vitro* differentiation of GATA-1 embryonic stem cells. *Genes Dev.*, **8**, 1184–1197.

Weiss,M.J., Yu,C.N. and Orkin,S.H. (1997) Erythroid-cell-specific properties of transcription factor GATA-1 revealed by phenotypic rescue of a gene-targeted cell line. *Mol. Cell. Biol.*, **17**, 1642–1651.

Whyatt,D.J., deBoer,E. and Grosfeld,F. (1993) The two zinc finger-like domains of GATA-1 have different DNA binding specificities. *EMBO J.*, **12**, 4993–5005.

Winick,J., Abel,T., Leonard,M.W., Michelson,A.M., Chardon-Loriaux,I., Holmgren,R.A., Maniatis,T. and Engel,J.D. (1993) A GATA family transcription factor is expressed along the embryonic dorsoventral axis in *Drosophila melanogaster*. *Development*, **119**, 1055–1065.

Yu,Y., Li,W., Su,K., Yussa,M., Han,W., Perrimon,N. and Pick,L. (1997) The nuclear hormone receptor Ftz-F1 is a cofactor for the *Drosophila* homeodomain protein Ftz. *Nature*, **385**, 552–555.

Received on May 23, 1997; revised on June 30, 1997

Factor V and Protein S as Synergistic Cofactors to Activated Protein C in Degradation of Factor VIIIa*

(Received for publication, May 16, 1994)

Lei Shen and Björn Dahlbäck†

From the Department of Clinical Chemistry, University of Lund, Malmö General Hospital, S-21401 Malmö, Sweden

Inherited resistance to activated protein C (APC) is a recently identified major cause of thrombosis. It is associated with a mutation in the factor V gene affecting one of the cleavage sites for APC. APC resistance was recently found to be corrected by factor V, suggesting that factor V may have anticoagulant properties as a cofactor to APC. To elucidate this further, we have studied the effect of factor V and protein S, which is a known cofactor to APC, on APC-mediated degradation of factor VIIIa in a purified system. The APC-mediated degradation of factor VIIIa was monitored by a factor X activation reaction using purified factor IXa, phospholipid, and calcium. In the presence of both factor V and protein S, APC was found to inhibit factor VIIIa activity efficiently. APC alone or together with factor V was ineffective, whereas APC in combination with protein S was less efficient than when factor V was also included in the reaction. Two monoclonal antibodies, one against protein S and the other directed toward factor V, were found to inhibit the APC cofactor activity of the factor V-protein S mixture. Factor Va did not express APC cofactor activity, and addition of excess factor Va over factor V did not inhibit the APC cofactor function of a factor V-protein S mixture. In conclusion, the results suggest that factor V and protein S work in synergy as phospholipid-bound cofactors to APC.

The blood coagulation cascade is regulated by the protein C anticoagulant system (reviewed in Refs. 1-3). Protein C, after its activation on the endothelial cell surface by thrombin-thrombomodulin, degrades the activated forms of factors VIIIa and Va. The anticoagulant effect of activated protein C (APC)¹ is potentiated by its cofactor protein S. Protein S, being a vitamin K-dependent protein with high affinity for negatively charged phospholipid, has been suggested to form a membrane-bound 1:1 stoichiometric complex with APC. The physiological importance of protein S as anticoagulant is demonstrated by

the association between protein S deficiency and thrombosis. However, its mode of action is incompletely understood, as the APC cofactor activity of protein S is weak in factor Va degradation systems using purified components (4).

Results recently presented from our laboratory have suggested that intact factor V, apart from being a precursor to factor Va, may also have anticoagulant properties functioning as cofactor to APC (5). This proposal was based on the observation that purified factor V corrected the anticoagulant defect of plasma from an individuals with inherited resistance to APC. APC resistance was originally characterized in a single individual with familial thrombophilia (6). It is now recognized as a major basis of venous thrombosis and prevalences between 20% and 60% in patients with thrombosis have been reported (7-11). The observation that factor V corrects the anticoagulant defect in APC-resistant plasma suggested that APC resistance is caused by mutations in the factor V gene (5). Recently, it was found that the same mutation is present in a majority of cases with APC resistance (12, 13). The mutation affects one of the APC cleavage sites of factor V, changing Arg-506 to Gln. Although the mutated factor Va is degradable by APC (there are several APC cleavage sites in factor Va), the mutation probably results in a qualitative resistance to APC, which affects the activation rate of the coagulation cascade.

The complicated nature of a plasma clotting system involving APC-resistant plasma makes it difficult to elucidate the potential role of factor V as cofactor to APC. For the purpose of determining whether factor V indeed is an APC cofactor, we have established a factor VIIIa degradation system using purified components, thus excluding potential influence of other factors in plasma. We now wish to report that both factor V and protein S, in a synergistic fashion, function as cofactors to APC in the degradation of factor VIIIa.

EXPERIMENTAL PROCEDURES

Hirudin and Russell viper venom (RVV) was obtained from Sigma. The chromogenic substrate S-2222, purified bovine factor IXa, bovine factor X, and phospholipid vesicles were components of the Coamatic Factor VIII kit (Chromogenix, Mölndal, Sweden) and was kindly provided by Dr. Steffen Rosén at Chromogenix. Octonate M (Pharmacia Biotech Inc.) was used as the source of factor VIII. Human factor V, protein S, activated human protein C, and bovine thrombin were purified according to previously described methods (5, 14). Factor V (0.6 mg/ml) in 50 mM Tris-HCl, 150 mM NaCl, 2 mM CaCl₂, pH 7.5, was activated by α -thrombin (final concentration of 6 NIH units/ml) at 37 °C for 15 min, and thrombin was then neutralized by hirudin (final concentration of 9 units/ml). The factor V activator from RVV was purified as previously reported (15). Factor V (170 µg/ml) was incubated with the factor V activator (8.7 µg/ml) in 50 mM Tris, 150 mM NaCl, 2 mM CaCl₂, pH 7.5, for 15 min at 37 °C. Protein S was cleaved by incubating protein S (0.67 mg/ml) with thrombin (final concentration of 5 NIH units/ml) in 50 mM Tris-HCl, pH 7.5, 150 mM NaCl, 2 mM EDTA for 60 min at 37 °C, after which hirudin (final concentration of 7.5 units/ml) was added to neutralize the excess thrombin.

Preparation of Factor VIIIa Reagent—Thrombin-activated factor VIII (factor VIIIa) was prepared by incubating a solution containing factor VIII (0.32 NIH units/ml), factor IXa (0.05 units/ml), and phospholipid vesicles (56 µm) with α -thrombin (0.002 NIH unit/ml). The buffer was 50 mM Tris-HCl, 10.5 mM CaCl₂, 0.2% bovine serum albumin, pH 7.3, and the incubation was kept at 37 °C in silicone-treated tubes. After 2 min, the reaction was stopped by the addition of hirudin to a final concentration of 0.003 unit/ml (1.5-fold molar excess over thrombin). Due to the labile nature of factor VIIIa, this factor IXa-factor VIIIa-PL mixture (reagent I) was prepared fresh for each series of experiments.

* This work was supported by the Swedish Medical Council (Grants 07143 and 10827), the Österlund Trust, King Gustaf Vs 80th Birthday Trust, the King Gustaf V and Queen Victoria Trust, the Magnus Bergwall Trust, the Albert Pahlsson Trust, the Johan and Greta Kock Trust, and research funds from Malmö General Hospital. The costs of publication of this article were defrayed in part by the payment of page charges. This article must therefore be hereby marked "advertisement" in accordance with 18 U.S.C. Section 1734 solely to indicate this fact.

† To whom correspondence should be addressed. Tel.: 46-40-331501; Fax: 46-40-929023.

¹ The abbreviations used are: APC, activated protein C; RVV, hirudin and Russell viper venom.

Factor V as Cofactor to Activated Protein C

Factor VIIIa Degradation Assay—Different combinations of APC (final concentration of 0–2 $\mu\text{g}/\text{ml}$), protein S (final concentration of 0–2.5 $\mu\text{g}/\text{ml}$), and factor V (final concentration of 0–11 $\mu\text{g}/\text{ml}$) were mixed in multiwell plates (Linbro, Flow Laboratories) in a final volume of 25 μl in 50 mM Tris-HCl, 10.5 mM CaCl₂, 0.2% bovine serum albumin, pH 7.3. Reagent I (80 μl) was added, and after 2 min 20 μl of factor X (1.2 units/ml) was added. After a 5-min incubation at room temperature, factor Xa was measured by S-2222 substrate hydrolysis; 50 μl of S-2222 was added; and after 5 min in the dark at room temperature, addition of 50 μl of 20% acetic acid stopped the reaction and the absorbance at 405 nm was measured. The factor Xa generated correlated linearly with the factor VIIIa activity, which was expressed as percent of activity of respective control.

Factor VIIIa Degradation in the Presence of an Excess of Factor Va—Fixed concentrations of APC (final concentration of 1.0 $\mu\text{g}/\text{ml}$), protein S (final concentration of 1.5 $\mu\text{g}/\text{ml}$) and factor V (final concentration of 6.6 $\mu\text{g}/\text{ml}$) were mixed with different concentrations of factor Va (0–200% as related to the factor V concentration) in a final volume of 25 μl . Reagent I (80 μl) and then factor X were added, and the remaining factor VIIIa activity was measured as described above.

Inhibition of Factor VIIIa Degradation by Monoclonal Antibodies against Protein S or Factor V—Monoclonal antibodies HFV-1 and HFV-4 react with the 150-kDa activation peptide of factor V, and they have been found to partially inhibit the factor V anticoagulant activity in normal plasma (5). Monoclonal antibody HPS-54 reacts with the first epidermal growth factor domain of human protein S and efficiently blocks APC cofactor activity of protein S (14). The antibodies (final concentration of 20 $\mu\text{g}/\text{ml}$) were incubated with the APC-protein S-factor V mixtures at room temperature for 10 min before addition of reagent I. The final concentration of APC was 1 $\mu\text{g}/\text{ml}$, factor V concentrations were between 0 and 11 $\mu\text{g}/\text{ml}$, and protein S concentrations were between 0 and 2.0 $\mu\text{g}/\text{ml}$.

RESULTS AND DISCUSSION

In the first identified patient with APC resistance, several potential causes for the poor anticoagulant response to APC were elucidated (6). Factor VIII gene mutations were excluded; inasmuch as the patient's factor Va appeared to be inhibited by APC in an essentially normal fashion, mutations changing the APC cleavage site of factor Va were found to be a less likely cause of the APC resistance, although it should be borne in mind that the possibility was not disproved. Deficiency of a previously unrecognized APC cofactor was another possible mechanism for APC resistance that we decided to elucidate. An assay for the hypothetical APC cofactor was established using plasma from an individual with almost complete APC resistance (5). A protein, which turned out to be identical to factor V, was purified from normal plasma and was found to correct APC resistance in a dose-dependent manner (5). This suggested that factor V possesses anticoagulant properties as a cofactor to APC. The addition of approximately 20 $\mu\text{g}/\text{ml}$ intact factor V (slightly higher than the normal plasma concentration of factor V) was found to completely normalize the APC response in plasma from this particular APC-resistant person.

The complicated nature of blood coagulation makes it difficult to draw firm conclusions regarding the role of factor V as an APC cofactor from results obtained in a plasma system. The recent finding that the majority of patients with APC resistance have a mutation affecting an APC cleavage sites in factor Va (12, 13) has cast doubt on our conclusion that factor V has a function as cofactor to APC. In order to elucidate the potential function of factor V as APC cofactor, we have developed a factor VIIIa degradation system using purified components. In this system, we find APC to be an efficient inhibitor of factor VIIIa only in the presence of a combination of factor V and protein S (Fig. 1). APC alone causes no inhibition of factor VIIIa activity, and protein S was found to have a weak potentiating effect on APC-mediated factor VIIIa inhibition. This is consistent with results on record, which demonstrate that protein S is also a poor APC cofactor in the degradation of factor Va in purified systems (4). In the presence of an equimolar mixture of APC

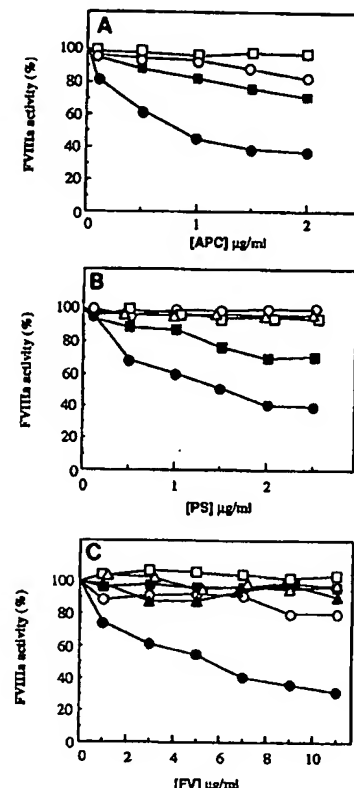


Fig. 1. Synergistic APC cofactor activity of protein S and factor V in degradation of factor VIIIa. A mixture of factor VIIIa, factor IXa, and phospholipid was incubated with different combinations of APC, protein S (or thrombin-cleaved protein S), and factor V (or factor Va). Factor X was added, and the rate of factor Xa formation was measured with a synthetic substrate. The absorbance was linearly related to the factor VIIIa activity, and results were expressed as percentage of respective control. *A*, increasing concentrations of APC (final concentrations are indicated) with fixed concentrations of the other components (final concentrations of 6.6 $\mu\text{g}/\text{ml}$ for factor V and 1.5 $\mu\text{g}/\text{ml}$ for protein S). \square , APC alone; \circ , APC plus factor V; \blacksquare , APC plus protein S; \bullet , APC plus factor V plus protein S. *B*, increasing concentrations of protein S or thrombin-cleaved protein S with other components kept at fixed concentration (1 $\mu\text{g}/\text{ml}$ APC and 6.6 $\mu\text{g}/\text{ml}$ factor V). Δ , protein S alone; \square , protein S plus factor V; \blacksquare , APC plus protein S; \bullet , APC plus factor V plus protein S; \circ , APC plus factor V plus thrombin-cleaved protein S. *C*, increasing concentrations of factor V or Va (thrombin- or RVV-activated) with other components kept at fixed concentration (1 $\mu\text{g}/\text{ml}$ APC and 1.5 $\mu\text{g}/\text{ml}$ protein S). \blacksquare , factor V alone; \blacktriangle , protein S plus factor V; \circ , APC plus factor V; \bullet , APC plus factor V plus protein S; Δ , APC plus protein S plus thrombin-activated factor Va; \square , APC plus protein S plus RVV-activated factor Va.

and protein S, the addition of factor V resulted in a dose-dependent increased inhibition of factor VIIIa activity. The APC cofactor activity of factor V reached its maximum at a molar concentration of factor V that was similar to those of APC and protein S. At equimolar concentrations of APC and factor V, addition of protein S yielded a dose-dependent increased inhibition of factor VIIIa activity, which leveled off at a molar protein S concentration close to that of factor V. This suggests that factor V is a required component for expression of maximum protein S anticoagulant activity and provides a basis for understanding the poor protein S activity observed in purified systems not including intact factor V (4). When factor V and protein S were kept constant at equimolar concentrations and increasing concentrations of APC were added, a dose-dependent increased inhibition of factor VIIIa activity was observed. The data were consistent with the formation of a 1:1:1 stoichiometric complex of APC, factor V, and protein S on the phos-

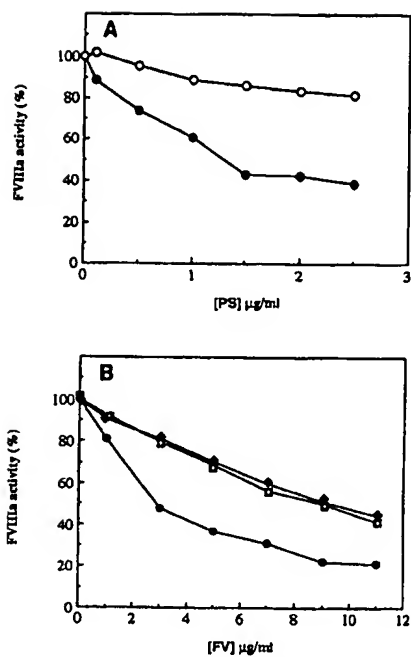


Fig. 2. Inhibition of APC-mediated factor VIIIa degradation by monoclonal antibodies against protein S and factor V. APC-mediated factor VIIIa degradation was studied as described in the legend to Fig. 1 in the presence or absence of monoclonal antibody against protein S or factor V. A, O, APC (1 µg/ml), factor V (6.6 µg/ml), plus monoclonal antibody HPS 54 against protein S (20 µg/ml) and increasing concentrations of protein S; ●, control without HPS 54. B, APC (1 µg/ml), protein S (1.5 µg/ml), and increasing concentrations of factor V in the presence of HFV-1 (20 µg/ml, ♦), HFV 4 (20 µg/ml, □), or in their absence (○).

pholipid surface, a complex that efficiently inhibited factor VIIIa activity. Factor V activated with thrombin or with the factor V activator from the RVV was found to be inefficient as APC cofactor. Moreover, cleavage of protein S by thrombin resulted in loss of APC cofactor activity.

Monoclonal antibodies against protein S and factor V were included in the factor VIIIa degradation assay (Fig. 2). Monoclonal antibodies HFV-1 and HFV-4, which were directed against the central part of factor V, were found to partially inhibit the APC cofactor activity of factor V. This is consistent with the observation that these two antibodies partially inhibit the factor V-dependent APC cofactor activity of normal plasma (5). Monoclonal antibody HPS-54, which is directed against the first epidermal growth factor-like module of protein S (14), efficiently inhibited the APC cofactor activity of the protein S-factor V mixture. These results support the concept that factor V and protein S function as synergistic cofactors to APC. Presumably, factor V and protein S form a 1:1 complex on the surface of negatively charged phospholipids and this complex provides efficient cofactor activity for APC. In a situation where the vessel wall is disrupted and the coagulation cascade is activated, the activity of this anticoagulant-APC cofactor complex may be inhibited by thrombin-mediated activation of factor V and possibly also by protein S cleavage by thrombin. This suggests that factor V functions as an anticoagulant protein under physiological conditions and that it is converted into a procoagulant factor in response to coagulation activation.

Both factors VIIIa and Va are substrates for APC, but it is not known which of the two is the preferred substrate. The concentration of factor V in plasma is at least 100-fold higher than that of factor VIII. If factor Va and factor VIIIa are equally good APC substrates, it follows that APC would preferentially in-

TABLE I
Effect of increasing factor Va concentrations on APC-protein S-factor V-mediated factor VIIIa inhibition

Reagent 1 (containing factor VIIIa, factor IXa, phospholipid, and calcium) and the mixture of APC (1 µg/ml), protein S (1.5 µg/ml), and factor V (6.6 µg/ml) were incubated with increasing concentrations of factor Va (0–200% as related to the factor V concentration) at room temperature for 2 min. Factor X was added and the factor Xa formation measured as described under "Experimental Procedures." Results were expressed as % inhibition of factor VIIIa activity using a mixture without factor V as reference.

(Factor Va/factor V) × 100%	Inhibition of FVIIIa activity
0	45
25	42
50	46
100	47
125	47
150	45
200	47

hibit factor Va after activation of the coagulation cascade *in vivo*. To elucidate whether factor VIIIa degradation was affected by factor Va, we included increasing concentrations of factor Va in a factor VIIIa degradation experiment using an APC-protein S-factor V mixture. The inhibitory effect on factor VIIIa of this trimolecular mixture was found to be unaffected by the added factor Va (Table I). Thus factor VIIIa appears to be the preferred substrate for APC. This makes sense, as it provides a mechanism for factor VIIIa degradation by APC even in the presence of an excess of factor Va.

Recently, we have found that the individual with pronounced APC resistance, the plasma of whom was used to identify factor V as a potential APC cofactor (5), has the APC cleavage site mutation in homozygous form, whereas the original patient (6) presents a more complicated picture with a heterozygous APC cleavage site mutation and an additional inherited, as yet unknown, disturbance that contributes to the severity of the APC resistance.² Mutated factor Va, when compared to normal factor Va, is presumably degraded at a lower rate by APC and consequently factor Va formed in APC-resistant plasma will result in a higher than normal rate of thrombin generation. Thrombin then feedback-activates factors VIII and V, with a resulting loss of the APC cofactor activity of factor V. The anticoagulant effect of added normal factor V to this kind of plasma may be partly due to increased APC-mediated degradation of factor VIIIa, as normal factor V is an APC cofactor. This would result in decreased rates of generation of factor Xa, thrombin, factor Va, and factor VIIIa and in preservation of the factor V-dependent APC cofactor activity. Moreover, assuming the normal and the mutated factor V to be activated at equal rates by thrombin, the majority of factor V molecules being activated after the addition of an excess of normal factor V would be the normal ones, which are degraded at a normal rate by APC in a factor V- and protein S-dependent reaction. Whether factor V with a mutation in the APC cleavage site expresses full activity as APC cofactor remains to be determined, but preliminary data suggest this to be the case.³

To sum up, using a purified system, we now provide experimental data demonstrating that factor V and protein S function as synergistic cofactors to APC in degradation of factor VIIIa and that cleavage of factor V and protein S by thrombin results in loss of this APC cofactor activity.

Acknowledgments—We gratefully acknowledge the technical assistance of Bergsia Hildebrand, Lise Borge, and Astra Anderson.

² B. Zöller and B. Dahlbäck, unpublished observation.

³ L. Shen and B. Dahlbäck, unpublished observation.

REFERENCES

1. Dahlbäck, B. (1991) *Thromb. Haemostasis* **66**, 49-61
2. Dahlbäck, B., and Stenflo, J. (1994) in *The Molecular Basis of Blood Diseases* (Stamatoyannopoulos, G., Majerus, P. W., Nienhuis, A. W., and Varmus, H., eds) pp 599-627, W. B. Saunders, Philadelphia
3. Esmon, C. T. (1989) *J. Biol. Chem.* **264**, 4743-4746
4. Bakker, H. M., Tans, G., Jansson-Claessen, T., Thomassen, M. C. L. G. D., Hemker, H. C., Griffin, J., and Rosing, J. (1992) *Eur. J. Biochem.* **208**, 171-178
5. Dahlbäck, B., and Hildebrand, B. (1994) *Proc. Natl. Acad. Sci. U. S. A.* **91**, 1398-1400
6. Dahlbäck, B., Carlsson, M., and Svensson, P. (1993) *Proc. Natl. Acad. Sci. U. S. A.* **90**, 1004-1008
7. Griffin, J., Evatt, B., Wideman, C., and Fernandez, J. A. (1993) *Blood* **82**, 1989-1993
8. Koster, T., Rosendaal, F. R., de Ronde, H., Briet, E., Vandenbroucke, J. P., and Bertina, R. M. (1993) *Lancet* **342**, 1503-1506
9. Faioni, E. M., Franchi, F., Asti, D., Sacchi, E., Bernardi, F., and Mannucci, P. M. (1993) *Thromb. Haemostasis* **70**, 1067-1071
10. Svensson, P., and Dahlbäck, B. (1994) *N. Engl. J. Med.* **330**, 517-567
11. Halbマイヤー, W.-M., Haushofer, A., Schön, R., and Fischer, M. (1994) *Blood Coag. Fibrinol.* **5**, 51-67
12. Bertina, R. M., Koelman, B. P. C., Koster, T., Rosendaal, F. R., Dirven, R. J., de Ronde, H., van der Velden, P. A., and Reitama, P. H. (1994) *Nature* **369**, 64-67
13. Zöller, B., and Dahlbäck, B. (1994) *Lancet* **343**, 1536-1538
14. Dahlbäck, B., Hildebrand, B., and Malm, J. (1990) *J. Biol. Chem.* **265**, 8127-8135
15. Esmon, C. T., and Jackson, C. M. (1974) *Thromb. Res.* **2**, 509-524

SYNERGY AMONG AGENTS INHIBITING GRANULOCYTE AGGREGATION^{1,2}

DALE E. HAMMERSCHMIDT,³ PATRICK J. FLYNN,³
PATRICIA A. COPPO,³ KEITH M. SKUBITZ,⁴ and
HARRY S. JACOB³

³Department of Medicine, University of Minnesota Medical School
Minneapolis, Minnesota

⁴Departments of Medicine and of Pharmacology and Experimental Therapeutics
Johns Hopkins University School of Medicine
Baltimore, Maryland

Abstract—Recent evidence suggests complement (C) -stimulated granulocytes (PMNs) are important in a variety of diseases, including shock and myocardial infarction (MI). Corticosteroids inhibit PMN response to C and show promise in some studies of shock and MI, but their use has not become routine for several reasons. Synergy was sought among agents inhibiting PMN aggregation *in vitro* in response to activated C: methylprednisolone (MP), with a 50% inhibitory dose (AD₅₀) of 0.6 mg/ml; ibuprofen (IBU), with AD₅₀ of 1.0 mg/ml, and betahistine (BH), with AD₅₀ of 1.6 mg/ml. Simultaneous use of all three agents produced 3.4-fold synergy; 3-fold synergy obtained between IBU + MP and IBU + BH, while 1.5-fold synergy was noted between MP + BH. Further, MP and IBU were at least additive in inhibiting $\cdot\text{O}_2^-$ generation by FMLP-stimulated PMNs and in blocking directed migration. In a preliminary *in vivo* test of this finding, cats were given MP and IBU—in known individually ineffective doses—immediately prior to coronary artery ligation. Neither MP nor the low dose of IBU chosen limited the size of the resultant MI, while both agents together reduced MI size by 42%. Synergy among these agents suggests that they inhibit PMN function of distinct cellular mechanisms (as yet not elucidated). Further, early *in vivo* results encourage speculation that such synergy might ultimately be exploited clinically, although such speculation must presently be regarded as preliminary.

INTRODUCTION

Recent evidence has suggested that the complement (C) -stimulated granulocyte (PMN) might play a role in the adult respiratory distress syndrome

¹Material presented in part to the plenary session of the 1981 annual meeting of the American Federation for Clinical Research, San Francisco, California.

²Work supported in part by the following grants: N.I.H.(U.S.A.): AM-15730, CA-09243, HL-19725, HL-07062, HL-25043, HL-26218.

(ARDS) (1-4) and in myocardial infarction (MI) (5-9). We have reported (10) that high-dose corticosteroids inhibit PMN responses to activated C and have postulated that this inhibition might explain in part the apparent efficacy of corticoids in both experimental and clinical shock and MI (11-14). While use of steroids in these syndromes has a rational basis, it has not become routine because of cost, fear of morbidity, uncertain efficacy (at least if not used very early) and the inability to identify early those patients likely to benefit.

Incidental to other studies, we noted that ibuprofen (IBU) also inhibited C-induced PMN aggregation, but only at drug concentrations several-fold higher than required to block fatty acid cyclooxygenase. A third agent, betahistine (BH), was noted to reduce the size of experimental MI (14) and was found to inhibit PMN aggregation. Aware of the limitations of corticosteroids alone in MI and shock, we sought synergy among these agents *in vitro* in hope of devising a drug combination which might be less costly, more effective, and/or less morbid than the use of steroids alone.

MATERIALS AND METHODS

PMN aggregometry was performed as previously described (15), using cells harvested from 12 normal volunteers' venous blood by our modification of the method of Bøyum (15, 16). Zymosan-activated plasma (ZAP) was prepared from minimally heparinized (1 unit/ml) human venous blood as previously described (15), incubating 2 mg zymosan (ICN Pharmaceuticals, Cincinnati, Ohio) per ml plasma (30 min at 37°C) and removing it by centrifugation (10,000g \times 15 min at 4°C). Aliquots were stored frozen (-70°C) until use; to assure a consistent potency of aggregation stimulus, aliquots of a single batch of ZAP were used for all aggregation studies. For each test, 50 μl of ZAP were added to 0.45 ml of PMN suspension (10^7 PMN/ml) containing the drug(s) under study, and maximal increment in light transmission (ΔT) was recorded and expressed as a percentage of the maximal ΔT in a simultaneous drug-free control. *N*-Formyl-methionyl-leucyl-phenylalanine (FMLP) (Peninsula, San Carlos, California) was dissolved at 10 mM in phosphate-buffered saline (PBS) (isotonic; pH = 7.4). Aliquots were stored frozen until use, when dilutions were prepared in PBS as needed.

Chemotaxis was measured by a leading-front modification (17) of the method of Boyden (18); 10^{-8} M FMLP was used as the stimulus, and results were expressed as net migration distance (stimulated migration distance less unstimulated migration distance). Superoxide generation was measured as previously described (19), as superoxide dismutase-inhibitable cytochrome *c* reduction on stimulation of cytochalasin-B-treated PMNs by 10^{-6} M FMLP.

MP sodium succinate (Upjohn Co., Kalamazoo, Michigan), IBU sodium (Upjohn), and BH hydrochloride (Unimed, Somerville, New Jersey) were gifts of the manufacturers. Each was dissolved in PBS to the desired concentrations. For each assay, one volume of drug solution or PBS blank was added to nine volumes of PMN suspension (10^7 cells/ml in Hanks' balanced salt solution) and incubated at 20°C for 10 min before adding the stimulus and measuring the response.

Each cell function-drug combination was tested in cells from at least six normal donors; each assay was performed in triplicate. For each agent and cell function studied, a 50% attenuative dose (AD_{50}) was determined by testing serial twofold drug dilutions and plotting the

Synergistic Inhibition of PMN Function

inhibitory effect logarithmically (10). Equipotent AD_{50} of each of the drugs in the mixtures were determined for each mixture; synergism was determined by comparing lower drug concentrations than those predicted by additive effects. Statistical significance of differences between observed and predicted values was determined by the Mann-Whitney *U* test.

RESULTS

As previously reported (10), MP AD_{50} of 0.64 mg/ml (1.7 mM) \pm 0.05 mg/ml (4.8 mM) (\pm 0.2 mg/ml), IBU AD_{50} of 0.50 mg/ml (1.3 mM) (\pm 0.3 mg/ml). Additive effect of equimolar mixtures of MP and IBU to 0.32 mg MP + 0.50 mg IBU/ml; in 1:6 dilution (0.11 mg MP + 0.18 mg IBU/ml), threefold synergy was observed (not shown). Only 1.4-fold synergy ($P < 0.05$) was observed between MP, suggesting IBU was the major component.

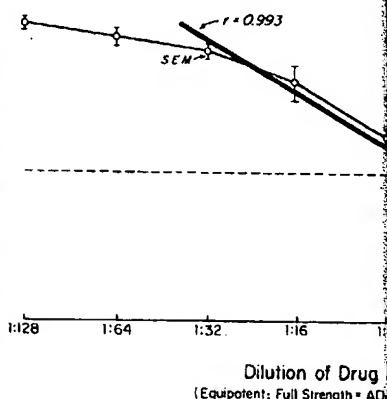


Fig. 1. Synergy between MP and IBU in inhibiting PMN function. The graph shows the inhibition of PMN function by MP and IBU. The y-axis represents the inhibition percentage, and the x-axis represents the dilution of the drug mixture. The data points show a linear decrease in inhibition percentage as the dilution increases, indicating synergy. The correlation coefficient $r = 0.993$. The graph also includes a dashed horizontal line representing the expected additive effect (50% inhibition at 1:16 dilution). The data points are labeled with error bars representing SEM.

dial infarction (MI) (5-9). We have reported that steroids inhibit PMN responses to activated C. Inhibition might explain in part the apparent experimental and clinical shock and MI (1). These syndromes has a rational basis, it has not yet, fear of morbidity, uncertain efficacy (at least, the inability to identify early those patients).

we noted that ibuprofen (IBU) also inhibits, but only at drug concentrations several-fold fatty acid cyclooxygenase. A third agent, to reduce the size of experimental MI (14) and aggregation. Aware of the limitations of corticosteroids, we sought synergy among these agents drug combination which might be less costly, and rapid than the use of steroids alone.

METHODS AND METHODS

As previously described (15), using cells harvested by our modification of the method of Bøyum (15, 16). Prepared from minimally heparinized (1 unit/ml) human (15), incubating 2 mg zymosan (ICN Pharmaceuticals) (30 min at 37°C) and removing it by centrifugation were stored frozen (-70°C) until use; to assure a consistent aliquots of a single batch of ZAP were used for all aggregation. ZAP were added to 0.45 ml of PMN suspension (10⁷ cells/ml) in a chamber, and maximal increment in light transmission was expressed as percentage of the maximal ΔT in a simultaneous drug-activated PMN suspension (FMLP) (Peninsula, San Carlos, California) in phosphate-buffered saline (PBS) (isotonic; pH = 7.4), when dilutions were prepared in PBS as needed. Leading-front modification (17) of the method of Boyden chamber, and results were expressed as net migration distance (unstimulated migration distance). Superoxide generation was described (19), as superoxide dismutase-inhibitable cytochrome c-oxidase-treated PMNs by 10⁻⁶ M FMLP. o., Kalamazoo, Michigan), IBU sodium (Upjohn), and (o., New Jersey) were gifts of the manufacturers. Each concentrations. For each assay, one volume of drug solution volumes of PMN suspension (10⁷ cells/ml in Hanks' balanced salt solution) was incubated at 37°C for 10 min before adding the stimulus and measuring aggregation was tested in cells from at least six normal donors. For each agent and cell function studied, a 50% attenuation testing serial twofold drug dilutions and plotting the

Synergistic Inhibition of PMN Function

inhibitory effect logarithmically (10). Equipotent mixtures of the agents were prepared, such that one AD_{50} of each of the drugs in the mixture was achieved in the final incubation with granulocytes; serial dilutions of such mixtures were then tested as inhibitors of PMN function. An AD_{50} was determined for each mixture; synergy was inferred when AD_{50} was achieved with lower drug concentrations than those predicted if effects were simply additive. Statistical significance of differences between observed and expected AD_{50} s was tested using Student's *t* test and the Mann-Whitney U test.

RESULTS

As previously reported (10), MP inhibited PMN aggregation with an AD_{50} of 0.64 mg/ml (1.7 mM) \pm 0.05 mg/ml (SEM). IBU had an AD_{50} of 1.0 mg/ml (4.8 mM) (\pm 0.2 mg/ml), and BH an AD_{50} of 1.6 mg/ml (11.7 mM) (\pm 0.3 mg/ml). Additive effect would predict the AD_{50} of an equipotent mixture of MP and IBU to appear at a 1:2 (part:total) dilution (0.32 mg MP + 0.50 mg IBU/ml); in fact, AD_{50} was observed at close to a 1:6 dilution (0.11 mg MP + 0.18 mg IBU/ml) ($P < 0.005$) (Figure 1). Similarly, threefold synergy was observed between IBU and BH ($P < 0.02$, data not shown). Only 1.4-fold synergy ($P \approx 0.08$) was noted between BH and MP, suggesting IBU was the major contributor to synergy. When all three

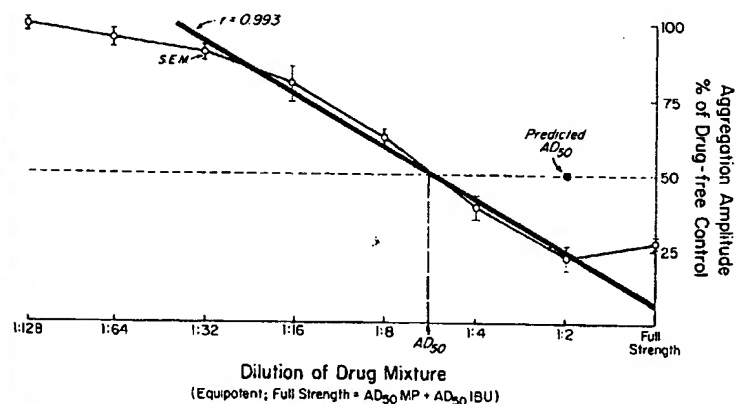


Fig. 1. Synergy between MP and IBU in inhibiting PMN aggregation in response to a constant source of activated C (as aliquots of a single batch of zymosan-activated plasma). The 50% attenuative dose of each agent was determined; a mixture providing one AD_{50} of each was prepared, and serial dilutions were tested as inhibitors of C-induced PMN aggregation. Additive (noncompetitive, nonsynergistic) effect would predict AD_{50} of the mixture to appear at a 1:2 dilution; instead it was observed close to 1:6 ($P < 0.005$). Similar synergy was found between BH and IBU and among BH, IBU and MP; a lesser synergy was found between BH and MP.

agents were used together, 3.4-fold synergy resulted, AD₅₀ appearing at 1:10.3 dilution (0.06 mg MP, 0.08 mg IBU, and 0.12 mg BH/ml).

Because aggregometry is a turbidometric assay (and therefore easier to perform in the absence of serum), these data are generated in a buffer system; to ensure that the conclusions were not limited to such a circumstance, several donors' cells were restudied suspended in a medium consisting of half autologous serum and half Hanks' balanced salt solution and concordant results were obtained (MP and IBU yielding similar AD₅₀ and approximately threefold synergy. Cell viability—assayed by trypan blue exclusion and by retention of cytoplasmic lactate dehydrogenase—remained greater than 98% in all incubations, excluding cumulative death as an explanation of apparent synergy.

FMLP-stimulated PMNs produced enough $\cdot\text{O}_2$ to reduce 7-17 nmol cytochrome *c* (12.2 ± 4.3 S.E.M.) per 10^6 PMNs in 20 min; IBU (AD₅₀ = 0.88 mM) and MP (AD₅₀ = 0.43 mM) inhibited this $\cdot\text{O}_2$ production. AD₅₀ of an equipotent mix was 1:2.3 (0.33 mM IBU + 0.16 mM MP) (*P* for synergy = 0.25); while weak synergy was not statistically significant, the drugs were at least additive in effect. 2.1 mM MP (± 0.12) inhibited net PMN chemotaxis by 50%, as did 4.8 mM IBU (± 0.25). An equipotent mix

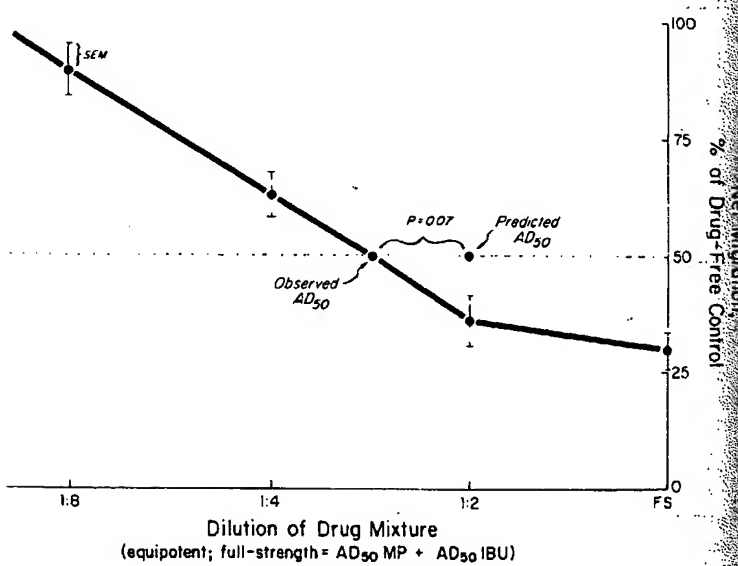


Fig. 2. Probable synergy between MP and IBU in inhibiting PMN chemotaxis in response to FMLP. As in aggregation (Figure 1), AD_{50} was determined for each agent, an equipotent mixture was prepared, and serial dilutions were then tested as inhibitors of chemotaxis. Moderate synergy was observed and was of borderline statistical significance.

ture achieved AD_{50} at a dilution of fifty percent attenuation of random 10 mM MP and 10 mM IBU).

DISCERN

Evidence has accumulated that C^1 -stimulated PMN—may play a role in determining the extent of infarctive reviewed elsewhere (1, 20) and has en C^1 -stimulated PMN in shock and infar-

Use of high-dose steroids in shock for several reasons. First, the therapy is based on the assumption that benefit is only derived from the presence of reliable predictors of drug benefit. Second, by requiring the treatment of most preventable mishaps. Third, while well tolerated in the short run, there is a risk of serious side effects after more than a few doses. The clinician lacks knowledge of the various options of uniform use and the potential for morbidity have encouraged nonuse.

We have reported (10) that high-doses to activated complement and PMN aggregation in response to activated cyclooxygenase. Other research in progress (11) suggested that IBU might also limit shock, at very high but clinical doses but no lasting ill effects if IBU was under study as a limiter of PMN aggregation in response to activated cyclooxygenase, and which mechanisms, we sought synergy among them. The theoretical foundation for multiple

fold synergy resulted, AD_{50} appearing at a 1.08 mg IBU, and 0.12 mg BH/ml. In a turbidometric assay (and therefore easier to perform), these data are generated in a buffer. Inclusions were not limited to such a circumstance; restudied suspended in a medium containing one half Hanks' balanced salt solution, obtained (MP and IBU yielding similar AD_{50} s) synergy. Cell viability—assayed by trypan blue exclusion of cytoplasmic lactate dehydrogenase—revealed all incubations, excluding cumulative cell count, apparent synergy.

produced enough $\cdot O_2$ to reduce 7-17 nmol M. per 10^6 PMNs in 20 min; IBU (AD_{50} = 43 mM) inhibited this $\cdot O_2$ production. AD_{50} 2.3 (0.33 mM IBU + 0.16 mM MP) (P for synergy was not statistically significant, the net effect. 2.1 mM MP (± 0.12) inhibited net $\cdot O_2$ and 4.8 mM IBU (± 0.25). An equipotent mix-

ture achieved AD_{50} at a dilution of 1:2.6 (P for synergy = 0.07) (Figure 2). Fifty percent attenuation of random migration was not achieved (maximum 6 mM MP and 10 mM IBU).

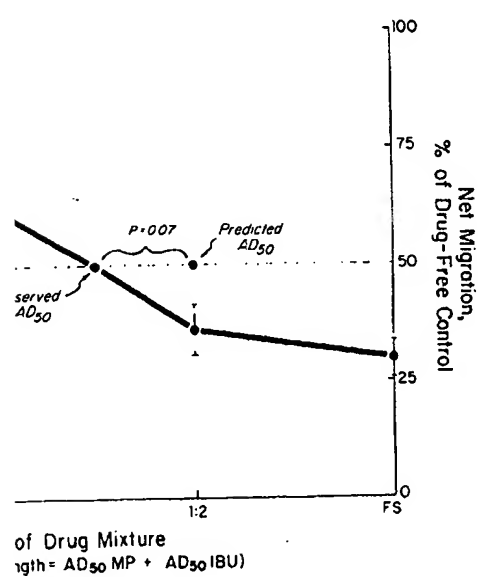
DISCUSSION

Evidence has accumulated that the stimulated PMN—specifically the C-stimulated PMN—may play a role in the complications of shock and in determining the extent of infarctive damage; this evidence has been reviewed elsewhere (1, 20) and has encouraged our continued study of the C-stimulated PMN in shock and infarction.

Very high dose corticosteroids have been tried (for a variety of reasons) in both clinical (12, 13) and experimental infarction (11, 14) and shock. In a number of models, these agents have reduced MI size or the morbidity and mortality of shock; studies showing benefit have generally been those in which very high doses (30 mg MP/kg body mass or equivalent) have been used very early in the insult. Clinical results have also been mixed, but the same generalization can be made.

Use of high-dose steroids in shock and MI has not become routine for several reasons. First, the therapy is expensive. Second, available data suggest that benefit is only derived from very early intervention; in the absence of reliable predictors of drug benefit, this compounds the cost problem by requiring the treatment of most or all patients at risk of a steroid-preventable mishap. Third, while high-dose steroids are remarkably well tolerated in the short run, there is concern for safety in use of more than a few doses. The clinician lacks a real option of selective steroid use; faced with options of uniform use and uniform nonuse, cost and fear of morbidity have encouraged nonuse.

We have reported (10) that high-dose corticosteroids inhibit PMN responses to activated complement and that this might explain apparent efficacy in shock. In that study, we also tested the ability of IBU to inhibit PMN aggregation in response to activated C; it did so, but only at doses several-fold those inhibiting platelet aggregation and reported to inhibit cyclooxygenase. Other research in progress in our laboratory and others (21) suggested that IBU might also limit experimental MI size and protect against shock, at very high but clinically achievable doses [associated with obtundation but no lasting ill effects in case reports to date (22)]. Finally, BH was under study as a limiter of MI size; we found it also to inhibit PMN aggregation in response to activated C. Having then three drugs which inhibited PMN aggregation, and which might well work by distinct mechanisms, we sought synergy among them. Were synergy to be found, it might lay the theoretical foundation for multiple-drug therapy in MI and shock,



MP and IBU in inhibiting PMN chemotaxis in response to C. AD_{50} was determined for each agent, an equipotent mixture was then tested as inhibitors of chemotaxis. Modest synergy was found, but not statistically significant.

allowing lower doses of several agents to be used, possibly in turn answering some of the objections to the use of steroids alone.

In fact, such synergy was easily demonstrable. The 50% attenuative concentration was determined for each drug (for a given stimulus and cell function), and equipotent mixtures were then prepared. Dose-response curves were then generated, using serial dilutions of the mixtures as test inhibitors of PMN aggregation in response to a fixed stimulus. In each case, 50% inhibition of aggregation was noted at drug concentrations well below those expected if mere additive effect is assumed; a similar synergy was also noted when aggregation was carried out in a serum-based suspending medium, or when FMLP was used as the aggregating stimulus (data not displayed). The combination of MP and IBU was further tested in other PMN responses. Each agent was able to inhibit superoxide production by FMLP-stimulated PMNs. Together, their effect is at least additive; weak synergy was observed, but did not reach statistical significance. Nonetheless, even a mere additive effect provides another potential benefit of the drug combination in limiting PMN-mediated tissue damage. Each agent also inhibited PMN chemotaxis to FMLP, simultaneous use resulting in similar modest synergy.

Encouraged by these *in vitro* findings, we sought drug synergy in experimental MI. In the model we were currently using—feline coronary artery ligation—MP proved of little or no benefit, while IBU reduced the size of resultant infarctions in a dose-dependent fashion. When MP was combined with an ineffective dose of IBU in a pilot study (data published in abstract form, *Clin. Res.* 29:334A, 1981), a 42% diminution in MI size resulted ($P \cong 0.06$), leading us to speculate that this synergy might one day prove clinically useful. This speculation is encouraged by an independent observation of apparent synergy between prednisolone and ibuprofen in experimental arthritis in rats (23). Nonetheless, such speculation must be made cautiously at this time. First, the apparent *in vivo* synergy has been tested only in a small group of animals in a single model¹; further animal studies will be necessary before the case for clinical trials becomes compelling. Further, even if synergy *in vivo* is confirmed, it may reflect totally separate effects of the two drugs on the intact organisms, rather than synergy between the drugs in a single cellular effect, as we postulate from our *in vitro* observation.

Synergy between MP and IBU suggests these agents act upon PMNs by distinct cellular mechanisms. We have recently reported that MP interferes (24) with the PMNs' receptor for chemotactic peptides; seeking the physiologic point at which IBU and MP differed, we also tested IBU in this system and were surprised to find that it, too, interfered.

¹These preliminary studies were carried out in the laboratory of the late Dr. Richard C. Lillehei, whose untimely death precluded their completion.

Synergistic Inhibition of PMN Function

Discordance between the synergistic inhibition of aggregation (more than threefold) and other PMN functions (less than twofold) is of particular interest. This may be due to a different mechanism of inhibition of aggregation than that of the mechanism whereby it (the PMN) is activated.

While the biological explanation is not yet elucidated, we are nonetheless optimistic that this may be clinically exploited.

REFERENCES

1. JACOB, H. S., P. R. CRADDOCK, D. E. HAMMERSCHMIDT, and R. G. WEAVER. 1980. Complement-induced granulocyte aggregation. *Eng. J. Med.* 302:789-794.
2. REDL, H., and G. SCHLAG. 1980. Modulation of the complement system in anaesthesia and intensive care. *Monatsschr. Anaesthesiol. und Intensivmedizin* 29:1-10.
3. HOSEA, S., E. BROWN, C. HAMMER, and R. G. WEAVER. 1980. Complement in a model of adult respiratory distress syndrome. *Am. J. Respir. Crit. Care Med.* 132:111-116.
4. HAMMERSCHMIDT, D. E., L. J. WEAVER, and H. S. JACOB. 1980. Association of complement and the respiratory distress syndrome: Pathophysiology. *Lancet* 1:947-949.
5. THAKUR, M. L., A. GOTTSCHALK, and B. H. HAMMERSCHMIDT. 1980. Complement and myocardial infarction with indium-111-labeled antibodies. *Am. J. Cardiol.* 45:100-104.
6. HILL, J. A., and P. A. WARD. 1971. The effect of complement on myocardial infarcts of rats. *J. Exp. Med.* 134:103-110.
7. LAUTER, C. B., M. R. EL KHATIB, J. A. HILL, and P. A. WARD. 1971. Complement and myocardial infarcts of rats. *J. Exp. Med.* 134:111-117.
8. BOYER, J. T., and R. A. O'ROURKE. 1977. The effect of complement on myocardial infarcts in rats. *Am. J. Pathol.* 83:740-750.
9. HARTMANN, J., J. ROBINSON, and R. G. WEAVER. 1977. Complement and myocardial infarcts in the rat. *Am. J. Cardiol.* 39:100-104.
10. HAMMERSCHMIDT, D. E., J. G. WHITE, P. R. WEAVER, and R. G. WEAVER. 1980. Complement and the myocardial infarct. *Am. J. Cardiol.* 45:105-109.
11. HAMMERSCHMIDT, D. E., J. G. WHITE, P. R. WEAVER, and R. G. WEAVER. 1980. Complement and the myocardial infarct. *Am. J. Cardiol.* 45:110-114.
12. HAMMERSCHMIDT, D. E., J. G. WHITE, P. R. WEAVER, and R. G. WEAVER. 1980. Complement and the myocardial infarct. *Am. J. Cardiol.* 45:115-119.
13. HAMMERSCHMIDT, D. E., J. G. WHITE, P. R. WEAVER, and R. G. WEAVER. 1980. Complement and the myocardial infarct. *Am. J. Cardiol.* 45:120-124.
14. HAMMERSCHMIDT, D. E., J. G. WHITE, P. R. WEAVER, and R. G. WEAVER. 1980. Complement and the myocardial infarct. *Am. J. Cardiol.* 45:125-129.
15. HAMMERSCHMIDT, D. E., J. G. WHITE, P. R. WEAVER, and R. G. WEAVER. 1980. Complement and the myocardial infarct. *Am. J. Cardiol.* 45:130-134.
16. HAMMERSCHMIDT, D. E., J. G. WHITE, P. R. WEAVER, and R. G. WEAVER. 1980. Complement and the myocardial infarct. *Am. J. Cardiol.* 45:135-139.
17. HAMMERSCHMIDT, D. E., J. G. WHITE, P. R. WEAVER, and R. G. WEAVER. 1980. Complement and the myocardial infarct. *Am. J. Cardiol.* 45:140-144.
18. HAMMERSCHMIDT, D. E., J. G. WHITE, P. R. WEAVER, and R. G. WEAVER. 1980. Complement and the myocardial infarct. *Am. J. Cardiol.* 45:145-149.
19. HAMMERSCHMIDT, D. E., J. G. WHITE, P. R. WEAVER, and R. G. WEAVER. 1980. Complement and the myocardial infarct. *Am. J. Cardiol.* 45:150-154.
20. HAMMERSCHMIDT, D. E., J. G. WHITE, P. R. WEAVER, and R. G. WEAVER. 1980. Complement and the myocardial infarct. *Am. J. Cardiol.* 45:155-159.
21. HAMMERSCHMIDT, D. E., J. G. WHITE, P. R. WEAVER, and R. G. WEAVER. 1980. Complement and the myocardial infarct. *Am. J. Cardiol.* 45:160-164.
22. HAMMERSCHMIDT, D. E., J. G. WHITE, P. R. WEAVER, and R. G. WEAVER. 1980. Complement and the myocardial infarct. *Am. J. Cardiol.* 45:165-169.
23. HAMMERSCHMIDT, D. E., J. G. WHITE, P. R. WEAVER, and R. G. WEAVER. 1980. Complement and the myocardial infarct. *Am. J. Cardiol.* 45:170-174.
24. HAMMERSCHMIDT, D. E., J. G. WHITE, P. R. WEAVER, and R. G. WEAVER. 1980. Complement and the myocardial infarct. *Am. J. Cardiol.* 45:175-179.
25. HAMMERSCHMIDT, D. E., J. G. WHITE, P. R. WEAVER, and R. G. WEAVER. 1980. Complement and the myocardial infarct. *Am. J. Cardiol.* 45:180-184.
26. HAMMERSCHMIDT, D. E., J. G. WHITE, P. R. WEAVER, and R. G. WEAVER. 1980. Complement and the myocardial infarct. *Am. J. Cardiol.* 45:185-189.
27. HAMMERSCHMIDT, D. E., J. G. WHITE, P. R. WEAVER, and R. G. WEAVER. 1980. Complement and the myocardial infarct. *Am. J. Cardiol.* 45:190-194.
28. HAMMERSCHMIDT, D. E., J. G. WHITE, P. R. WEAVER, and R. G. WEAVER. 1980. Complement and the myocardial infarct. *Am. J. Cardiol.* 45:195-199.
29. HAMMERSCHMIDT, D. E., J. G. WHITE, P. R. WEAVER, and R. G. WEAVER. 1980. Complement and the myocardial infarct. *Am. J. Cardiol.* 45:200-204.
30. HAMMERSCHMIDT, D. E., J. G. WHITE, P. R. WEAVER, and R. G. WEAVER. 1980. Complement and the myocardial infarct. *Am. J. Cardiol.* 45:205-209.
31. HAMMERSCHMIDT, D. E., J. G. WHITE, P. R. WEAVER, and R. G. WEAVER. 1980. Complement and the myocardial infarct. *Am. J. Cardiol.* 45:210-214.
32. HAMMERSCHMIDT, D. E., J. G. WHITE, P. R. WEAVER, and R. G. WEAVER. 1980. Complement and the myocardial infarct. *Am. J. Cardiol.* 45:215-219.
33. HAMMERSCHMIDT, D. E., J. G. WHITE, P. R. WEAVER, and R. G. WEAVER. 1980. Complement and the myocardial infarct. *Am. J. Cardiol.* 45:220-224.
34. HAMMERSCHMIDT, D. E., J. G. WHITE, P. R. WEAVER, and R. G. WEAVER. 1980. Complement and the myocardial infarct. *Am. J. Cardiol.* 45:225-229.
35. HAMMERSCHMIDT, D. E., J. G. WHITE, P. R. WEAVER, and R. G. WEAVER. 1980. Complement and the myocardial infarct. *Am. J. Cardiol.* 45:230-234.
36. HAMMERSCHMIDT, D. E., J. G. WHITE, P. R. WEAVER, and R. G. WEAVER. 1980. Complement and the myocardial infarct. *Am. J. Cardiol.* 45:235-239.
37. HAMMERSCHMIDT, D. E., J. G. WHITE, P. R. WEAVER, and R. G. WEAVER. 1980. Complement and the myocardial infarct. *Am. J. Cardiol.* 45:240-244.
38. HAMMERSCHMIDT, D. E., J. G. WHITE, P. R. WEAVER, and R. G. WEAVER. 1980. Complement and the myocardial infarct. *Am. J. Cardiol.* 45:245-249.
39. HAMMERSCHMIDT, D. E., J. G. WHITE, P. R. WEAVER, and R. G. WEAVER. 1980. Complement and the myocardial infarct. *Am. J. Cardiol.* 45:250-254.
40. HAMMERSCHMIDT, D. E., J. G. WHITE, P. R. WEAVER, and R. G. WEAVER. 1980. Complement and the myocardial infarct. *Am. J. Cardiol.* 45:255-259.
41. HAMMERSCHMIDT, D. E., J. G. WHITE, P. R. WEAVER, and R. G. WEAVER. 1980. Complement and the myocardial infarct. *Am. J. Cardiol.* 45:260-264.
42. HAMMERSCHMIDT, D. E., J. G. WHITE, P. R. WEAVER, and R. G. WEAVER. 1980. Complement and the myocardial infarct. *Am. J. Cardiol.* 45:265-269.
43. HAMMERSCHMIDT, D. E., J. G. WHITE, P. R. WEAVER, and R. G. WEAVER. 1980. Complement and the myocardial infarct. *Am. J. Cardiol.* 45:270-274.
44. HAMMERSCHMIDT, D. E., J. G. WHITE, P. R. WEAVER, and R. G. WEAVER. 1980. Complement and the myocardial infarct. *Am. J. Cardiol.* 45:275-279.
45. HAMMERSCHMIDT, D. E., J. G. WHITE, P. R. WEAVER, and R. G. WEAVER. 1980. Complement and the myocardial infarct. *Am. J. Cardiol.* 45:280-284.
46. HAMMERSCHMIDT, D. E., J. G. WHITE, P. R. WEAVER, and R. G. WEAVER. 1980. Complement and the myocardial infarct. *Am. J. Cardiol.* 45:285-289.
47. HAMMERSCHMIDT, D. E., J. G. WHITE, P. R. WEAVER, and R. G. WEAVER. 1980. Complement and the myocardial infarct. *Am. J. Cardiol.* 45:290-294.
48. HAMMERSCHMIDT, D. E., J. G. WHITE, P. R. WEAVER, and R. G. WEAVER. 1980. Complement and the myocardial infarct. *Am. J. Cardiol.* 45:295-299.
49. HAMMERSCHMIDT, D. E., J. G. WHITE, P. R. WEAVER, and R. G. WEAVER. 1980. Complement and the myocardial infarct. *Am. J. Cardiol.* 45:300-304.
50. HAMMERSCHMIDT, D. E., J. G. WHITE, P. R. WEAVER, and R. G. WEAVER. 1980. Complement and the myocardial infarct. *Am. J. Cardiol.* 45:305-309.
51. HAMMERSCHMIDT, D. E., J. G. WHITE, P. R. WEAVER, and R. G. WEAVER. 1980. Complement and the myocardial infarct. *Am. J. Cardiol.* 45:310-314.
52. HAMMERSCHMIDT, D. E., J. G. WHITE, P. R. WEAVER, and R. G. WEAVER. 1980. Complement and the myocardial infarct. *Am. J. Cardiol.* 45:315-319.
53. HAMMERSCHMIDT, D. E., J. G. WHITE, P. R. WEAVER, and R. G. WEAVER. 1980. Complement and the myocardial infarct. *Am. J. Cardiol.* 45:320-324.
54. HAMMERSCHMIDT, D. E., J. G. WHITE, P. R. WEAVER, and R. G. WEAVER. 1980. Complement and the myocardial infarct. *Am. J. Cardiol.* 45:325-329.
55. HAMMERSCHMIDT, D. E., J. G. WHITE, P. R. WEAVER, and R. G. WEAVER. 1980. Complement and the myocardial infarct. *Am. J. Cardiol.* 45:330-334.
56. HAMMERSCHMIDT, D. E., J. G. WHITE, P. R. WEAVER, and R. G. WEAVER. 1980. Complement and the myocardial infarct. *Am. J. Cardiol.* 45:335-339.
57. HAMMERSCHMIDT, D. E., J. G. WHITE, P. R. WEAVER, and R. G. WEAVER. 1980. Complement and the myocardial infarct. *Am. J. Cardiol.* 45:340-344.
58. HAMMERSCHMIDT, D. E., J. G. WHITE, P. R. WEAVER, and R. G. WEAVER. 1980. Complement and the myocardial infarct. *Am. J. Cardiol.* 45:345-349.
59. HAMMERSCHMIDT, D. E., J. G. WHITE, P. R. WEAVER, and R. G. WEAVER. 1980. Complement and the myocardial infarct. *Am. J. Cardiol.* 45:350-354.
60. HAMMERSCHMIDT, D. E., J. G. WHITE, P. R. WEAVER, and R. G. WEAVER. 1980. Complement and the myocardial infarct. *Am. J. Cardiol.* 45:355-359.
61. HAMMERSCHMIDT, D. E., J. G. WHITE, P. R. WEAVER, and R. G. WEAVER. 1980. Complement and the myocardial infarct. *Am. J. Cardiol.* 45:360-364.
62. HAMMERSCHMIDT, D. E., J. G. WHITE, P. R. WEAVER, and R. G. WEAVER. 1980. Complement and the myocardial infarct. *Am. J. Cardiol.* 45:365-369.
63. HAMMERSCHMIDT, D. E., J. G. WHITE, P. R. WEAVER, and R. G. WEAVER. 1980. Complement and the myocardial infarct. *Am. J. Cardiol.* 45:370-374.
64. HAMMERSCHMIDT, D. E., J. G. WHITE, P. R. WEAVER, and R. G. WEAVER. 1980. Complement and the myocardial infarct. *Am. J. Cardiol.* 45:375-379.
65. HAMMERSCHMIDT, D. E., J. G. WHITE, P. R. WEAVER, and R. G. WEAVER. 1980. Complement and the myocardial infarct. *Am. J. Cardiol.* 45:380-384.
66. HAMMERSCHMIDT, D. E., J. G. WHITE, P. R. WEAVER, and R. G. WEAVER. 1980. Complement and the myocardial infarct. *Am. J. Cardiol.* 45:385-389.
67. HAMMERSCHMIDT, D. E., J. G. WHITE, P. R. WEAVER, and R. G. WEAVER. 1980. Complement and the myocardial infarct. *Am. J. Cardiol.* 45:390-394.
68. HAMMERSCHMIDT, D. E., J. G. WHITE, P. R. WEAVER, and R. G. WEAVER. 1980. Complement and the myocardial infarct. *Am. J. Cardiol.* 45:395-399.
69. HAMMERSCHMIDT, D. E., J. G. WHITE, P. R. WEAVER, and R. G. WEAVER. 1980. Complement and the myocardial infarct. *Am. J. Cardiol.* 45:400-404.
70. HAMMERSCHMIDT, D. E., J. G. WHITE, P. R. WEAVER, and R. G. WEAVER. 1980. Complement and the myocardial infarct. *Am. J. Cardiol.* 45:405-409.
71. HAMMERSCHMIDT, D. E., J. G. WHITE, P. R. WEAVER, and R. G. WEAVER. 1980. Complement and the myocardial infarct. *Am. J. Cardiol.* 45:410-414.
72. HAMMERSCHMIDT, D. E., J. G. WHITE, P. R. WEAVER, and R. G. WEAVER. 1980. Complement and the myocardial infarct. *Am. J. Cardiol.* 45:415-419.
73. HAMMERSCHMIDT, D. E., J. G. WHITE, P. R. WEAVER, and R. G. WEAVER. 1980. Complement and the myocardial infarct. *Am. J. Cardiol.* 45:420-424.
74. HAMMERSCHMIDT, D. E., J. G. WHITE, P. R. WEAVER, and R. G. WEAVER. 1980. Complement and the myocardial infarct. *Am. J. Cardiol.* 45:425-429.
75. HAMMERSCHMIDT, D. E., J. G. WHITE, P. R. WEAVER, and R. G. WEAVER. 1980. Complement and the myocardial infarct. *Am. J. Cardiol.* 45:430-434.
76. HAMMERSCHMIDT, D. E., J. G. WHITE, P. R. WEAVER, and R. G. WEAVER. 1980. Complement and the myocardial infarct. *Am. J. Cardiol.* 45:435-439.
77. HAMMERSCHMIDT, D. E., J. G. WHITE, P. R. WEAVER, and R. G. WEAVER. 1980. Complement and the myocardial infarct. *Am. J. Cardiol.* 45:440-444.
78. HAMMERSCHMIDT, D. E., J. G. WHITE, P. R. WEAVER, and R. G. WEAVER. 1980. Complement and the myocardial infarct. *Am. J. Cardiol.* 45:445-449.
79. HAMMERSCHMIDT, D. E., J. G. WHITE, P. R. WEAVER, and R. G. WEAVER. 1980. Complement and the myocardial infarct. *Am. J. Cardiol.* 45:450-454.
80. HAMMERSCHMIDT, D. E., J. G. WHITE, P. R. WEAVER, and R. G. WEAVER. 1980. Complement and the myocardial infarct. *Am. J. Cardiol.* 45:455-459.
81. HAMMERSCHMIDT, D. E., J. G. WHITE, P. R. WEAVER, and R. G. WEAVER. 1980. Complement and the myocardial infarct. *Am. J. Cardiol.* 45:460-464.
82. HAMMERSCHMIDT, D. E., J. G. WHITE, P. R. WEAVER, and R. G. WEAVER. 1980. Complement and the myocardial infarct. *Am. J. Cardiol.* 45:465-469.
83. HAMMERSCHMIDT, D. E., J. G. WHITE, P. R. WEAVER, and R. G. WEAVER. 1980. Complement and the myocardial infarct. *Am. J. Cardiol.* 45:470-474.
84. HAMMERSCHMIDT, D. E., J. G. WHITE, P. R. WEAVER, and R. G. WEAVER. 1980. Complement and the myocardial infarct. *Am. J. Cardiol.* 45:475-479.
85. HAMMERSCHMIDT, D. E., J. G. WHITE, P. R. WEAVER, and R. G. WEAVER. 1980. Complement and the myocardial infarct. *Am. J. Cardiol.* 45:480-484.
86. HAMMERSCHMIDT, D. E., J. G. WHITE, P. R. WEAVER, and R. G. WEAVER. 1980. Complement and the myocardial infarct. *Am. J. Cardiol.* 45:485-489.
87. HAMMERSCHMIDT, D. E., J. G. WHITE, P. R. WEAVER, and R. G. WEAVER. 1980. Complement and the myocardial infarct. *Am. J. Cardiol.* 45:490-494.
88. HAMMERSCHMIDT, D. E., J. G. WHITE, P. R. WEAVER, and R. G. WEAVER. 1980. Complement and the myocardial infarct. *Am. J. Cardiol.* 45:495-499.
89. HAMMERSCHMIDT, D. E., J. G. WHITE, P. R. WEAVER, and R. G. WEAVER. 1980. Complement and the myocardial infarct. *Am. J. Cardiol.* 45:500-504.
90. HAMMERSCHMIDT, D. E., J. G. WHITE, P. R. WEAVER, and R. G. WEAVER. 1980. Complement and the myocardial infarct. *Am. J. Cardiol.* 45:505-509.
91. HAMMERSCHMIDT, D. E., J. G. WHITE, P. R. WEAVER, and R. G. WEAVER. 1980. Complement and the myocardial infarct. *Am. J. Cardiol.* 45:510-514.
92. HAMMERSCHMIDT, D. E., J. G. WHITE, P. R. WEAVER, and R. G. WEAVER. 1980. Complement and the myocardial infarct. *Am. J. Cardiol.* 45:515-519.
93. HAMMERSCHMIDT, D. E., J. G. WHITE, P. R. WEAVER, and R. G. WEAVER. 1980. Complement and the myocardial infarct. *Am. J. Cardiol.* 45:520-524.
94. HAMMERSCHMIDT, D. E., J. G. WHITE, P. R. WEAVER, and R. G. WEAVER. 1980. Complement and the myocardial infarct. *Am. J. Cardiol.* 45:525-529.
95. HAMMERSCHMIDT, D. E., J. G. WHITE, P. R. WEAVER, and R. G. WEAVER. 1980. Complement and the myocardial infarct. *Am. J. Cardiol.* 45:530-534.
96. HAMMERSCHMIDT, D. E., J. G. WHITE, P. R. WEAVER, and R. G. WEAVER. 1980. Complement and the myocardial infarct. *Am. J. Cardiol.* 45:535-539.
97. HAMMERSCHMIDT, D. E., J. G. WHITE, P. R. WEAVER, and R. G. WEAVER. 1980. Complement and the myocardial infarct. *Am. J. Cardiol.* 45:540-544.
98. HAMMERSCHMIDT, D. E., J. G. WHITE, P. R. WEAVER, and R. G. WEAVER. 1980. Complement and the myocardial infarct. *Am. J. Cardiol.* 45:545-549.
99. HAMMERSCHMIDT, D. E., J. G. WHITE, P. R. WEAVER, and R. G. WEAVER. 1980. Complement and the myocardial infarct. *Am. J. Cardiol.* 45:550-554.
100. HAMMERSCHMIDT, D. E., J. G. WHITE, P. R. WEAVER, and R. G. WEAVER. 1980. Complement and the myocardial infarct. *Am. J. Cardiol.* 45:555-559.
101. HAMMERSCHMIDT, D. E., J. G. WHITE, P. R. WEAVER, and R. G. WEAVER. 1980. Complement and the myocardial infarct. *Am. J. Cardiol.* 45:560-564.
102. HAMMERSCHMIDT, D. E., J. G. WHITE, P. R. WEAVER, and R. G. WEAVER. 1980. Complement and the myocardial infarct. *Am. J. Cardiol.* 45:565-569.
103. HAMMERSCHMIDT, D. E., J. G. WHITE, P. R. WEAVER, and R. G. WEAVER. 1980. Complement and the myocardial infarct. *Am. J. Cardiol.* 45:570-574.
104. HAMMERSCHMIDT, D. E., J. G. WHITE, P. R. WEAVER, and R. G. WEAVER. 1980. Complement and the myocardial infarct. *Am. J. Cardiol.* 45:575-579.
105. HAMMERSCHMIDT, D. E., J. G. WHITE, P. R. WEAVER, and R. G. WEAVER. 1980. Complement and the myocardial infarct. *Am. J. Cardiol.* 45:580-584.
106. HAMMERSCHMIDT, D. E., J. G. WHITE, P. R. WEAVER, and R. G. WEAVER. 1980. Complement and the myocardial infarct. *Am. J. Cardiol.* 45:585-589.
107. HAMMERSCHMIDT, D. E., J. G. WHITE, P. R. WEAVER, and R. G. WEAVER. 1980. Complement and the myocardial infarct. *Am. J. Cardiol.* 45:590-594.
108. HAMMERSCHMIDT, D. E., J. G. WHITE, P. R. WEAVER, and R. G. WEAVER. 1980. Complement and the myocardial infarct. *Am. J. Cardiol.* 45:595-599.
109. HAMMERSCHMIDT, D. E., J. G. WHITE, P. R. WEAVER, and R. G. WEAVER. 1980. Complement and the myocardial infarct. *Am. J. Cardiol.* 45:600-604.
110. HAMMERSCHMIDT, D. E., J. G. WHITE, P. R. WEAVER, and R. G. WEAVER. 1980. Complement and the myocardial infarct. *Am. J. Cardiol.* 45:605-609.
111. HAMMERSCHMIDT, D. E., J. G. WHITE, P. R. WEAVER, and R. G. WEAVER. 1980. Complement and the myocardial infarct. *Am. J. Cardiol.* 45:610-614.
112. HAMMERSCHMIDT, D. E., J. G. WHITE, P. R. WEAVER, and R. G. WEAVER. 1980. Complement and the myocardial infarct. *Am. J. Cardiol.* 45:615-619.
113. HAMMERSCHMIDT, D. E., J. G. WHITE, P. R. WEAVER, and R. G. WEAVER. 1980. Complement and the myocardial infarct. *Am. J. Cardiol.* 45:620-624.
114. HAMMERSCHMIDT, D. E., J. G. WHITE, P. R. WEAVER, and R. G. WEAVER. 1980. Complement and the myocardial infarct. *Am. J. Cardiol.* 45:625-629.
115. HAMMERSCHMIDT, D. E., J. G. WHITE, P. R. WEAVER, and R. G. WEAVER. 1980. Complement and the myocardial infarct. *Am. J. Cardiol.* 45:630-634.
116. HAMMERSCHMIDT, D. E., J. G. WHITE, P. R. WEAVER, and R. G. WEAVER. 1980. Complement and the myocardial infarct. *Am. J. Cardiol.* 45:635-639.
117. HAMMERSCHMIDT, D. E., J. G. WHITE, P. R. WEAVER, and R. G. WEAVER. 1980. Complement and the myocardial infarct. *Am. J. Cardiol.* 45:640-644.
118. HAMMERSCHMIDT, D. E., J. G. WHITE, P. R. WEAVER, and R. G. WEAVER. 1980. Complement and the myocardial infarct. *Am. J. Cardiol.* 45:645-649.
119. HAMMERSCHMIDT, D. E., J. G. WHITE, P. R. WEAVER, and R. G. WEAVER. 1980. Complement and the myocardial infarct. *Am. J. Cardiol.* 45:650-654.
120. HAMMERSCHMIDT, D. E., J. G. WHITE, P. R. WEAVER, and R. G. WEAVER. 1980. Complement and the myocardial infarct. *Am. J. Cardiol.* 45:655-659.
121. HAMMERSCHMIDT, D. E., J. G. WHITE, P. R. WEAVER, and R. G. WEAVER. 1980. Complement and the myocardial infarct. *Am. J. Cardiol.* 45:660-664.
122. HAMMERSCHMIDT, D. E., J. G. WHITE, P. R. WEAVER, and R. G. WEAVER. 1980. Complement and the myocardial infarct. *Am. J. Cardiol.* 45:665-669.
123. HAMMERSCHMIDT, D. E., J. G. WHITE, P. R. WEAVER, and R. G. WEAVER. 1980. Complement and the myocardial infarct. *Am. J. Cardiol.* 45:670-674.
124. HAMMERSCHMIDT, D. E., J. G. WHITE, P. R. WEAVER, and R. G. WEAVER. 1980. Complement and the myocardial infarct. *Am. J. Cardiol.*

al agents to be used, possibly in turn answer the use of steroids alone. As easily demonstrable. The 50% attenuative for each drug (for a given stimulus and cell mixtures were then prepared. Dose-response using serial dilutions of the mixtures as test in response to a fixed stimulus. In each aggregation was noted at drug concentrations well additive effect is assumed; a similar synergy was carried out in a serum-based suspension. FMLP was used as the aggregating stimulus. Combination of MP and IBU was further tested in agent was able to inhibit superoxide production. MNs. Together, their effect is at least additive; but did not reach statistical significance. None effect provides another potential benefit of limiting PMN-mediated tissue damage. Each chemotaxis to FMLP, simultaneous use result.

In vitro findings, we sought drug synergy in model we were currently using—feline coronary of little or no benefit, while IBU reduced the in a dose-dependent fashion. When MP was a dose of IBU in a pilot study (data published 29:334A, 1981), a 42% diminution in MI size us to speculate that this synergy might one. This speculation is encouraged by an independent synergy between prednisolone and ibuprofen in us (23). Nonetheless, such speculation must be. First, the apparent in vivo synergy has been of animals in a single model⁵; further animal before the case for clinical trials becomes confirmed, it may reflect totally drugs on the intact organisms, rather than synergy in vivo is confirmed, it may reflect totally drugs on the intact organisms, rather than synergy in a single cellular effect, as we postulate from our

and IBU suggests these agents act upon PMNs. We have recently reported that MP is receptor for chemotactic peptides; seeking the IBU and MP differed, we also tested IBU in this to find that it, too, interfered.

carried out in the laboratory of the late Dr. Richard C. Lillehei, their completion.

Discordance between the synergy observed in inhibition of PMN aggregation (more than threefold) and that observed in inhibition of two other PMN functions (less than twofold and less than statistically convincing) is of particular interest. This may well indicate that the cellular mechanism of inhibition of aggregation by one or both drugs is different from the mechanism whereby it (they) inhibit(s) chemotaxis and superoxide production.

While the biological explanation of the observed synergy remains to be elucidated, we are nonetheless excited by the prospect that it might ultimately be clinically exploited.

REFERENCES

1. JACOB, H. S., P. R. CRADDOCK, D. E. HAMMERSCHMIDT, and C. F. MOLDOW. 1980. Complement-induced granulocyte aggregation: An unsuspected mechanism of disease. *N. Eng. J. Med.* 302:789-794.
2. REDL, H., and G. SCHLAG. 1980. Morphologische Untersuchungen der Lunge im Schock. In *Anästhesiologie und Intensivmedizin*, Band 25, Kreislaufsschock. Springer-Verlag, Berlin.
3. HOSEA, S., E. BROWN, C. HAMMER, and M. FRANK. 1980. Role of complement activation in a model of adult respiratory distress syndrome. *J. Clin. Invest.* 66:375-382.
4. HAMMERSCHMIDT, D. E., L. J. WEAVER, L. D. HUDSON, P. R. CRADDOCK, and H. S. JACOB. 1980. Association of complement activation and elevated plasma-C5a with adult respiratory distress syndrome: Pathophysiologic relevance and possible prognostic value. *Lancet* 1:947-949.
5. THAKUR, M. L., A. GOTTSCHALK, and B. L. ZARET. 1979. Imaging experimental myocardial infarction with indium-111-labeled autologous leukocytes: Effects of infarct age and residual regional myocardial blood flow. *Circulation* 60:297-305.
6. HILL, J. A., and P. A. WARD. 1971. The phlogistic role of C3 leukotactic fragments in myocardial infarcts of rats. *J. Exp. Med.* 133:885-900.
7. LAUTER, C. B., M. R. EL KHATIB, J. A. RISING, and E. ROBIN. 1973. The nitroblue-tetrazolium test in acute myocardial infarction. *Ann. Intern. Med.* 79:59-62.
8. BOVER, J. T., and R. A. O'ROURKE. 1974. Consumption of classical complement by heart subcellular membranes in vitro and in patients after acute myocardial infarction. *J. Clin. Invest.* 56:740-750.
9. HARTMANN, J., J. ROBINSON, and R. GUNNAR. 1977. Chemotactic activity in the coronary sinus after experimental myocardial infarction: Effects of pharmacologic interventions on ischemic injury. *Am. J. Cardiol.* 40:550-555.
10. HAMMERSCHMIDT, D. E., J. G. WHITE, P. R. CRADDOCK, and H. S. JACOB. 1979. Corticosteroids inhibit complement-mediated granulocyte aggregation: A possible mechanism for their efficacy in shock states. *J. Clin. Invest.* 63:798-803.
11. WHITE, G. L., L. T. ARCHER, B. K. BELLER, and L. B. HINSHAW. 1978. Increased survival with methylprednisolone treatment in canine endotoxin shock. *J. Surg. Res.* 25:357-364.
12. SCHUMER, W. 1976. Steroids in the treatment of clinical septic shock. *Ann. Surg.* 184:333-341.
13. SLADEN, A. 1976. Methylprednisolone. Pharmacologic doses in shock lung syndrome. *J. Thorac. Cardiovasc. Surg.* 21:800-805.

14. JOYCE, L. D., J. M. SMITH, H. G. MAUER, and R. C. LILLEHEI. 1979. Reduction of experimental myocardial infarct size by combined treatment with methylprednisolone sodium succinate and betahistine hydrochloride. *Adv. Shock Res.* 1:235-249.
15. CRADDOCK, P. R., D. E. HAMMERSCHMIDT, J. G. WHITE, A. P. DALMASSO, and H. S. JACOB. 1977. Complement (C5a)-induced granulocyte aggregation in vitro: A possible mechanism of complement-mediated leukostasis and leukopenia. *J. Clin. Invest.* 60:261-264.
16. BØYUM, A. 1968. Isolation of mononuclear cells and granulocytes from blood. Isolation of mononuclear cells by one centrifugation and of granulocytes by combining centrifugation and sedimentation at 1 g. *Scand. J. Lab. Invest.* 21(Suppl. 97):77-89.
17. ZIMOND, S. H., and J. G. HIRSCH. 1973. Leukocyte locomotion and chemotaxis. New methods for evaluation and demonstration of cell-derived chemotactic factor. *J. Exp. Med.* 137:387.
18. BOYDEN, S. 1962. The chemotactic effect of mixtures of antibody and antigen on polymorphonuclear leukocytes. *J. Exp. Med.* 115:453.
19. WEENING, R. S., R. WEVER, and D. ROOS. 1975. Quantitative aspects of the production of superoxide radicals by phagocytizing human granulocytes. *J. Lab. Clin. Med.* 85:245-252.
20. CRADDOCK, P. R., D. E. HAMMERSCHMIDT, C. F. MOLDOW, O. YAMADA, and H. S. JACOB. 1979. Granulocyte aggregation as a manifestation of membrane interactions with complement: Possible role in leukocyte margination, microvascular occlusion and endothelial damage. *Sem. Haematol.* 16:140-147.
21. DARSE, J. R., R. A. KLONER, and E. BRAUNWALD. 1981. Demonstration of lateral and epicardial border zone salvage by flurbiprofen using an in vivo method for assessing myocardium at risk. *Circulation* 63:29-35.
22. HUNT, D. P., and R. J. LEIGH. 1980. Overdose of ibuprofen causing unconsciousness and hypotension. *Brit. Med. J.* 281:1458.
23. Boots Pharmaceutical Co. Brufen 400: Pharmakologie und Klinische Erfahrung. Braum-pharm Ges.m.b.H., Vienna, 1981. 34-35.
24. SKUBITZ, K. M., P. R. CRADDOCK, D. E. HAMMERSCHMIDT, and J. T. AUGUST. 1981. Corticosteroids block binding of chemotactic peptide to its receptors on granulocytes and cause disaggregation of granulocyte aggregates in vitro. *J. Clin. Invest.* 68:13-20.

NONSPECIFIC PRO ACTIVITIES IN

J. VARANI, D. WA

Depart
University of M
Ann Arbor

Abstract—Extracts were prepared after glycogen injection and assayed on various substrates. The substrates included hemoglobin, bovine serum albumin, a portion of basement membrane, bovine neck with elastase specificity. A high level of elastase was used as the substrate. The serum fraction were also readily hydrolyzed native elastin and synthetic elastin. Although the leukocyte extract demonstrated potentiated the elastolytic activity, it was mixed with a commercial h

INTR

Human polymorphonuclear leukocytes contain several neutral proteases: elastase, chymotrypsin, and cathepsin G. These enzymes have been identified in the neutrophil. It is apparent that considerable species differences exist between these proteases. These differences may be critical to their role in various pathological processes. The protease activity obtained from rat neutrophils is a high level of neutral protease activity on synthetic substrates. However, when native substrates are used as substrates, very little activity is observed.

¹This study was supported in part by NIH grant

0360-3

Strategic Design and Three-Dimensional Analysis of Antiviral Drug Combinations

MARK N. PRICHARD,^{1,2} LYNN E. PRICHARD,¹ AND CHARLES SHIPMAN, JR.^{1,2*}

Department of Biologic and Materials Sciences, School of Dentistry,¹ and Department of Microbiology and Immunology, Medical School,² The University of Michigan, Ann Arbor, Michigan 48109

Received 17 August 1992/Accepted 23 December 1992

The development of new drugs effective against human viral diseases has proven to be both difficult and time-consuming. Indeed, there are but 10 drugs licensed for such applications in the United States today. An attractive solution to this problem may be to optimize the efficacy and selectivity of existing antiviral drugs by combining them with agents that strategically block carefully selected metabolic pathways. This approach was used in the rational design of a three-drug combination to increase the apparent potency of acyclovir against herpes simplex virus. Recent advances in analytical techniques have made the evaluation of this complex drug strategy both possible and practical. A modified version of a previously described analytical method was used to identify optimal drug concentrations and to quantitate statistically significant synergy. Concentrations of 0.25 μ M 5-fluorodeoxyuridine, 3.6 μ M 2-acetylpyridine thiosemicarbazone, and 0.3 μ M acyclovir were determined to be optimal in terms of antiviral activity. The volume of synergy produced was nearly 2,000 μ M³% at a 95% level of confidence (corresponding to a 186-fold decrease in the apparent 50% inhibitory concentration of acyclovir with the addition of 0.25 μ M 5-fluorodeoxyuridine and 3.6 μ M 2-acetylpyridine thiosemicarbazone). We anticipate that this strategic approach and the supporting three-dimensional analytical method will prove valuable in designing and understanding multidrug therapies.

Antiviral drugs derive their specificity through the preferential inhibition of virus-encoded enzymes present in infected cells (13). The usefulness of these agents is limited by the degree to which they concomitantly affect uninfected cells, producing untoward toxicity. Additionally, the emergence of drug-resistant mutants is a significant problem in single-drug therapy (3). Treatment with combinations of antiviral agents is generally thought to minimize drug resistance (1, 6, 14) but may or may not offer increased selectivity and efficacy. Traditionally, drug combinations have been chosen on the basis of the potency and/or efficacy of the individual agents. The component drugs often have been active against the same target, and detailed evaluations of drug interactions often have been lacking. Combinations of drugs that inhibit different targets, however, often offer surprising potency, even though one or more of the constituent compounds may be weakly active. We now describe the rational design of an antiviral combination of three drugs that strategically inhibits the replication of herpes simplex virus (HSV) by blocking carefully chosen metabolic pathways. Evaluation of this strategy and the determination of optimal drug concentrations were made possible by recent advances in existing three-dimensional analytical procedures (21, 22).

The rational design of a combination of drugs relies on a thorough understanding of drug metabolism in both virus-infected and uninfected cells. The antiherpesvirus drug acyclovir (ACV; Zovirax) is a potent inhibitor of HSV replication and is an apparent inactivator of the HSV DNA polymerase (5). This drug is initially phosphorylated by the HSV pyrimidine deoxyribonucleoside kinase and is further phosphorylated by cellular kinases to ACV triphosphate (ACVTP) (Fig. 1), the active form of the drug (25).

In HSV-infected cells, ACV limits its own effectiveness on

at least two levels. Treatment with ACV results in an increase in both thymidylate synthase activity and the size of intracellular thymidine pools (11). Thymidine competes with ACV for phosphorylation by the HSV pyrimidine deoxyribonucleoside kinase (TK) (9). This alteration of nucleoside metabolism adversely affects the efficiency with which ACV can inhibit the HSV DNA polymerase, as less ACV is phosphorylated (Fig. 1). ACV also significantly increases the size of deoxyribonucleoside triphosphate (dNTP) pools, including dGTP (7, 11). Thus, the effectiveness of ACV is further limited, as dGTP competes with ACVTP for binding by the HSV DNA polymerase (Fig. 1).

ACV increases the sizes of both thymidine and dGTP pools. Thus, for optimization of the antiviral activity of ACV, it would be desirable to decrease the sizes of both the pyrimidine deoxyribonucleoside pools and the dGTP pools in infected cells. This strategy would remove molecules that compete with ACV for both activation and incorporation, theoretically resulting in increased phosphorylation of ACV to its active form and maximizing the incorporation of ACVTP by the HSV DNA polymerase. The predicted result of this increased activation and incorporation would be synergistic inhibition of viral replication by drugs that decrease the size of either thymidine (dThd) or dGTP pools. This strategy also predicts that even more synergy would be produced by a combination of inhibitors that simultaneously decrease the sizes of both dThd and dGTP pools.

Early experiments by Cohen demonstrated that HSV stimulated the synthesis of DNA in thymidine-blocked cells (4). Cohen and coworkers later demonstrated that this effect was due primarily to the expression of a viral ribonucleoside diphosphate reductase (ribonucleotide reductase; RR) (18). We have shown that HSV type 1 (HSV-1) requires this increased synthesis of deoxynucleotides to replicate efficiently (22a). Inhibitors of the RR have been shown to potentiate the antiviral effects of ACV (21, 29-31). These inhibitors have been shown to decrease the size of intracellular

* Corresponding author. Electronic mail address: usergb5h@umich.edu.

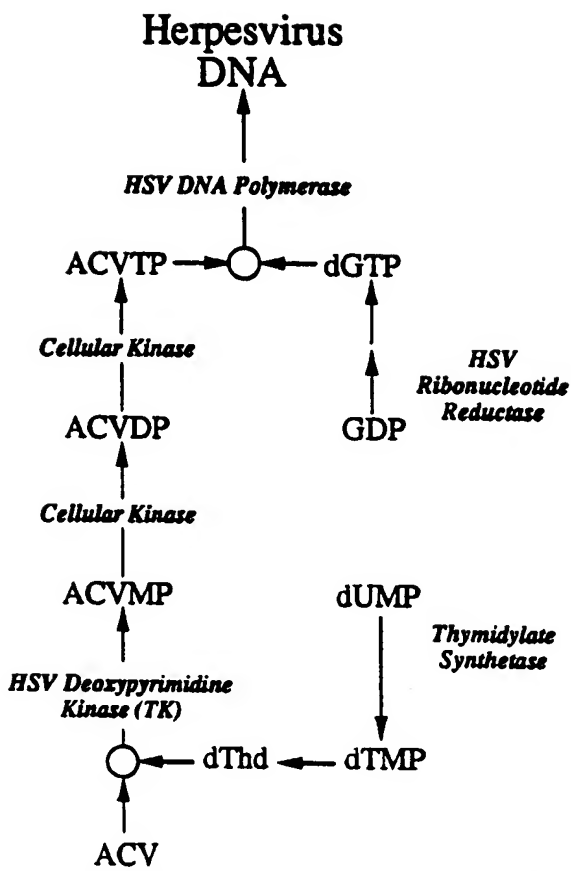


FIG. 1. Anabolism of ACV to ACVTP by viral and cellular enzymes. Competition is represented by circles at the intersections of the competing substrates. Thymidine competes with ACV for phosphorylation, and dGTP competes with ACVTP for incorporation by the DNA polymerase.

lular pools of dGTP, which competes with ACVTP for binding by the HSV DNA polymerase (29).

One such inhibitor, 2-acetylpyridine thiosemicarbazone (APTS), is a selective inhibitor of the HSV RR (32, 33) and is also a potent inhibitor of HSV both *in vitro* and *in vivo* (27, 28). This drug has been shown to decrease the size of purine dNTP pools in infected cells and should be effective in decreasing the size of pools of dGTP, which competes with ACVTP for incorporation by the HSV DNA polymerase (22a). To limit the size of intracellular pools of pyrimidine deoxyribonucleosides, 5-fluorodeoxyuridine (5-FdUrd) was used to inhibit thymidylate synthase, the key enzyme responsible for the conversion of dUMP to dTMP. This inhibitor has been shown to decrease the sizes of intracellular pools of thymidine and cytidine at nontoxic concentrations (10). Previous experiments in our laboratory showed that this drug also potentiates the antiviral effects of ACV (20). Thus, we predicted that the three-drug combination of ACV, APTS, and 5-FdUrd should act in a synergistic manner to inhibit the replication of HSV. Furthermore, the three-drug combination should produce more synergy than any of the three possible two-drug combinations.

MATERIALS AND METHODS

Chemicals. APTS was prepared by Derse and Schroeder Associates, Ltd., Madison, Wis. ACV was provided through the courtesy of Sandra Lehrman of the Burroughs Wellcome Co., Research Triangle Park, N.C. 5-FdUrd was obtained from Sigma Chemical Co., St. Louis, Mo., and KH_2PO_4 was obtained from ICN Biomedicals Inc., Costa Mesa, Calif.

Cell line and virus. BS-C-1 cells, an established line of African green monkey kidney cells, were grown in monolayers in minimal essential medium with Earle salts and supplemented with 10% calf serum as described previously (23). Cells were routinely passaged with 0.05% trypsin-0.02% EDTA in *N*-2-hydroxyethylpiperazine-*N'*-2-ethanesulfonic acid (HEPES)-buffered saline (HBS) (26). The KOS strain of HSV-1 was obtained from Sandra Weller of the University of Connecticut, Farmington. The virus was grown and its titers were determined as described previously (23).

dNTP pool size determinations. Exponentially growing BS-C-1 cells were passaged 12 h prior to infection and/or drug treatment. The cell sheets, containing 3×10^6 to 6×10^6 exponentially growing BS-C-1 cells, were infected at a multiplicity of infection of 10 with HSV-1 (strain KOS). The medium was replaced, and drugs were added after a 1-h adsorption period. At 6 h postinfection, the cells were washed twice with HBS at 37°C and trypsinized as described above. The extraction protocol is based on the procedure described by Garret and Santi (8). In brief, the cells were pelleted, and 75 μl of ice-cold 0.6 M trichloroacetic acid and an internal standard, [^3H]dThd, were added to the cell pellet. The cells were extracted for a minimum of 15 min on ice, and the solution was filtered through a 0.22- μm -pore-size SPIN-X centrifuge filter unit (Costar, Cambridge, Mass.) at 4°C. The trichloroacetic acid was extracted from the solution by adding 125 μl of Freon-0.5 M triethylamine to the filtrate and vortexing the mixture. The upper aqueous phase containing the dNTPs was divided into aliquots and frozen at -77°C.

Ribonucleotides were cleaved via a periodate oxidation reaction (24). In brief, to each sample, 8 μl of 0.25 M sodium metaperiodate (Fisher Scientific, Fair Lawn, N.J.) was added, and the mixture was vortexed. Following 4 min of incubation at 20°C, 10 μl of 4 M methylamine phosphate (pH 7.5) was added, and the mixture was vortexed and incubated for 30 min at 37°C. The reaction was stopped by the addition of 10 μl each of 1 M HCl and 1 M glucose, and the samples were frozen at -77°C until separated by high-pressure liquid chromatography (HPLC).

The dNTPs were separated by use of an HPLC from Spectraphysics Inc., San Jose, Calif., with an Ultrasil AX column (4.6 mm by 25 cm) and an Ultrasil AX precolumn (3.2 mm by 4.5 cm) (Beckman Instruments, Inc., Fullerton, Calif.). The column was equilibrated with 0.3 M KH_2PO_4 at pH 3.75, and samples were separated by 5 min of isocratic elution at 2 ml/min with 0.3 M KH_2PO_4 at pH 3.75 and 25 min of elution with a linear gradient of 0.3 to 0.75 KH_2PO_4 at pH 3.75.

Antiviral EIA. The antiviral enzyme immunoassay (EIA) used is similar to the one described previously (21). In brief, an EIA was performed directly in the wells of 96-well plates containing the infected-cell sheets. The wells were first blocked with 200 μl of HBS containing 0.05% Tween 20 and supplemented with 10% horse serum for 1 h at 37°C. The plates were then shaken out, and 50 μl of a 1:400 dilution of horseradish peroxidase-conjugated rabbit anti-HSV-1 antibodies (Dako Corp., Santa Barbara, Calif.) in HBS supple-

mented with 10% horse serum was added to each well. Following 1 h of incubation, the plates were washed four times with HBS-0.05% Tween 20. The plates were subsequently developed with 150 μ l of a substrate solution consisting of 35 mM citric acid, 67 mM Na_2HPO_4 (pH 5.0), 0.005% (vol/vol) 30% H_2O_2 , and 1 mg of tetramethylbenzidine (Sigma) per ml. The reaction was stopped with 50 μ l of 2 N H_2SO_4 and read at 450 and 570 nm in a Microplate Bio-Kinetics Reader (model EL312; Biotek Instruments, Inc., Winooski, Vt.).

Synergy analysis. For characterization of the drug-drug interactions present, a three-dimensional analytical method was used (21, 22). The analysis was performed with a modified version of the shareware developed in our laboratory (MacSynergy II). In brief, theoretical additive interactions were calculated from the dose-response curves of the individual drugs. The calculated additive surface, which represents the predicted additive interactions, was then subtracted from the experimental surface to reveal regions of greater-than-expected interactions (synergy). The resulting surface would appear as a horizontal plane at 0% inhibition above the calculated additive surface if the interactions were merely additive. Any peaks above this plane would be indicative of synergy. Similarly, any depressions below the plane would indicate antagonism.

The 95% confidence intervals for the experimental dose-response surface were used to evaluate the data statistically. For each point in the plot, if the lower 95% confidence limit of the experimental data was greater than the calculated additive surface, then the synergy was considered significant. Conversely, if the upper 95% confidence limit of the experimental data was less than the calculated additive surface, then the antagonism was considered significant. All plots and values presented here are at the level of 95% confidence.

Since three drugs were used in this experiment, the existing software was modified to accommodate the expanded experimental design. Furthermore, additive drug interactions were calculated with the following equation:

$$I = 1 - \prod_{n=1}^{\infty} (1 - i_n) \quad (1)$$

where I is the predicted fractional inhibition produced by the combination and i is the fractional inhibition produced by n drugs used individually. Equation 1 is the general form of equation 2, which is the dissimilar-site additivity equation described previously (21, 22):

$$Z = X + Y(1 - X) \quad (2)$$

where Z represents the total inhibition produced by the combination of drugs X and Y and X and Y represent the inhibition produced by drugs X and Y alone, respectively. Both equations 1 and 2 correspond to the independent-effects equations used by some investigators (16, 17, 34).

The results presented here were based on data from checkerboard dilution matrices, which included the drugs used individually (21, 22). This experimental design was used to identify regions at which significant drug interactions occurred (19). Drug concentrations were initially chosen on the basis of the efficacy and cytotoxicity of each drug alone. A range of concentrations that produced no inhibition of replication at the lower concentrations and maximal inhibition at the highest concentration were chosen. This range was subsequently modified to encompass the regions of

significant synergy. Although replicates are not necessary for an analysis of this type, at least three replicates are required to obtain reasonable 95% confidence intervals. This experimental design and analytical method compare favorably with other designs and methods used to analyze three-drug combinations (12-14).

Cytotoxicity determinations. Simultaneous cytotoxicity control experiments were done as described above, except that the plates were not infected with virus. The evaluation of cytotoxicity was based on a procedure described previously (19). In brief, cell growth was quantitated by staining the cell sheets with crystal violet and measuring the bound dye by elution with 1% (vol/vol) HCl in ethanol. The optical density was determined at 570 and 405 nm in a Microplate Bio-Kinetics Reader.

RESULTS

To test the strategically designed drug combination, we measured the antiviral effect of the three-drug combination and experimentally determined the optimal concentrations of each drug. Data were generated by use of an EIA with horseradish peroxidase-conjugated polyclonal antibodies to HSV-1. With this technique, the replication of HSV-1 (strain KOS) was measured in triplicate at 300 different combinations of concentrations of the three drugs. The data were analyzed as described above and plotted as a vertical series of contour plots (Fig. 2).

Synergistic antiviral interactions between APTS and ACV are shown in the bottom tier of Fig. 2. Dark red regions indicate combinations of concentrations at which additive interactions were observed. Increasingly synergistic interactions are displayed by red, orange, and then yellow regions. The volume of synergy produced was 112 $\mu\text{M}^2\%$ (volumes are expressed as micromolar concentration times micromolar concentration times percentage, or $\mu\text{M}^2\%$) and attained a maximum at concentrations of 3.6 μM APTS and 0.33 μM ACV. Synergy was also seen with combinations of ACV and 5-FdUrd (right front edges of Fig. 2 at 0 μM APTS). The synergy observed with ACV and 5-FdUrd had a volume of 206 $\mu\text{M}^2\%$ and reached a maximum at concentrations of 1.0 μM ACV and 0.5 μM 5-FdUrd. No synergy was observed with APTS and 5-FdUrd.

The addition of 0.25 μM 5-FdUrd dramatically increased the volume of synergy to 602 $\mu\text{M}^2\%$ (Fig. 2, second tier), more than fivefold higher than that observed with the combination of ACV and APTS alone (Fig. 2, bottom tier). As the concentrations of 5-FdUrd were increased, synergy among the three drugs decreased because of the antiviral activity of 5-FdUrd. The optimal combination of ACV, APTS, and 5-FdUrd was at a molar ratio of approximately 2:14:1. The volume of synergy produced by the three-drug combination was 1,988 $\mu\text{M}^3\%$. This value corresponded to a 186-fold decrease in the apparent 50% inhibitory concentration of ACV with the addition of 3.6 μM APTS and 0.25 μM 5-FdUrd. Calculations revealed that the volume of synergy produced by the three-drug combination was larger than expected on the basis of the synergy produced by the synergistic two-drug combinations (APTS and ACV; 5-FdUrd and ACV). It is clear that the three-drug combination inhibited the replication of HSV-1 better than any drug by itself or any two-drug combination.

We have shown that the three-drug combination is highly efficacious in inhibiting the replication of HSV-1. It is equally important, however, to evaluate any combination of drugs for potential synergistic cytotoxicity. The cytotoxicity

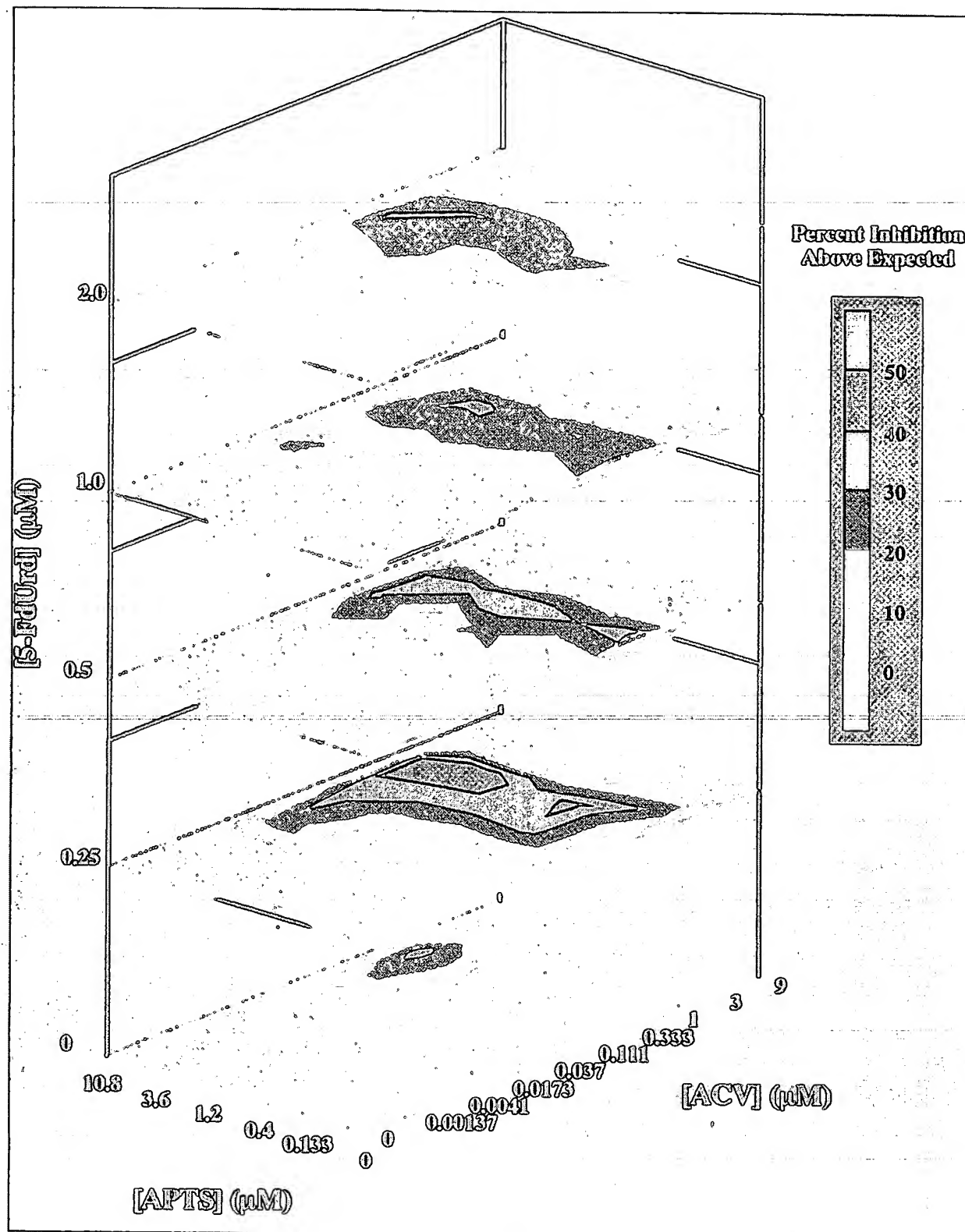


FIG. 2. Synergistic inhibition of the replication of HSV-1 by combinations of ACV, APTS, and 5-FdUrd. Calculated additive antiviral interactions were subtracted from experimentally determined values to reveal regions and corresponding concentrations at which synergistic antiviral interactions occurred. Peaks of statistically significant (confidence level, 95%) synergy are shown in shades of red to yellow, with yellow indicating the strongest synergy. Concentrations of each drug are indicated on the axes. Values used to describe the percentage of inhibition above that expected were derived from averaged triplicate data. The experiment was repeated four times with essentially identical results.

TABLE 1. Sizes of dNTP pools in infected cells treated with the three-drug combination of ACV (3 μ M), APTS (10 μ M), and 5-FdUrd (2 μ M)

Drug(s)	pmol of the following/10 ⁶ cells ^a :					ACVTP/dGTP ratio
	dCTP	dTTP	dATP	dGTP	ACVTP	
None (uninfected)	69 \pm 9.2	77 \pm 6	69 \pm 2	25 \pm 4		
None (HSV-1 KOS infected)	420 \pm 31	2,180 \pm 204	146 \pm 6	167 \pm 18		
ACV	554 \pm 34	2,480 \pm 156	261 \pm 21	272 \pm 29	3.0 \pm 0.02	0.011
APTS	134 \pm 14	2,290 \pm 149	9 \pm 5	22 \pm 2		
5-FdUrd	342 \pm 31	1,990 \pm 164	144 \pm 12	184 \pm 22		
ACV-APTS	137 \pm 13	2,570 \pm 176	17 \pm 2	35 \pm 3	7.5 \pm 0.3	0.22
ACV-APTS-5-FdUrd	130 \pm 15	2,270 \pm 301	11 \pm 2	23 \pm 2	8.3 \pm 1.6	0.36

^a Each value is the arithmetic mean from three determinations \pm the standard error of the mean.

of the three-drug combination was evaluated in BS-C-1 cells by a cytotoxicity assay described previously (19) and analyzed by the three-dimensional dose-response method described above. No significant synergistic cytotoxicity or antagonism of cytotoxicity was observed in any of the regions of Fig. 2 (data not shown). Thus, we concluded that the effects seen in Fig. 2 were not due to synergistic cytotoxicity and that the toxicity of the three-drug combination was additive.

To confirm the mechanism(s) of the observed synergistic effect of the three-drug combination, we measured dNTP pools in HSV-1-infected cells treated with the individual drugs and the three-drug combination at the optimal ratio (Table 1). The results confirm that ACV increased the sizes of all of the dNTP pools, an observation consistent with results published previously (7). Infected cells treated with APTS had greatly reduced purine deoxyribonucleoside pool sizes as a direct result of the inhibition of the RR. This effect was also seen for infected cells treated with the two-drug combination of ACV and APTS. Here, APTS prevented the increase in the size of dGTP pools, thus increasing the ratio of ACVTP to its competitor dGTP by 20-fold. APTS did not prevent the increase in the size of pools of dTTP or dCTP; this phenomenon, although not understood, has been reported for other inhibitors of the RR, such as hydroxyurea (2). As predicted, 5-FdUrd decreased the size of dTTP pools in infected cells. The three-drug combination of ACV, APTS, and 5-FdUrd resulted in decreased dTTP and dGTP pool sizes and in a 33-fold increase in the ratio of ACVTP to dGTP.

DISCUSSION

The drug combination presented here was rationally designed to optimize the efficacy of the antiviral drug ACV. Previous studies demonstrated that decreasing dGTP pools with RR inhibitors increases the apparent potency of ACV by increasing the ACVTP/dGTP ratio (29-31). Inhibitors of RR, however, are unable to inhibit the increase in the size of pools of pyrimidine deoxyribonucleosides (2), which reduces the phosphorylation of ACV (9). Our strategy used (i) an inhibitor of the cellular thymidylate synthase to decrease the size of the intracellular dThd pools and (ii) an inhibitor of the HSV RR to decrease the size of the intracellular dGTP pools. As predicted, the combination of APTS, 5-FdUrd, and ACV synergistically inhibited the replication of HSV and was a much more potent combination than ACV and an RR inhibitor alone.

The measurement of intracellular dNTP pool sizes confirmed the proposed mechanism of synergy. In infected cells,

5-FdUrd decreased the sizes of dTTP and dCTP pools but did not eliminate them. Previous experiments by Nutter and coworkers (15) suggested that the large increase in the size of dTTP pools seen in infected cells was due mainly to thymidine salvaged from degraded cellular DNA. Furthermore, these pools appeared to be compartmentalized, as salvaged thymidine not efficiently used for incorporation into viral DNA (15, 22a). The inability of 5-FdUrd to eliminate dTTP pools in infected cells would appear to confirm that some salvage does occur. We also showed that the inhibition of thymidylate synthase correlated well with the potentiation of ACV (20). Thus, the small decrease in the size of dTTP pools in infected cells treated with the three-drug combination may reflect the suppression of the small pools of thymidine that are used in the synthesis of viral DNA.

The data presented in this communication describe the rational design and evaluation of a combination of drugs that optimized the efficacy and selectivity of ACV. A novel analytical procedure demonstrated that the three drugs acted cooperatively to inhibit the replication of HSV-1 and identified the optimal concentration of each drug. The apparent potency of ACV could be increased by more than 186-fold without producing synergistic cytotoxicity. We do not endorse this particular drug combination for clinical use because of the toxicity known to be associated with 5-FdUrd. Nevertheless, we have clearly shown that it is possible to rationally design and evaluate efficacious and selective combinations of drugs *in vitro*. One would hope that this approach would be helpful in predicting the usefulness of combinations of drugs in the treatment of human disease.

ACKNOWLEDGMENTS

We thank Kimberly R. Aseltine for excellent technical assistance and Donald Nelson of Burroughs Wellcome Co. for scientific advice and suggestions in the determination of dNTP pools.

This work was supported by USPHS grant DE08510 from the National Institute of Dental Research and USPHS contract AI05077 from the National Institute of Allergy and Infectious Diseases.

REFERENCES

1. Ban, J., and G. Weber. 1992. Synergistic action of tiazofurin and difluorodeoxycytidine on differentiation and cytotoxicity. *Biochem. Biophys. Res. Commun.* 184:551-559.
2. Bianchi, V., E. Pontis, and P. Reichard. 1986. Changes of deoxyribonucleoside triphosphate pools induced by hydroxyurea and their relation to DNA synthesis. *Proc. Natl. Acad. Sci. USA* 83:16037-16042.
3. Coen, D. M. 1991. The implications of resistance to antiviral agents for herpesvirus drug targets and drug therapy. *Antiviral Res.* 15:287-300.
4. Cohen, G. H. 1972. Ribonucleotide reductase activity of syn-

chronized KB cells infected with herpes simplex virus. *J. Virol.* 9:408-418.

- Elion, G. B., P. A. Furman, J. A. Fye, P. De Miranda, L. Beauchamp, and H. J. Schaffer. 1977. Selectivity of action of an antiherpetic agent, 9-(2-hydroxyethoxymethyl)guanine. *Proc. Natl. Acad. Sci. USA* 74:5716-5720.
- Freestone, D. S. 1985. The need for new antiviral agents. *Antiviral Res.* 5:307-324.
- Furman, P. A., C. U. Lambe, and D. J. Nelson. 1982. Effect of acyclovir on the deoxyribonucleotide triphosphate pool levels in Vero cells infected with herpes simplex virus type 1. *Am. J. Med.* 73:14-17.
- Garret, C., and D. V. Santi. 1979. A rapid and sensitive high pressure liquid chromatography assay for deoxyribonucleoside triphosphates in cell extracts. *Anal. Biochem.* 99:268-273.
- Harmenber, J. 1983. Intracellular pools of thymidine reduce the antiviral action of acyclovir. *Intervirology* 20:48-51.
- Heidelberger, C. 1975. Fluorinated pyrimidines and their nucleosides, p. 193-231. In A. C. Sartorelli and D. G. Johns (ed.), *Handbook of experimental pharmacology*, vol. 38, part 2. Springer-Verlag, New York.
- Karlsson, A. H. J., J. G. Harmenber, and B. E. Wahren. 1986. Influence of acyclovir and buyclovir on nucleotide pools in cells infected with herpes simplex virus type 1. *Antimicrob. Agents Chemother.* 29:821-824.
- Kong, X.-B., Q.-Y. Zhu, R. M. Ruprecht, K. A. Watanabe, J. M. Zeidler, J. W. M. Gold, B. Polksky, D. Armstrong, and T.-C. Chou. 1991. Synergistic inhibition of human immunodeficiency virus type 1 replication in vitro by two-drug and three-drug combinations of 3'-azido-3'-deoxythymidine, phosphonofomate, and 2',3'-dideoxythymidine. *Antimicrob. Agents Chemother.* 35:2003-2011.
- McKinley, M. A., and M. G. Rossman. 1989. Rational design of antiviral agents. *Annu. Rev. Pharmacol. Toxicol.* 29:111-122.
- Meng, T.-C., M. A. Fischl, A. M. Boota, S. A. Spector, D. Bemmet, Y. Bassiakos, S. Lal, B. Wright, and D. D. Richman. 1992. Combination therapy with zidovudine and dideoxycytidine in patients with advanced human immunodeficiency virus infection. *Ann. Intern. Med.* 116:13-20.
- Nutter, L. M., S. P. Grill, and Y.-C. Cheng. 1985. The sources of thymidine nucleotides for virus DNA synthesis in herpes simplex virus type 2-infected cells. *J. Biol. Chem.* 260:13272-13275.
- Pöch, G. 1990. Application of the isobogram technique for the analysis of combined effects with respect to additivity as well as independence. *Can. J. Physiol. Pharmacol.* 68:682-688.
- Pöch, G. 1991. Evaluation of combined effects with respect to independent action. *Arch. Complex Environ. Studies* 3:65-74.
- Ponce de Leon, M., R. J. Eisenberg, and G. H. Cohen. 1977. Ribonucleotide reductase from herpes simplex virus (types 1 and 2) infected and uninfected KB cells: properties of the partially purified enzyme. *J. Gen. Virol.* 36:163-173.
- Prichard, M. N., L. E. Prichard, W. A. Baguley, M. R. Nassiri, and C. Shipman, Jr. 1991. Three-dimensional analysis of the synergistic cytotoxicity between ganciclovir and zidovudine. *Antimicrob. Agents Chemother.* 35:1060-1065.
- Prichard, M. N., L. E. Prichard, and C. Shipman, Jr. Inhibitors of thymidylate synthase and dihydrofolate reductase potentiate the antiviral effect of acyclovir. *Antiviral Res.*, in press.
- Prichard, M. N., and C. Shipman, Jr. 1990. A three-dimensional model to analyze drug-drug interactions. *Antiviral Res.* 14:181-206.
- Prichard, M. N., and C. Shipman, Jr. 1992. Letter to the editor in response to J. Sühnel's comment on the paper, "a three-dimensional model to analyze drug-drug interactions." *Antiviral Res.* 17:95-98.
- Prichard, M. N., and C. Shipman, Jr. Unpublished observations.
- Prichard, M. N., S. R. Turk, L. A. Coleman, S. L. Engelhardt, C. Shipman, Jr., and J. C. Drach. 1990. A microtiter virus yield reduction assay for the evaluation of antiviral compounds against human cytomegalovirus and herpes simplex virus type 1. *J. Virol. Methods* 28:101-106.
- Rammier, D. H. 1971. Periodate oxidations of enamines. I. Oxidation of adenosine monophosphate in the presence of methylamine. *Biochemistry* 10:4699-4705.
- Reardon, J. E., and T. Spector. 1991. Acyclovir: mechanism of antiviral action and potentiation by ribonucleotide reductase inhibitors. *Adv. Pharmacol.* 22:1-27.
- Shipman, C., Jr. 1969. Evaluation of 4-(2-hydroxyethyl)-1-piperazineethanesulfonic acid (HEPES) as a tissue culture buffer. *Proc. Soc. Exp. Biol.* 130:305-310.
- Shipman, C., Jr., S. H. Smith, J. C. Drach, and D. L. Klayman. 1981. Antiviral activity of 2-acetylpyridine thiosemicarbazones against herpes simplex virus. *Antimicrob. Agents Chemother.* 19:682-685.
- Shipman, C., Jr., S. H. Smith, J. C. Drach, and D. L. Klayman. 1986. Thiosemicarbazones of 2-acetylpyridine, 2-acetylquinone, 1-acetylquinone, and related compounds as inhibitors of herpes simplex virus in vitro and in a cutaneous herpes guinea pig model. *Antiviral Res.* 6:197-222.
- Specter, T., D. R. Averett, D. J. Nelson, C. U. Lambe, R. W. Morrison, Jr., M. H. St. Claire, and P. A. Furman. 1985. Potentiation of antiherpetic activity of acyclovir by ribonucleotide reductase inhibition. *Proc. Natl. Acad. Sci. USA* 82:4254-4257.
- Specter, T., J. A. Harrington, R. Morrison, Jr., C. U. Lambe, D. J. Nelson, D. R. Averett, K. K. Biron, and P. A. Furman. 1989. 2-Acetylpyridine 5-[(dimethylamino)thiocarbonyl]-thiocarbonohydrazone (A1110U), a potent inactivator of ribonucleotide reductases of herpes simplex and varicella-zoster viruses and a potentiator of acyclovir. *Proc. Natl. Acad. Sci. USA* 86:1051-1055.
- Specter, T., J. A. Harrington, and D. J. T. Porter. 1991. Herpes and human ribonucleotide reductases. Inhibition by 2-acetylpyridine 5-[(2-chloroanalino)-thiocarbonyl] thiocarbonohydrazone (348U87). *Biochem. Pharmacol.* 42:91-96.
- Turk, S. R., C. Shipman, Jr., and J. C. Drach. 1986. Selective inhibition of herpes simplex virus ribonucleoside diphosphate reductase by derivatives of 2-acetylpyridine thiosemicarbazone. *Biochem. Pharmacol.* 35:1539-1545.
- Turk, S. R., C. Shipman, Jr., and J. C. Drach. 1986. Structure activity relationships among α -(N)-heterocyclic acyl thiosemicarbazones and related compounds as inhibitors of herpes simplex virus type 1 specified ribonucleoside diphosphate reductase. *J. Gen. Virol.* 67:1625-1632.
- Unkelbach, H.-D., and G. Pöch. 1988. Comparison of independence and additivity in drug combinations. *Arzneim. Forsch.* 38:1-6.

HU and Y.-C. CHENG

KALA, Properties of dihydrofolate reductase in KB cells and comparison with enzyme from cells, *Mol. Pharmacol.* 21, 231-238 (1982).

CAVAZIERI, DNA complementary to rabbit *iochem. Biophys. Res. Commun.* 55, 1-7 (1973).

I characterization of the drosophila alcohol U.S.A. 77, 5794-5798 (1980).

biologically active globin messenger RNA by cellulose, *Proc. Natl. Acad. Sci. U.S.A.* 69,

cient translation of tobacco mosaic virus RNA from commercial wheat germ, *Proc. Natl.*

ODMAN and P. H. SEEBURG, Regulation of ad and glucocorticoid hormones, *Proc. Natl.*

KAUFMAN, H. A. ERLICH, R. T. SCHIMKE in *E. coli* of a DNA sequence coding for mouse 24 (1978).

quences among DNA fragments separated by 17 (1975).

OTTE and G. ATTARDI, Multiple forms of *Mol. Biol.* 156, 583-607 (1982).

BERTINO and R. T. SCHIMKE, Selective genes in methotrexate-resistant variants of 357-1370 (1978).

BIEDLER and C. HESSION, Antifolate-evidence for dihydrofolate reductase gene sublines overproducing different dihydrofolate 1980).

GRILL, B. A. DOMIN and Y.-C. CHENG, ty stained regions on chromosome 10 with cells, *Proc. Natl. Acad. Sci. U.S.A.* 80, 807-809

PFENDT, F. W. ALT and R. T. SCHIMKE, d control of dihydrofolate reductase mRNA fibroblasts, *J. Biol. Chem.* 254, 309-318 (1979).

dihydrofolate reductase messenger ribonucleic 1 (1981).

HENG, Modulation of dihydrofolate reductase in cells, *AACR Abstracts*, 1115 (1983).

ELERA, Selective amplification of polymorphic e hamster lung cells, *Proc. Natl. Acad. Sci. U.S.A.*

ES, DNA binding by dihydrofolate reductase in 52-12155 (1981).

ant of Chinese hamster ovary cells-resistant to at. *Cell. Genet.* 7, 219-233 (1981).

QUANTITATIVE ANALYSIS OF DOSE-EFFECT RELATIONSHIPS: THE COMBINED EFFECTS OF MULTIPLE DRUGS OR ENZYME INHIBITORS

TING-CHAO CHOU* and PAUL TALALAY†

*Laboratory of Pharmacology, Memorial Sloan-Kettering Cancer Center, New York, NY 10021, and †Department of Pharmacology and Experimental Therapeutics, The Johns Hopkins University School of Medicine, Baltimore, Maryland 21205

INTRODUCTION

The quantitative relationship between the dose or concentration of a given ligand and its effect is a characteristic and important descriptor of many biological systems varying in complexity from isolated enzymes (or binding proteins) to intact animals. This relationship has been analyzed in considerable detail for reversible inhibitors of enzymes. Such analyses have made assumptions on the mechanism of inhibition (competitive, noncompetitive, uncompetitive), and on the mechanism of the reaction for multi-substrate enzymes (sequential or ping-pong), and have required knowledge of kinetic constants (1-4). More recently, it has been possible to describe the behavior of such enzyme inhibitors by simple generalized equations that are independent of inhibitor or reaction mechanisms and do not require knowledge of conventional kinetic constants (i.e. K_m , K_i , V_{max}) (5-8).

Our understanding of dose-effect relationships in pharmacological systems has not advanced to the same level as those of enzyme systems. Many types of mathematical transformations have been proposed to linearize dose-effect plots, based on statistical or empirical assumptions, e.g. probit (9, 10), logit (11) or power-law functions (12). Although these methods often provide adequate linearizations of plots, the slopes and intercepts of such graphs are usually devoid of any fundamental meaning.

THE MEDIAN EFFECT PRINCIPLE

We demonstrate here the application of a single and generalized method for analyzing dose-effect relationships in enzymatic, cellular and whole animal systems. We also examine the problem of quantitating the effects of multiple inhibitors on such systems and provide definitions of summation of effects, and consequently of synergism and antagonism.

Since the proposed method of analysis is derived from generalized mass action considerations, we caution the reader that the analysis of dose-effect

data is concerned with basic mass-action characteristics rather than with proof of specific mechanisms. Nevertheless, it is convenient and intuitively attractive to analyze and normalize all types of dose-response results by a uniform method which is based on sound fundamental considerations that have physicochemical and biochemical validity in simpler systems. Our analysis is based on the median effect principle of the mass action law (5-8), and has already been shown to be simple to apply and useful in the analysis of complex biological systems (13).

The Median Effect Equation

The median effect equation (6, 8) states that:

$$f_a/f_u = (D/D_m)^m \quad (1)$$

where D is the dose, f_a and f_u are the fractions of the system affected and unaffected, respectively, by the dose D , D_m is the dose required to produce the median effect (analogous to the more familiar IC_{50} , ED_{50} , or LD_{50} values), and m is a Hill-type coefficient signifying the sigmoidicity of the dose-effect curve, i.e., $m = 1$ for hyperbolic (first order or Michaelis-Menten) systems. Since by definition, $f_a + f_u = 1$, several useful alternative forms of equation 1 are:

$$f_a/(1 - f_a) = [(f_u)^{-1} - 1]^{-1} = [(f_u)^{-1} - 1] = (D/D_m)^m$$

$$f_a = 1/[1 + (D_m/D)]^m$$

$$D = D_m[f_a/(1 - f_a)]^{1/m}$$

The median effect equation describes the behavior of many biological systems. It is, in fact, a generalized form of the enzyme kinetic relations of Michaelis-Menten (14) and Hill (15), the physical adsorption isotherm of Langmuir (16), the pH-ionization equation of Henderson and Hasselbalch (17), the equilibrium binding equation of Scatchard (18), and the pharmacological drug-receptor interaction (19). Furthermore, the median effect equation is directly applicable not only to primary ligands such as substrates, agonists, and activators, but also to secondary ligands such as inhibitors, antagonists, or environmental factors (5, 6).

When applied to the analysis of the inhibition of enzyme systems, the median effect equation can be used without knowledge of conventional kinetic constants (i.e. K_m , V_{max} or K_i) and irrespective of the mechanism of inhibition (i.e. competitive, noncompetitive or uncompetitive). Furthermore, it is valid for multisubstrate reactions irrespective of mechanism (sequential or ping-pong) (5-8).

ANALYSIS OF

The Median Effect Plot

The median effect equation logarithms of both sides, i.e.

$$\begin{aligned} \log (f_a/f_u) &= m \log (D/D_m) \\ \text{or} \quad \log [(f_u)^{-1} - 1]^{-1} &= m \log (D/D_m) \\ \text{or} \quad \log [(f_u)^{-1} - 1] &= m \log (D/D_m) \end{aligned}$$

The median effect plot (Fig. 1) with respect to $x = \log (D/D_m)$ is a general pharmacological median doses, agonist drugs (ED_{50}), and effect effect principle of the mass applications. The plot gives the plot with the median-effect axis ($f_a/f_u = 0$) which gives $\log (D/D_m)$ consequence relationship that g two basic parameters, m and describes such a system. The lin from linear regression coefficient method.

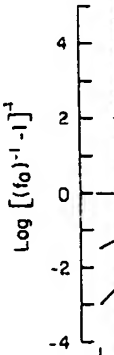


FIG. 1. The median-effect plot at different doses. The plot is based on the median-effect equation. The plot is normalized by taking the ratio to the median dose (ED_{50}). The plot is identical to the plot of $\log [(f_u)^{-1} - 1]$ versus $\log (D/D_m)$.

in characteristics rather than with respect to the dose. It is convenient and intuitively types of dose-response results by a few fundamental considerations that are valid in simpler systems. Our principle of the mass action law (5-8), is to apply and useful in the analysis of

es that:

$$f_a / f_u = (D / D_m)^m \quad (1)$$

fractions of the system affected and D_m is the dose required to produce the median effect (i.e., 50% of the system affected, IC_{50} , ED_{50} , or LD_{50} values), and the sigmoidicity of the dose-effect curve, (Michaelis-Menten) systems. Since by alternative forms of equation 1 are:

$$[(f_a / f_u)^{-1} - 1] = (D / D_m)^m$$

es the behavior of many biological systems, the enzyme kinetic relations of the physical adsorption isotherm of the Henderson and Hasselbalch equation of Scatchard (18), and the equation (19). Furthermore, the median effect applies not only to primary ligands such as but also to secondary ligands such as extrinsic factors (5, 6).

In inhibition of enzyme systems, the inhibition is without knowledge of conventional competitive or noncompetitive (uncompetitive). Furthermore, the inhibition is irrespective of the mechanism of action (sequential or

The Median Effect Plot

The median effect equation (equation 1) may be linearized by taking the logarithms of both sides, i.e.

$$\begin{aligned} \log (f_a / f_u) &= m \log (D) - m \log (D_m) \\ \text{or} \quad \log [(f_a)^{-1} - 1] &= m \log (D) - m \log (D_m) \\ \text{or} \quad \log [(f_a)^{-1} - 1] &= m \log (D) - m \log (D_m) \end{aligned}$$

The median effect plot (Fig. 1) of $y = \log (f_a / f_u)$ or its equivalents with respect to $x = \log (D)$ is a general and simple method (13, 30) for determining pharmacological median doses for lethality (LD_{50}), toxicity (TD_{50}), effect of agonist drugs (ED_{50}), and effect of antagonist drugs (IC_{50}). Thus, the median-effect principle of the mass-action law encompasses a wide range of applications. The plot gives the slope, m , and the intercept of the dose-effect plot with the median-effect axis [i.e. when $f_a = f_u$, $f_a / f_u = 1$ and hence $y = \log (f_a / f_u) = 0$] which gives $\log (D_m)$ and consequently the D_m value. Any cause-consequence relationship that gives a straight line for this plot will provide the two basic parameters, m and D_m , and thus, an apparent equation that describes such a system. The linearity of the median-effect plot (as determined from linear regression coefficients) determines the applicability of the present method.

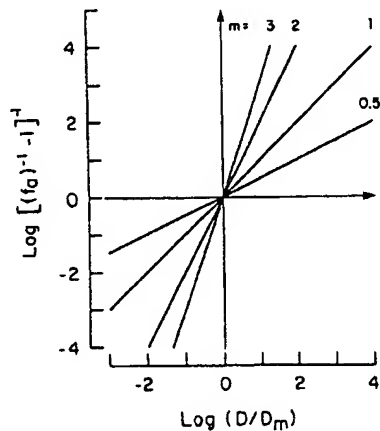


FIG. 1. The median-effect plot at different slopes corresponding to m values of 0.5, 1, 2 and 3. The plot is based on the median-effect equation (equation 1) in which the dose (D) has been normalized by taking the ratio to the median-effect dose (D_m). Note that the ordinate $\log [(f_a)^{-1} - 1]$ is identical to $\log [(f_a)^{-1} - 1]$ or $\log (f_a / f_u)$.

Relation of the Median-Effect Equation to Michaelis-Menten and Hill Equations

In the special case, when $m = 1$, equation 1 becomes $f_e = [1 + (D_m/D)]^{-1}$ which has the same form as the Michaelis-Menten equation (14), $v/V_{max} = [1 + (K_m/S)]^{-1}$. In addition, when the effector ligand is an environmental factor such as an inhibitor, the equation, $f_e = [1 + (D_m/D)]^{-1}$, is valid not only for a single substrate reaction (Michaelis-Menten equation) but also for multiple substrate reactions; the fractional effect is expressed with respect to the control velocity rather than to the maximal velocity (6). Furthermore, f_e in equation 1 is simple to obtain, whereas the determination of V_{max} in the Michaelis-Menten (or Hill) equations requires approximation or extrapolation (6, 7). The logarithmic form of equation 1 describes the Hill equation.

The Utility of the Median Effect Principle

The median-effect equation has been used to obtain accurate values of IC_{50} , ED_{50} , LD_{50} , or the relative potencies of drugs or inhibitors in enzyme systems (6-8, 21-26), in cellular systems (20, 27, 28) and in animal systems (13, 29-32). An alternative form of the median-effect equation (5) has been used for calculating the dissociation constant (K_i or K_a) of ligands for pharmacological receptors (33-35). It has also permitted the analysis of chemical carcinogenesis data and has predicted especially accurately tumor incidence at low dose carcinogen exposure (30, 31). By using the median-effect principle, the general equation for describing a standard radioimmunoassay or ligand displacement curve has been derived recently by Smith (36). It has also been used to show that there is marked synergism among chemotherapeutic agents in the treatment of hormone-responsive experimental mammary carcinomas (32). In recent preliminary reports (13, 37), we have shown that, in conjunction with the multiple drug effect equations (see below), the median-effect plot forms the basis for the quantitation of synergism, summation and antagonism of drug effects.

ANALYSIS OF MULTIPLE DRUG EFFECTS

An Overview

Over the past decades, numerous authors have claimed synergism, summation or antagonism of the effects of multiple drugs. However, there is still no consensus as to the meanings of these terms. For instance, in a review, Goldin and Mantel in 1957 (38) listed seven different definitions of these terms. Confusion and ambiguity persist (39) despite increasing use of multiple drugs in experimentation and in therapy. This emphasizes the lack of a

ANALYSIS OF M

theoretical basis that would permit the effects of drug combinations.

Attempts to interpret the effects of drug combinations have been made for more than a century (39). Since Loewe in 1928 (40, 41) and the French in 1934 (42), the theoretical basis has been the subject of many reviews. There have been many possible mechanisms that may lead to the observed effects. The methods of data analysis have been the subject of many reviews (4, 42, 52-58), but the usefulness of these methods has not been specifically stated. Although not specifically stated, the methods are valid only for inhibitors; others are valid only for systems but not for higher order systems or for mutually nonexclusive inhibitors.

The present authors, therefore, propose to analyze the problem. An understanding of the principles is a prerequisite for any meaningful analysis of drug interactions. Ironically, two principles are often used in two opposite situations. The former are mutually exclusive, and the latter are not (13, 49), and thus these methods are not interchangeable (see Appendix). In this paper, we propose to show that they are merely special cases of a more general method recently (59). We also propose to show the applicability of experimental data to the analysis of synergism, summation and antagonism of nonexclusive drugs, and to obtain a quantitative analysis of synergism, summation and antagonism.

Requirements for Analyzing Multiple Drug Effects

The following information is required for analyzing multiple drug effects and for quantitating synergism, summation and antagonism of drugs.

1. A quantitative definition of synergism, summation and antagonism implies more than summation and antagonism.
2. Dose-effect relationships for the two drugs (i.e., the dose ratio of drug 1 to drug 2) are required.
- a. Measurements made with single drugs (13, 49) and with mixtures of drugs (59) can never alone determine synergism, summation and antagonism.

Michaelis-Menten and Hill

tion 1 becomes $f_a = [1 + (D_m/D)]^{-1}$. The Michaelis-Menten equation (14), $v/V_{max} = [1 + (D_m/D)]^{-1}$, is valid not only for a single ligand (where D is an environmental factor and D_m is the Michaelis constant) but also for multiple ligands (where D is expressed with respect to the total concentration of ligands) and for multiple enzymes (6). Furthermore, f_a in equation 1 is valid for the determination of V_{max} in the presence of multiple ligands, provided that the approximation or extrapolation 1 describes the Hill equation.

Attempts to obtain accurate values of IC_{50} , the concentration of drugs or inhibitors in enzyme systems (13, 29-32) and in animal systems (13, 29-32) have been used for the calculation of K_a of ligands for pharmacological systems. In addition, the analysis of chemical carcinogenesis has been carried out by using the median-effect principle, which is based on the standard radioimmunoassay or ligand-binding assay (36). It has also been used for the analysis of experimental mammary carcinomas (13, 37). We have shown that, in addition to the equations (see below), the median-effect principle can be used for the analysis of synergism, summation and antagonism.

LE DRUG EFFECTS

Authors have claimed synergism, summation and antagonism of multiple drugs. However, there is no agreement on the definition of these terms. For instance, in a review, seven different definitions of synergism (39) despite increasing use of multiple ligands and enzymes. This emphasizes the lack of a

theoretical basis that would permit rigorous and quantitative assessment of the effects of drug combinations.

Attempts to interpret the effect of multiple drugs have been documented for more than a century (39). Since the introduction of the isobol concept by Loewe in 1928 (40, 41) and the fractional product concept (see Appendix) by Webb in 1963 (42), the theoretical and practical aspects of the problem have been the subject of many reviews (38, 43-51). Some authors have discussed the possible mechanisms that may lead to synergism, and others have emphasized methods of data analysis. The kinetic approach was used earlier by some investigators (4, 42, 52-58), but the formulations were frequently too complex to be of practical usefulness or were restricted to individual situations. Although not specifically stated, some formulations are limited to two inhibitors; others are valid only for first order (Michaelis-Menten type) systems but not for higher order (Hill type) systems, and still others are valid only for mutually nonexclusive inhibitors but not for mutually exclusive inhibitors.

The present authors, therefore, have undertaken a kinetic approach to analyze the problem. An unambiguous definition of summation is a prerequisite for any meaningful conclusions with respect to synergism and antagonism. Ironically, two prevalent concepts for calculating summation i.e., the isobol and the fractional-product method, are shown to conform to two opposite situations. The former concept is valid for drugs whose effects are mutually exclusive, and the latter is valid for mutually nonexclusive drugs (13, 49), and thus these methods cannot be used indiscriminately (see Appendix). In this paper, we provide the equations for both situations and show that they are merely special cases of the general equations described recently (59). We also propose a general diagnostic plot to determine the applicability of experimental data, to distinguish mutually exclusive from nonexclusive drugs, and to obtain parameters that can be directly used for the analysis of summation, synergism or antagonism.

Requirements for Analyzing Multiple Drug Effects

The following information is essential for analyzing multiple drug effects and for quantitating synergism, summation and antagonism of multiple drugs.

1. A quantitative definition of summation is required since synergism implies more than summation and antagonism less than summation of effects.
2. Dose-effect relationships for drug 1, drug 2 and their mixture (at a known ratio of drug 1 to drug 2) are required.
 - a. Measurements made with single doses of drug 1, drug 2 and their mixture can never alone determine synergism since the sigmoidicity of dose-effect

curves and the exclusivity of drug effects cannot be determined from such measurements.

b. The dose-effect relationships should follow the basic mass-action principle relatively well (e.g. median-effect plots with correlation coefficients for the regression lines greater than 0.9).

c. Determination of the sigmoidicity of dose-effect curves and the exclusivity of effects of multiple drugs is necessary. The slope of the median-effect plot gives a quantitative estimation of sigmoidicity. When $m = 1$, the dose-effect curve is hyperbolic; when $m \neq 1$, the dose-effect curve is sigmoidal, and the greater the m value, the greater its sigmoidicity; $m < 1$ is a relatively rare case which in allosteric systems indicates negative cooperativity of drug binding at the receptor sites. When the dose-effect relationships of drug 1, drug 2 and their mixture are all parallel in the median-effect plot, the effects of drug 1 and drug 2 are mutually exclusive (59). If the plots of drugs 1 and 2 are parallel but the plot of their mixture is concave upward with a tendency to intersect the plot of the more potent of the two drugs, their effects are mutually nonexclusive (59). If the plots for drugs 1 and 2 and their mixture are not parallel to each other, exclusivity of effects cannot be established. Alternatively, exclusivity of effects may not be ascertained because of a limited number of data points or limited dose range. In these cases, the data may be analyzed for the "combination index" (see below) on the basis of both mutually exclusive and mutually nonexclusive assumptions. Note that exclusivity may occur at a receptor site, at a point in a metabolic pathway, or in more complex systems, depending on the endpoint of the measurements.

Equations for the Effects of Multiple Drugs

A systematic analysis in enzyme kinetic systems using the basic principles of the mass action law has led to the derivation of generalized equations for multiple inhibitors or drugs (8, 59).

1. *For two mutually exclusive drugs that obey first order conditions.* If two drugs (e.g., inhibitors D_1 and D_2) have effects that are mutually exclusive, then the summation of combined effects $(f_a)_{1,2}$, in first-order systems (i.e., each drug follows a hyperbolic dose-effect curve) can be calculated from (59):

$$\begin{aligned} \frac{(f_a)_{1,2}}{(f_u)_{1,2}} &= \frac{(f_a)_1}{(f_u)_1} + \frac{(f_a)_2}{(f_u)_2} \\ &= \frac{(D)_1}{(ED_{50})_1} + \frac{(D)_2}{(ED_{50})_2} \end{aligned} \quad (2)$$

ANALYSIS OF

where f_a is the fraction affected at the concentration of the drug that $f_a + f_u = 1$ or $f_a = 1 - f_u$.

2. *For two mutually nonexclusive effects of two drugs (D_1 and D_2) with different modes of action or active effects, $(f_a)_{1,2}$, in a first-order system.*

$$\begin{aligned} \frac{(f_a)_{1,2}}{(f_u)_{1,2}} &= \frac{(f_a)_1}{(f_u)_1} \\ &= \frac{(D)_1}{(ED_{50})_1} \end{aligned}$$

Similar relationships apply to inhibitors, for which generalized systems, equations 2 and 3 are irrespective of the number of inhibition (competitive, noncompetitive) mechanisms (sequential or ping-pong). The simplicity of the above equations (substrate concentration factors derivation) suggests their general mechanism-specific reactions complex. In more organized relationships of drugs or inhibitors, the curves are hyperbolic.

3. *For two mutually exclusive drugs that obey first order conditions.* The above concepts have been extended to the case in which each drug has a sigmoidal dose-effect curve or exhibits positive cooperativity. Such drugs are mutually exclusive.

$$\left[\frac{(f_a)_{1,2}}{(f_u)_{1,2}} \right]^{\frac{1}{m}} = \left[\frac{(f_a)_1}{(f_u)_1} \right]^{\frac{1}{m}} + \left[\frac{(f_a)_2}{(f_u)_2} \right]^{\frac{1}{m}}$$

where m is a Hill-type coefficient for the sigmoidal dose-effect curve.

cts cannot be determined from such should follow the basic mass-action effect plots with correlation coefficients 9). city of dose-effect curves and the is necessary. The slope of the medianation of sigmoidicity. When $m = 1$, the $n/m \neq 1$, the dose-effect curve is the greater its sigmoidicity; $m < 1$ is a stems indicates negative cooperativity When the dose-effect relationships of parallel in the median-effect plot, the y exclusive (59). If the plots of drugs 1 ir mixture is concave upward with a re potent of the two drugs, their effects lots for drugs 1 and 2 and their mixture vity of effects cannot be established. may not be ascertained because of a ed dose range. In these cases, the data index" (see below) on the basis of both onexclusive assumptions. Note that , at a point in a metabolic pathway, or on the endpoint of the measurements.

drugs

tic systems using the basic principles of derivation of generalized equations for

that obey first order conditions. If two effects that are mutually exclusive, then , in first-order systems (i.e., each drug) can be calculated from (59):

$$\frac{f_a}{f_a} + \frac{(f_a)_2}{(f_u)_2} = \frac{(D)_1}{(ED_{50})_1} + \frac{(D)_2}{(ED_{50})_2} \quad (2)$$

where f_a is the fraction affected and f_u is the fraction unaffected, and ED_{50} is the concentration of the drug that is required to produce a 50% effect. Note that $f_a + f_u = 1$ or $f_a = 1 - f_u$.

2. For two mutually nonexclusive drugs that obey first order conditions. If the effects of two drugs (D_1 and D_2) are mutually non-exclusive (i.e., they have different modes of action or act independently) the summation of combined effects, $(f_a)_{1,2}$, in a first-order system is (59):

$$\begin{aligned} \frac{(f_a)_{1,2}}{(f_u)_{1,2}} &= \frac{(f_a)_1}{(f_u)_1} + \frac{(f_a)_2}{(f_u)_2} + \frac{(f_a)_1 (f_a)_2}{(f_u)_1 (f_u)_2} \\ &= \frac{(D)_1}{(ED_{50})_1} + \frac{(D)_2}{(ED_{50})_2} + \frac{(D)_1 (D)_2}{(ED_{50})_1 (ED_{50})_2} \quad (3) \end{aligned}$$

Similar relationships apply to situations involving more than two inhibitors, for which generalized equations are given in ref. 59. In enzyme systems, equations 2 and 3 express summation of inhibitory effects, irrespective of the number of substrates, the type or mode of reversible inhibition (competitive, noncompetitive or uncompetitive) or the kinetic mechanisms (sequential or ping-pong) of the reaction under consideration. The simplicity of the above equations (in which all specific kinetic constants, substrate concentration factors, and V_{max} have been cancelled out during derivation) suggests their general applicability (5, 6). This is in contrast to the mechanism-specific reactions (3, 5) for which the equations are far more complex. In more organized cellular or animal systems, the dose-effect relationships of drugs or inhibitors are frequently sigmoidal rather than hyperbolic.

3. For two mutually exclusive drugs that obey higher order conditions. The above concepts have been extended to higher-order (Hill-type) systems in which each drug has a sigmoidal dose-effect curve (i.e., has more than one binding site or exhibits positive or negative cooperativity). If the effects of such drugs are mutually exclusive:

$$\left[\frac{(f_a)_{1,2}}{(f_u)_{1,2}} \right]^{\frac{1}{m}} = \left[\frac{(f_a)_1}{(f_u)_1} \right]^{\frac{1}{m}} + \left[\frac{(f_a)_2}{(f_u)_2} \right]^{\frac{1}{m}} = \frac{(D)_1}{(ED_{50})_1} + \frac{(D)_2}{(ED_{50})_2} \quad (4)$$

where m is a Hill-type coefficient which denotes the sigmoidicity of the dose-effect curve.

4. For two mutually nonexclusive drugs that obey higher order conditions. If the effects of two drugs (D_1 and D_2) are mutually nonexclusive and if each drug and their combination follow a sigmoidal dose-effect relationship with m^{th} order kinetics, then this relationship becomes (59):

$$\left[\frac{(f_a)_{1,2}}{(f_a)_{1,2}} \right]^{\frac{1}{m}} = \left[\frac{(f_a)_1}{(f_a)_1} \right]^{\frac{1}{m}} + \left[\frac{(f_a)_2}{(f_a)_2} \right]^{\frac{1}{m}} + \left[\frac{(f_a)_1 (f_a)_2}{(f_a)_1 (f_a)_2} \right]^{\frac{1}{m}}$$

$$= \frac{(D)_1}{(ED_{50})_1} + \frac{(D)_2}{(ED_{50})_2} + \frac{(D)_1 (D)_2}{(ED_{50})_1 (ED_{50})_2} \quad (5)$$

In the special case where $(f_a)_{1,2} = (f_a)_1,2 = 0.5$, equations 2 and 4 become:

$$\frac{(D)_1}{(ED_{50})_1} + \frac{(D)_2}{(ED_{50})_2} = 1 \quad (6)$$

which describes the ED_{50} isobogram.

Similarly, equations 3 and 5 become:

$$\frac{(D)_1}{(ED_{50})_1} + \frac{(D)_2}{(ED_{50})_2} + \frac{(D)_1 (D)_2}{(ED_{50})_1 (ED_{50})_2} = 1 \quad (7)$$

which does not describe an isobogram, because of the additional term on the left.

In the Appendix it is shown that equation 3 or 7 can be readily used for deriving the fractional product equation of Webb (42), and equation 4 can be used for deriving the generalized isobogram equation for any desired f_a value. Thus, for the isobogram at any fractional effect $f_a = x$ per cent, the generalized equation is:

$$\frac{(D)_1}{(D_x)_1} + \frac{(D)_2}{(D_x)_2} = 1 \quad (8)$$

The limitations of the fractional product concept and the isobogram method are detailed in the Appendix.

ANALYSIS OF M

5. Quantitation of synergism: experimental results are entered in equation 2 or 4, or the sum of than, equal to, or smaller than summation or synergism of effect fore, from equations 2-5, if the calculated additive effect, $(f_a)_{1,2}$ antagonism is indicated.

It is, however, convenient to quantifying synergism, summation

$$CI =$$

for mutually exclusive drugs, an

$$CI = \frac{(D)_1}{(D_x)_1}$$

for mutually nonexclusive drugs

For mutually exclusive or non when $CI < 1$, synergism is indi

$CI = 1$, summation is ind

$CI > 1$, antagonism is in

To determine synergism, sum (i.e., for any f_a value), the prod median-effect plot (Eqn. 1) wh drug 2 and their combination; value representing x per cent aff $(D_x)_1$, $(D_x)_2$ and $(D_x)_{1,2}$ by using $[f_a/(1-f_a)]^{1/m}$; iii) calculate the CI, where $(D_x)_1$ and $(D_x)_2$ are to be dissected into $(D)_1$ and $(D)_2$ $\times P/(P+Q)$ and $(D)_2 = (D_x)_1,2$ equal to, or greater than 1, respectively.

To facilitate the calculation automatic graphing of CI with this computer simulation are sample calculation of CI witho

is that obey higher order conditions. If they are mutually nonexclusive and if each sigmoidal dose-effect relationship with respect to f_a becomes (59):

$$\left[\frac{f_a}{f_u} \right]^{\frac{1}{m}} + \left[\frac{(f_a)_1 (f_a)_2}{(f_u)_1 (f_u)_2} \right]^{\frac{1}{m}} = \frac{(D)_2}{(ED_{50})_2} + \frac{(D)_1 (D)_2}{(ED_{50})_1 (ED_{50})_2} \quad (5)$$

When $f_a = 0.5$, equations 2 and 4 become:

$$\frac{D_2}{ED_{50}2} = 1 \quad (6)$$

∴

$$\frac{(D)_1 (D)_2}{(ED_{50})_1 (ED_{50})_2} = 1 \quad (7)$$

because of the additional term on the

equation 3 or 7 can be readily used for the method of Webb (42), and equation 4 can be used to obtain the isobogram equation for any desired fractional effect $f_a = x$ per cent, the

$$\frac{(D)_2}{(D_x)_2} = 1 \quad (8)$$

product concept and the isobogram

5. Quantitation of synergism, summation and antagonism. When experimental results are entered into equations 2-5, if the sum of the two terms in equation 2 or 4, or the sum of the three terms in equation 3 or 5 is greater than, equal to, or smaller than 1, it may be inferred that antagonism, summation or synergism of effects, respectively, has been observed. Therefore, from equations 2-5, if the combined observed effect is greater than the calculated additive effect, $(f_a)_{1,2}$, synergism is indicated; if it is smaller, antagonism is indicated.

It is, however, convenient to designate a "combination index" (CI) for quantifying synergism, summation, and antagonism, as follows:

$$CI = \frac{(D)_1}{(D_x)_1} + \frac{(D)_2}{(D_x)_2} \quad (9)$$

for mutually exclusive drugs, and

$$CI = \frac{(D)_1}{(D_x)_1} + \frac{(D)_2}{(D_x)_2} + \frac{(D)_1 (D)_2}{(D_x)_1 (D_x)_2} \quad (10)$$

for mutually nonexclusive drugs.

For mutually exclusive or nonexclusive drugs, when $CI < 1$, synergism is indicated.

$CI = 1$, summation is indicated.

$CI > 1$, antagonism is indicated.

To determine synergism, summation and antagonism at any effect level (i.e., for any f_a value), the procedure involves three steps: i) Construct the median-effect plot (Eqn. 1) which determines m and D_m values for drug 1, drug 2 and their combination; ii) for a given degree of effect (i.e., a given f_a value representing x per cent affected), calculate the corresponding doses [i.e., $(D_x)_1$, $(D_x)_2$ and $(D_x)_{1,2}$] by using the alternative form of equation 1, $D_x = D_m [f_a/(1 - f_a)]^{1/m}$; iii) calculate the combination index (CI) by using equations 9 or 10, where $(D_x)_1$ and $(D_x)_2$ are from step (ii), and $(D_x)_{1,2}$ [also from step (ii)] can be dissected into $(D)_1$ and $(D)_2$ by their known ratio, P/Q . Thus, $(D)_1 = (D_x)_{1,2} \times P/(P + Q)$ and $(D)_2 = (D_x)_{1,2} \times Q/(P + Q)$. CI values that are smaller than, equal to, or greater than 1, represent synergism, summation and antagonism, respectively.

To facilitate the calculation, a computer program written in BASIC for automatic graphing of CI with respect to f_a has been developed. Samples of this computer simulation are shown in the examples to be given later. A sample calculation of CI without using a computer is also given in Example 1.

APPLICATIONS OF THE MEDIAN EFFECT EQUATION
AND PLOTS TO THE ANALYSIS OF MULTIPLE
DRUGS OR INHIBITORS

Example 1. Inhibition of Alcohol Dehydrogenase by Two Mutually Exclusive Inhibitors

Yonetani and Theorell (55) have reported the inhibition of horse liver alcohol dehydrogenase by two inhibitors (I_1 = ADP-ribose and I_2 = ADP) both of which are competitive with respect to NAD. Velocity measurements in the presence of a range of concentrations of the two inhibitors (alone and in combination) and control velocities were retrieved from the original plot, and tabulated in ref. 59. The results are most conveniently expressed as fractional velocities (f_v) which are the ratios of the inhibited velocities to the control velocities, and therefore correspond to the fraction of the process unaffected (f_u). The fractional velocities in the presence of ADP-ribose (95–375 μM), ADP (0.5–2.5 μM), and a combination of ADP-ribose and ADP at a constant molar ratio of 190:1, have been plotted as $\log[(f_v)^{-1} - 1]$ with respect to $\log(I)$ (Fig. 2). For ADP-ribose, $m = 0.968$, $I_{50} = 156.1 \mu\text{M}$ with a regression coefficient of $r = 0.9988$. For ADP, $m = 1.043$, $I_{50} = 1.657 \mu\text{M}$ and $r = 0.9996$. For ADP-ribose and ADP in combination (molar ratio 190:1), $m_{1,2} = 1.004$, $(I_{50})_{1,2} = 107.0 \mu\text{M}$ and $r = 0.9997$. It is clear that both inhibitors follow first-order kinetics (i.e., $m \approx 1$) and that ADP-ribose and ADP are mutually exclusive inhibitors (i.e., the

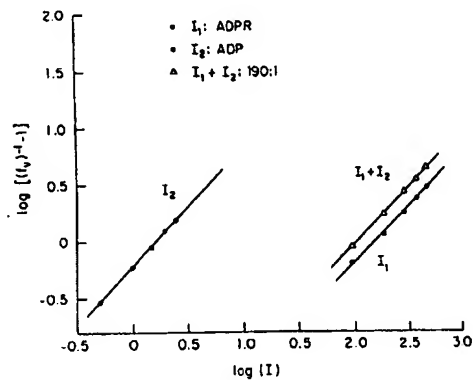


FIG. 2. Median-effect plots of the experimental data of Yonetani and Theorell (55) for the inhibition of horse liver alcohol dehydrogenase by two mutually exclusive inhibitors. I_1 is ADP-ribose (ADPR), I_2 is ADP, and $I_1 + I_2$ is a mixture of ADP-ribose and ADP in a molar ratio of 190:1. The abscissa represents $\log(I_1)$ (●), $\log(I_2)$ (○), or $\log[(I_1 + I_2)/(190:1)]$ (Δ). In this case it is convenient to use the terms fractional velocity (f_v) which is the ratio of the inhibited to the control velocity and therefore corresponds to the fraction that is unaffected (f_u). [from Chou and Talalay (59)].

ANALYSIS OF MU

plot for the combination of inhib component inhibitors). These co interpretations obtained by Yonetan (59) using different methods. For constants and type of inhibition is agreement between theory and ex

With this knowledge of the m combination at a constant molar r combination index (CI) for a series close to 1 over the entire range of inhibitory effects of ADP-ribose a

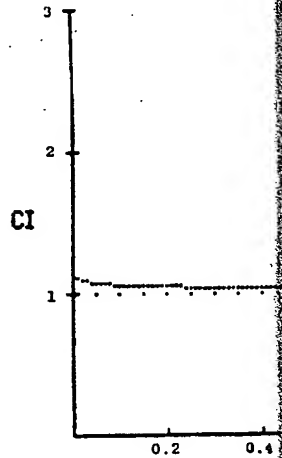


FIG. 3. Computer-generated graphical presentation of the combination index (CI) with respect to the fraction affected (f_u) for the additive inhibition of horse liver alcohol dehydrogenase. The CI is described in the section entitled "Quantitative analysis of inhibition" which is equal to $(D_{90})_1 / (D_{90})_2$. $CI < 1$, $= 1$ and > 1 represent synergy, additive and antagonism, respectively. Although plots of CI with respect to f_u can be more convenient to use computer simulations, this can be done by the use of linear regression.

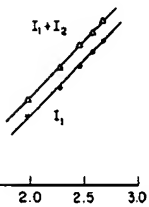
We now give a sample calculation for the CI for an arbitrarily selected value of $f_u = 0.3$. From equation 1, $D_x = D_m [f_u / (1 - f_u)]$.

Since I_1 is ADP-ribose and I_2 is ADP, then $(D_{90})_1 = 156.1 \mu\text{M}$ [0.9/(1 - 0.3)] = 234.4 μM , $(D_{90})_2 = 1.657 \mu\text{M}$ [0.9/(1 - 0.3)] = 2.439 μM , and $(D_{90})_{1,2} = 107.0 \mu\text{M}$ [0.9/(1 - 0.3)] = 159.9 μM .

DIAN EFFECT EQUATION LYSIS OF MULTIPLE HIBITORS

ogenase by Two Mutually Exclusive

orted the inhibition of horse liver rs (I_1 = ADP-ribose and I_2 = ADP) to NAD. Velocity measurements is of the two inhibitors (alone and in retrieved from the original plot, and conveniently expressed as fractional e inhibited velocities to the control he fraction of the process unaffected ice of ADP-ribose ($95-375 \mu\text{M}$), ADP -ribose and ADP at a constant molar $\sqrt{r_1} - 1$] with respect to $\log(I)$ (Fig. 2). M with a regression coefficient of $r = \mu\text{M}$ and $r = 0.9996$. For ADP-ribose 90:1), $m_{1,2} = 1.004$, $(I_{50})_{1,2} = 107.0 \mu\text{M}$ tors follow first-order kinetics (i.e., m mutually exclusive inhibitors (i.e., the



data of Yonetani and Theorell (55) for the two mutually exclusive inhibitors. I_1 is ADP- of ADP-ribose and ADP in a molar ratio of 90:1, or $\log[(I_1 + I_2)/(190:1)]$. In this case it is which is the ratio of the inhibited to the control hat is unaffected (I_0). [from Chou and Talalay

plot for the combination of inhibitors parallels the plots for each of the component inhibitors). These conclusions are in agreement with the interpretations obtained by Yonetani and Theorell (55) and Chou and Talalay (59) using different methods. For the present analysis, knowledge of kinetic constants and type of inhibition is not required. The plots show excellent agreement between theory and experiment.

With this knowledge of the m and I_{50} values for each inhibitor and the combination at a constant molar ratio, it is possible to calculate the inhibitor combination index (CI) for a series of values of f_a (Fig. 3). The CI values are close to 1 over the entire range of f_a values, suggesting strongly that the inhibitory effects of ADP-ribose and ADP are additive.

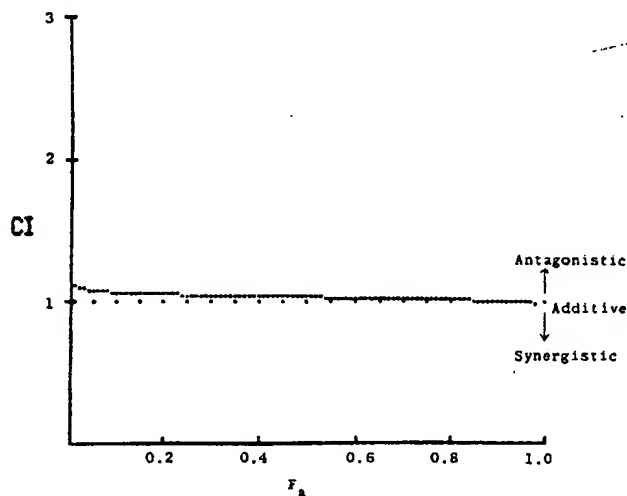


FIG. 3. Computer-generated graphical presentation of the combination index (CI) with respect to fraction affected (f_a) for the additive inhibition by ADP-ribose and ADP (molar ratio of 190:1) of horse liver alcohol dehydrogenase. The plot is based on equation 9 (mutually exclusive) as described in the section entitled "Quantitation of Synergism, Summation and Antagonism." CI is the combination index which is equal to $(D_x)/(D_{x1}) + (D_x)/(D_{x2})$ (see text for sample calculation). $CI < 1$, $= 1$ and > 1 represent synergistic, additive and antagonistic effects, respectively. Although plots of CI with respect to f_a can be obtained by step-by-step calculations, it is much more convenient to use computer simulation. The parameters were obtained as described in Fig. 2, by the use of linear regression analysis or computer simulation.

We now give a sample calculation of the combination index (CI) for an arbitrarily selected value of $f_a = 0.9$:

From equation 1, $D_x = D_m [f_a/(1 - f_a)]^{1/m}$.

Since I_1 is ADP-ribose and I_2 is ADP,

then $(D_{90})_1 = 156.1 \mu\text{M} [0.9/(1 - 0.9)]^{1/0.968} = 1511 \mu\text{M}$

$(D_{90})_2 = 1.657 \mu\text{M} [0.9/(1 - 0.9)]^{1/1.043} = 13.62 \mu\text{M}$

$(D_{90})_{1,2} = 107.0 \mu\text{M} [0.9/(1 - 0.9)]^{1/1.004} = 954.6 \mu\text{M}$

Since in the mixture $I_1 : I_2 = 190 : 1$, then, $(D_{50})_{1,2}$ can be dissected into:

$$(D)_1 = 954.6 \times [190/(190 + 1)] = 949.6 \mu\text{M}$$

$$(D)_2 = 954.6 \times [1/(190 + 1)] = 4.998 \mu\text{M}$$

therefore, $(CI)_{50} = \frac{949.6 \mu\text{M}}{1511 \mu\text{M}} + \frac{4.998 \mu\text{M}}{13.62 \mu\text{M}} = 0.9955$.

Since value of $(CI)_{50}$ is close to 1, an additive effect of ADP-ribose and ADP at $f_a = 0.9$ is indicated.

A computer program for automated calculation of m , D_m , D_a , r , and CI at different f_a values has been developed.

Example 2. Inhibition of Alcohol Dehydrogenase by Two Mutually Non-Exclusive Inhibitors

Yonetani and Theorell (55) also studied the inhibition of horse liver alcohol dehydrogenase by the two competitive, mutually nonexclusive inhibitors: *o*-phenanthroline (I_1) and ADP (I_2). The fractional velocity (f_v) values retrieved from the original plot are given in ref. 59, and are presented in the form of a median-effect plot, i.e., $\log [(f_v)^{-1} - 1]$ with respect to $\log (I)$ (Fig. 4). *o*-Phenanthroline gives $m = 1.303$, $I_{50} = 36.81 \mu\text{M}$ and $r = 0.9982$, and ADP gives $m = 1.187$, $I_{50} = 1.656 \mu\text{M}$ and $r = 0.9842$. These data again show that both inhibitors follow first order kinetics (i.e., $m \approx 1$). However, when the data for

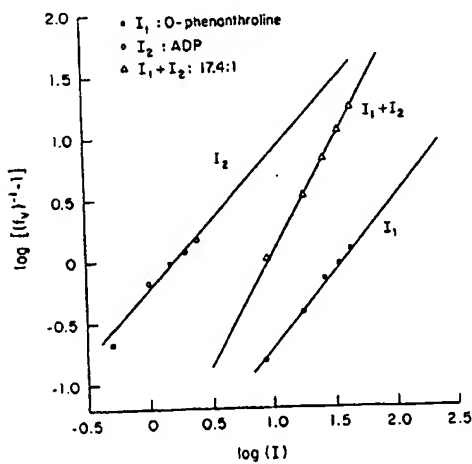


FIG. 4. The median-effect plot of experimental data of Yonetani and Theorell (55) for the inhibition of horse liver alcohol dehydrogenase by two mutually nonexclusive inhibitors. I_1 is *o*-phenanthroline, I_2 is ADP, and $I_1 + I_2$ is a mixture of *o*-phenanthroline and ADP (molar ratio 17.4:1). The abscissa represents $\log (I_1)$ (●), $\log (I_2)$ (○), or $\log [(I_1 + I_2)]$ (Δ) [from Chou and Talalay (59)].

ANALYSIS OF

the mixture of *o*-phenanthroline plotted in the same manner, a (apparent), $(I_{50})_{1,2} = 9.116 \mu\text{M}$ a slope of the plot for the mixture clearly indicates that *o*-phenanthroline inhibitors.

The combination indices at results indicate that there is a marked synergism at high f_a va

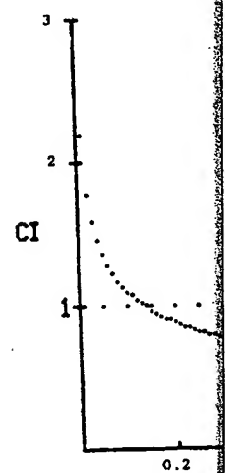


FIG. 5. Computer-generated graphic of the combination index (CI) versus the fraction affected (f_a) for the inhibition of horse liver alcohol dehydrogenase by *o*-phenanthroline and ADP (molar ratio 17.4:1) as described in the legend to Fig. 3.

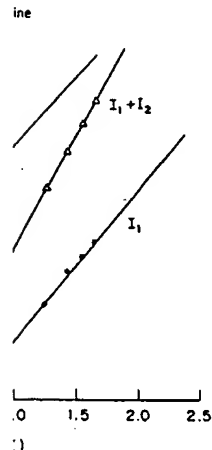
Example 3. Inhibition of the L1210 Leukemia Cells by Mixture of MTX and Arabinofuranosylcytosine (ara-C)

Murine L1210 leukemia cells were treated with different concentrations of MTX (0.1-10 μM) and a fixed molar ratio mixture of MTX and arabinofuranosylcytosine (ara-C) (1:10). The deoxyuridine into DNA was measured and the results of dUrd incorporation are shown in the median effect plot (Fig. 6). The data are: $D_m = 1.091$, $D_a = 2.554 \mu\text{M}$, $r = 0.999$.

49.6 μM
 98 μM
 $\frac{\mu\text{M}}{\mu\text{M}} = 0.9955$.
 additive effect of ADP-ribose and
 calculation of m , D_m , D_1 , r , and CI at

Inhibition of Alcohol Dehydrogenase by Two Mutually Non-

in the inhibition of horse liver alcohol dehydrogenase by two mutually nonexclusive inhibitors: *o*-phenanthroline and ADP. The fractional velocity (f_v) values retrieved from the data are plotted in the form of a graph with respect to $\log (I)$ (Fig. 4). *o*-phenanthroline gives $I_{50} = 31 \mu\text{M}$ and $r = 0.9982$, and ADP gives $I_{50} = 2 \mu\text{M}$ and $r = 1.0$ ($m \approx 1$). However, when the data for



data of Yonetani and Theorell (55) for the two mutually nonexclusive inhibitors. I_1 is *o*-phenanthroline and ADP (molar ratio 17.4:1) (\circ), or $\log [(I_1) + (I_2)]$ (\square) [from Chou and Talalay (9)].

the mixture of *o*-phenanthroline and ADP (constant molar ratio 17.4:1) are plotted in the same manner, a very different result is obtained: $m_{1,2} = 1.742$ (apparent), $(I_{50})_{1,2} = 9.116 \mu\text{M}$ and $r = 0.9999$. The dramatic increase in the slope of the plot for the mixture (in comparison to each of its components), clearly indicates that *o*-phenanthroline and ADP are mutually nonexclusive inhibitors.

The combination indices at various f_a levels are given in Figure 5. The results indicate that there is a moderate antagonism at low f_a values and a marked synergism at high f_a values.

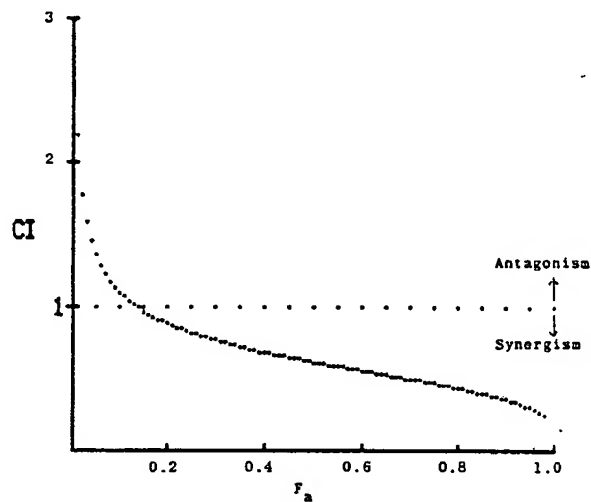


FIG. 5. Computer-generated graphical presentation of the combination index (CI) with respect to fraction affected (f_a) for the inhibition of horse liver alcohol dehydrogenase by a mixture of *o*-phenanthroline and ADP (molar ratio 17.4:1). The method of analysis is the same as that described in the legend to Fig. 3, except that equation 10 (mutually non-exclusive) is used.

Example 3. Inhibition of the Incorporation of Deoxyuridine into the DNA of L1210 Leukemia Cells by Methotrexate (MTX) and 1- β -D-Arabinofuranosylcytosine (ara-C)

Murine L1210 leukemia cells were incubated in the presence of a range of concentrations of MTX (0.1–6.4 μM), of ara-C (0.0782–5.0 μM), or a constant molar ratio mixture of MTX and ara-C (1:0.782), and the incorporation of deoxyuridine into DNA was then determined. The fractional inhibitions (f_a) of dUrd incorporation are shown in Table 1. Analysis of the results by the median effect plot (Fig. 6) gave the following parameters: for MTX, $m = 1.091$, $D_m = 2.554 \mu\text{M}$, $r = 0.9842$; for ara-C, $m = 1.0850$, $D_m = 0.06245 \mu\text{M}$, and

TABLE I. INHIBITION OF [6^3 H]DEOXYURIDINE (dUrd) INCORPORATION INTO DNA IN L1210 LEUKEMIA CELLS BY METHOTREXATE (MTX) AND 1- β -D-ARABINOFURANOSYLCYTOSINE (ara-C), ALONE AND IN COMBINATION

MTX μM	Fractional inhibition (f_i) at [ara-C] of							
	0 μM	0.782 μM	0.156 μM	0.313 μM	0.625 μM	1.25 μM	2.5 μM	5.0 μM
0	0	0.582	0.715	0.860	0.926	0.955	0.980	0.993
0.1	0.0348	0.405						
0.2	ND*		0.587					
0.4	ND			0.775				
0.8	0.140				0.878			
1.6	0.415					0.943		
3.2	0.573						0.970	
6.4	0.755							ND

*Result not used because of large variation between duplicates.

L1210 murine leukemia cells (8×10^6 cells) were incubated in Eagle's basal medium (20) in the presence and absence of various concentrations of MTX and ara-C and their mixture (molar ratio, 1:0.782) at 37°C for 20 min and then incubated with 0.5 μM (1 μCi) of [6^3 H]dUrd, at 37°C for 30 min. Fractional inhibition (f_i or f_d) of [6^3 H]dUrd incorporation into perchloric acid-insoluble DNA fraction was then measured as previously described (20). All measurements were made in duplicate.

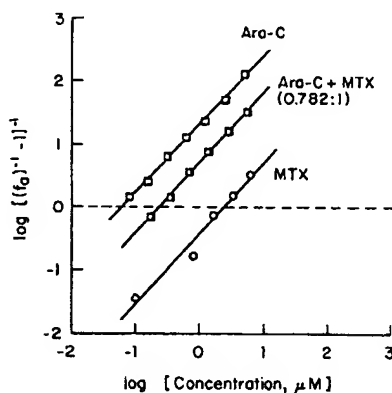


FIG. 6. Median-effect plot showing the inhibition of [6^3 H]dUrd incorporation into DNA of L1210 murine leukemia cells by methotrexate (MTX), (O); arabinofuranosylcytosine (ara-C), (X); or their mixture (1:0.782), (+). Data from Table I have been used.

$r = 0.9995$. For the combination of MTX and ara-C (1:0.782), the parameters were: $m = 1.1296$, $D_m = 0.2496 \mu M$, and $r = 0.9995$. The combination index (Fig. 7) shows a moderate antagonism between the two drugs at all values of fractional inhibition.

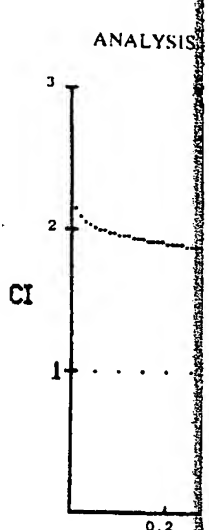


FIG. 7. Computer-generated graph respect to fraction affected (f_d) for arabinofuranosylcytosine (ara-C) in DNA of L1210 murine leukemia cell. Fig. 6 have been used for this plot

Example 4. Inhibition of the L1210 Leukemia Cells by Hydroxyurea and 5-Fluorouracil

Murine L1210 leukemia cells were incubated with various concentrations of hydroxyurea and of a constant molar ratio of 5-fluorouracil (12.5:1), and the incorporation of [3^3 H]thymidine was determined. The fractional inhibition data are given in Table 2. Analysis of the results by the median-effect method gives the following parameters: for hydroxyurea, $m = 0.9908$; for 5-fluorouracil, $m = 0.9995$; for the mixture of hydroxyurea and 5-fluorouracil, $m = 0.2496 \mu M$, and $r = 0.9776$. It is interesting to note that the median-effect plot for the mixture is a straight line, whereas the degree of this antagonism for the mixture increases as the concentration of 5-fluorouracil increases (Table 3). The reason for this may be of practical importance.

URIDINE (dUrd) INCORPORATION INTO METHOTREXATE (MTX) AND 1- β -D-C, ALONE AND IN COMBINATION

fraction (f_a) at [ara-C] of			
0.625 μM	1.25 μM	2.5 μM	5.0 μM
0.926	0.955	0.980	0.993
0.878	0.943	0.970	ND

between duplicates.

incubated in Eagle's basal medium (20) in the presence of MTX and ara-C and their mixture (molar ratio 1:0.782) and of [6- H]dUrd, at 37°C. [6- H]dUrd incorporation into perchloric acid-soluble fraction was determined as previously described (20). All measurements were

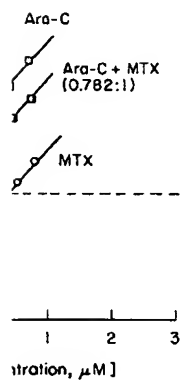


Fig. 6. Median effect plot showing the fraction affected (f_a) of [6- H]dUrd incorporation into DNA of L1210 murine leukemia cells versus concentration (μM) for Ara-C, Ara-C + MTX (0.782:1), and MTX. The data from Table 1 have been used.

and ara-C (1:0.782), the parameters are $m = 1.196$, $D_m = 34.09 \mu\text{M}$, and $r = 0.9995$. The combination index is 1.0 for all values of f_a .

ANALYSIS OF MULTIPLE DRUG EFFECTS

41

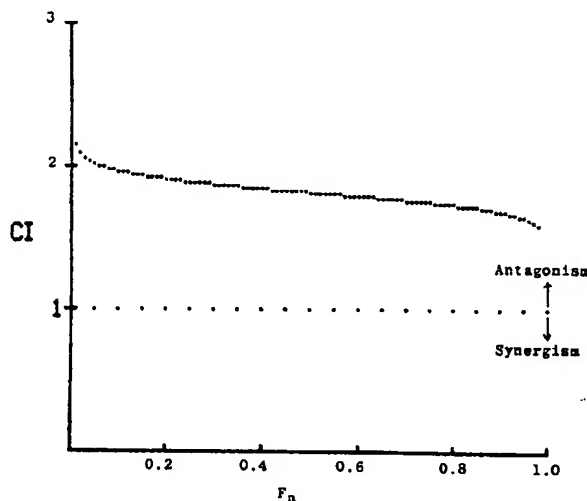


Fig. 7. Computer-generated graphical presentation of the drug combination index (CI) with respect to fraction affected (f_a) for the inhibitory effect of a mixture of methotrexate (MTX) and arabinofuranosylcytosine (ara-C) (molar ratio, 1:0.782) on the incorporation of [6- H]dUrd into DNA of L1210 murine leukemia cells. The data from Table 1 and the parameters obtained from Fig. 6 have been used for this plot on the assumption that the drugs act in a mutually exclusive manner (equation 9).

Example 4. Inhibition of the Incorporation of Deoxyuridine into the DNA of L1210 Leukemia Cells by Hydroxyurea (HU) and 5-Fluorouracil (5-FU)

Murine L1210 leukemia cells were incubated in the presence of a range of concentrations of hydroxyurea (50–3,200 μM), or 5-fluorouracil (4.0–256 μM), and of a constant molar ratio mixture of hydroxyurea and 5-fluorouracil (12.5:1), and the incorporation of deoxyuridine (dUrd) into DNA was then determined. The fractional inhibitions (f_a) of dUrd incorporation are shown in Table 2. Analysis of the results by the median effect plot (Fig. 8) gave the following parameters: for hydroxyurea, $m = 1.196$, $D_m = 34.09 \mu\text{M}$, and $r = 0.9908$; for 5-fluorouracil, $m = 1.187$, $D_m = 8.039 \mu\text{M}$, and $r = 0.9978$; and for the mixture of hydroxyurea and 5-fluorouracil (12.5:1), $m = 1.407$, $D_m = 225.8 \mu\text{M}$, and $r = 0.9776$. It is immediately apparent from Figure 8 that the effects of hydroxyurea and 5-fluorouracil are markedly antagonistic since the median-effect plot for the mixture lies to the right of both parent compounds. The degree of this antagonism falls as the level of inhibition increases, i.e. as f_a increases (Table 3). The reasons for this marked antagonism are obscure, but may be of practical importance.

TABLE 2. INHIBITION OF [6-³H]DEOXYURIDINE INCORPORATION INTO DNA IN L1210 LEUKEMIA CELLS BY HYDROXYUREA (HU), AND 5-FLUOROURACIL (5-FU), ALONE AND IN COMBINATION

HU μM	Fractional inhibition (f_0) at [5-FU] of							
	0 μM	4 μM	8 μM	16 μM	32 μM	64 μM	128 μM	256 μM
0	0	0.348	0.475	0.661	0.827	0.923	0.966	0.985
50	0.605	0.208						
100	0.741		0.168					
200	0.889			0.345				
400	0.962				0.747			
800	0.984					0.885		
1,600	0.990						0.957	
3,200	0.994							0.977

L1210 murine leukemia cells (4.5×10^6) were incubated as described in the legend to Table 1, except that the incubation period with drugs prior to the addition of [6-³H]dUrd was 40 min. The results are analyzed in Fig. 8 and Table 3.

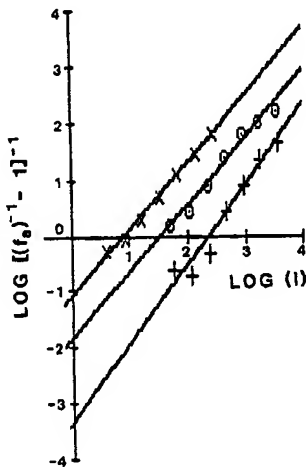


FIG. 8. Computer-generated median effect plot showing the inhibition of the incorporation of [6-³H]dUrd into DNA of L1210 murine leukemia cells by hydroxyurea (HU), (●); 5-fluorouracil (5-FU), (×), or their mixture (12.5:1), (+). The data given in Table 2 have been used. The parameters (m , D_m and r) can be obtained automatically.

Example 5. The Lethal Effects of Two Insecticides on Houseflies

Nearly 50 years ago Le Pelley and Sullivan (60) reported very careful dose-effect data for the lethality of rotenone, pyrethrins, and a mixture of these insecticides on houseflies. Adult houseflies were sprayed with alcoholic solutions of rotenone, pyrethrins, and a mixture of the two insecticides in a

ANALYSIS O

TABLE 3. CALCULATED VALUE OF COMBINATION INDEX AS A FUNCTION OF FRACTIONAL INHIBITION OF [6-³H]DEOXYURIDINE INTO DNA BY HYDROXYUREA AND

Fractional inhibition (f_0)	Combination index (CI)
0.05	
0.10	
0.20	
0.30	
0.40	
0.50	
0.60	
0.70	
0.80	
0.90	
0.95	

The combination index was calculated by the method of Finney (61) as a function of the fractional inhibition of [6-³H]dUrd by hydroxyurea and 5-FU, respectively (Eqn. 9). The combination index values are given in Table 3.

ratio by weight of 1:5. One of the main purposes of this paper is to answer the question whether the numerical results were retrieved from the original paper (60).

These quantal data were evaluated by the method of Finney (61) as were the earlier data. We have recently published the results (13). The parameters of the model are given in Table 2.

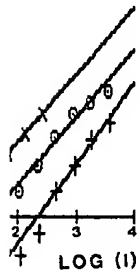
The dose-effect relationship is clearly sigmoidal (Fig. 9A) with a median-lethal dose (LD_{50}) of 1.25 μ g/cc (Fig. 9B and Table 4). The results are given in Table 4, indicating that the applicability of the model to the median-lethal doses (LD_{50} 's) is good, as calculated from the median-lethal doses (LD_{50} 's) of rotenone and pyrethrins, respectively (Fig. 9B). These values are 0.012 and 0.0012 μ g/cc from probit analysis by Finney (61) and 0.012 and 0.0012 μ g/cc, respectively.

The original authors interpreted the results as being antagonistic or synergistic effects. We have used the method for the mixture equivalence analysis to conclude that there was pronounced synergism, and Finney, after

IDINE INCORPORATION INTO DNA IN UREA (HU), AND 5-FLUOROURACIL IN COMBINATION

Fraction (f_0) at [5-FU] of				
32 μM	64 μM	128 μM	256 μM	
0.827	0.923	0.966	0.985	
0.747	0.885	0.957	0.977	

Incubated as described in the legend to Table 1, or to the addition of [^3H]dUrd was 40 min.



owing the inhibition of the incorporation of [^3H]dUrd by hydroxyurea (HU), (6); 5-fluorouracil (5-FU) in Table 2 have been used. The parameters were obtained automatically.

Insecticides on Houseflies

Sullivan (60) reported very careful studies on rotenone, pyrethrins, and a mixture of these insecticides. Houseflies were sprayed with alcoholic mixtures of the two insecticides in a

ANALYSIS OF MULTIPLE DRUG EFFECTS

43

TABLE 3. CALCULATED VALUES FOR THE COMBINATION INDEX AS A FUNCTION OF FRACTIONAL INHIBITION (F_0) OF THE INCORPORATION OF [^3H]DEOXYURIDINE INTO DNA OF L1210 LEUKEMIA CELLS BY A MIXTURE OF HYDROXYUREA AND 5-FLUOROURACIL (MOLAR RATIO 12.5:1)

Fractional inhibition (F_0)	Combination index (CI)	Diagnosis of combined effect
0.05	11.95	Antagonism
0.10	10.86	Antagonism
0.20	9.80	Antagonism
0.30	9.15	Antagonism
0.40	8.65	Antagonism
0.50	8.21	Antagonism
0.60	7.80	Antagonism
0.70	7.38	Antagonism
0.80	6.89	Antagonism
0.90	6.21	Antagonism
0.95	5.61	Antagonism

The combination index was calculated on the assumption that the two drugs are mutually exclusive (Eqn. 9). The combination index was generated by computer on the basis of parameters obtained from the median effect plot (Fig. 8).

ratio by weight of 1:5. One thousand flies were used for each dose. The data are of historical interest since four different laboratories have attempted to answer the question whether there is synergism among these insecticides. The numerical results were retrieved by Finney (9) from the diagrams contained in the original paper (60).

These quantal data were equally suitable for analysis by the median effect principles as were the earlier examples in which graded responses were analyzed. We have recently provided a preliminary analysis of these results (13). The parameters of the median effect equation are shown in Table 4.

The dose-effect relationships for rotenone, pyrethrins and their mixture are clearly sigmoidal (Fig. 9A) with slopes (m values) ranging from 2.52 to 2.75 (Fig. 9B and Table 4). The regression coefficients (r) are greater than 0.993, indicating that the applicability of the method to the data is excellent. The median-lethal doses (LD_{50} 's) for rotenone, pyrethrins and their mixture (1:5) as calculated from the median-effect plot are 0.157, 0.916 and 0.450 mg/cc, respectively (Fig. 9B). These values are in close agreement with those obtained from probit analysis by Finney (9) who obtained 0.156, 0.918 and 0.455 mg/cc, respectively.

The original authors interpreted the results as indicating no striking antagonistic or synergistic effect of the mixture. Richardson used a predictive method for the mixture equivalent to the similar action law (9) and asserted that there was pronounced synergism. Bliss supported Richardson's conclusion, and Finney, after a new analysis of data, also agreed that there

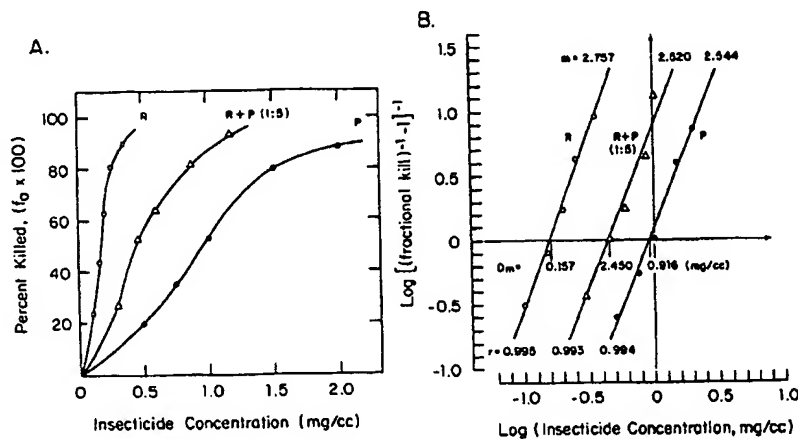


FIG. 9. Lethality of rotenone and pyrethrins to houseflies. Experimental data of LePelley and Sullivan (60), retrieved in ref. 13, were plotted for rotenone (R), pyrethrins (P), and their mixture (1:5, by weight) (R + P), on an arithmetic scale (A), and according to the median effect plot (B).

TABLE 4. TOXICITY OF ROTENONE AND PYRETHRINS TO HOUSEFLIES (60)

Insecticide	Parameters of median effect equation			
	m	D _m (mg/cc)	y-intercept	r
Rotenone	2.757 (± 0.157)	0.1571	2.216	0.9952
Pyrethrins	2.528 (± 0.158)	0.9097	0.0964	0.9960
Rotenone-Pyrethrins mixture (1:5)	2.519 (± 0.162)	0.4497	0.8743	0.9938

The m values (\pm S.E.) are the slopes of plots of $\log [(f_0)^{-1} - 1]^{-1}$ with respect to $\log (D)$, and were obtained by simple regression analysis on a programmable electronic calculator which also gives the y-intercepts and the linear regression coefficients (r). The median effect concentration is given by $\text{antilog}(-y\text{-intercept}/m)$. These results may also be obtained by the use of a computer program developed for this purpose (37).

was evidence of synergism (9). The present paper uses a new method and shows that rotenone and pyrethrins are indeed somewhat synergistic, as shown quantitatively in Figure 10.

SUMMARY

A generalized method for analyzing the effects of multiple drugs and for determining summation, synergism and antagonism has been proposed. The

ANALYSIS OF

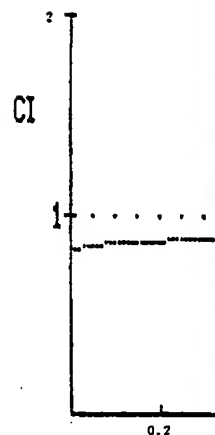
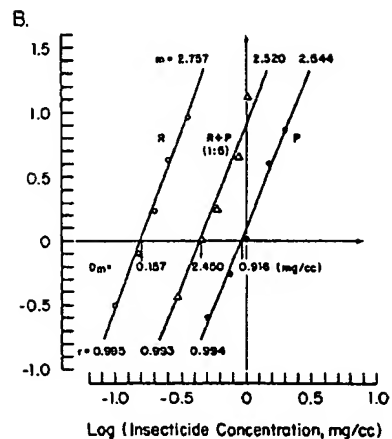


FIG. 10. Computer-generated graphical analysis to fraction affected (f_0) for the lethality to houseflies of rotenone and pyrethrins (1:5, by weight). The data of ref. 13 were used. See legend for symbols.

derived, generalized equations are relatively simple and is not limited to 1) the curves are hyperbolic or sigmoidal, 2) the interactions are exclusive or nonexclusive, 3) whether the drugs are noncompetitive or uncompetitive antagonists, or 5) the number of drugs.

The equations for the two extremes of synergism, antagonism and summation, the isobogram and fractional product method, have been shown to have limitations in their use and are used indiscriminately. The equations derived from a more generalized approach can be shown that the isobogram is mutually exclusive, whereas the fractional product method is mutually nonexclusive drugs. Furthermore, in the isobogram method combinations of drugs that would give a fractional product method tend to underestimate the summation of the effects of drugs that have sigmoidal dose-effect curves. These deficiencies and limitations



houseflies. Experimental data of LePelley and rotenone (R), pyrethrins (P), and their mixture (4), and according to the median effect plot (B).

D PYRETHRINS TO HOUSEFLIES (60)

Parameters of median effect equation

D_m (mg/cc)	$y_{\text{intercept}}$	r
0.1571	2.216	0.9952
0.9097	0.0964	0.9960
0.4497	0.8743	0.9938

$\log \{(\frac{f_0}{f_0})^{-1} - 1\}^{-1}$ with respect to $\log (D)$, and were amenable electronic calculator which also gives r . The median effect concentration is given to be obtained by the use of a computer program

present paper uses a new method and are indeed somewhat synergistic, as

ARY

the effects of multiple drugs and for antagonism has been proposed. The

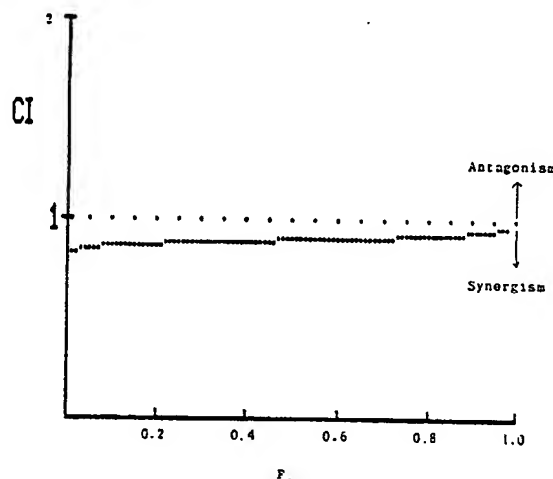


FIG. 10. Computer-generated graphical presentation of the combination index (CI) with respect to fraction affected (f_a) for the lethality to houseflies of a mixture of rotenone and pyrethrins (ratio of 1:5, by weight). The data of ref. 13 (Fig. 9) and the method of calculation described in the legend to Fig. 3 were used.

derived, generalized equations are based on kinetic principles. The method is relatively simple and is not limited by 1) whether the dose-effect relationships are hyperbolic or sigmoidal, 2) whether the effects of the drugs are mutually exclusive or nonexclusive, 3) whether the ligand interactions are competitive, noncompetitive or uncompetitive, 4) whether the drugs are agonists or antagonists, or 5) the number of drugs involved.

The equations for the two most widely used methods for analyzing synergism, antagonism and summation of effects of multiple drugs, the isobologram and fractional product concepts, have been derived and been shown to have limitations in their applications. These two methods cannot be used indiscriminately. The equations underlying these two methods can be derived from a more generalized equation previously developed by us (59). It can be shown that the isobologram is valid only for drugs whose effects are mutually exclusive, whereas the fractional product method is valid only for mutually nonexclusive drugs which have hyperbolic dose-effect curves. Furthermore, in the isobol method, it is laborious to find proper combinations of drugs that would produce an iso-effective curve, and the fractional product method tends to give indication of synergism, since it underestimates the summation of the effect of mutually nonexclusive drugs that have sigmoidal dose-effect curves. The method described herein is devoid of these deficiencies and limitations.

The simplified experimental design proposed for multiple drug-effect analysis has the following advantages: 1) It provides a simple diagnostic plot (i.e., the median-effect plot) for evaluating the applicability of the data, and provides parameters that can be directly used to obtain a general equation for the dose-effect relation; 2) the analysis which involves logarithmic conversion and linear regression can be readily carried out with a simple programmable electronic calculator and does not require special graph paper or tables; and 3) the simplicity of the equation allows flexibility of application and the use of a minimum number of data points. This method has been used to analyze experimental data obtained from enzymatic, cellular and animal systems.

ACKNOWLEDGEMENTS

The authors wish to thank Joseph H. I. Chou of The Lawrenceville School, Lawrenceville, New Jersey, for developing the computer programs. These studies were supported by Grants from the National Institutes of Health (CA 27569, CA 18856 and AM 07422) and from the American Cancer Society (SIG-3).

REFERENCES

1. J. L. WEBB, *Enzyme and Metabolic Inhibitors*, Vol. 1, pp. 55-79. Academic Press, New York (1963).
2. M. DIXON and E. C. WEBB, *Enzymes*, 3rd ed., pp. 332-381, Academic Press, New York (1979).
3. W. W. CLELAND, The kinetics of enzyme catalyzed reactions with two or more substrates or products, *Biochim. Biophys. Acta* 67, 173-196 (1963).
4. I. H. SEGEL, Multiple inhibition analysis, pp. 465-503 in *Enzyme Kinetics*, John Wiley & Sons, New York (1975).
5. T. C. CHOU, Relationships between inhibition constants and fractional inhibition in enzyme-catalyzed reactions with different numbers of reactants, different reaction mechanisms, and different types and mechanisms of inhibition, *Mol. Pharmacol.* 10, 235-247 (1974).
6. T. C. CHOU, Derivation and properties of Michaelis-Menten type and Hill type equations for reference ligands, *J. Theor. Biol.* 59, 253-276 (1976).
7. T. C. CHOU, On the determination of availability of ligand binding sites in steady-state systems, *J. Theor. Biol.* 65, 345-356 (1977).
8. T. C. CHOU and P. TALALAY, A simple generalized equation for the analysis of multiple inhibitions of Michaelis-Menten kinetic systems, *J. Biol. Chem.* 252, 6438-6442 (1977).
9. D. J. FINNEY, *Probit Analysis*, 2nd ed., pp. 146-153, Cambridge University Press, Cambridge (1952).
10. C. I. BLISS, *Statistics in Biology I*, McGraw-Hill, New York (1967).
11. L. J. REED and J. BERKSON, The application of the logistic function to experimental data, *J. Physical Chem.* 33, 760-779 (1929).
12. C. O. NORDLING, A new theory of the cancer-inducing mechanism, *Brit. J. Cancer* 7, 68-72 (1953).
13. T. C. CHOU and P. TALALAY, Analysis of combined drug effects: A new look at a very old problem, *Trends in Pharmacol. Sci.* 4, 450-454 (1983).
14. L. MICHAELIS and M. L. MENTEN, 333-369 (1913).
15. A. V. HILL, The combinations of *Biochem. J.* 7, 471-480 (1913).
16. I. LANGMUIR, The adsorption of *Am. Chem. Soc.* 40, 1361-1403 (1918).
17. W. M. CLARK, *The Determination of Insecticides*, Baltimore (1928).
18. G. SCATCHARD, The attractions of *Acad. Sci.* 51, 660-672 (1949).
19. R. J. TALLARIDA and L. S. JACOBI, *Handbook of Pharmacology*, Academic, New York (1979).
20. T. C. CHOU, D. J. HUTCHINSON, Selective effects of 1- β -D-arabinofuranose on *Escherichia coli*, *Res.* 35, 225-236 (1975).
21. A. B. KREMER, R. M. EGAN and J. H. TALLARIDA, Arginine residues are essential for *Acinetobacter* *glutamate dehydrogenase* activity, *Res.* 36, 237-244 (1976).
22. M. BOUNIAS, Correlations between *glucosidase* kinetics in *Apis mellifera* and *Acinetobacter* *glutamate dehydrogenase* activity, *Res.* 36, 245-252 (1976).
23. P. FINOTTI and P. PALATINI, Carboxypeptidase A: Activation by *Ca*²⁺ and inhibition by *sodium-potassium-activated adenosine triphosphatase*, *Res.* 36, 784-790 (1981).
24. K. HATA, M. HAYAKAWA, Y. KAWABE and T. KAWABE, Properties of γ -glutamyl transpeptidase, *Res.* 36, 681-692 (1981).
25. M. BOUNIAS, Kinetic study of the inhibition of *Acinetobacter* *glutamate dehydrogenase* by *BAYe* 4609, *BAYg* 5421, *Res.* 36, 537-544 (1982).
26. J. STECKEL, J. ROBERT, F. S. TELLER and J. TALLARIDA, Inhibition of *Acinetobacter* *glutamate dehydrogenase* by *Acinetobacter* *glutamate dehydrogenase* inhibitor, *Res.* 36, 545-552 (1983).
27. S. J. FRIEDMAN and P. SKEHAN, Inhibition of *Acinetobacter* *glutamate dehydrogenase* by *D-glucosamine*, *Proc. Natl. Acad. Sci. USA* 73, 1000-1004 (1976).
28. R. ROSENBERG, A kinetic analysis of the inhibition of *Acinetobacter* *glutamate dehydrogenase* by *D-glucosamine*, *Biochim. Biophys. Acta* 649, 262-268 (1981).
29. T. C. CHOU, A general procedure for the analysis of multiple inhibitions, *Res.* 36, 269-276 (1982).
30. T. C. CHOU, Comparison of dose-response curves for low-dose and high-dose *DMBA* in *carcinogenesis*, *Carcinogenesis* 1, 203-213 (1980).
31. T. C. CHOU, Carcinogenic risk assessment by *Acinetobacter* *glutamate dehydrogenase* assay, *Res.* 36, 277-284 (1982).
32. M. N. TELLER, C. STOCK, M. BOUNIAS, DMBA-induced rat mammary carcinogenesis and inhibition by *Acinetobacter* *glutamate dehydrogenase*, *Res.* 36, 285-292 (1982).
33. K. M. MURPHY and S. H. SNEYD, Inhibition of *Acinetobacter* *glutamate dehydrogenase* by *DMBA*, *Mol. Pharmacol.* 22, 111-116 (1982).
34. G. VAUQUELIN, C. ANDRE, J. STROSBERG, Agonist-mediated inhibition of *Acinetobacter* *glutamate dehydrogenase* by *DMBA*, *Europ. J. Biochem.* 125, 117-122 (1982).
35. T. VISWANATHAN and W. H. HARRIS, Inhibition of *Acinetobacter* *glutamate dehydrogenase* by naphthoflavones, *Res.* 36, 303-310 (1982).
36. S. M. SMITH, A model of ligand binding to *Acinetobacter* *glutamate dehydrogenase*, *Res.* 36, 311-318 (1982).
37. J. CHOU, T. C. CHOU and P. TALALAY, Inhibition of *Acinetobacter* *glutamate dehydrogenase* by *DMBA*, *Res.* 36, 319-326 (1982).

ANALYSIS OF DRUG EFFECTS

proposed for multiple drug-effect
1) It provides a simple diagnostic plot
ing the applicability of the data, and
used to obtain a general equation for
which involves logarithmic conversion
ried out with a simple programmable
especial graph paper or tables; and 3)
bility of application and the use of a
s method has been used to analyze
natic, cellular and animal systems.

GEMENTS

I. Chou of The Lawrenceville School,
ping the computer programs. These
the National Institutes of Health (CA
from the American Cancer Society

NCES

s, Vol. 1, pp. 55-79. Academic Press, New York

led., pp. 332-381, Academic Press, New York

atalyzed reactions with two or more substrates
-196 (1963).

pp. 465-503 in *Enzyme Kinetics*, John Wiley &

bition constants and fractional inhibition in
t numbers of reactants, different reaction
hanisms of inhibition, *Mol. Pharmacol.* 10,

Michaelis-Menten type and Hill type equations
1-276 (1976).

ability of ligand binding sites in steady-state

eneralized equation for the analysis of multiple
tems, *J. Biol. Chem.* 252, 6438-6442 (1977).
, pp. 146-153, Cambridge University Press,

w-Hill, New York (1967).
ation of the logistic function to experimental
cancer-inducing mechanism, *Brit. J. Cancer* 7,
combined drug effects: A new look at a very old
454 (1983).

ANALYSIS OF MULTIPLE DRUG EFFECTS

47

14. L. MICHAELIS and M. L. MENTEN, Die Kinetik der Invertinwirkung, *Biochem. Z.* 49, 333-369 (1913).
15. A. V. HILL, The combinations of hemoglobin with oxygen and with carbon monoxide, *Biochem. J.* 7, 471-480 (1913).
16. I. LANGMUIR, The adsorption of gases on plane surfaces of glass, mica and platinum, *J. Am. Chem. Soc.* 40, 1361-1403 (1918).
17. W. M. CLARK, *The Determination of Hydrogen Ions*, Williams and Wilkins, 3rd ed., Baltimore (1928).
18. G. SCATCHARD, The attractions of proteins for small molecules and ions, *Ann. N. Y. Acad. Sci.* 51, 660-672 (1949).
19. R. J. TALLARIDA and L. S. JACOB, *Dose-Response Relation in Pharmacology*, Springer-Verlag, New York (1979).
20. T. C. CHOU, D. J. HUTCHINSON, F. A. SCHMID and F. S. PHILIPS, Metabolism and selective effects of 1- β -D-arabinofuranosylcytosine in L1210 and host tissues *in vivo*, *Cancer Res.* 35, 225-236 (1975).
21. A. B. KREMER, R. M. EGAN and H. Z. SABLE, The active site of transketolase: Two arginine residues are essential for activity, *J. Biol. Chem.* 255, 2405-2410 (1980).
22. M. BOUNIAS, Correlations between glucose-inhibition and control parameters of α -glucosidase kinetics in *Apis mellifica* haemolymph, *Experientia* 36, 157-159 (1980).
23. P. FINOTTI and P. PALATINI, Canrenone as a partial agonist at the digitalis receptor site of sodium-potassium-activated adenosine triphosphatase, *J. Pharmacol. Exptl. Therap.* 217, 784-790 (1981).
24. K. HATA, M. HAYAKAWA, Y. ABIKO and H. TAKIGUCHI, Purification and properties of γ -glutamyl transpeptidase from bovine parotid gland, *Int. J. Biochem.* 13, 681-692 (1981).
25. M. BOUNIAS, Kinetic study of the inhibition of the honeybee haemolymph α -glucosidase *in vitro* by BAYe 4609, BAYg 5421 and BAYn 5595, *Biochem. Pharmacol.* 31, 2769-2775 (1982).
26. J. STECKEL, J. ROBERT, F. S. PHILIPS and T. C. CHOU, Kinetic properties and inhibition of *Acinetobacter* glutaminase-asparaginase, *Biochem. Pharmacol.* 32, 971-977 (1983).
27. S. J. FRIEDMAN and P. SKEHAN, Membrane-active drugs potentiate the killing of tumor cells by D-glucosamine, *Proc. Natl. Acad. Sci. USA* 77, 1172-1176 (1980).
28. R. ROSENBERG, A kinetic analysis of L-tryptophan transport in human red blood cells, *Biochim. Biophys. Acta* 649, 262-268 (1981).
29. T. C. CHOU, A general procedure for determination of median-effect doses by a double logarithmic transformation of dose-response relationships, *Federation Proc.* 34, 228 (1975).
30. T. C. CHOU, Comparison of dose-effect relationships of carcinogens following low-dose chronic exposure and high-dose single injection: An analysis by the median-effect principle, *Carcinogenesis* 1, 203-213 (1980).
31. T. C. CHOU, Carcinogenic risk assessment by a mass-action law principle: Application to large scale chronic feeding experiment with 2-acetylaminofluorene (2-AAF), *Proc. Am. Assoc. Cancer Res.* 22, 141 (1981).
32. M. N. TELLER, C. STOCK, M. BOWIE, T. C. CHOU and J. M. BUDINGER, Therapy of DMBA-induced rat mammary carcinomas with combinations of 5-fluorouracil and 2 α -methylidihydrotestosterone propionate, *Cancer Res.* 42, 4408-4412 (1982).
33. K. M. M. MURPHY and S. H. SNYDER, Heterogeneity of adenosine A₁ receptor binding in brain tissue, *Mol. Pharmacol.* 22, 250-257 (1982).
34. G. VAUQUELIN, C. ANDRE, J. P. DeBACKER, P. LAUDURON and A. D. STROSBERG, Agonist-mediated conformational changes of muscarinic receptors in rat brain, *Europ. J. Biochem.* 125, 117-124 (1982).
35. T. VISWANATHAN and W. F. ALWORTH, Effects of 1-arylpurroles and naphthoflavones upon cytochrome P-450 dependent monooxygenase activities, *J. Med. Chem.* 24, 822-830 (1981).
36. S. M. SMITH, A model of labelled-ligand displacement assay resulting in logit-log relationships, *J. Theor. Biol.* 98, 475-499 (1982).
37. J. CHOU, T. C. CHOU and P. TALALAY, Computer simulation of drug effects:

Quantitation of synergism, summation and antagonism of multiple drugs. *Pharmacologist* 25, 175 (1983).

38. A. GOLDIN and N. MANTEL, The employment of combinations of drugs in the chemotherapy of neoplasia: A review, *Cancer Res.* 17, 635-654 (1957).
39. M. C. BERENBAUM, Synergy, additivism and antagonism in immunosuppression: A critical review, *Clin. Exptl. Immunol.* 28, 1-18 (1977).
40. S. LOEWE, Die quantitation probleme der pharmakologie, *Ergebn. Physiol.* 27, 47-187 (1928).
41. S. LOEWE, The problem of synergism and antagonism of combined drugs, *Arzneimittelforsch.* 3, 285-320 (1953).
42. J. L. WEBB, Effect of more than one inhibitor, pp. 66-79, 488-512, in *Enzyme and Metabolic Inhibitors*, Vol. 1, Academic Press, New York (1963).
43. H. VELDSTRA, Synergism and potentiation with special reference to the combination of structural analogues, *Pharmacol. Rev.* 8, 339-388 (1956).
44. B. W. LACEY, Mechanisms of chemotherapeutic synergy, pp. 247-287, in *The Strategy of Chemotherapy* (S. T. COWAN and E. ROWATT, eds.), Cambridge University Press, Cambridge (1958).
45. L. S. GOODMAN, The problem of drug efficacy: An exercise in dissection, pp. 49-67 in *Drugs in Our Society* (P. TALALAY, ed.), The Johns Hopkins University Press, Baltimore (1964).
46. J. M. VENDITTI and A. GOLDIN, Drug synergism in anti-neoplastic chemotherapy, pp. 397-498 in *Advances in Chemotherapy*, Vol. 1 (A. GOLDIN and F. HAWKING, eds.), Academic Press, New York (1964).
47. A. C. SARTORELLI, Approaches to the combination chemotherapy of transplantable neoplasms, pp. 229-273 in *Progress in Experimental Tumor Research*, Vol. 6 (F. HOMBURGER, ed.), Hanfer Publishing Co. Inc., New York (1965).
48. A. GOLDIN, J. M. VENDITTI, N. MANTEL, I. KLINE and M. GANG, Evaluation of combination chemotherapy with three drugs, *Cancer Res.* 28, 950-960 (1968).
49. H. E. SKIPPER, Combination therapy: Some concepts and results, *Cancer Chemother. Rep.* 5, 137-146 (1974).
50. F. M. SCHABEL, Synergism and antagonism among antitumor agents, pp. 595-623 in *Pharmacological Basis of Cancer Chemotherapy*, Williams & Wilkins Co., Baltimore (1975).
51. G. B. GRINDEY, R. G. MORAN and W. C. WERKHEISER, Approaches to the rational combination of antimetabolites for cancer chemotherapy, pp. 169-249 in *Drug Design*, Vol. 5 (E. J. ARIENS, ed.), Academic Press, New York (1975).
52. F. H. JOHNSON, H. EYRING, R. STEBLAY, H. CHAPLIN, C. HUMBER and G. GHERADI, The nature and control of reactions in bioluminescence. *J. Gen. Physiol.* 28, 463-537 (1945).
53. K. YAGI and T. OZAWA, Complex formation of apo-enzyme, coenzyme and substrate of D-amino acid oxidase, *Biochim. Biophys. Acta* 42, 381-387 (1960).
54. E. J. ARIENS and A. M. SIMONIS, Analysis of the action of drugs and drug combinations, pp. 286-311, 318-327, in *Quantitative Methods in Pharmacology* (H. DE JONGE, ed.), Interscience, New York (1961).
55. T. YONETANI and H. THEORELL, Studies on liver alcohol dehydrogenase complexes. III. Multiple inhibition kinetics in the presence of two competitive inhibitors, *Arch. Biochem. Biophys.* 106, 243-251 (1964).
56. T. KELETI and C. FAJSZI, The system of double inhibitions, *Math. Biosci.* 12, 197-215 (1971).
57. C. FAJSZI, Methods of analysis of double inhibitor experiments, *Symp. Biol. Hung.* 18, 77-103 (1974).
58. D. B. NORTHRUP and W. W. CLELAND, The kinetics of pig heart triphosphopyridine nucleotide-isocitrate dehydrogenase, *J. Biol. Chem.* 249, 2928-2931 (1974).
59. T. C. CHOU and P. TALALAY, Generalized equations for the analysis of inhibitions of Michaelis-Menten and higher-order kinetic systems with two or more mutually exclusive and nonexclusive inhibitors, *Europ. J. Biochem.* 115, 207-216 (1981).
60. R. H. LE PELLEY and W. N. SULLIVAN, Toxicity of rotenone and pyrethrins alone and in combination, *J. Econom. Entomol.* 29, 791-797 (1936).

ANALYSIS OF M

A
DERIVATION OF FRA
AND ISOBOLOGRAM
APPLICABILITY AN
M

Derivation of Fractional Product E

Many investigators have assumed that inhibitors can be expressed by the equation $f_u = (f_u)_1 \times (f_u)_2$, as formalized by Williams (1964). The independence of inhibitor action is assumed.

Since $f_u = 1 - f_u$, equation 3 can be written as

$$(f_u)_{1,2} = (f_u)_1 \times (f_u)_2$$

or $[1 - (f_u)_{1,2}] = [1 - (f_u)_1] [1 - (f_u)_2]$

It is, therefore, clear that the analysis of the data is based on the assumption of mutually nonexclusive first-order reactions.

Limitations of Fractional Product E

The widely used fractional product method has serious limitations when applied to enzyme systems. This method does not take into consideration the dose-effect curve and the case where the dose-effect curve is not linear. The following sample calculations shown in Table 5 illustrate that the fractional product method is valid with respect to the following conditions: 1) the drugs are noncompetitive, 2) the dose-effect curve is linear, and 3) the Michaelis-Menten-type hyperbolic curve is valid.

As shown in Table 5, when the fractional product method is applied to the data obtained with two mutually nonexclusive drugs and two competitive drugs, and, thus, may lead to false conclusions. The dose-effect curve is inversely sigmoidal, the fractional product method will overestimate the combined antagonism. However, the inverse sigmoidal dose-effect curve is particularly prominent at low f_u values, and the two nonexclusive drugs produce greater inhibition than the two competitive drugs at any level of sigmoidicity.

Peptide and Small Molecule Microarray for High Throughput Cell Adhesion and Functional Assays

James R. Falsey,[†] M. Renil,[†] Steven Park, Shijun Li, and Kit S. Lam*

UC Davis Cancer Center, Division of Hematology/Oncology, and Department of Internal Medicine, University of California Davis, 4501 X Street, Sacramento, California 95817. Received November 21, 2000

A novel class of chemical microchips consisting of glass microscope slides was prepared for the covalent attachment of small molecule ligands and peptides through site-specific oxime bond or thiazolidine ring ligation reaction. Commercially available microscope slides were thoroughly cleaned and derivatized with (3-aminopropyl)triethoxysilane (APTES). The amino slides were then converted to glyoxylyl derivatives via two different routes: (1) coupling of Fmoc-Ser followed by deprotection and oxidation, or (2) coupling with protected glyoxylic acid and final deprotection with HCl. Biotin or peptide ligands derivatized at the carboxyl terminus with a 4,7,10-trioxa-1,13-tridecanediamine succinimic acid linker and an amino-oxy group or a 1,2-amino-thiol group (e.g., cysteine with a free N^{α} -amino group) were printed onto these slides using a DNA microarray spotter. After chemical ligation, the microarray of immobilized ligands was analyzed with three different biological assays: (1) protein-binding assay with fluorescence detection, (2) functional phosphorylation assay using $[\gamma^{33}\text{P}]\text{-ATP}$ and specific protein kinase to label peptide substrate spots, and (3) adhesion assay with intact cells. In the cell adhesion assay, not only can we determine the binding specificity of the peptide against different cell lines, we can also determine functional cell signaling of attached cells using immuno-fluorescence techniques *in situ* on the microchip. This chemical microchip system enables us to rapidly analyze the functional properties of numerous ligands that we have identified from the “one-bead one-compound” combinatorial library method.

INTRODUCTION

Ever since the introduction of solid-phase peptide synthesis by Professor Bruce Merrifield in 1963, there has been a revolutionary advancement in peptide and organic synthesis (1). This technique was rapidly improved and modified for the synthesis of long peptides or proteins, peptide libraries and even small organic molecule libraries (2–5). A decade ago, by adopting the solid-phase peptide synthesis method, we reported the synthesis and screening of a “one-bead one-compound” combinatorial peptide library (6, 7). In this method, using a split synthesis approach (6, 8, 9), millions of peptide-beads were generated such that each bead displays only one chemical entity (6, 7). Because each compound-bead is spatially separable, the “one-bead one-compound” combinatorial library can be viewed as a huge microarray platform that is not addressable. Using various screening techniques (7), we can identify the compound-beads with a specific biological, chemical, or physical property and isolate them for structural determination. Over the last 10 years, we have successfully used this technology to identify ligands for various protein targets (6, 10–13) or small molecule dyes (14), and peptide substrates for various protein kinases (15–17). In addition, using intact cell lines as a probe, we were able to identify ligands that bind to cell surface receptors (18). Many ligands for various molecular targets can be identified with this combinatorial approach. There is an urgent need for the development of a highly miniaturized and high-throughput technique to characterize the binding specificity of

these ligands. The DNA microarray technique has been developed in recent years as a powerful tool for genomic analysis. In this method, thousands of genes (cDNA) are immobilized as individual tiny spots on microscope slides, and fluorescent-labeled cDNA derived from mRNA of whole cell lysate is then used to probe the gene microarray (19, 20). This elegant technique enables one to determine expression levels of multiple genes in one single experiment. This method has inspired us to develop a peptide and small molecule microarray based technique to achieve our goal of rapidly analyzing the binding and functional properties of the leads identified from our combinatorial libraries. We reported the chemical microarray work at the American Peptide Symposium in June of 1999 (21). Independently, a similar microarray method has also been reported by Schreiber's group (22). More recently, MacBeath and Schreiber modified their method to protein microarrays (23).

Spot synthesis on cellulose sheets and light-directed parallel synthesis on special glass slides have already been reported for the generation of peptides in a microarray format (24, 25). Photogenerated acids have been introduced to make the light-directed synthesis simpler on a glass slide for microarray preparation (26). Proteins and enzymes have been immobilized on either acrylamide-gel pads or glass slides with special Teflon cover in a microarray format for high throughput screening (27, 28). In these cases, proteins or enzymes are bound to the slides through covalent nonspecific site of attachment, or noncovalently by hydrophobic or electrostatic interaction. Several types of chemistries have been applied in a DNA microarray system using glass surface modified with amino, epoxide, carboxylic acid, aldehyde, or sulfhydryl groups (29, 30). Schreiber's group has reported

* Corresponding author: Kit S. Lam, Tel (916)734-8012, Fax (916)734-7946, Kit.lam@ucdmc.ucdavis.edu.

[†] J. Falsey and M. Renil contributed equally to the project.

the Michael addition of thiol-containing compounds onto maleimide-derivatized glass slides for the microarray printing of small molecules (22). In the last five years, chemoselective ligation methods have been developed to chemically link unprotected peptide fragments together to form larger peptides or proteins (31–34). These coupling reactions are efficient and highly specific. We have reported the use of these ligation methods to iodinate peptide (35) and to derivatize the N-terminal cysteine of a single chain monoclonal antibody molecule via thiazolidine ring formation (36). In this report we applied this chemoselective ligation reaction to covalently attach peptides or small molecules onto the glyoxylyl-derivatized glass slide via oxime bond or thiazolidine ring formation. These chemical microarrays were then subjected to a number of biological assays, including protein binding, substrate phosphorylation, and cell adhesion.

EXPERIMENTAL PROCEDURES

Materials. Avidin-Cy5 and Streptavidin-Cy3 were obtained from Pharmacia, Amersham; anti-phosphotyrosine antibody-FITC and anti-Mouse IgG-Cy5 conjugates from Sigma, St. Louis, MO; Calcein AM or Cell-Tracker Orange from Molecular Probes, Eugene, OR; anti- β -endorphin monoclonal antibody (clone 3-E7) was obtained from Boehringer Mannheim, Indianapolis, IN; *O*-(hydrazinocarbonyl methyl) *O*-methyl-poly(ethylene glycol)-5000 (PEG₅₀₀₀-NHNH₂) from Fluka, Milwaukee, WI; stearic acid, glyoxylic acid, all other fatty acids and other chemicals used in this study were obtained from Aldrich Chem Co., Milwaukee, WI. All Fmoc-protected amino acids and resins were purchased from Nova-Bachem, Switzerland or Advanced ChemTech, Louisville, KY; human p60^{src} protein tyrosine kinase was purchased from Upstate Biotechnology Inc., Lake Placid, NY. Thin-wall polycarbonate 96 well plates were obtained from Corning Inc. New York, NY. Ordinary microscope slides were obtained from Corning or Fisher, and amino-functionalized slides from CEL Associates, Houston TX. The anti-human insulin antibody was purified from ascites derived from HB125 murine hybridoma cell line (ATCC) using a protein G column (Pharmacia).

Preparation of Glyoxylyl Modified Glass Slides. Ordinary glass microscope slides (75 mm \times 25 mm; 1.06 mm thickness) were cleaned extensively by dipping in 1% NaOH followed by 3% HCl both at 90 °C for 10 min. The slides were then placed in boiling 35% HNO₃ in a reaction vessel fitted with a water condenser and the outlet passed through cold 1% NaOH solution for 1 h. The slides were thoroughly washed six times with distilled water, followed by methanol, and dried under vacuum overnight. The dry slides were dipped in 2% (3-amino-propyl)triethoxysilane (APTES) in dry toluene containing anhydrous NaSO₄ or 4 Å molecular sieves and stirred at room temperature for 3 h. The amino slides were thoroughly washed with toluene followed by dichloromethane (DCM) and N₂ dried. The slides were then cured overnight at 190 °C. The amino slides were placed in a Fmoc-Ser-OH solution (50 mM) in DMF along with DIC and HOBr (50 mM each) for 1.5 h and washed five times with DMF. The Fmoc group was removed by 20% (v/v) piperidine in DMF, and the deprotected Ser was oxidized by a NaIO₄ solution (100 mM) for 2 h. This procedure results in surface derivatization of both sides of the slides by a glyoxylyl group.

Alternatively, we have also used protected glyoxylic acid to derivatize the amino slide. To a solution of glyoxylic acid (1 M) in DMF was added HCl to give a

concentration of 0.1 mM, followed by addition of ethylene glycol to give a final concentration of 5 M. The solution was allowed to react in a boiling water bath for 30 min to obtain protected glyoxylic acid. The product was directly used for DIC-HOBr coupling reaction. The amino slides were placed in a solution of freshly prepared protected glyoxylic acid (10 mM), stearic acid (40 mM), DIC (50 mM), and HOBr (50 mM) dissolved in DMF and stirred at room temp for 2 h. The slides were washed with DMF (four times) and DCM (three times) and air-dried. The acetal protecting group was removed by placing the slides in 0.01 M HCl solution with stirring at room temp for 2 h. Finally the glyoxylyl slides were washed four times with distilled water and three times with methanol and dried under vacuum overnight. In a similar manner, different fatty acids (in place of stearic acid) along with different proportions of glyoxylic acid were used for the slide preparation.

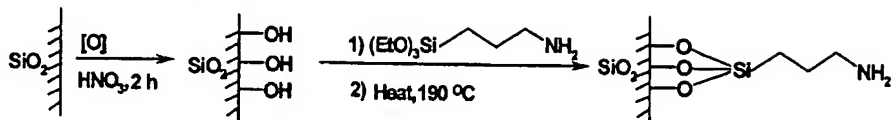
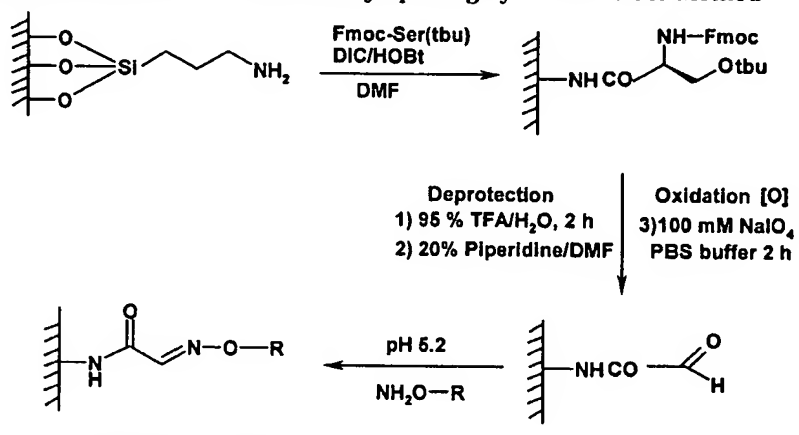
Peptide Synthesis. Peptides were synthesized according to standard Fmoc-chemistry on Rink resin. After TFA cleavage, the peptides were purified on a C-18 reverse phase column (Vydac, Hesperia, CA) using a Beckman HPLC system and characterized by ESMS. The hydrophilic linker, Fmoc-4,7,10-trioxa-1,13-tridecanediamine succinimic acid (Fmoc-Ttds-OH), was synthesized according to our previous report (36), and its purity was confirmed by HPLC and ES MS.

Microarray Spotting. Peptides or biotin containing a Ttds-linker and an amino-oxyacetyl group or Lys (Cys) at their carboxyl termini were used for microarray spotting. The compounds were dissolved in 300 mM NaCl and 250 mM NaOAc (pH 5.2) at a concentration of 1–3 mM and distributed into a thin-wall polycarbonate 96 well plate (15 μ L per well). Both linear and array mode of spotting were carried out using the Affymatrix 417 arrayer (Santa Clara, CA). A spacing of 500 μ m or 300 μ m was employed between the spots with one to three repetitions for each spot. Soon after spotting, the slides were transferred to a plastic rack inside a plastic box containing saturated NaCl and incubated at room temperature overnight. The slides were thoroughly washed with distilled water, air-dried, and stored under N₂.

Fluorescent Binding Assay. The microarray slides were blocked for 3 h with 1% (w/v) BSA solution in PBS (1 mL per slide), rinsed with water (six times), and air-dried. Protein labeled with fluorescent dye Cy3 or Cy5 (1–2 μ g /ml) was added to the slides and kept in dark for 45 min. In the case of secondary antibody detection technique, the slides were first incubated with the primary antibody (anti-insulin antibody or anti- β -endorphin antibody) for 1.5 h and washed with distilled water, followed by incubation with fluorescent dye conjugated secondary antibody for 45 min. The slides were washed with deionized water, air-dried, and scanned on both channels of the General Scanning (ScanArray 3000) confocal microscope fluorescence scanner.

Protein Kinase Functional Assay. The microarray slides were blocked with 1% BSA solution in PBS as mentioned above. Human p60^{src} protein tyrosine kinase (30 units) and [γ ³³P]-ATP (3000 Ci/mmol) were mixed in 1 mL of MES buffer (50 mM, pH 6.8) and placed over the slides and allowed to react for 5 h. The slides were washed thoroughly with deionized water and placed in boiling HCl (1 M) for 5 min. The slide was rinsed with water, air-dried, and exposed to low energy X-ray film (Kodak Biomax MR film) for 5 h, after which the film was developed.

Cell Adhesion Assay. To block nonspecific binding of the cells, each slide was covered with 1 mL of

Scheme 1. Preparation of Amino Slides**Scheme 2. Preparation of Glass Slides for Microarray Spotting by the Fmoc-Ser Method**

O-(hydrazinocarbonyl methyl)-*O*-methyl-poly(ethylene glycol)-5000 (PEG₅₀₀₀-NHNH₂, 2 mM) in 0.2 mM NaOAc buffer at pH 5.2. After 4 h, the slides were rinsed with deionized H₂O and dried in a desiccator. The slides were then covered with a suspension of intact cancer cell line (2×10^6 cells in 1 mL of medium) and incubated at room temperature for 30 min. After gentle washing with PBS, if the slides were to be studied under fluorescent microscope or array scanner, the cells were then stained with Calcein AM or Cell-Tracker Orange, respectively. After 30 min of incubation, the slides were washed gently with PBS before analysis. In some experiments, the bound cells were fixed with acetone and stained with Giemsa stain.

Immunofluorescence Microscopy. Immunofluorescence microscopy was performed in continuation of cell adhesion assay. After cell binding, the slides were covered with 1 mL of 3.7% paraformaldehyde to fix the cells. After 15 min, paraformaldehyde solution was aspirated, and the slides were washed with 0.5% Triton X-100 in TBS buffer for 5 min and TBS for another 5 min. To detect the effect of cell adhesion on intracellular tyrosine phosphorylation of proteins, 45 μ L of FITC conjugated anti-phosphotyrosine antibody (1/40 dilution) was added. The slides were incubated for 1 h at room temperature and washed in TBS for 5 min. The slides were then mounted for observation under fluorescent microscope. For the negative control slide (without peptide), cell attachment to the glass slide was accomplished with cytopsin. The cells were then fixed, processed, and examined under the fluorescent microscope as above.

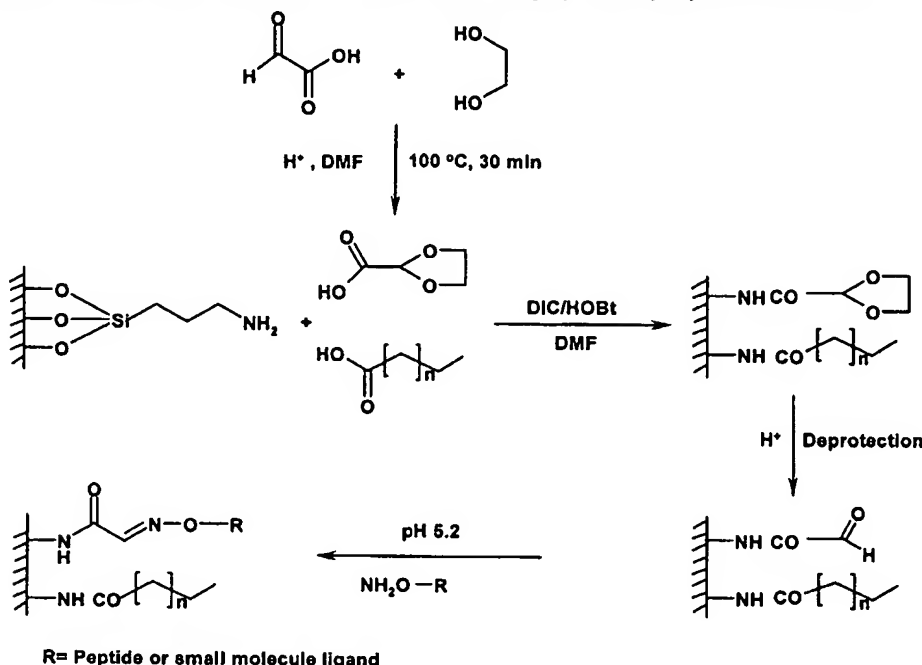
RESULTS AND DISCUSSION

Slide Preparation. We have tried various commercially available microscope slides for this microarray technique. Corning and Fisher slides were found to be the best for our purpose. First the slides were treated with NaOH and HCl, followed by boiling with HNO₃ to remove all organic matter and free up more surface Si-OH groups for the derivatization with APTES. Optimal conditions for the amino modification was to incubate 2% APTES solution in dry toluene for 3 h (Scheme 1). Strict

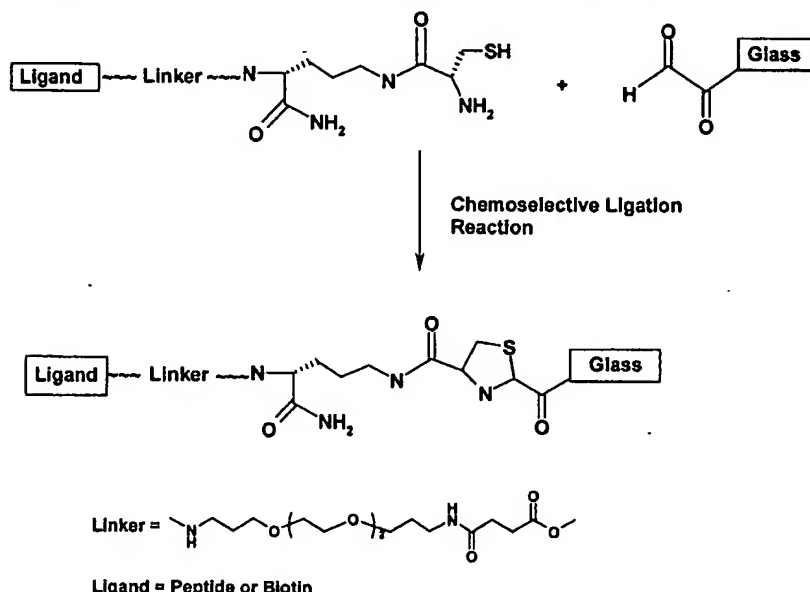
anhydrous conditions were maintained during this step to avoid white precipitate formation on the surface of the slides (probably a polymer of the silane). We have also tried prederivatized amino slides from CEL Associates with satisfactory results. The amino slides reacted with Fmoc-Ser in the presence of DIC, HOBt, followed by removal of the Fmoc group. Final oxidation with NaIO₄ will generate slides with a uniform coating of glyoxyl groups (Scheme 2). Alternatively acetal protected glyoxylic acid was directly coupled to the amino slides followed by deprotection with dilute HCl (Scheme 3). We have found that this alternative method is more convenient, efficient, and consistent. To maximize the signal-to-noise ratio, we need to create a glass surface that has minimal nonspecific binding during biological assays. In addition, the printed chemical spots need to be uniform, precise, and cannot spread to the adjacent areas of the microarray. We believe that these requirements can be achieved through (1) the creation of an optimal hydrophobic-hydrophilic balance on the glass surface, and (2) the use of appropriate blocking agents prior to the biological assays. To achieve these goals, we added various fatty acids such as butyric, valeric, hexanoic, heptanoic, octanoic, decanoic, lauric, myristic, palmitic, and stearic acids separately along with protected glyoxylic acid during the coupling step. Stearic acid was found to be best in this regard. We also tried various ratios of glyoxylic acid to stearic acid and found that a 1:4 ratio was optimal for the least nonspecific binding and reproducible well-defined spots. These slides are designated as (10:40) slides. Slides without the addition of fatty acids tend to generate larger spots that often spread to the adjacent areas. This is probably due to the hydrophilic character of the modified glass surface that leads to greatly reduced surface tension between the aqueous spot and the surface of the slide. Spots generated from the (10:40) slides are smaller and usually do not have the problem with spreading.

Peptides were synthesized by Fmoc-chemistry using DIC/HOBt as coupling reagents. The Ttds-linker was used to connect the carboxyl terminus of the peptide to the glass slide as shown in Scheme 4. The linker is

Scheme 3. Preparation of Glass Slides for Microarray Spotting by the Glyoxylic Acid Method



Scheme 4. Covalent Attachment of Peptides or Small Molecules to a Glass Slide via a Thiazolidine Ring



critical in some biological assays (see below). The glyoxylyl group exhibits desirable reactivity in that it will react specifically with oxy-amine to form oximes, with 1,2-amino-thiols (e.g., N-terminal cysteine) to form thiazolidine rings, or with hyrazines to form hydrazones at acidic pH. We have tried various additives for this ligation reaction. These include glycerol, ethylene glycol, PEG-1000, PEG-4000, and PEG-6000. High molecular weight PEG caused more spreading of the spots, and hence they were avoided. We have tried various blocking agents such as *O*-allyl-hydroxylamine, *O*-ethyl-hydroxylamine, trimethylsilyl hydroxylamine, *tert*-butyldimethylsilyl-hydroxylamine, *O*-*tert*-butyl-hydroxylamine, and PEG₅₀₀₀NHNH₂ to improve the background of slides. PEG₅₀₀₀NHNH₂ was found to be the best in the case of cell adhesion assay. For protein binding assay, we found

that chemical blocking of the glyoxylyl group is not needed. Blocking with 1% BSA prior to biological assay is sufficient.

Fluorescent Binding Assay. Previously we have identified peptide sequences that bind specifically to avidin (e.g., HPYPP) and streptavidin (e.g., HPQ) using the "one-bead one-compound" combinatorial library approach (6, 12). Biotin and peptides (WSHPQFEK and HPYPP) containing Ttds-linker with Dpr (Aoa) at the carboxyl end were printed onto the glass slide and then probed with a mixture of streptavidin-Cy3 and avidin-Cy5 conjugates. As expected, biotin bound to both streptavidin and avidin. Peptide WSHPQFEK only bound to streptavidin, whereas peptide HPYPP bound to avidin only (Figure 1). This result validates that the microarray methodology could be applied to both peptides and small

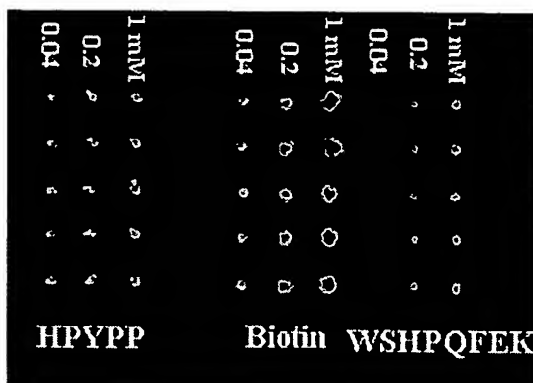


Figure 1. Binding of streptavidin-Cy3 (red) and avidin-Cy5 (green) conjugates to a microarray of biotin, and peptides HPYPP and WSHPQFEK. As expected, avidin bound to HPYPP, streptavidin bound to WSHPQFEK, and both avidin and streptavidin bound to biotin.

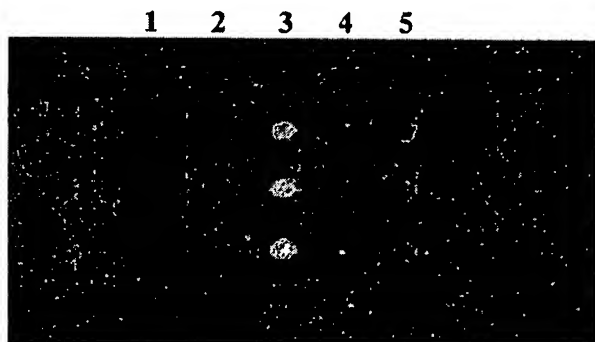


Figure 2. Binding of anti-human insulin monoclonal antibody to the immobilized mimotope peptide pqrGstG in a microarray format. The microarray was first treated with the primary anti-human insulin antibody, followed by secondary anti-mouse IgG-Cy5 conjugate. The peptides were spotted in triplets. Column 1: YGGFL, 2: wGeyidvk, 3: pqrGstG, 4: WSHPQFEK, and 5: biotin. As expected, anti-human insulin antibody bound to pqrGstG peptide only.

molecules, such as biotin. In another experiment, several peptides (YGGFL, wGeyidvk, pqrGstG, WSHPQFEK) and biotin were spotted in a microarray format, and their binding specificity to an anti-insulin MoAb (HB125) was evaluated. From our previous epitope mapping effort, pqrGstG was a mimotope peptide that we had discovered for the anti-insulin MoAb (37). As expected, after incubating with the primary HB125 MoAb followed by anti-mouse IgG-Cy3, only peptide pqrGstG was positive (Figure 2, column 3). To confirm the applicability of this technique in a microarray format, we spotted the pqrGstG peptide on five identical (10:40) slides along with biotin in an alternate pattern. Four of the five slides were incubated with the primary anti-insulin MoAb (HB125) for 1.5 h, followed by one of the following secondary reagents: streptavidin-Cy3, avidin-Cy5, anti-mouse IgG-Cy3, or a mixture of avidin-Cy5 and anti-mouse IgG-Cy3. The remaining slide was treated with a mixture of avidin Cy5 and anti-mouse IgG-Cy3. As expected, no staining was observed in the microarray that had been incubated with the secondary antibody anti-mouse IgG-Cy3 alone. For the slide that had been incubated with HB125 MoAb followed by a mixture of avidin-Cy5 and anti-mouse IgG-Cy3, the biotin spot was labeled with Cy5 and the pqrGstG spot labeled with Cy3 (Figure 3). On the same slide, the reference spot that had both biotin and pqrGstG was labeled with both Cy3 and Cy5 (see arrow in Figure

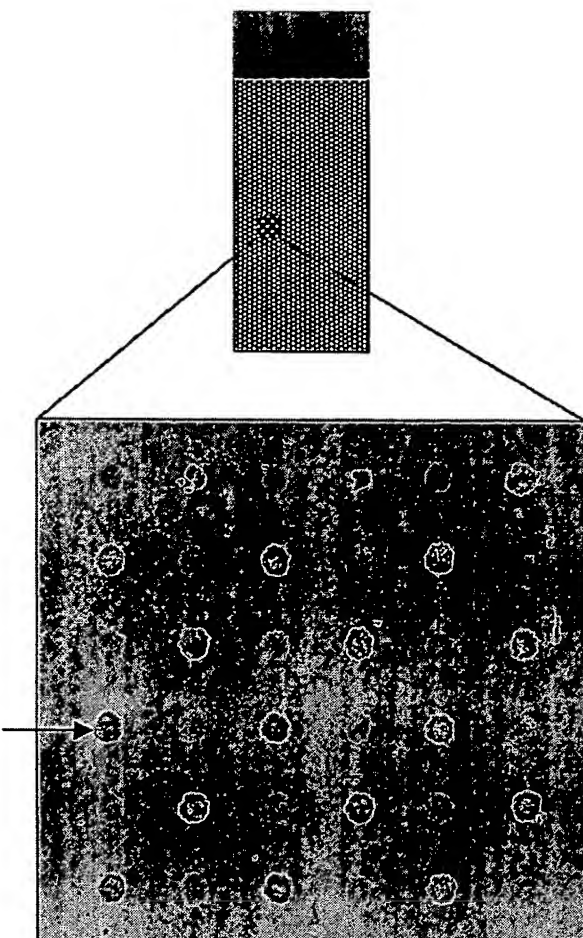


Figure 3. Biotin-linker-Dpr (Aoa) and pqrGstG-linker-Dpr(Aoa) peptide were spotted alternatively on this slide. The amino slide was functionalized with 10:40 glyoxylic acid:stearic acid. The green spots are due to the avidin-Cy5 binding to biotin and red spots due to the anti-insulin monoclonal antibody binding to pqrGstG peptide. The slides were first treated with anti-insulin antibody (1 μ g/mL) followed by a mixture of avidin-Cy5 and anti-mouse IgG-Cy3 (1:1000 each). The slide was scanned under red and green channels. The color shown is not original. The final image was obtained by overlaying the two pictures that were scanned separately. The distance between the spots is 500 μ m. The arrow marks the spot that both pqrGstG peptide and biotin were printed onto the glass. As expected, this spot bound to both avidin and anti-insulin antibody.

3). For the slides that had been incubated with HB125 MoAb followed by streptavidin-Cy3 or avidin-Cy5, only the biotin spots were labeled (data not shown). For the slide that had been incubated with HB125 MoAb followed by anti-mouse IgG-Cy3, only the pqrGstG spots were labeled (data not shown).

Protein Kinase Functional Assay. To demonstrate the versatility of the chemical microarray approach for functional assays, we carried out a solid-phase phosphorylation assay that is very similar to the condition we used to screen a combinatorial bead library for peptide substrates with specific protein kinases (15–17). A known peptide substrate for p60^{c-src} protein tyrosine kinase EEIYGEFF (38, 39) was used in this study. Figure 4 shows the autoradiogram of the peptide microarray that has been phosphorylated by p60^{c-src} using [γ ³³P]ATP, instead of [γ ³²P]ATP as the phosphoryl donor. ³³P was used because it gives a much better resolution of the radiolabeled microarray. In another experiment, we

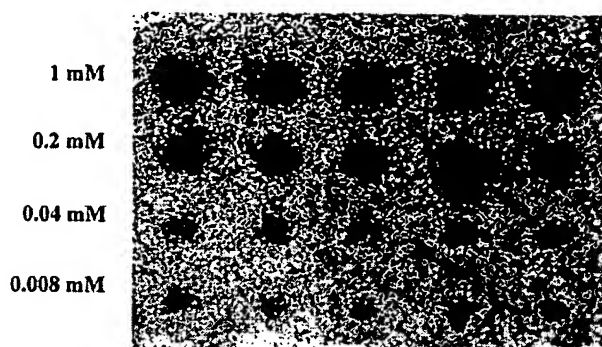


Figure 4. Autoradiogram of $[^{33}\text{P}]$ -labeled EEIYGEFF peptide microarray (spotted at various concentrations) that had been phosphorylated by p60^{c-src} protein tyrosine kinase.

evaluated the importance of the Ttds linker in the phosphorylation assay. The peptide substrate EEIYGEFF was ligated directly to the glass slide without the use of the Ttds linker. No phosphorylation was observed on this peptide microarray (data not shown), indicating the importance of a long flexible hydrophilic linker in this assay.

Cell Adhesion Assay. We have reported the use of a whole cell binding assay to screen a "one-bead one-compound" combinatorial library peptide library for the identification of cell surface binding ligands (18). In addition, we have previously reported the use of an enzyme-linked colorimetric screening method, with purified idiotype derived from WEHI-231 murine lymphoma cell line, to screen an all-D-amino acid 8-mer peptide library. We identified wGeyidvk as a peptide that bound specifically to the surface idiotype of the WEHI-231 cells (40). Furthermore, this peptide (in a tetrameric form) was able to induce tyrosine phosphorylation of intact WHEI231 but not WEHI279 cells. We have decided to use this peptide as a model system for the development of a cell adhesion assay for the microarray. Peptide wGeyidvk was synthesized with a Ttds linker and Lys(Cys) at the carboxyl terminus (Scheme 4) and spotted onto the glyoxylyl-functionalized (10:40) slides. After reaction overnight in a moisture chamber, the slide was treated with PEG₅₀₀₀NHNH₂. Each of the areas of the microarray were then covered separately with various cell lines which includes WEHI-231, Jurkat, OC1LY8, K562, MOLT-4, and HL-60. The slides were then washed and stained with Giemsa stain and observed under a light microscope. Only the WEHI 231 cell was found to bind to the spotted area of the slide with minimal background (Figure 5). The slides that were incubated with other cell lines had no binding (data not shown). To determine whether the cell binding could be quantified, different concentrations of wGeyidvk peptide were spotted on the slide. The slide was then treated with Cell-Tracker Orange stained WEHI 231 cells and scanned by the microarray scanner. The scanned picture was analyzed and quantitated by the ImageQuant 5.0 program. With this quantitative analysis, we were able to determine that maximal cell binding to the microarray spots could be reached with 30 min of incubation (data not shown). As indicated above, wGeyidvk peptide was known to induce tyrosine phosphorylation in WEHI 231 cell line (40). To confirm this finding by the microarray method, cells were fixed after the cell adhesion assay. After permeation with nonionic detergent, FITC-conjugated anti-phosphotyrosine antibody was added. After incubation and washing, the cells were examined under a fluorescent microscope. Cells bound to wGeyidvk peptide fluoresced brightly

(Figure 6a), whereas the negative control where WEHI 231 cells were bound to the slide by cytopsin was completely dark (data not shown). To make sure we still had bound cells in the negative control slide, we turned the background light on and showed that the cells were present but did not fluoresce (Figure 6b). To avoid nonspecific binding of cell onto the slide, PEG₅₀₀₀NHNH₂ blocking was essential.

Comparison with Other Microarray Techniques. One of the earlier reports on peptide or chemical microarray was the light-directed photolithographic synthetic microchip system first reported by Fodor et al. (29). They synthesized 1042 peptides on microscope slides and used a fluorescent-labeled antibody to probe the peptide microarray. The method, while elegant, is inefficient as the synthetic method requires new synthesis on each slide and requires expensive instrumentation that is not readily available. The spotting of peptides or small molecules onto the slide (the method described in this report and that of Schreiber's (22), on the other hand, is much more efficient. Similar to the DNA microarray method, once the peptides or chemical compounds are synthesized, they can be spotted repeatedly onto hundreds of slides. The main difference between the Schreiber's approach and our approach is that Schreiber used the Michael addition chemistry to couple free thiol group of the ligand to the maleimide-functionalized slide. This free radical addition reaction, while efficient, is not site-specific as the ligation chemistries described in this report and cannot be used for ligands with a sulphydryl group that may be essential for binding. Furthermore, the chemoselective ligation method employed in this study can also be used to generate a protein microarray by ligating specifically to proteins with a free N-terminal cysteine (36).

Potential Applications. In this report, we describe three distinct biological assays to analyze the chemical microarrays: the fluorescent-protein binding assay, the functional phosphorylation assay, and the whole cell adhesion assay. All these assays have been used in the screening of the "one-bead one-compound" combinatorial libraries (7). As indicated earlier, each compound-bead is spatially separable and the bead-library can be viewed as a huge microarray platform (10^7 compounds) that is nonaddressable. The identity of the compound-bead is known only after one picks up the positive bead and determines the chemical structure. On the other hand, the chemical microarray described in this report can be viewed as a mini-microarray (up to 10 000 compounds per slide) that is addressable. That is, the chemical identity of each spot is known prior to the biological assays. The two methods, although quite different, are highly complementary. Many ligands can be identified from bead-library screening. Once the chemical structure of these positive ligands are identified, they can be resynthesized, spotted as multiple sets of ligands onto the microscope slide, and characterized under several conditions. For instance, one may use the bead-library method to identify hundreds to thousands of specific peptide substrates for a large number of different protein kinases. These peptide substrate sets can then be used to profile protein kinase activities of cell extracts derived from patient specimens. This profile may be able to direct us to use the appropriate kinase inhibitor for cancer therapy. Similarly, the whole cell binding assay in conjunction with the peptide microarray method may enable us to select the most appropriate peptide or peptide cocktails for targeted-therapy of cancer (41). The *in situ* functional assay after cell adhesion on the

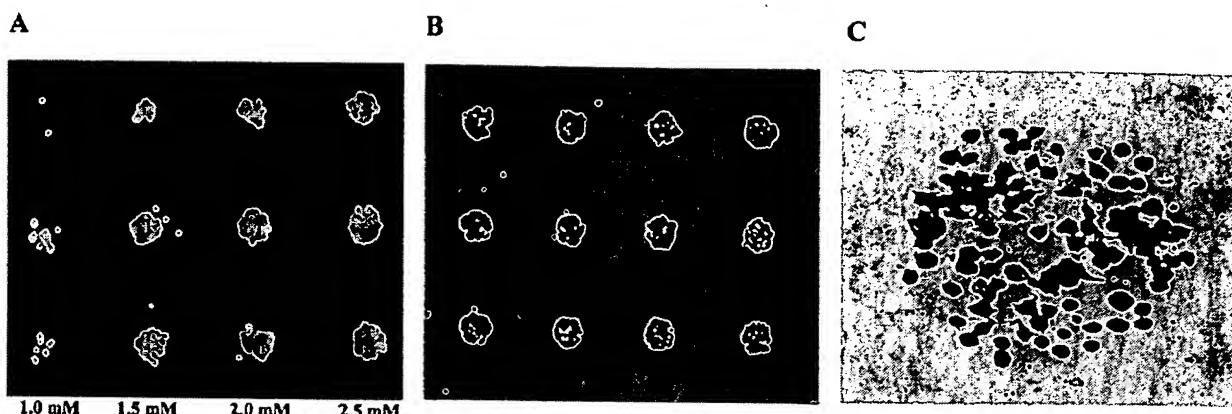


Figure 5. Cell adhesion assay of intact WEHI 231 murine lymphoma cell to wGeyidvk peptide microarray. (A) Fluorescent micrograph of calcein AM-labeled cells bound to peptide microarray that was spotted at different peptide concentrations. (B) Giemsa staining of cells bound to the peptide microarray (low power). (C) Giemsa staining of cells bound to the peptide microarray (higher power).

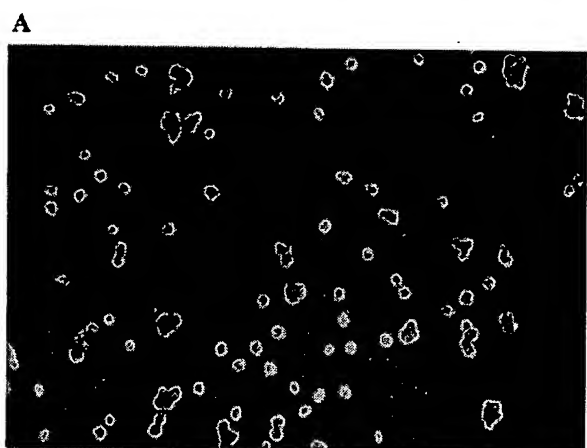


Figure 6. (A) Fluorescent micrograph of WEHI 231 lymphoma cells bound to immobilized wGeyidvk peptide. The bound cells were first fixed with paraformaldehyde and then treated with FITC-labeled anti-phosphotyrosine antibody. Strong fluorescence indicates that cell binding to the immobilized peptide triggers cell signaling. (B) Control slide with WEHI 231 cells bound to the glass by cytospin, fixed with paraformaldehyde, and treated with FITC-labeled anti-phosphotyrosine antibody as above. No fluorescence was observed (data not shown), but the cells could still be seen with dim background light.

microarray is particularly powerful because one can easily envision that hundreds to thousands of interactions between different cell lines and many ligands can

be examined concurrently with respect to binding as well as the different functional responses after binding. Using the appropriate fluorescent-labeled antibodies against a large number of signaling proteins, one can perform numerous experiments and answer many questions on one single microarray slide, using only a minute amount of cell suspension. The method is highly miniaturized and could potentially be fully automatic, from peptide synthesis, to peptide spotting, to cell adhesion, to immuno-fluorescence staining, to final image analysis with confocal microscopy.

CONCLUSION

We have demonstrated the preparation and optimization of a novel class of microchip, which consists of glyoxylyl-modified microscope glass slides and their application for high-throughput analysis of biomolecules and even whole cells. Peptides or small molecules were spotted and covalently attached to slides by site-specific chemical ligation procedure via thiazolidine ring or oxime bond formation. Slides with optimal hydrophobic-hydrophilic balance were obtained by coupling-protected glyoxylic acid and stearic acid in a ratio of 1:4. The peptide and biotin spots on this microchip bound specifically with their receptor protein conjugates (with dye Cy3 or Cy5) and could be easily visualized under a confocal array scanner. We were able to carry out functional phosphorylation assay as well as whole cell binding assay on this microchip. In the cell adhesion assay, nonspecific binding could be eliminated by modifying the glass surface with PEG₅₀₀₀NHNH₂. One major advantage of this type of slide comes from the site-specific attachment of C-terminal modified peptides or small molecules with a Ttds linker molecule to the solid-support, thereby facilitating the binding or functional assays on these chemical microarrays.

ACKNOWLEDGMENT

We would like to thank Professor Jeff Gregg and Ms. Stephenie Liu of the Pathology Department of UC Davis for their assistance with the operation of the DNA Arrayer and Scanner. This work was supported by grants NIH CA78868, NIH CA78909, NIH CA86364, and NSF MCB950621. The Undergraduate Biology Research Program (UBRP) of the University of Arizona, that partly funded Mr. Falsey, was supported by the Howard Hughes Foundation.

LITERATURE CITED

- (1) Merrifield, R. B. (1963) Solid-phase peptide synthesis I The synthesis of a tetrapeptide. *J. Am. Chem. Soc.* 85, 2149–2154.
- (2) Lam, K. S. (1997) Application of combinatorial library methods in cancer research and drug discovery. *Anti-Cancer Drug Design* 12, 145–167.
- (3) Renil, M., Ferreras, M., Delaisse, J. M., Foged, N. T., and Meldal, M. (1998) PEGA supports for combinatorial peptide synthesis and solid-phase enzymatic library assays. *J. Pept. Sci.* 4, 195–210.
- (4) Dolle, R. E., and Nelson, N., Jr. (1999) Comprehensive survey of combinatorial library synthesis: 1998. *J. Comb. Chem.* 1 (4), 235–282.
- (5) St. Hilaire, P. M., and Meldal, M. (2000) Glycopeptide and oligosaccharide libraries. *Angew. Chem., Int. Ed.* 39, 1162–1179.
- (6) Lam, K. S., Salmon, S. E., Hersh, E. M., Hruby, V. J., Kazmierski, W. M., and Knapp, R. J. (1991) One-bead, One-peptide: A new type of synthetic peptide library for identifying ligand-binding activity. *Nature* 354, 82–83.
- (7) Lam, K. S., Krchnak, V., and Lebl, M. (1997) The “one-bead one-compound” combinatorial library method. *Chem. Rev.* 97, 411–448.
- (8) Furka, A., Sebestyen, F., Asgedom, M., and Dibo, G. (1991) General method for rapid synthesis of multicomponent peptide mixtures. *Int. J. Pept. Protein Res.* 37, 487–493.
- (9) Houghten, R. A., Pinilla, C., Blondelle, S. E., Appel, J. R., Dooley, C. T., and Cuervo, J. H. (1991) Generation and use of synthetic peptide combinatorial libraries for basic research and drug discovery. *Nature* 354, 84–86.
- (10) Lam, K. S., Hruby, V. J., Lebl, M., Kazmierski, W. M., Hersh, E. M., and Salmon, S. E. (1993) The chemical synthesis of large random peptide libraries and their use for the discovery of ligands for macromolecular acceptors. *Bioorg. Med. Chem. Lett.* 3, 419–424.
- (11) Lam, K. S., Lebl, M., Krchnak, V., Wade, S., Abdul-Latif, F., Ferguson, R., Cuzzocrea, C., and Wertman, K. (1993) Discovery of D-amino acid containing ligands with Selectide technology. *Gene* 137, 13–16.
- (12) Lam, K. S., and Lebl, M. (1992) Streptavidin and avidin recognize peptide ligands with different motifs. *Immuno-Methods* 1, 11–15.
- (13) Lam, K. S., and Lebl, M. (1994) Selectide technology – bead binding screening. *Methods: A Companion to Methods in Enzymology* 6, 372–380.
- (14) Lam, K. S., Zhao, Z. G., Wade, S., Krchnak, V., and Lebl, M. (1994) Identification of small peptides that interact specifically with a small organic dye. *Drug Dev. Res.* 33, 157–160.
- (15) Wu, J., Ma, Q. N., and Lam, K. S. (1994) Identifying substrate motifs of protein kinases by a random library approach. *Biochemistry* 33, 14825–14833.
- (16) Lam, K. S., Wu, J. S., and Lou, Q. (1995) Identification and characterization of a novel peptide substrate specific for src-family tyrosine kinase. *Int. J. Protein Pept. Res.* 45, 587–592.
- (17) Lou, Q., Leftwich, M., and Lam, K. S. (1996) Identification of GIYWHY as a novel peptide substrate for human p60^{src} protein tyrosine kinase. *Bioorg. Med. Chem.* 4, 677–682.
- (18) Pennington, M. E., Lam, K. S., and Cress, A. E. (1996) *Mol. Divers.* 2, 19–28.
- (19) Schena, M., Shalon, D., Heller, R., Chai, A., Brown, P. O., and Davis, R. W. (1996) Parallel human genome analysis: Microarray-based expression monitoring of 1000 genes. *Proc. Natl. Acad. Sci.* 93, 10614–10619.
- (20) Niemeyer, C. M., and Blohm, D. (1999) DNA microarrays. *Angew. Chem. Int. Ed.* 39, 2865–2869.
- (21) Falsey, J., Li, S., and Lam, K. S. (2000) Development of a chemical microarray technology. In *Peptides: Chemistry, Structure and Biology* (Proceeding of the 16th American Peptide Symposium, June 26–July 1, 1999), pp 736–737.
- (22) MacBeath, G., Hoehler, A. N., and Schreiber, S. L. (1999) Printing small molecules as microarrays an detecting protein–ligand interactions en Masse. *J. Am. Chem. Soc.* 121, 7967–7968.
- (23) MacBeath, G., and Schreiber, S. L. (2000) Printing proteins as microarrays for high-throughput function determination. *Science* 289, 1760–1763.
- (24) Frank, R. (1992) Spot-Synthesis: An easy technique for the positionally addressable, parallel chemical synthesis on a membrane support. *Tetrahedron* 48, 9217–9232.
- (25) Fodor, S., Read, J. L., Pirrung, M. C., Stryer, L., Tsai, Lu, A., and Solas, D. (1991) Light-directed, spatially addressable parallel chemical synthesis. *Science* 251, 767–773.
- (26) (a) Pellois, J. P., Wang, W., and Gao, X. (2000) Peptide synthesis based on t-Boc chemistry and solution photogenerated acids. *J. Comb. Chem.* 2 (4), 355–60. (b) LeProust, E., Pellois, J. P., Yu, P., Zhang, H., Gao, X., Srivannavit O., Gulari, E., and Zhou, X. (2000) Digital light-directed synthesis. A microarray platform that permits rapid reaction optimization on a combinatorial basis. *J. Comb. Chem.* 2 (4), 349–354.
- (27) Arenkove, P., Kukhtin, A., Gemmell, A., Voloshchuk, S., Chupeeva, V., and Mirzabekov, A. (2000) Protein microchips: use for immunoassay and enzymatic reactions *Anal. Biochem.* 278, 123–131.
- (28) Mendoza, L. G., McQuarry, P., Mongan, A., Gangadharan, R., Brignac, S., and Eggers, M. (1999) High-throughput microarray-based enzyme-linked immunosorbent assay (ELISA) *BioTechniques* 27, 778–788.
- (29) Zammateo, N., Jeanmart, L., Hamels, S., Courtois, S., Louette, P., Hevesi, L., and Remacle, J. (2000) Comparison between different strategies of covalent attachment of DNA to glass surfaces to build DNA microarrays *Anal. Biochem.* 280, 143–150.
- (30) Joos, B., Kuster, H., and Cone, R. (1997) Covalent attachment of hybridizable oligonucleotides to glass supports. *Anal. Biochem.* 247, 96–101.
- (31) Liu, C. F., Rao, C., and Tam, J. P. (1996) Orthogonal ligation of unprotected peptide segments through pseudo-proline formation for the synthesis of HIV-1 protease analogues. *J. Am. Chem. Soc.* 118, 307–312.
- (32) Shao, J., and Tam, J. P. (1995) Unprotected peptides as building blocks for the synthesis of peptide dendrimers with oxime, hydrazone, and thiazolidine linkages. *J. Am. Chem. Soc.* 117, 3893–3899.
- (33) Wahl, F., and Mutter, M. (1996) Analogues of oxytocin with an oxime bridge using chemoselectively addressable building blocks. *Tetrahedron Lett.* 37, 6861.
- (34) Tam, J. P., Yu, W., and Miao, Z. (1999) Orthogonal ligation strategies for peptides and proteins. *Biopolymers (Pept. Sci.)* 51, 311–332.
- (35) Zhao, Z.-G., and Lam, K. S. (1995) A novel approach for iodolabeling synthetic peptides. *J. Chem. Soc., Chem. Commun.* 1739–1740.
- (36) Zhao, Z.-G., Im, J. S., Lam, K. S., and Lake, D. (1999) Site specific modification of a single chain antibody using a novel glyoxyl-based labeling reagent. *Bioconjugate Chem.* 10, 424–430.
- (37) Lam, K. S., Lake, D., Salmon, S. E., et al. (1996) A one-bead one-peptide combinatorial library method for B-cell epitope mapping. *Methods: a Companion to Methods in Enzymology* 9, 482–493.
- (38) Songyang, Z., Carrway, K. L., III, Eck, M. J., et al. (1995) Catalytic specificity of protein tyrosine kinases is critical for selective signaling. *Nature* 373, 536.
- (39) Al-Obeidi, F. A., Wu, J. J., and Lam, K. S. (1998) Protein tyrosine kinases: Structure, substrate, specificity, and drug discovery. *Biopolymers (Pept. Sci.)* 47, 197–203.
- (40) Lam, K. S. et al. (1995) Idiotypic specific peptides bind to the surface immunoglobulins of two murine B-cell lymphoma lines, inducing signal transduction. *Biomed. Pept., Proteins Nucleic Acids* 1, 205–210.
- (41) Lam, K. S., and Zhao, Z.-G. (1997) Targeted therapy for lymphoma with peptides. *Hematology/Oncology Clinic of North America* 11, 1007–1019.

The Search for Synergy: A Critical Review from a Response Surface Perspective*

WILLIAM R. GRECO, GREGORY BRAVO, AND JOHN C. PARSONS

Department of Biomathematics, Roswell Park Cancer Institute, Buffalo, New York

I. Introduction	332
II. Review of reviews	334
III. General overview of methods from a response surface perspective	334
IV. Debate over the best reference model for combined-action	344
V. Comparison of rival approaches for continuous response data	348
A. Isobologram by hand	349
B. Fractional product method of Webb (1963)	351
C. Method of Valeriote and Lin (1975)	352
D. Method of Drewinko et al. (1976)	352
E. Interaction index calculation of Berenbaum (1977)	352
F. Method of Steel and Peckham (1979)	353
G. Median-effect method of Chou and Talalay (1984)	354
H. Method of Berenbaum (1985)	358
I. Bliss (1939) independence response surface approach	360
J. Method of Prichard and Shipman (1990)	360
K. Nonparametric response surface approaches	362
1. Bivariate spline fitting (Sühnel, 1990)	362
L. Parametric response surface approaches	363
1. Models of Greco et al. (1990)	364
2. Models of Weinstein et al. (1990)	365
VI. Comparison of rival approaches for discrete success/failure data	367
A. Approach of Gessner (1974)	369
B. Parametric response surface approaches	371
1. Model of Greco and Lawrence (1988)	371
2. Multivariate linear logistic model	371
VII. Overall conclusions on rival approaches	373
VIII. Experimental design	373
IX. General proposed paradigm	376
X. Appendix A: Derivation of a model for two mutually nonexclusive noncompetitive inhibitors for a second order system	377
A. Motivation	377
B. Elements of the derivation of the mutually nonexclusive model for higher order systems from Chou and Talalay (1981)	377
C. Assumptions of the derivation of the model for mutual nonexclusivity for two noncompetitive higher order inhibitors	378
D. Derivation	378
E. Possible rationalization of the mutually nonexclusive model of Chou and Talalay (1981)	379
XI. Appendix B: Problems with the use of the median effect plot and combination index calculations to assess drug interactions	379
A. Nonlinear nature of the median effect plot for mutual nonexclusivity	380
B. Incorrect combination index calculations for the mutually nonexclusive case	382
C. Nonlinear nature of the median effect plot for mutual exclusivity with interaction	382
XII. References	382

I. Introduction

The search for synergy has followed many tortuous paths during the past 100 years, and especially during the last 50 years. Claims of synergism for the effects, both therapeutic and toxic, of combinations of chemicals are ubiquitous in the broad field of Biomedicine. Over 20,000 articles in the biomedical literature from 1981 to 1987 included "synergism" as a key word (Greco and Lawrence, 1988). Travelers on the search for synergy have included scientists from the disciplines of Pharmacology, Toxicology, Statistics, Mathematics, Epidemiology, Entomology, Weed Science, and others. Travelers have independently found the same trails, paths have crossed, bitter fights have ensued, and alliances have been made. The challenge of assessing the nature and intensity of agent interaction is universal and is especially critical in the chemotherapy of both infectious diseases and cancer. In the mature field of anticancer chemotherapy, with minor exceptions, combination chemotherapy is required to cure all drug-sensitive cancers (DeVita, 1989). For the nascent field of Antiviral Chemotherapy, combination chemotherapy is of great research interest because of its great clinical potential (Schinazi, 1991). Our review should aid investigators in understanding the various rival approaches to the assessment of drug interaction and assist them in choosing appropriate approaches.

We will make no attempt to offer advice on the use of a discovery of synergy. The interpretation of the impact of both qualitative and quantitative measures of agent interaction is dependent upon the field of application. At the very least, an agent combination that displays moderate to extreme synergy can be labeled as interesting and deserving of further study. (Inventors may use proof of synergy as support for the characteristic of "unobviousness," which will assist them in receiving a patent for a combination device or formulation with the United States Patent Office.)

There have been many previous reviews of this controversial subject of agent interaction assessment. These critiques are summarized in the next section. However, our review is unique in several ways. First, our bias is toward the use of response surface concentration-effect models to aid in the design of experiments, to use for fitting data and estimating parameters, and to help in visualizing the results with graphs. In fact, because a major strength of response surface approaches is that they can help to explain the similarities and differences among other approaches, the entire review is from

a response surface perspective. [Response surface methodology is composed of a group of statistical techniques, including techniques for experimental design, statistical analyses, empirical model building, and model use (Box and Draper, 1987). A response surface is a mathematical equation, or the graph of the equation, that relates a dependent variable, such as drug effect, to inputs such as drug concentrations.] Second, two common data sets, one with continuous responses and one with discrete success/failure responses, are used to compare 13 specific rival approaches for continuous data, and three rival approaches for binary success/failure data, respectively. Third, many detailed criticisms of many approaches are included in our review; these criticisms have not appeared elsewhere.

It should be noted that the goal of this review is to underscore the similarities, differences, strengths, and weaknesses of many approaches, but not to provide a complete recipe for the application of each approach. Readers who need the minute details of the various approaches should refer to the original articles. A good compendium of recipes for many of the approaches included in this review is the fourth chapter of a book by Calabrese (1991). It should also be noted that many of the approaches were originally written as guidelines, not detailed algorithms. Therefore, our specific implementations of several of the methods may have differences from the approaches actually intended by the original authors.

There is no uniform agreement on the definitions of agent interaction terms. Sources for extensive discussions of rival nomenclature include the following: Berenbaum (1989); Calabrese (1991); Copenhaver et al. (1987); Finney (1952, 1971); Gessner (1988); Hewlett and Plackett (1979); Loewe (1953); Kodell and Pounds (1985; 1991); Valeriote and Lin (1975); Unkelbach and Wolf (1984); and Wampler et al. (1992). It is our view that many of the naming schemes are unnecessarily complex. We will use a simple scheme that was the consensus of six scientists who debated concepts and terminology for agent interaction at the Fifth International Conference on the Combined Effects of Environmental Factors in Saariselkä, Finnish Lapland, September 6 to 10, 1992 (Greco et al., 1992). The six scientists, from the fields of Pharmacology, Toxicology and Biometry, comprised a good representative sample of advocates of diametrically opposing views on many issues.

Table 1 lists the consensus terminology for the joint action of two agents, the major part of the so-called Saariselkä agreement. The foundation for this set of terms includes two empirical models for "no interaction" for the situation in which each agent is effective alone. (Even though the term "interaction" has a mechanistic connotation when applied to agent combinations, it will be used throughout this article in a purely empirical sense. Also, the less-mechanistic term, "combined-action" will be often substituted for "interaction" when

* Supported by grants from the National Cancer Institute, CA46732, CA16056 and RR10742.

† Abbreviations: 3-D, three-dimensional; 2-D, two-dimensional; Eq., equation; vs., versus; see table 2 for mathematical/statistical abbreviations.

To whom correspondence should be addressed: Dr. William R. Greco, Department of Biomathematics, Roswell Park Cancer Institute, Buffalo, NY 14263

TABLE 1
Consensus terminology for two-agent combined-action concepts

	Both agents effective individually; Eq. 6 is the reference model	Both agents effective individually; Eq. 11 or 14 is the reference model	Only one agent effective individually	Neither agent effective individually
Combination effect greater than predicted	Loewe synergism	Bliss synergism	synergism	coalism
Combination effect equal to prediction from reference model	Loewe additivity	Bliss independence	inertism	inertism
Combination effect less than predicted	Loewe antagonism	Bliss antagonism	antagonism	

feasible.) The mathematical details of these two models are described in Section III, and the debate over which of these is the best null reference model is the subject of Section IV. The first model is that of Loewe additivity (Loewe and Muischnek, 1926), which is based on the idea that, by definition, an agent cannot interact with itself. In other words, in the sham experiment in which an agent is combined with itself, the result will be Loewe additivity. The second model is Bliss independence (Bliss, 1939), which is based on the idea of probabilistic independence; i.e., two agents act in such a manner that neither one interferes with the other, but each contributes to a common result. The cases in which the observed effects are more or less than predicted by Loewe additivity or Bliss independence are Loewe synergism, Loewe antagonism, Bliss synergism, and Bliss antagonism, respectively. The use of the names Loewe and Bliss as adjectives emphasizes the historical origin of the specific models and deemphasizes the mechanistic connotation of the terms additivity and independence. Both Loewe additivity and Bliss independence are included as reference models, because each has some logical basis, and especially because each has its own coterie of staunch advocates who have successfully defended their preferred model against repeated vicious attacks (see Section IV). As shown in table 1, when only one agent in a pair is effective alone, inertism is used for "no interaction," synergism (without a leading adjective) for an increased effect caused by the second agent, and antagonism for the opposite case. Alternate common terms for the latter two cases are potentiation and inhibition. When neither drug is effective alone, an ineffective combination is a case of inertism, whereas an effective combination is termed coalism.

For the cases in which more than two agents are present in a combination, it may not always be fruitful to assign special names to the higher order interactions. It may be better to just quantitatively describe the results of a three-agent or more complex interaction than to pin a label on the combined-action. However, in some fields, such as Environmental Toxicology, it may be useful to assign a descriptive name to a complex mixture of chemicals at specific concentrations. Then, six of the above-mentioned terms have clear, useful extensions to higher order interactions: Loewe additivity, Loewe synergism,

Loewe antagonism, Bliss independence, Bliss synergism, and Bliss antagonism. Note also that all ten terms are defined so that as the concentration or intensity of the agent(s) increases, the pharmacological effect monotonically increases. This is why the lower right-hand cell of table 1 is missing; a pharmacological effect less than zero is not defined. However, because in the field of chemotherapy it is common for increased concentrations of drugs to decrease the survival or growth of infectious agents or of tumor cells, most of the concentration-effect (dose-response) equations and curves in this review will assume a monotonically decreasing observed effect (response), such as virus titer. The dependent response variable will be labeled as effect, % effect, % survival, or % control in most graphs and will decrease with increasing drug concentration. In contrast, ID_X values such as ID_{25} will refer to the concentration of drug resulting in $X\%$ of pharmacological effect (e.g., 25% inhibition, leaving 75% of control survival). The above definitions and conventions will become clearer in later sections with the introduction of defining mathematical equations.

The emphasis of this review will be on approaches to assess combinations of agents that yield an unexpectedly enhanced pharmacological effect. Loewe additivity and Bliss independence will be used as references to give meaning to claims of Loewe synergism and Bliss synergism, respectively. Loewe antagonism will be only briefly discussed, as will synergism, antagonism, and coalism. Most concentration-effect models and curves in this review will be monotonic. Therapeutic synergy in *in vivo* and in clinical systems, which involves a mixture of efficacy and toxicity, and which often involves nonmonotonic concentration-effect curves for each agent individually and for the combination, will not be discussed.

The preceding discussion referred to global properties of agent combinations; i.e., it was implied that a particular type of named interaction, such as Loewe synergism, appropriately described the entire 3-D⁺ concentration-effect surface. Some agent combinations may demonstrate different types of interaction at different local regions of the concentration-effect surface. When this occurs, the interaction terms in table 1 can be used to describe well defined regions. However, it is important to differentiate true mosaics of different interaction types from random statistical variation and/or artifacts

caused by faulty data analysis methods. Unfortunately, rigorous methods to identify true mosaics are not yet available.

II. Review of Reviews

We have divided reviews on the subject of synergy into three classes: (a) whole books, some of which include new methodology, and some of which do not; (b) book chapters and journal articles entirely dedicated to review; and (c) book chapters and articles with noteworthy introductions and discussions of combined-action assessment, but which also include new specific methodology development or data analyses. Books include: Brunden et al. (1988); Calabrese (1991); Carter et al. (1983); Chou and Rideout (1991); National Research Council (1988); Pöch (1993); and Vollmar and Unkelbach (1985). Book chapters and articles dedicated to a review of the field include: Berenbaum (1977, 1981, 1988, 1989); Copenhaver et al. (1987); Finney (1952, 1971); Gessner (1988); Hewlett and Plackett (1979); Jackson (1991); Kodell and Pounds (1991); Lam et al. (1991); Loewe (1953, 1957); Rideout and Chou (1991); and Unkelbach and Wolf (1984). Book chapters and articles that include significant reviews of various approaches, but which also include either new methodology development and/or analyses of new data include: Chou and Talalay (1983, 1984); Gennings et al. (1990); Greco (1989); Greco and Dembinski (1992); Hall and Duncan (1988); Kodell and Pounds (1985); Prichard and Shipman (1990); Sühnel (1990); Syracuse and Greco (1986); Tallarida (1992); and Machado and Robinson (1994).

Although not exhaustive, this list includes a comprehensive, redundant account of the interaction assessment literature. This list includes critical and non-critical reviews of history, philosophy, semantics, approaches advocated by statisticians, and approaches advocated by pharmacologists. Most of the reviews are biased toward the respective authors' point of view, and many of the reviews harshly criticize the work of rival groups. Our review is no exception. A subset of these reviews, which along with our own, will provide a comprehensive, but not overly redundant view of the field include: chapters 1 to 4 of Calabrese (1991), which provide a relatively noncritical recipe-like description of concepts, terminology, and assessment approaches, including many disagreements with our review; chapters 1 to 2 of Chou and Rideout (1991), which also provide a contrasting view to our review on many issues; Copenhaver et al. (1987), which accents the approaches developed by statisticians; Berenbaum (1981, 1988, 1989), which critically review the approaches developed by pharmacologists; Gessner (1988), which examines approaches developed both by statisticians and pharmacologists; and Kodell and Pounds (1991), which may be the best source for a rigorous comparison of rival concepts and nomenclature.

III. General Overview of Methods from a Response Surface Perspective

Figure 1 is a schematic diagram of a general approach to the assessment of the nature and intensity of drug interactions. This scheme includes all of the approaches examined in later sections. This is because, in essence, figure 1 describes the scientific method. A formal statistical response surface way of thinking underlies all of this section. With such an orientation, the similarities and differences among rival approaches for the assessment of drug interactions, both mathematically rigorous ones and not-so-rigorous ones, can be readily explained.

Step 1 is to choose a good concentration-effect (dose-response) structural model for each agent when applied individually. A common choices is the Hill model (Hill, 1910), which is also known as the logistic model (Waud and Parker, 1971; Waud et al., 1978). The Sigmoid-Emax model (Holford and Sheiner, 1981), is equivalent to a nonlinear form of the median-effect model (Chou and Talalay, 1981, 1984). However, the equivalence of the median-effect and Hill models is disputed by Chou (1991). The Hill model is shown in figure 2 and as Eq. 1 for an inhibitory drug. Symbol definitions are listed in table 2.

$$E = \frac{Emax \left(\frac{D}{IC_{50}} \right)^m}{1 + \left(\frac{D}{IC_{50}} \right)^m} \quad [1]$$

Strategy & Tactics for Assessing Agent Interactions

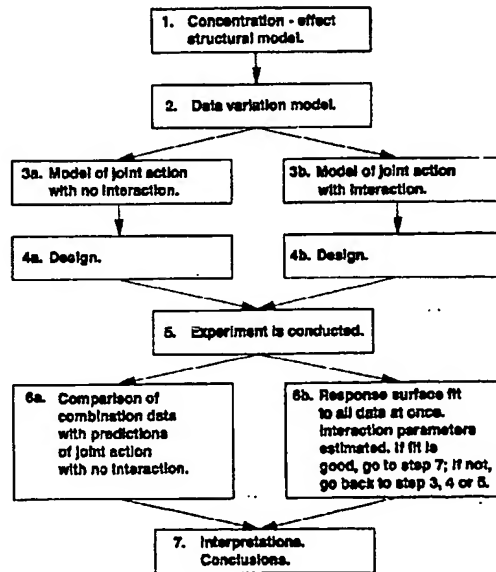


FIG. 1. Schematic diagram of a general approach to the assessment of the nature and intensity of agent interactions, which includes all specific approaches.

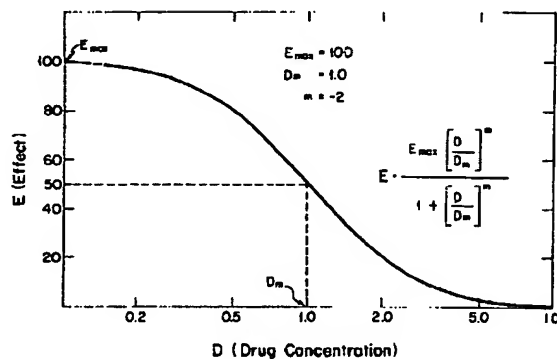


FIG. 2. Graph of the Hill (1910) model, which is also referred to as the Sigmoid-Emax model (e.g., Holford and Sheiner, 1981), and which is also a nonlinear form of the median-effect equation (Chou and Talalay, 1984).

In Eq. 1, E is the measured effect (response), such as the virus titer remaining in a culture vessel after drug exposure; D is concentration of drug; E_{max} is the full range of response that can be affected by the drug; D_m or IC_{50} is the median effective dose (or concentration) of drug (or ID_{50} , ED_{50} , LD_{50} , etc.); and m is a slope parameter. When m has a negative sign, the curve falls with increasing drug concentration; when m is positive, the curve rises with increasing drug concentration. The concentration-effect curve in figure 2 can be thought of as an ideal curve formed by data with no discernible variation, or as the true curve known only to God or to Mother Nature, or as the average curve formed by an infinite number of data points at each of an infinite number of evenly spaced concentrations. Equations 2 to 4 are additional candidate structural models for single agents.

$$E = \frac{Econ \left(\frac{D}{IC_{50}} \right)^m}{1 + \left(\frac{D}{IC_{50}} \right)^m} \quad [2]$$

$$E = \frac{(Econ - B) \left(\frac{D}{IC_{50}} \right)^m}{1 + \left(\frac{D}{IC_{50}} \right)^m} + B \quad [3]$$

$$E = Econ \exp(aD) = Econ \exp \left(D \ln \left(\frac{1}{2} \right) \right) \quad [4]$$

In Eqs. 2 and 3, the parameter $Econ$ is the control effect (or response when no inhibitory drug is applied). When there is no B (background response observed at infinite drug concentration), then $Econ$ is equivalent to E_{max} , as in Eq. 2. However, when there is a finite B , then $Econ =$

$E_{max} + B$. Eq. 4 is the exponential concentration-effect model, which can also be parameterized with an IC_{50} .

Because real experiments rarely generate data that fall on the ideal curve, Step 2 in figure 1 is to choose an appropriate data variation model. Model candidates include the normal distribution for continuous data, such as found in growth assays in which the absorbance of a dye bound to cells is the measured signal; the binomial distribution (Larson, 1982) for proportions of failures or successes, such as in acute toxicology experiments; and the Poisson distribution for low numbers of counts, such as in clonogenic assays. A composite model is formed from one structural model plus one data variation model and eventually used for fitting to real experimental data. This concept, called generalized nonlinear modeling (McCullagh and Nelder, 1989) is illustrated in figure 3, with the Hill model as the structural model, and the normal, binomial, and Poisson distributions (respectively from left to right) as the random models. (Note that only one random component is usually assumed for a particular data set. Graphs of three random components are pictured in figure 3 to illustrate the universal nature of the approach. The lower equation in the figure is a variant of the Hill model, and the upper one is for the binomial distribution. These equations will be described in detail in Section VI.)

In Step 3, most approaches can be categorized into one of two main strategies. In Step 3a, a structural model is derived for joint action of two or more agents with the assumption of "no interaction" (Loewe additivity, Bliss independence, or another null reference model). Then, after the experiment is designed and conducted, data from the combination of agents is compared with predictions of joint action from a null reference combined-action model. This comparison can be made with formal statistical rejections of null hypotheses, or by less formal methods. In contrast, in Step 3b, a structural model is derived for joint action that includes interaction terms. Then, after the experiment is designed and conducted, the full combined-action model is fit to all of the data at once, and interaction parameters are estimated. Both the left-hand and right-hand strategies end in a set of guidelines for making conclusions.

Examples of approaches that use the left-hand strategy include: the classical isobologram approach (Loewe and Muischnek, 1926); the fractional product method of Webb (1963); the method of Valeriote and Lin (1975); the method of Drewinko (1976); the method of Steel and Peckham (1979); the method of Gessner (1974); the methods of Berenbaum (1977, 1985); the median-effect method (Chou and Talalay, 1981, 1984); the method of Prichard and Shipman (1990); and the method of Laska et al. (1994). Examples of approaches that use the right-hand strategy include the universal response surface approach (Greco et al., 1990; Greco and Lawrence, 1988; Greco, 1989; Greco and Tung, 1991; Syracuse and Greco, 1986); the response surface approaches of Carter's group

TABLE 2
Mathematical/statistical symbol definitions

Symbol	Definition
E	Measured effect (or response), in this review, usually a measure of survival
Y	Transformed response variable, continuous or discrete
y	A particular value of Y
$P(\cdot)$	Probability that the function in parenthesis is true
μ	Mean or expected value of a transformed response
k	Number of successes in a binomial trial
n	Number of attempts in a binomial trial
D , [drug], D_1 , [drug 1], D_2 , [drug 2]	Concentration (or dose) of drug, drug 1, drug 2
I, I_1, I_2	Inhibitor concentrations for an inhibitor, inhibitor 1, inhibitor 2
$Econ$	Control effect (or response)
E_{max}	Maximum effect (response), is equal to $Econ$ for an inhibitory drug in the absence of a background, B
B	Background effect (response) observed at infinite concentration for an inhibitory drug
fa	Fraction of effect affected
fu	Fraction of effect unaffected
fi	Fraction enzyme velocity inhibited
$IC_{50}, I_{50}, IC_{50,1}, IC_{50,2}$	Concentration (or dose) of drug resulting in 50% inhibition of E_{max} , of drug 1, of drug 2
$D_m, D_{m1}, D_{m2}, D_{m12}$	Median effective dose (or concentration) of drug, of drug 1, of drug 2, of a combination of drugs 1 and 2 in a constant ratio (equivalent to IC_{50})
$ID_x, D_x, IC_x, ID_{x,1}, D_{x,1}, ID_{x,2}, D_{x,2}, D_{x,12}$	Concentration (or dose) of drug resulting in $X\%$ inhibition of E_{max} , of drug 1, of drug 2, or a combination of drugs 1 and 2 in a constant ratio
X	% inhibition
m, m_1, m_2, m_{12}	Slope parameter, for drug 1, for drug 2, for a combination of drugs 1 and 2 in a constant ratio
α	Synergism-antagonism interaction parameter
a, b	Empirical parameters for exponential concentration-effect model
PC_1, PC_2, bp_1, bp_2	Interaction parameters of model 29
η	Interaction parameter of model 30
$\beta_0, \beta_1, \beta_2, \beta_{12}$	Empirical parameters for probit and logistic models
I	Interaction index of Berenbaum (1977)
CI	Combination index of Chou and Talalay (1984)
R	Ratio of D_1 to D_2

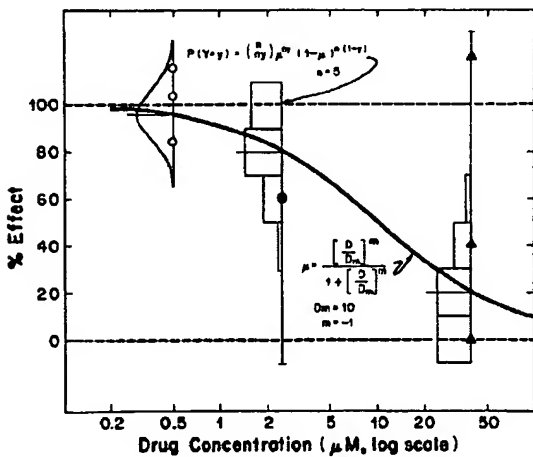


FIG. 3. General scheme for the dissection of a generalized non-linear model into random and structural components for a concentration-effect curve for a single drug.

(Carter et al., 1983, 1986, 1988; Gennings et al., 1990); the response surface approach of Weinstein et al. (1990); the generalized linear model approach of Lam et al. (1991); and the response surface approach of Machado

and Robinson (1994). The method proposed by Sühnel (1990) has elements of both the left-hand and right-hand strategies.

Although most, and possibly all, approaches for assessing agent combinations may fall under the scheme presented in figure 1, the different approaches differ from each other in many respects. The approaches developed by pharmacologists usually stress structural models, e.g., the median-effect approach (Chou and Talalay, 1984), whereas the approaches developed by statisticians usually stress data variation models, e.g., the approaches of Finney based on probit analysis (Finney, 1952). There are differences in the definitions of key terms, especially that of "synergism." Some approaches only yield a qualitative conclusion (e.g., Loewe synergism, Loewe antagonism, or Loewe additivity), such as the classical isobogram approach, whereas others also provide a quantitative measure of the intensity of the interaction, such as the universal response surface approach. There are differences in the degree of mathematical and statistical rigor, i.e., some approaches are performed entirely by hand (e.g., the classical isobogram approach), whereas others require a computer (e.g., universal response surface approach). Some approaches use

parametric models (e.g., Greco et al., 1990), whereas others emphasize nonparametric models (e.g., Sühnel, 1990; Kelly and Rice, 1990). The suggested designs for experiments differ widely among the different approaches. It is therefore not surprising that it is possible to generate widely differing conclusions on the nature of a specific agent interaction when applying different methods to the same data set. This will be illustrated dramatically in Sections V and VI.

We are highly biased in our view that the right-hand strategy in figure 1 for assessing agent interactions is superior to the left-hand strategy when used for the cases in which an appropriate response surface model can be found to adequately model the biological system of interest. However, for preliminary data analyses for all systems, for the final data analyses of complex systems, and for cases in which the data is meager, the left-hand approaches are often very useful.

The derivation of Eq. 5, the flagship equation for two-agent combined-action developed by our group, is provided in detail in Greco et al. (1990). Although we do not put forward Eq. 5 as the model of two-agent combined-action, it is a model of two-agent combined-action that has proved to be very useful for both practical applications (Greco et al., 1990; Greco and Dembinski, 1992; Gaumont et al., 1992; Guimaraes et al., 1994) and methodology development (Syracuse and Greco, 1986; Greco and Lawrence, 1988; Greco, 1989; Greco and Tung, 1991; Khinkis and Greco, 1993; Khinkis and Greco, 1994; Greco et al., 1994). Eq. 5 will be used throughout this review to illustrate concepts of combined-action and to assist in the comparison of rival data analysis approaches. Eq. 5 was derived with an adaptation of an approach suggested by Berenbaum (1985), with the assumption of Eq. 2 as the appropriate model for each agent alone. The interaction parameter is α .

$$1 = \frac{D_1}{IC_{50,1} \left(\frac{E}{Econ - E} \right)^{1/m_1}} + \frac{D_2}{IC_{50,2} \left(\frac{E}{Econ - E} \right)^{1/m_2}} + \frac{\alpha D_1 D_2}{IC_{50,1} IC_{50,2} \left(\frac{E}{Econ - E} \right)^{(1/2m_1 + 1/2m_2)}} \quad [5]$$

Eq. 5 allows the slopes of the concentration-effect curves for the two drugs to be unequal. It is this key feature that distinguishes Eq. 5 from many other response surface models used by others to describe agent interactions (e.g., Carter et al., 1988). (This point is expanded in Section VI. B.2.). Because Eq. 5 is in unclosed form (the dependent variable, E , cannot be isolated on the left-hand side of the equation), a one-dimensional bisection root finder (a computer numerical procedure explained, e.g., by Thisted, 1988) is used to calculate E for simulations. Eq. 5 was not derived from biological theory,

rather it is an empirical equation that often matches the shape of real data (e.g., Gaumont et al., 1992; Greco et al., 1990; Greco and Dembinski, 1992; Greco and Lawrence, 1988). However, as shown below, it is consistent with Eq. 6, the equation for Loewe additivity (Loewe and Muischnek, 1926), which is the basis of many interaction assessment approaches.

$$1 = \frac{D_1}{ID_{X,1}} + \frac{D_2}{ID_{X,2}} \quad [6]$$

For an inhibitory drug, Eq. 6 refers to a particular $X\%$ (percent inhibition level), e.g., 58% inhibition. $ID_{X,1}$, $ID_{X,2}$ are the concentrations of drugs to result in $X\%$ inhibition for each respective drug alone, and D_1 , D_2 are concentrations of each drug in the mixture that yield $X\%$ inhibition. When the right-hand side of Eq. 6 [equal to the Interaction index, I , of Berenbaum (1977) or to the combination index, CI , for the mutually exclusive case of Chou and Talalay (1984)] is less than 1, then Loewe synergism is indicated, and when the right-hand side is greater than 1, Loewe antagonism is indicated. When Eq. 2 is an appropriate concentration-effect model for each drug alone, then Eq. 7, which is a rearrangement of Eq. 2 [similar to a rearrangement of the median-effect equation from Chou and Talalay (1984)], relates the ID_X value for any $X\%$ inhibition to the observed response level, E , and the parameters, $Econ$, IC_{50} , and m .

$$ID_X = IC_{50} \left(\frac{E}{Econ - E} \right)^{1/m} \quad [7]$$

Note that the right-hand expression of Eq. 7 is the same as the denominators of the first two right-hand terms of Eq. 5. Therefore, the first two right-hand terms of Eqs. 5 and 6 are equivalent. It follows that Eq. 8 defines I [or CI for the mutually exclusive case of Chou and Talalay (1984)] for two-drug combinations whose individual components have concentration-effect curves that follow Eq. 2.

$$I = CI = \frac{D_1}{IC_{50,1} \left(\frac{E}{Econ - E} \right)^{1/m_1}} + \frac{D_2}{IC_{50,2} \left(\frac{E}{Econ - E} \right)^{1/m_2}} = 1 - \frac{\alpha D_1 D_2}{IC_{50,1} IC_{50,2} \left(\frac{E}{Econ - E} \right)^{(1/2m_1 + 1/2m_2)}} \quad [8]$$

Therefore, based upon the interaction index, I —when α is positive, Loewe synergism is indicated, when α is negative, Loewe antagonism is indicated, and when α is 0, Loewe additivity is indicated. The magnitude of α indicates the intensity of the interaction. Thus, although Eq. 5 is not the model for Loewe synergism (or Loewe antagonism), it is a model for Loewe synergism (or Loewe antagonism) that is consistent with the more general Loewe additivity model, Eq. 6.

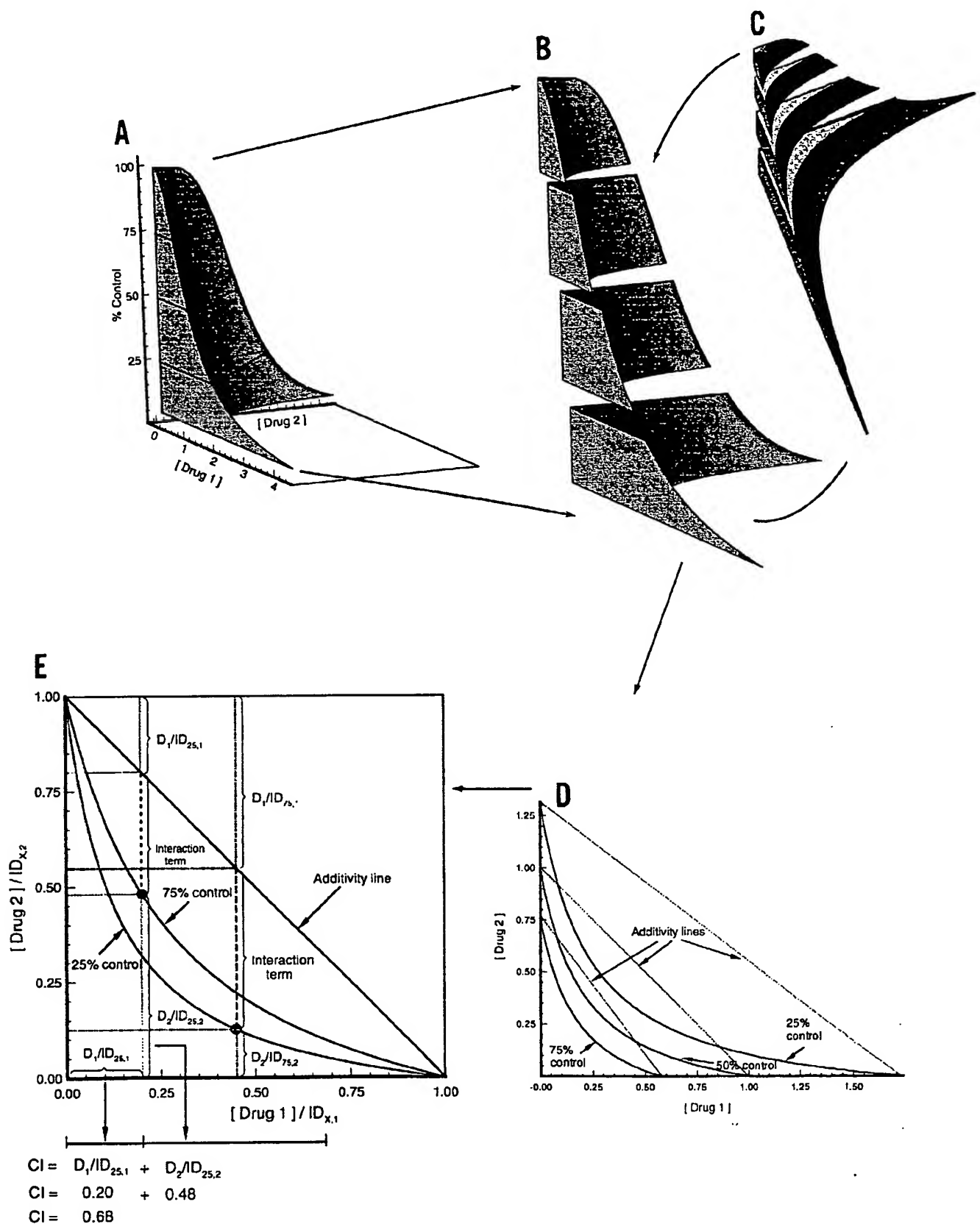


FIG. 4.

We now use the concept that Eq. 5 generates a Loewe synergistic response surface at all effect levels, and we present several 3-D and 2-D graphical representations of Eq. 5 to help to show the similarities and differences among the various approaches to the assessment of Loewe synergism.

Figure 4 shows the relationship between a 3-D response surface of Loewe synergism, the construction of isobols, and the calculation of interaction indices. The 3-D surface was simulated with Eq. 5, our flagship model for agent interaction for the case in which the individual drugs follow the Hill model, Eq. 2, with unequal slope parameters. The interaction parameter, α , was made equal to 5 to demonstrate strong synergism. The other parameters used and additional technical details are listed in the figure legend. Note the scooped out nature of the Loewe synergistic surface in contrast to the three Loewe additivity bars at 75%, 50%, and 25% of control. A complete Loewe additivity surface ($\alpha = 0$) would consist of straight lines running across the surface parallel to these bars at every effect level. To show the 3-D origin of 2-D isobols, the surface is cut and separated at the 25%, 50%, and 75% effect levels and rotated so that the viewer sees the surface from the top. The isobols in panel (D) are not symmetric because of the different slope parameters for drug 1 ($m = -1$) and drug 2 ($m = -2$). However, as seen in panel (E), normalizing the drug concentrations by the respective ID_x values (from Eq. 7) makes the isobols symmetric. In addition, the normalization reverses the order of the isobols and makes the Loewe additivity lines lie on top of each other for all effect levels. Panel (E) shows the geometrical relationships among normalized isobols, interaction (or combination) indices, and response surface equations. One specific CI calculation is given for one specific point on the 25% pharmacological effect (75% control) isobol. The calculated CI is 0.68, indicating Loewe synergism. Vertical lines, made up of three different line patterns, run through the two data points. The three segments of each line correspond to the three right-hand parts of the response surface model, Eq. 5.

The geometrical relationships between interaction models and isobols are further examined in figure 5. Note in panel A that lines at a 45° angle in the northeast

direction between the isobol and the Loewe additivity diagonal are equal to the interaction term divided by $\sqrt{2}$. In panel (B), panel (A) is redrawn with the curves removed, with many horizontal, vertical and diagonal lines drawn, and with vertices labeled. These reference lines and ubiquitous 45° triangles all aid in the interpretation of the geometry of the 25% isobol (75% control). In panel (B), the length of each thick line represents the magnitude of the interaction term. This is a general result and will be true for a large class of specific equations that follow the general interaction equation, Eq. 9.

$$1 = \frac{D_1}{ID_{X,1}} + \frac{D_2}{ID_{X,2}} + f\left(\frac{D_1}{ID_{X,1}}, \frac{D_2}{ID_{X,2}}, \alpha, p\right) \quad [9]$$

Eq. 9 is a general form that is independent of the specific concentration-effect models for each drug (that may be different for each drug). Also, the interaction term may be any function of the normalized concentrations, may include any number of interaction parameters, α , and may include any number of additional parameters, p . Additional specific response surface interaction models, including ones from Weinstein et al. (1990) and Machado and Robinson (1994), which are consistent with Eq. 9, are described in Section V.L.

Figure 6 shows the geometrical relationships for 50% effect isobols for Eq. 5, with various values of α listed in the figure legend. When α is positive, the isobols are to the left of the Loewe additivity diagonal ($\alpha = 0$), line E; larger α values increase the bowing of the isobols, indicating more intense Loewe synergism. When α is negative, the isobols are to the right of the Loewe additivity diagonal; as α increases in absolute value, the isobols become more bowed, indicating more intense Loewe antagonism. The degree of bowing of the isobols can be quantitated as the ratio of the line segments, $S = o_n/o_m$ (Hewlett, 1969) or by the sum of $o_p + o_q$ (Elion et al., 1954). The interaction parameter, α , is related to these geometrical measures (Greco et al., 1990). Eq. 10 was derived by Greco et al. (1990) and shows the relationship between α and S for the 50% effect isobols of Eq. 5.

$$\alpha = 4(S^2 - S) \quad [10]$$

FIG. 4. Illustration of the relationship between a 3-D response surface of Loewe synergism, the construction of isobols, and the calculation of combination (interaction) indices. (A) A hypothetical 3-D solid shaded graph of measured effect (response, survival, or some other endpoint) expressed as a percent of control effect vs. the concentrations of drug 1 and drug 2. This graph was simulated with Eq. 5, with parameters: $Econ = 100$, $IC_{50,1} = 1$, $IC_{50,2} = 1$, $m_1 = -1$, $m_2 = -2$, $\alpha = 5$. The horizontal lines connecting the edges of the surface at 75%, 50%, and 25% of control are part of a Loewe additivity surface (Eq. 5, $\alpha = 0$). (B) The surface is cut and separated at the 75%, 50%, and 25% of control levels, and the sections are pulled apart to accent the inward curved shape of the surface. (C) The sectioned surface is being rotated so that the viewer will be able to see the surface from the top. (D) A view of the surface from the top; a set of 2-D isobols at 75%, 50%, and 25% of control, along with their corresponding Loewe additivity lines. (E) An isobogram in which the isobols at 75% and 25% of control each have their drug concentrations normalized by their respective ID_x values. This makes all of the isobols symmetrical, makes all of the Loewe additivity lines coincide, and reverses the order of the isobols. Two vertical lines, each running the full length of the Y-axis, and each comprised of three segments of different line patterns, one for the 25% isobol (75% of control) and one for the 75% isobol (25% of control) show the correspondence between the isobol diagram and Eq. 5. Each of the three segments corresponds to one of the three right-hand expressions of Eq. 5. In addition, the correspondence of the combination (or interaction) index, CI , and the isobols and Eq. 5 is illustrated.

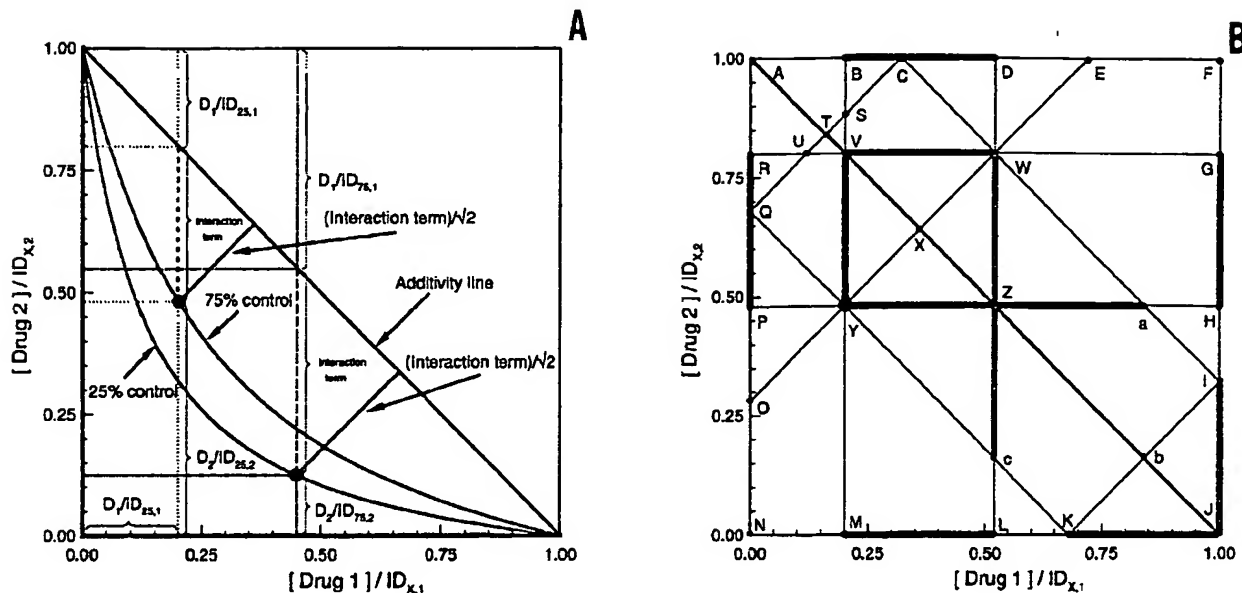


FIG. 5. Diagram to show the general correspondence between the geometry of interaction isobols and the algebraic expressions of interaction mathematical models. (A) An elaboration of Figure 4, Panel (E), which shows the correspondence between the lengths of line segments in the normalized isobogram and the value of the three right-hand expressions in Eq. 5 at 75% of control. Note that the interaction term that contains α , is the vertical distance between the curved isobol and the additivity line. (B) Panel (A) is redrawn, but only for the 25% isobol (75% of control) (with the curve removed), and many horizontal, vertical, and diagonal lines drawn and vertices labeled. The length of each thick line is equal to the value of the interaction term. This is a general correspondence, and will be true for many specific models that follow the general form of Eq. 9.

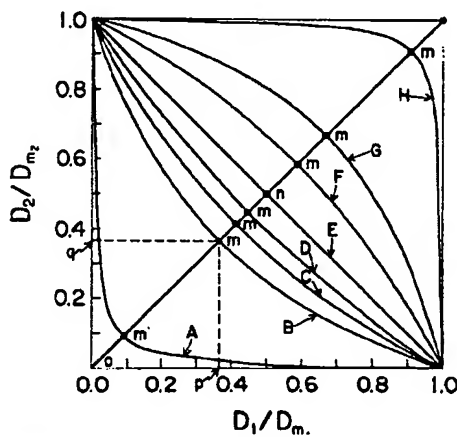


FIG. 6. Examples of isobols for the 50% effect level, simulated from equation 5, for a range of α values. For curves A through H, α was 100, 2, 1, 0.5, 0, -0.5, -0.75, and -0.99. Curves A through D represent varying degrees of Loewe synergism; curves F through H represent varying degrees of Loewe antagonism, and curve E is the straight line of Loewe additivity. The point n is the center of the straight Loewe additivity line, and points m are the centers of the other isobols. Points p and q are the abscissa and ordinate of the point m. The degree of bowing of the isobols can be quantitated as the ratio of the line segments, $S = on/on$ (Hewlett, 1969) or by the sum of $op + oq$ (Elion et al., 1954).

Figure 7 shows the relationship between the same 3-D response surface described in figure 5 and the concept of the CI vs. fa plot (mutually exclusive case) of the median-effect approach (Chou and Talalay, 1984). Although

the exact calculations for the CI vs. fa plot suggested by Chou and Talalay (1984) will be disputed in Section V.G, we believe that the general idea has great merit. Essentially, the 3-D surface is cut lengthwise along a fixed ratio of $D_1:D_2$ (for example, a ratio of 1:1 in fig. 7). Then, both the Loewe synergistic ray and the predicted Loewe additivity ray are drawn on a 2-D concentration-effect graph, both rays are normalized by the ID_X values along their whole lengths, and then the normalized graph is rotated counterclockwise by 90° . The details are provided in the figure legend.

Figure 8 is another graphical sequence, using the same simulated 3-D surface as shown in figures 4, 5, and 7, created to illustrate the concept of the CI vs. fa plot. In panel (A), the Loewe synergistic surface is deleted except for one vertical, infinitely thin slice for the fixed ratio of $D_1:D_2$ of 1:1. The length of the short horizontal line segments at various effect levels drawn from the curve to the backplanes are the values of D_1 and D_2 used to construct the Loewe synergistic surface. Panels (B) and (C) show the unnormalized and normalized set of isobols, respectively. The solid points in these panels are the same ones as in figure 7. The sum of one vertical and one horizontal line from each point in Panel C is equal to the CI at that effect level. Details are provided in the figure legend.

Thus, in essence, the isobogram approach consists of making horizontal slices through a 3-D surface, and the median-effect approach (mutually exclusive case) con-

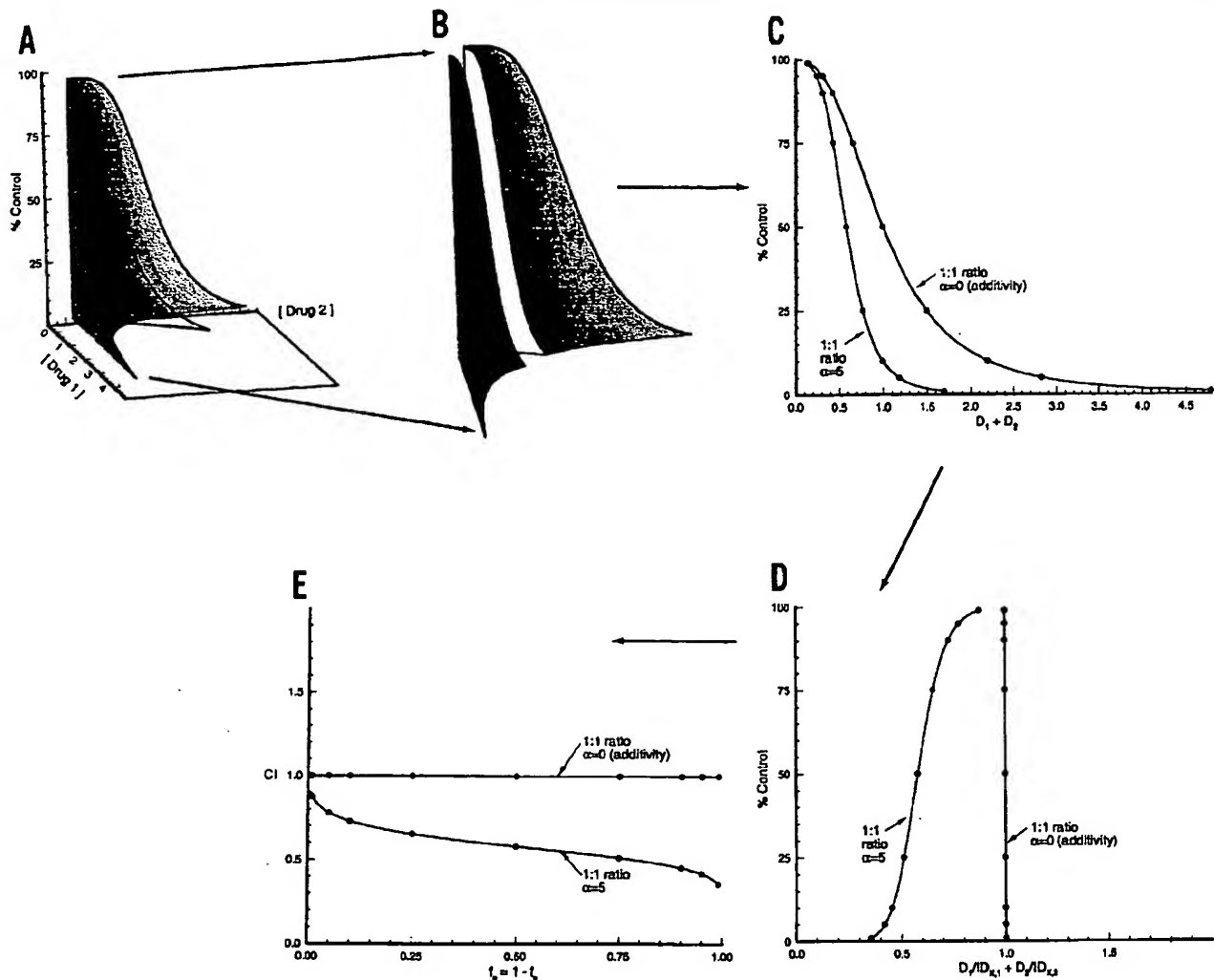


FIG. 7. Illustration of the relationship between a 3-D response surface of Loewe synergism and the CI vs. fa plot of the median-effect approach (Chou and Talalay, 1984). (A) The same hypothetical 3-D solid shaded graph shown in figure 4 is shown here. A curve is drawn on the surface for a fixed ratio of $D_1:D_2$ of 1:1, and a corresponding Loewe additivity curve, to the right of the solid surface, is drawn for the same fixed ratio of $D_1:D_2$ ($\alpha = 0$). (B) The solid surface is cut and separated at the fixed ratio of $D_1:D_2$ to accent the shape of the curved Loewe synergistic surface (the Loewe additivity curve was removed for clarity). (C) A 2-D plot of the Loewe synergistic and additive curves at the same fixed ratio of $D_1:D_2$, with $D_1 + D_2$ as the X -axis. The solid points in Panels (C) through (E) correspond to % Control levels of 99, 95, 90, 75, 50, 25, 10, 5, and 1. (D) The drug concentrations have been normalized by their respective ID_{50} s, and the X -axis is now the sum of the normalized concentrations. (E) Because the normalized sum is the same as the combination index, CI , for the mutually exclusive model, Eq. 8 (Chou and Talalay, 1984), and the % control is the same as 100 [$1 - fa$] (where fa is the fraction of effect affected), the CI vs. fa plot can be obtained by rotating the graph in Panel D counterclockwise by 90°.

sists of making vertical slices through the same 3-D surface. Both approaches and their variants then include examination of the shape of the slices, with or without data transformations, and/or making some calculations to summarize the shape of the slices, usually with comparison to a Loewe additivity reference.

The difference between a Loewe synergistic surface and a Loewe additivity reference surface can also be examined in 3-D. The difference can be calculated in the horizontal or vertical directions, and plotted, with or without additional transformations. The use of difference surfaces to examine combined-actions has been introduced by Prichard and Shipman (1990) and Sühnel

(1992c). The 3-D CI plot in figure 9 was calculated with Eq. 8 for the same simulated Loewe synergistic surface ($\alpha = 5$) shown in the previous figures. Note that CI starts at 1 for each drug alone, and decreases toward zero for combinations as either drug concentration increases toward infinity. Thus, for Loewe synergistic drug combinations that follow Eq. 5, there is more intense interaction, as quantified by CI (or I), at higher drug concentrations. In contrast, figure 10 [panels (A) and (C)] shows the results of plotting the vertical difference between the Loewe synergistic ($\alpha = 5$) and additivity surface. Panel (A) shows the Loewe synergistic surface with a fishnet and the Loewe additivity surface as a

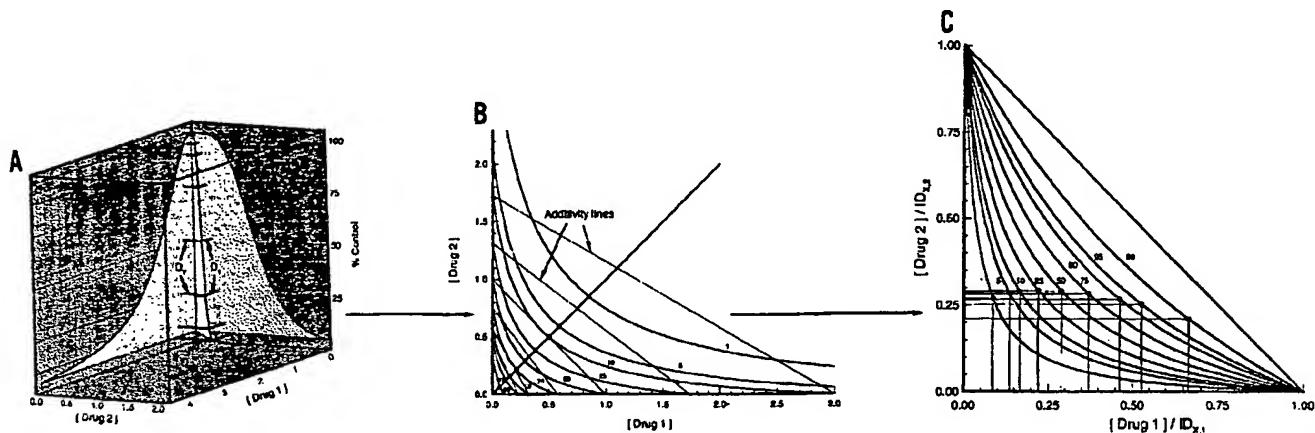


FIG. 8. An additional illustration of the relationship between a 3-D response surface of Loewe synergism and the combination index, CI . (A) For the same hypothetical surface shown in Figs. 4, 5, and 7, the concentration-effect curves for drug 1 and drug 2 alone are shown along the back walls of the figure, together with the Loewe synergistic middle curve for a fixed ratio of $D_1:D_2$ of 1:1. Line segments from the joint drug curve to the back walls represent the values of D_1 and D_2 used to construct the curve at % Control values of 99, 95, 90, 75, 50, 25, 10, and 5. (B) A view of the isobols for the surface from the top. The numbers next to the isobols indicate the % Control. The solid dots along the northeast-pointing diagonal indicate the points corresponding to the fixed ratio of $D_1:D_2$ of 1:1 at the indicated levels of % Control. Although not included in Panel (B), the line segments in Panel A would be horizontal and vertical lines from the dots to the axes. (C) The [Drug 1] and [Drug 2] axes are normalized by the respective ID_{50} values. The addition of the lengths of a horizontal plus a vertical line segment for each solid dot equals the CI for the respective % Control level. These points correspond to the respective points in figure 7.

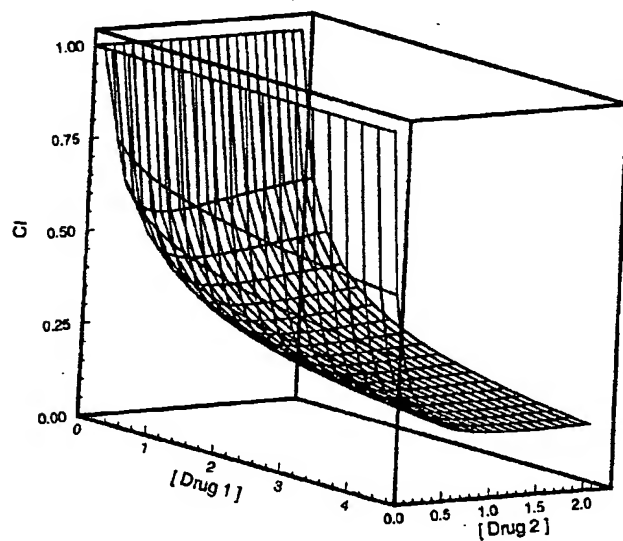


FIG. 9. A 3-D fishnet plot of the CI calculated from Eq. 8 for the Loewe synergistic concentration-effect surface described in Figs. 4, 5, 7, and 8.

solid sheet on top of the fishnet. Note that the difference between the two surfaces, shown in panel (C), has a peak near $D_1 = D_2 = 1$. Thus, when looking at vertical differences, the largest synergism is not at infinite drug concentrations, but rather at achievable drug concentrations near (but not exactly at) the IC_{50} 's of each drug. This critical difference in the two ways of forming differences between Loewe synergistic and Loewe additive surfaces, i.e., either in the horizontal or vertical direction, has profound implications for experimental design, as discussed in Section VIII.

In figure 10, panels (B) and (D) were constructed in an analogous manner to panels (A) and (C), except that the null reference model was that for Bliss independence, not for Loewe additivity. The general form of the Bliss independence effects equation is Eq. 11, and a specific form, which assumes that Eq. 2 is appropriate for each drug individually, is Eq. 12.

$$fu_{12} = fu_1 fu_2 \quad [11]$$

$$E = \frac{Econ \left(\frac{D_1}{IC_{50,1}} \right)^{m_1} \left(\frac{D_2}{IC_{50,2}} \right)^{m_2}}{\left(1 + \left(\frac{D_1}{IC_{50,1}} \right)^{m_1} \right) \left(1 + \left(\frac{D_2}{IC_{50,2}} \right)^{m_2} \right)} \quad [12]$$

In Eq. 11, fu_1 , fu_2 , and fu_{12} are the fractions of possible response for drug 1, drug 2, and the combination (e.g., % survival, %control) unaffected (Chou and Talalay, 1984). For Eqs. 2, 5, and 12, $fu = E/Econ$. Eq. 12 was used to generate the upper solid surface in panel B. Note that the difference plot in panel (D) has a central peak, but the peak is higher than the analogous one for the Loewe additivity reference in panel (C).

Which is a more appropriate reference, Loewe additivity (generally represented by Eq. 6) or Bliss independence (generally represented by Eq. 11)? Some of the approaches for interaction assessment examined in Section V use the Loewe additivity reference and others use the Bliss independence reference. This controversy is examined in detail in Section IV.

Our preferred paradigm of interaction assessment is most closely akin to the philosophical principles expressed by Berenbaum (1981, 1985, 1988, 1989), but

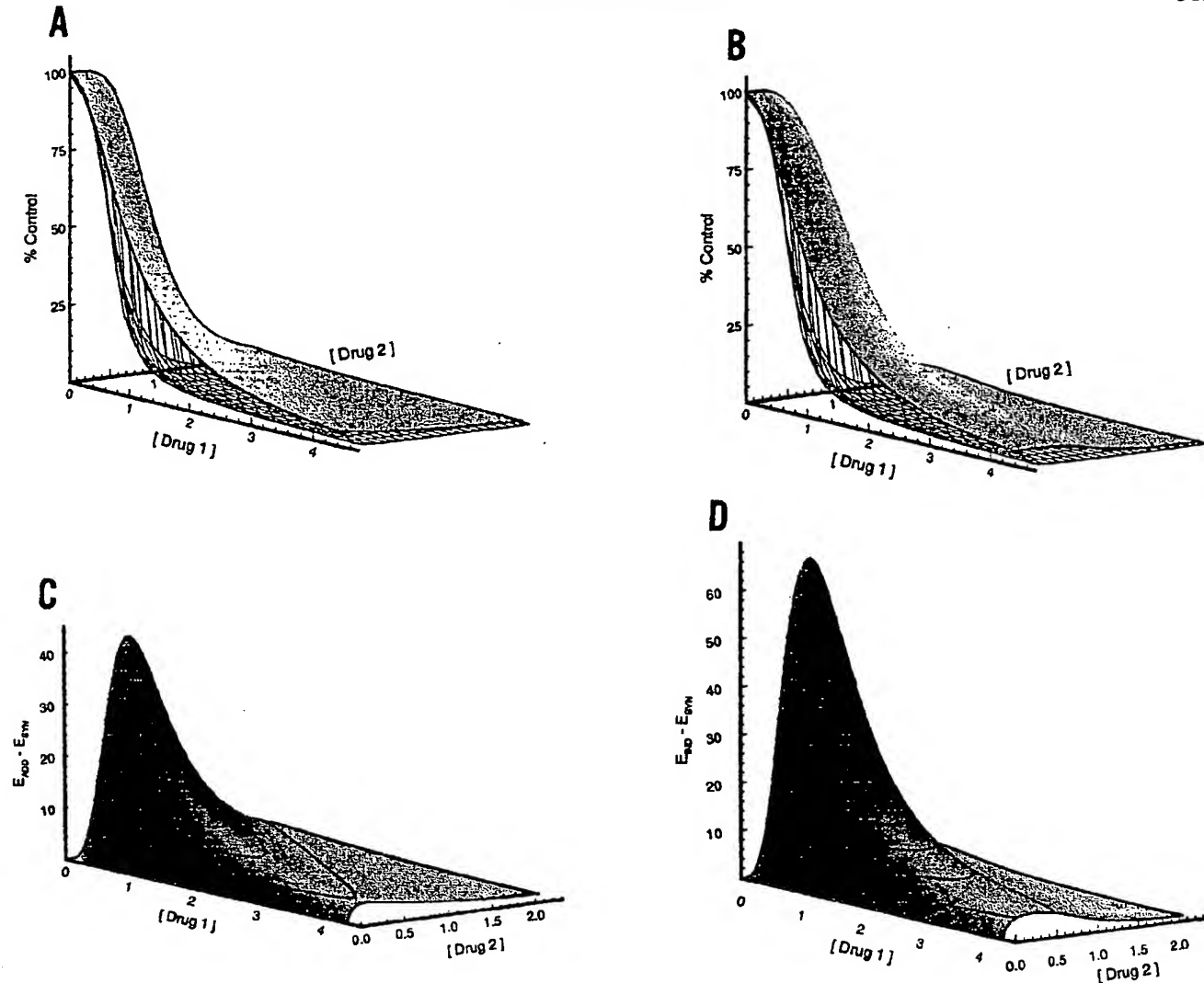


FIG. 10. (A) 3-D fishnet Loewe synergistic surface simulated with Eq. 5, with parameters: $E_{\text{con}} = 100$, $IC_{50,1} = 1$, $IC_{50,2} = 1$, $m_1 = -1$, $m_2 = -2$, $\alpha = 5$, the same as in Figs. 4, 5, and 7 through 9. The solid surface on the top of the fishnet is a Loewe additivity surface simulated with the same values for the first five parameters, but with $\alpha = 0$. (B) The 3-D fishnet Loewe synergistic surface is the same one as in Panel (A), but the solid top surface was simulated from the Bliss independence model, Eq. 12, with parameters: $E_{\text{con}} = 100$, $IC_{50,1} = 1$, $IC_{50,2} = 1$, $m_1 = -1$, $m_2 = -2$. C. A 3-D solid shaded graph of the difference between the Loewe additivity and Loewe synergistic surfaces in Panel (A). The contour lines are at five-unit intervals. (D) A 3-D solid shaded graph of the difference between the Bliss independence and Loewe synergistic surfaces in Panel (B).

with several major differences. The elements of the paradigm include: (a) combined-action assessment is most appropriate for complex systems in which a complete correct description of the mechanisms by which the agents cause their single and joint effects does not exist. If such a description does exist, then mathematical models based upon a mechanistic understanding of the concentration-effect relationships should be applied to data, not general combined-action mathematical models; (b) the degree of departure from "no interaction" of the concentration-effect surface for an agent combination is a quantitative measure of the ignorance of the investigator, i.e., if the system were well understood by the investigator, and this understanding were incorporated

into the "no interaction" model, then the experimental results would be as predicted (e.g., Loewe additivity)—no more, no less; (c) the Loewe additivity equation, Eq. 6, the Bliss independence equation, Eq. 11 or 14, or response surface interaction models adapted directly from them, should be used in an initial step to evaluate departures from the no interaction reference, without regard to mechanistic interpretation; (d) a later useful step in interaction assessment may involve the interpretation of Loewe synergism, Loewe additivity, Loewe antagonism, Bliss synergism, Bliss independence, Bliss antagonism, synergism, inertism, antagonism, or coalism via mechanistic arguments. For relatively simple systems, such as individual enzymes or receptors or small

networks of enzymes and receptors, it may be useful to establish the relationship between empirical interaction models and mechanistic biochemical models. However, except for very well understood simple systems, it is unlikely that the results of a combined-action analysis will unambiguously lead to a correct mechanistic explanation of an observed agent interaction; (e) the main uses of general combined-action analyses are:

(1) to summarize a large amount of data with a joint concentration-effect surface, with relatively few parameters, for a combination of agents.

(2) to facilitate good predictions of joint effects in regions in which no real data was collected (interpolation and judicious extrapolation).

(3) to empirically find and characterize agent combinations with intense interactions, in order to use or to avoid the combinations for specific practical purposes.

(4) to quantitatively characterize a system, so that the effect of changes in some other factor can be quantified.

(5) to provide a lead to a mechanistic explanation of joint action.

IV. Debate Over the Best Reference Model for Combined-action

Because synergism (and antagonism) are commonly defined as a greater (or lesser) pharmacological effect for a two-drug combination than what would be predicted for "no interaction" from the knowledge of the effects of each drug individually, their definitions critically depend upon the reference model for "no interaction." It is our view that there are only two reference models that deserve extensive consideration. The first, and our preference, is Loewe additivity, which is defined by Eq. 6. A specific model for Loewe additivity that assumes the Hill equation, Eq. 2, for the concentration-effect model for each drug individually, is Eq. 13.

$$1 = \frac{D_1}{IC_{50,1} \left(\frac{E}{Econ - E} \right)^{1/m_1}} + \frac{D_2}{IC_{50,2} \left(\frac{E}{Econ - E} \right)^{1/m_2}} \quad [13]$$

Note that Eq. 13 is equivalent to Eq. 5 with the third right-hand term, the interaction expression, dropped. Also note that Eq. 13 is merely the Loewe additivity model, Eq. 6, with the substitution of the definition of ID_X for the Hill model, Eq. 7, for both drugs. This derivation for a specific Loewe additivity model follows the guidelines of Berenbaum (1985), and the examples of Hewlett (1969) and Sühnel (1992c). The additivity reference concept was first mentioned by Frei (1913) and was first defined formally by Loewe and Muischnek (1926). The Loewe additivity reference is the diagonal Northwest-Southeast line in isobolograms of figures 4, 5, 6, and 8 and is a key part of the classical isobogram approach (Loewe and Muischnek, 1926; Elion et al., 1954; Gessner, 1974).

The simplest intuitive explanation of the concept of Loewe additivity is the following sham experiment: an aliquot of a solution of drug 1 from a tube is poured into a second tube and then diluted with an appropriate solvent. When these two preparations are falsely labeled as different agents and their combination is examined, the result will be Loewe additivity. [Gennings et al. (1990) experimentally illustrated and verified this concept by examining the loss of righting reflex of mice treated with the combination of sodium hexobarbital with itself.] Thus, by definition, one agent is noninteractive with itself. Advocates of the Loewe additivity reference for no interaction use this sham study of one drug with itself as a litmus test to invalidate other reference models (e.g., Berenbaum, 1981). From this logic, Loewe additivity implies that each of two drugs act similarly, presumably at the same site of action, differing only in potency. However, Eq. 6 is less restrictive than this narrow interpretation. The constraint of Eq. 6 can be obeyed for two drugs with different concentration-effect slopes, (e.g., Eq. 13) that presumably would not act at the same site. In fact, each of the two drugs in a combination could follow different concentration-effect functions and still obey Loewe additivity, Eq. 6. This flexibility is considered a weakness, with no theoretical justification, by opponents of the Loewe additivity reference [Greco et al., (1992)]. They contend that the rare observation of Loewe additivity in real complex experimental systems is only fortuitous and does not lead one to any mechanistic conclusion.

The strongest advocate of approaches based upon the Loewe additivity reference has been Berenbaum (1977, 1978, 1981, 1985, 1988, 1989). Of the approaches evaluated in our review, the following use the Loewe additivity reference: isobogram by hand; interaction index of Berenbaum (1977); median-effect method of Chou and Talalay (1984); mutually exclusive model method of Berenbaum (1985); bivariate spline fitting (Sühnel, 1990); parametric response surface approaches of Greco et al. (1990) and Weinstein et al. (1990); approach of Gessner (1974); parametric response surface approach of Greco and Lawrence (1988); and the use of the multivariate linear logistic model (Carter et al., 1983, 1986, 1988; Brunden et al., 1988). The concepts of similar joint action (Bliss, 1939), simple similar action (Plackett and Hewlett, 1952), and concentration (dose) addition (Shelton and Weber, 1981) are all consistent with Loewe additivity, as defined by Eq. 6. However, as discussed above, Loewe additivity also includes cases not consistent with these more restrictive concepts.

In our view, the most convincing argument in favor of the use of the Loewe additivity model, Eq. 6, as a universal reference to define "synergism" and "antagonism," is that it can best survive criticism. With the possible exception of Bliss independence, all of the other candidate reference models can be fatally wounded from well aimed attacks; whereas, the Loewe additivity

model, although not completely unscathed, is still standing after the smoke of battle clears. The Loewe additivity reference model, by definition, yields the intuitive correct evaluation of the sham combination of one drug with itself to be Loewe additivity (or as preferred by Berenbaum, 1981, "no interaction"). The Loewe additivity reference model is, in fact, merely a reasonable assumption. The interpretation of an assessment of Loewe additivity, Loewe synergism, or Loewe antagonism is, in general, free of mechanistic restrictions and implications. [In principle, the mathematical models and parameters of specific biological systems can be mapped to empirical combined-action models and parameters to facilitate a mechanistic interpretation of a combined-action analysis, but work on such mappings is in its infancy (e.g., Bravo et al., 1992; Jackson, 1993).] From a response surface perspective, the Loewe additivity model, Eq. 6, can be adapted to yield many useful empirical models of combined-action, such as Eq. 5.

In our view, the only other major contender for a universal reference of noninteraction (worthy of the silver medal) is Bliss independence, Eq. 11, or its equivalents. Eq. 12 is a specific Bliss independence model that assumes that the Hill model, Eq. 2, is an appropriate concentration-effect model for each drug individually. Bliss independence implies that two agents do not physically or chemically or biologically cooperate; i.e., each agent acts independently of the other. Berenbaum (1981) describes an interesting hypothetical experiment that provides an intuitive feel for independently acting agents. His thought experiment involves randomly throwing either bushels of nails or pebbles or both at a collection of eggs. None of the causal units, nails or pebbles, cooperate with each other in the cracking of an egg, an all-or-none phenomenon. But rather, each causal unit has a certain probability (different for nails or pebbles) of hitting an egg, and the cumulative damage is merely the result of correctly combining probabilities.

The Bliss independence reference model has an intuitive, theoretical basis: the concept of noninteraction; it has a simple general formula, Eq. 11. Testing of the model usually requires frugal experimental designs, and many specific approaches for interaction assessment incorporate it. These approaches include: the fractional product method of Webb (1963); the method of Valeriote and Lin (1975); the method of Drewinko et al. (1976); the method of Steel and Peckham (1979), Mode I; and the method of Prichard and Shipman (1990). Synonyms for Bliss independence include: independent effects, independent joint action (Bliss, 1939); independent action (Plackett and Hewlett, 1952); response (effect) addition (Shelton and Weber, 1981); effect summation (Gessner, 1988); and effect multiplication (Berenbaum, 1981). [Note: if Eq. 11 is recast in terms of the fraction of possible effect, with subscripts referring to specific concentrations of agent 1, agent 2, and the corresponding combination of agents 1 and 2, then Eq. 14 is the result.

This equation is analogous to the common formula for the combination of probabilities (e.g., Larson, 1982).]

$$fa_{12} = fa_1 + fa_2 - fa_1fa_2 \quad [14]$$

Gessner (1974; 1988) offered a philosophical argument against the Bliss independence model: *he questioned whether, given the high degree of integration of a living organism, the action of an agent on one receptor type, target organ, or system can ever be envisaged as not altering to some degree the responsiveness of other receptors, organs, or systems to a simultaneously present second agent.* Certainly, complex systems with extensive positive and negative feedback pathways at all levels of biological organization are ubiquitous and are the chief targets of drug therapy (Jackson, 1992). Most examples of theoretical systems that follow the Bliss independence model are relatively simple, such as single enzymes (e.g., Webb, 1963) and simple biochemical pathways (e.g., Jackson, 1991).

Gessner (1988) also mentioned that he had never seen a published isobologram for the 50% effect level for quantal data in which an isobol reasonably followed the Bliss independence model throughout the whole curve. In contrast, Pöch and coworkers have reported several examples of Bliss independence (e.g., Pöch, 1990; Pöch et al., 1990a, b, c; Pöch, 1991; Pöch, 1993). An objective survey would be necessary to estimate the frequency of occurrence of exact Bliss independence for combinations of agents in real experimental work. However, just as with Loewe additivity, it is also our impression that pure Bliss independence in complex systems is a rare occurrence.

The most convincing arguments against the Bliss independence model as a universal reference model for noninteraction use the pair of concentration-effect curves in figure 11 (Greco, 1989). [Similar figures and arguments were previously published by Grindey et al. (1975) and Berenbaum (1977, 1981)]. Figure 11 includes individual simulated data points and simulated concentration-effect curves for two different hypothetical inhibitory drugs. Suppose that 0.5 μM of drug 1 results in 95%

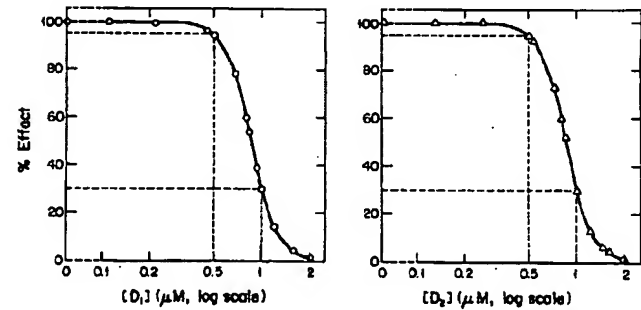


FIG. 11. Hypothetical concentration-effect curves for two drugs to demonstrate a logical inconsistency for approaches to assess drug synergism based upon the assumption of Bliss independence, Eq. 11 or Eq. 14, as the "no interaction" reference model.

survival of cells in a typical growth inhibition experiment, likewise for drug 2. From Eq. 11, one would predict that the noninteractive response for $0.5 \mu\text{M}$ of drug 1 plus $0.5 \mu\text{M}$ of drug 2 would be about 90% survival. Therefore, if one found that this drug combination elicited, let's say, 40% survival of cells, one would conclude strong, undeniable Bliss synergism. However, note in figure 11 that either $1 \mu\text{M}$ of drug 1 alone or $1 \mu\text{M}$ of drug 2 alone brings the survival of cells down to 30%. Therefore, a total of $1 \mu\text{M}$ of the hypothetical combined drug preparation elicits less of a cell kill than $1 \mu\text{M}$ of either drug alone, yet one would conclude strong Bliss synergism under methods based upon the Bliss independence reference assumption, Eq. 11.

Figure 11 can also be used to illustrate the paradox of the sham combination of one drug with itself. Let's say that a drug preparation is divided into two tubes, and then each tube is treated as if it contained a different drug. The two concentration-effect curves in figure 11, which are in fact identical, would result. Using the same logic as used in the beginning of the previous paragraph, one would conclude that the drug is Bliss synergistic with itself. This absurd conclusion is inconsistent with the intuitive definitions of "synergism," "additivity," and "antagonism" used by many researchers.

It is our view that these two aspects of the same basic criticism illustrated by figure 11 are persuasive enough to relegate Bliss independence to second place for the optimal routine reference for defining "synergism" and "antagonism." However, proponents of the Bliss independence reference have several counterarguments: (a) when concentration-effect curves are steep, such as in figure 11, the joint effects of a Bliss synergistic combination may be disappointingly small relative to the effects of each drug individually, but this result is neither paradoxical nor absurd; (b) a drug with a steep concentration-effect curve is Bliss synergistic with itself (this is a fundamental tenet of Biology); (c) the sham combination of a drug with itself is a silly experiment, and the so-called paradox is, at worst, a minor exception to a generally useful concept; (d) if it is known that two drugs in a combination act at the same biochemical site, a relatively rare situation, then their actions cannot be independent, and one shouldn't use the Bliss independence reference. Figure 11 is merely an illustration of the extreme case of this situation, in which the two dose response curves are identical.

Our rejoinders to these counterarguments include: (a) the search for synergy will often involve agents, drugs, and preparations with multiple, complex, possibly unknown mechanisms of action, and therefore, guidelines for the assessment of interaction must not depend upon knowledge of mechanisms of action; (b) a general concept must encompass rare cases; (c) the first argument illustrated by figure 11 did not require that the two drugs be the same or that they have similar sites of action, but only that they have steep concentration-

effect curves; (d) a reference model that can result in the counterintuitive result, that a synergistic combination is less effective than its components applied individually, is not useful.

As pointed out by Berenbaum (1981), the fundamental explanation underlying both forms of the above paradox involves the functional form of the individual concentration-effect curves. Only when each individual concentration-effect curve follows Eq. 4, that for exponential decline with dose, will there be no paradox: Loewe additivity will be concluded from the sham combination of one drug with itself. Eq. 15 would be the resulting equation for no interaction of two drugs, from combining either Eq. 4 and Eq. 6 (Loewe additivity) or Eq. 4 and Eq. 11 (Bliss independence). Concentration-effect curves steeper than the exponential model will lead to the above paradox; whereas, concentration-effect curves less steep than the exponential model will lead to an opposite paradox. (Note: the data points and curves in figure 11 were simulated with Eq. 2 with $Econ = 100$, $IC_{50} = 0.86 \mu\text{M}$, and $m = -5.6$, resulting in relatively steep curves.)

$$E = Econ \exp(aD_1)\exp(bD_2) = Econ \exp(aD_1 + bD_2) \quad [15]$$

However, we disagree with Berenbaum's inference from the above logic that the Bliss independence model, Eq. 11, is appropriate for describing the joint action of a combination only when each of the component drugs have exponential concentration-effect curves, Eq. 4. Berenbaum (1981) argues that in order for molecules of drug 1 to act independently from molecules of drug 2, all molecules of drug 1 must act independently of all other molecules of drug 1, resulting in an exponential concentration-effect curve for drug 1; all molecules of drug 2 must act independently of all other molecules of drug 2, resulting in an exponential concentration-effect curve for drug 2. This argument can be refuted by a specific counterexample from Jackson (1991). Jackson (1991) modeled a hypothetical biochemical pathway consisting of: a substrate, A, being converted to substrate B by enzyme 1; substrate B being converted to substrate C by enzyme 2, and to substrate D by enzyme 3; a competitive inhibitor of enzyme 1; and a competitive inhibitor of enzyme 2. When the enzyme kinetic parameters are adjusted to give a high sink capacity (the ratio of the sum of the maximal velocities of enzymes 2 and 3 divided by the maximal velocity of enzyme 1), exact Bliss independence of the effects of the two inhibitors can be achieved. The individual concentration-effect curves for the two inhibitors followed the Hill model, Eq. 2, and thus were nonexponential, yet the specific Bliss independence model, Eq. 12, fit the data perfectly over a wide range of inhibitor concentrations (Bravo et al., 1992). In addition, Pöch (1991) provides several specific examples of Bliss independence found with real laboratory data, in which the individual concentration-effect curves follow the Hill model, Eq. 2 or 3. Thus, this specific argument

of Berenbaum against the independent effects model is questionable.

Although we prefer Loewe additivity to Bliss independence as a universal reference for the lack of "synergism" or "antagonism," we must concede that the Bliss independence camp has successfully resisted total defeat. It is clear that adherents of Loewe additivity and Bliss independence have heard all of the most compelling arguments for and against each model and cannot be persuaded to switch allegiances. Thus, the debate can progress no further, and we join in the recommendation that both models be accepted as legitimate empirical reference standards for "no interaction." It must be emphasized, however, that neither model is well suited for unambiguously indicating mechanistic explanations for the joint action of agents in complex systems, such as whole cells, single organisms, or populations of organisms. In order for researchers to make mechanistic conclusions for a specific experimental system, the correspondence between empirical concepts—such as Loewe synergism or Bliss antagonism—and theoretical mechanisms must be derived. This is a rich source for future research initiatives.

The shapes of isobols for Loewe additivity and Bliss independence will, in general, be very different. Figure 12 shows a set of isobols at the 50% effect level for the specific Bliss independence model, Eq. 12, which incorporates the Hill model, Eq. 2, for the individual concentration-effect curves. The shape of the isobols is determined only by the two slope parameters, m_1 and m_2 ; these are listed in figure 12 next to each respective isobol. [Note: Similar figures and observations are provided by Gessner (1988) and Pöch et al. (1990c)]. When the slope parameters are the same for the two drugs, the isobols are symmetrical; when they are different, the

isobols have an S shape and may cross the Loewe additivity diagonal. Slope parameters that are large in magnitude result in Loewe antagonism; whereas, slope parameters that are small in magnitude result in Loewe synergism. It may be useful to superimpose the predicted Bliss independence model on both 2-D and 3-D representations of two-drug combination concentration-effect surfaces. If the superimposed Bliss independence curves lie close to the data, then it may be useful to infer, after making necessary assumptions, that the two drugs may, in some sense, act independently.

Four other candidates for a universal reference for no interaction will be briefly described and critiqued below. The first is Eq. 16, that for effect addition, and the second is almost the same, Eq. 17, that for fractional effect addition. [Note: Some authors call Eq. 11 and 14 the effect addition model (e.g., Shelton and Weber, 1981).]

$$E_{12} = E_1 + E_2 \quad [16]$$

$$fa_{12} = fa_1 + fa_2 \quad [17]$$

According to Eq. 16, if the effect for a particular concentration of drug 1 was 20 units and that for a particular dose of drug 2 was 30 units, then the no interaction prediction would be 50 units. As pointed out by Berenbaum (1981), this intuitive definition of no interaction may underlie the claims of synergism and antagonism for which authors provide no explicit definitions. Eq. 16 is not easily applied to the common case in which the drugs have some maximum possible effect, because if E_1 and E_2 are both reasonably large, 60 and 70, let's say, and close to the maximum possible effect, 100, let's say, then E_{12} would be 130, greater than the maximum possible effect, resulting in an inconsistency. For one restricted situation, when each of the individual concentration-effect curves are linear and increasing, Berenbaum (1981) showed that Eq. 16 is consistent with the Loewe additivity model, Eq. 6.

A somewhat more credible variation of effect addition, Eq. 16, is fractional effect addition, Eq. 17. According to Eq. 17, if the fraction of possible effect affected for drug 1 is 0.20 and the fraction affected for drug 2 is 0.30, then the no interaction prediction would be 0.50. Eq. 17 is also easily eliminated as a candidate for a universal standard by considering an example in which the fractional effects are both large, let's say, $fa_1 = 0.60$ and $fa_2 = 0.70$. Because fa_{12} has an upper limit of 1.0, the sum of $fa_1 + fa_2$, which equals 1.30, leads to an inconsistency. In addition, paradoxes regarding synergy, similar to those described above for the Bliss independence reference model, can be contrived using figure 11. However, Eq. 17 is valid or approximately valid under several restricted situations. The first is the case in which fa_1 and fa_2 are both very small. Then Eq. 17 will approximate Eq. 14, that for Bliss independence, because the product term will be very small (Pöch, 1991). The second

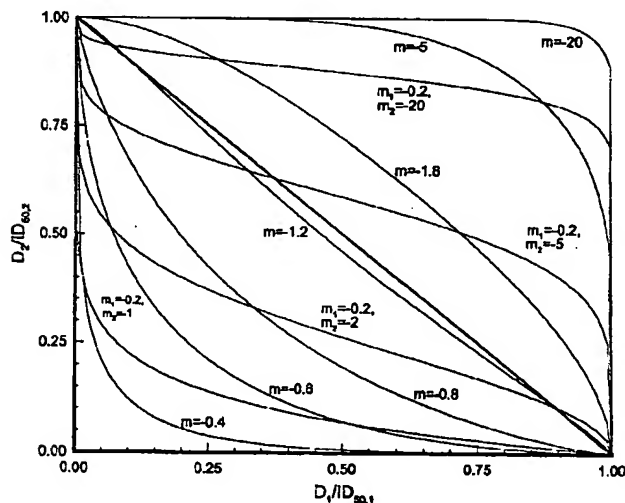


FIG. 12. Normalized isobols at the 50% effect level, for the Bliss independence model, Eq. 12, for various values of m_1 and m_2 , which are set next to each corresponding curve. A single m indicates that $m_1 = m_2 = m$. The thick diagonal line is the line of Loewe additivity.

is independent effects for quantal responses, in which the susceptibilities of the individual organisms to the two drugs are completely negatively correlated (any organism that is affected by drug 1 will not be affected by drug 2, and vice versa) (Plackett and Hewlett, 1948). The third is the joint effects of two inhibitors in a metabolic network in which two converging reactions that lead to a single product are both inhibited (Jackson, 1991). Note that these latter two examples of restricted conditions both impose upper limits upon the magnitudes of fa_1 and fa_2 ; their sum never exceeds 1.0.

Another candidate for a universal reference for no interaction is the mutually nonexclusive model of Chou and Talalay (1984), Eq. 18. An alternate form is Eq. 19, which is equivalent to Eq. 5, our model for drug interaction, with $m = m_1 = m_2$ and $\alpha = 1$. As emphasized by Chou and Talalay (1984), their mutually nonexclusive model is equivalent to the Bliss independence model only under restricted conditions; specifically, when the median-effect model (equivalent to Eq. 1 or Eq. 2) adequately describes the individual concentration-effect curves for both drugs and $m_1 = m_2 = -1$ for monotonically decreasing curves [or $m_1 = m_2 = 1$ for monotonically increasing curves, as preferred by Chou and Talalay (1984)]. They further conclude that the Bliss independence model is inadequate under conditions in which $|m| \neq 1$. However, it is our view that it is the mutually nonexclusive model that is suspect. Only an abbreviated general derivation of this model, for the case of multiple mutually nonexclusive inhibitors of a single enzyme, is provided in Chou and Talalay (1981). A specific derivation, for the case of two mutually nonexclusive noncompetitive inhibitors, is provided in Appendix A. An equation equivalent to Eq. 12, not to Chou and Talalay's mutually nonexclusive model, is the result. Because their model is of questionable validity, we feel that it is not appropriate as a universal reference. An extensive discussion of the median-effect approach to the assessment of drug interaction is provided in Section V.G.

$$\left(\frac{fa_{12}}{fu_{12}}\right)^{1/m} = \left(\frac{fa_1}{fu_1}\right)^{1/m} + \left(\frac{fa_2}{fu_2}\right)^{1/m} + \left(\frac{fa_1fa_2}{fu_1fu_2}\right)^{1/m} \quad [18]$$

$$= \frac{D_1}{Dm_1} + \frac{D_2}{Dm_2} + \frac{D_1D_2}{Dm_1Dm_2}$$

$$E = \frac{Econ \left(\frac{D_1}{IC_{50,1}} + \frac{D_2}{IC_{50,2}} + \frac{D_1D_2}{IC_{50,1}IC_{50,2}} \right)^m}{1 + \left(\frac{D_1}{IC_{50,1}} + \frac{D_2}{IC_{50,2}} + \frac{D_1D_2}{IC_{50,1}IC_{50,2}} \right)^m} \quad [19]$$

A final candidate for a universal reference for no interaction is the Mode II additivity model of Steel and Peckham (1979). A compact way to express the model is

Eq. 20. An equivalent form is provided by Kodell and Pounds (1991).

$$D_2 = ID_{[X-fa(D_1)]/2} \quad [20]$$

Eq. 20 can be used to construct an isobol for D_2 versus D_1 for a particular $X\%$ inhibition. To do this, D_1 is varied, and the fraction affected (% inhibition) for the particular D_1 is calculated and subtracted from the target $X\%$. Then, the D_2 needed to achieve this resulting difference $X\%$ is determined. Interestingly, this reference model will give the correct answer of no interaction for a sham combination of drug 1 with itself; the isobol will be a straight diagonal NW-SE line, such as in figure 6. However, Eq. 20 is not equivalent to the Loewe additivity model, Eq. 6. This will be shown and discussed in detail in Section V.F. A fatal flaw of the Mode II reference model is that it has a polarity; i.e., for two different drugs, different isobols will be drawn, depending upon the arbitrary assignment of drug 1 and drug 2 (Berenbaum, 1981).

The issue of the preferred reference model for no interaction has been recently debated in the antiviral literature by Sühnel (1990; 1992a) and Prichard and Shipman (1990; 1992). We endorse Sühnel's advocacy of the Loewe additivity model, Eq. 6 over Prichard and Shipman's advocacy of Bliss independence, Eq. 11 or Eq. 14. However, this is mainly because of personal preference and because our specific response surface models incorporate Loewe additivity. We do not endorse Sühnel (1990, 1992a) and Berenbaum's (1981) main argument that the Bliss independence model is only valid for the case in which each individual concentration-effect curve follows an exponential concentration-effect curve. Rather, we feel that the paradoxes illustrated with figure 11 are sufficient to place Bliss independence in second place for the competition for a universal null reference model.

In summary, we advocate the use of the Loewe additivity model, Eq. 6, as the best choice for a universal standard reference for defining "synergism" and "antagonism." Adaptations of Eq. 6 can be used to derive concentration-effect response surface functions, such as Eq. 5, containing interaction parameters, such as α . To the best of our knowledge, response surface models for agent interaction that incorporate Bliss independence have not been developed. However, some ideas of Ashford and Smith (1964) and Ashford (1981), which have been recently reviewed by Unkelbach (1992), have the potential to lead to the development of such models.

V. Comparison of Rival Approaches for Continuous Response Data

There are many published methods for assessing drug interactions. We have carefully chosen 13 of them for continuous response data to compare in a head-to-head competition. (Section VI includes a comparison of three

rival approaches for discrete success/failure data.) Some methods consist of general guidelines, whereas others include very specific recipes. This set of 13 methods was chosen because, as a group, they have a high frequency of use, have a high relative impact on biomedicine, have many similarities and differences, provide a good summary of the practical history of drug interactions, include good examples of the pleasures, pitfalls, controversies and paradoxes inherent in the field, and point toward the future of interaction assessment. Noteworthy additional approaches not extensively evaluated in this review include the ones by Pöch (1990b), Kodell and Pounds (1985), Tallarida et al. (1989), Kelly and Rice (1990), and Laska et al. (1994). The 13 rival approaches will be compared in two ways: (a) Theoretical aspects, both positive and negative, of each approach will be listed and discussed. Although a large number of these comments will be summarized from previous work of other reviews, there will be many new comments. Several of the theoretical comments will refer back to Sections I to IV. (b) An abbreviated recipe for the application of each approach to a common data set, for an inhibitory drug, will be described. For a complete recipe of each approach, the reader is encouraged to consult the original references. Each approach will then be applied to a common data set. Pitfalls, problems, and results will be listed and compared.

The common data set consists of the 38 data points in columns 2 to 4 of table 3, simulated with the approach described completely in footnote *a* of the table. Briefly, this data set was simulated with Eq. 5 as the structural model, with different slope parameters for the two drugs ($m_1 = -1$, $m_2 = -2$) and with a small amount of synergism ($\alpha = 0.5$). The data contains normally distributed random relative errors; the coefficient of variation is 10%. A simulated Monte Carlo data set was used, as opposed to a real data set, because: (a) the "true" answer is known, so there is an absolute reference for making comparisons between rival approaches; and (b) specific characteristics can be imbedded in the data set to illustrate specific differences among rival approaches. To the best of our knowledge, this approach to making comparisons among rival methods to assess agent interaction has not been used by groups other than ours (Syracuse and Greco, 1986; Greco, 1989).

A. Isobogram by Hand

The graphical isobogram approach, performed by hand, with the aid of pencil, ruler, graph paper, and possibly French curve, has its origins in the work of Fraser (1870–1871; 1872), Loewe (Loewe and Muischnek, 1926; Loewe, 1928, 1953, 1957), and Eliot, Singer, and Hitchings (1954). It is a general approach and has many interpretations and variants. Our interpretation is described here. The first step is to plot the measured data, such as those found in columns 2 to 4 of table 3, as concentration-effect curves, such as in figure 13. Two

separate graphs are drawn, usually by hand with a French curve or a straight edge, one for drug 1 and the other for drug 2. Each graph has a family of concentration-effect curves, one curve for each level of the other drug. The IC_{50} (or D_m , ID_{50} , ED_{50} , LD_{50} , etc.) values are then determined, by eye, for each curve on both graphs. From Figure 13, six IC_{50} values can be determined, three from the left panel and three from the right panel. (An IC_{50} value cannot be determined for six of the concentration-effect curves, because for each of them, the measured response at the first drug concentration is already below 50% of the maximum measured response.) From the left panel, the IC_{50} values for drug 1 are recorded along with the level of drug 2 used to generate the respective concentration-effect curves. Then, these IC_{50} values for drug 1 are divided by the IC_{50} value for drug 1 in the absence of drug 2, and the levels of drug 2 are divided by the IC_{50} for drug 2 alone. The resulting data points, $(D_1/D_{m1}, D_2/D_{m2})$, are the solid points on the left isobogram of figure 14. The analogous procedure is performed on the concentration-effect curves of the right panel of figure 13, resulting in the open points in the left panel of figure 14. In the isobograms of figure 14, each data point is labeled (a-l) to correspond to the curve in figure 13 from which it was derived. Occasionally, smooth curves are drawn through points on an isobogram, possibly with a French curve; occasionally, straight lines are drawn connecting the points, and occasionally, no curve is drawn at all. In figure 14, curve W is not a curve drawn by hand, but rather is the theoretically correct isobol simulated with Eq. 21 (an isobol model that assumes that Eq. 5 is appropriate for the entire concentration-effect surface), for the 50% level and for $\alpha = 0.5$. As explained in Section III and shown in figures 4, 5, 6, and 8, the diagonal NW-SE line is the line of Loewe additivity; points below the line indicate Loewe synergism and points above the line indicate Loewe antagonism.

$$\frac{D_2}{IC_{X,2}} = \frac{1 - \frac{D_1}{IC_{X,1}}}{1 + \frac{\alpha D_1}{IC_{X,1}} \left[\frac{100 - X}{X} \right]^{(1/2m_1 + 1/2m_2)}} \quad [21]$$

In principle, any constant effect level can be used for an isobogram analysis, not just the 50% level. Because most of the concentration-effect curves from figure 13 did not yield a D_m value, IC_{80} (D_{80}) values were also determined. The right panel of figure 14 is the isobogram analysis of the D_{80} values.

If one only used the D_m isobogram from figure 14, one would conclude that the experiment should be repeated. If one also used the D_{80} isobogram from figure 14, one would conclude that the interaction between drug 1 and drug 2 is Loewe synergistic.

TABLE 3

Data set, with a continuous response variable, used for comparison of rival data analysis approaches, and the results from four approaches

Data point number	D_1	D_2	Measured effect*	Predicted effect from Bliss independence model†	Conclusion from fractional product comparison‡	Conclusion from V and L system§	Drewinko's Score	Predicted effect from Loewe additivity model¶	Berenbaum's interaction index, I#	Conclusion from Loewe additivity comparison**
1	0	0	106					99.2		
2	0	0	99.2					99.2		
3	0	0	115					99.2		
4	0	0.2	79.2					94.6		
5	0	0.5	70.1					77.4		
6	0	1	49.0					47.9		
7	0	2	21.0					19.6		
8	0	5	3.88					4.00		
9	2	0	74.2					81.7		
10	5	0	71.5					64.9		
11	10	0	48.1					48.4		
12	20	0	30.9					32.2		
13	50	0	16.3					16.1		
14	2	0.2	76.3	55.0	BANT	INT	21.3	74.3	1.10	LANT
15	2	0.5	48.8	48.6	BANT	SUB	0.2	61.1	0.713	LSYN
16	2	1	44.5	34.0	BANT	SUB	10.5	40.6	1.10	LANT
17	2	2	15.5	14.6	BANT	SUB	0.9	18.2	0.901	LSYN
18	2	5	3.21	2.66	BANT	SUB	0.55	3.94	0.895	LSYN
19	5	0.2	56.7	52.9	BANT	SUB	3.8	58.3	0.944	LSYN
20	5	0.5	47.5	46.9	BANT	SUB	0.6	48.2	0.978	LSYN
21	5	1	26.8	32.7	BSYN	BSYN	-5.9	33.6	0.811	LSYN
22	5	2	16.9	14.0	BANT	SUB	2.9	16.5	1.02	LANT
23	5	5	3.25	2.56	BANT	SUB	0.69	3.85	0.911	LSYN
24	10	0.2	46.7	35.6	BANT	SUB	11.1	43.5	1.13	LANT
25	10	0.5	35.6	31.5	BANT	SUB	4.1	36.5	0.968	LSYN
26	10	1	21.5	22.1	BSYN	BSYN	-0.6	26.7	0.818	LSYN
27	10	2	11.1	9.44	BANT	SUB	1.66	14.4	0.836	LSYN
28	10	5	2.94	1.72	BANT	SUB	1.22	3.72	0.878	LSYN
29	20	0.2	24.8	22.9	BANT	SUB	1.9	29.2	0.809	LSYN
30	20	0.5	21.6	20.3	BANT	SUB	1.3	25.1	0.844	LSYN
31	20	1	17.3	14.1	BANT	SUB	3.2	19.4	0.899	LSYN
32	20	2	7.78	6.07	BANT	SUB	1.71	11.6	0.751	LSYN
33	20	5	1.84	1.10	BANT	SUB	0.74	3.47	0.698	LSYN
34	50	0.2	13.6	11.3	BANT	SUB	2.3	15.0	0.898	LSYN
35	50	0.5	11.1	9.96	BANT	SUB	1.14	13.4	0.824	LSYN
36	50	1	6.43	7.47	BSYN	BSYN	-1.04	11.1	0.613	LSYN
37	50	2	8.34	3.20	BANT	SUB	0.14	7.66	0.539	LSYN
38	50	5	0.890	0.583	BANT	SUB	0.307	2.93	0.496	LSYN
Totals			BSYN = 3	BSYN = 3	mean = 2.59				LSYN = 21	
			BANT = 22	SUB = 21	S.D. = 5.1				LANT = 4	
				INT = 1	S.E. = 1.02					

* The "Measured Effects" were generated by: (a) calculating ideal data with Eq. 5 with parameters, $Econ = 100$, $IC_{50,1} = 10$, $IC_{50,2} = 1$, $m_1 = -1$, $m_2 = -2$, $\alpha = 0.5$; (b) generating normally distributed random numbers with a mean of 0 and a variance of 1 (Box and Müller, 1958); (c) calculating relative errors by the equation, error = [(normal random number)/10] \times [ideal effect]; (d) adding the errors to the ideal effects to generate simulated data with relative error (a coefficient of variation of 10%).

† Each measured effect from column 4 was divided by the average of the control effects (107) to yield a fraction of control effect, then the fractional effects for the appropriate D_1 and D_2 were multiplied, then this product was multiplied by the average of control effects to yield the entries in column 5.

‡ For the fractional product approach to the assessment of drug interaction (Webb, 1963), when the entry in column 4, the measured effect, is greater than the entry in column 5, the predicted effect, then Bliss antagonism (BANT) (less inhibition than predicted) is recorded; when the column 4 entry is less than the column 5 entry (more inhibition than predicted), then Bliss synergism (BSYN) is recorded.

§ The Valeriote and Lin (1975) system differs from the Webb approach by further subdividing the Bliss antagonism into 3 categories, subadditivity (SUB), interference (INT), and antagonism (ANT). Details are in the text.

|| Column 8 is the difference between columns 4 and 5. From the mean and standard error of the mean for this difference score (Drewinko et al., 1976) one would conclude significant antagonism ($P < 0.05$). See the text for details.

¶ The predictions in column 9 are based on the best fit of Eq. 13 to the data points for which drug 1 and drug 2 were not simultaneously present, i.e., the data in columns 2-4, rows 1-13, and then the simulation of Eq. 13 with these 5 best fit parameters for all of the 38 data points.

Berenbaum's interaction index (I) is calculated from Eq. 22, with the ID_{Xs} for drug 1 and drug 2 calculated from Eq. 7 with the parameter values from the best fit of Eq. 13 to the first 13 data points.

** When $I > 1$, then Loewe antagonism (LANT) is concluded; when $I < 1$, then Loewe synergism (LSYN) is concluded.

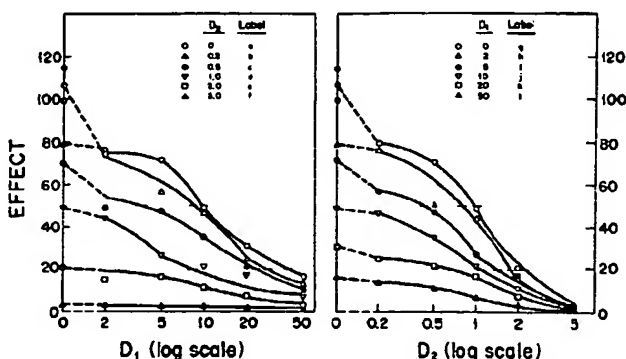


FIG. 13. Hand-drawn (with the aid of a French curve) concentration-effect curves for the data in columns 2 through 4 from table 3. The IC_{50} and IC_{80} values for each curve are indicated by short horizontal lines intersecting the curves.

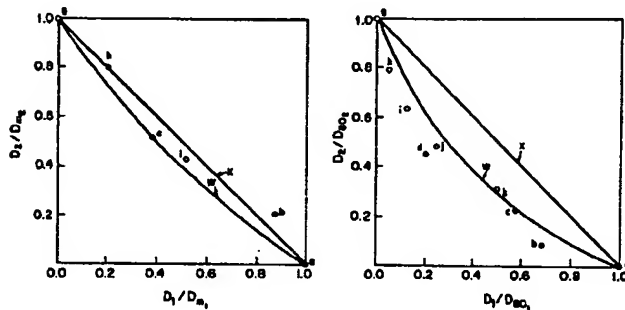


FIG. 14. Isobolograms made from IC_{50} values (left panel) and IC_{80} values (right panel). Line x in each panel is the Loewe additivity line. The data points in each panel are labeled with a lowercase letter that corresponds to the appropriate curve from figure 13. The solid points were derived from the left panel of figure 13, and the open points from the right panel. Curves W in each panel of figure 14 are the theoretically correct isobols and were simulated from Eq. 21 with parameters: $Econ = 100$, $IC_{50,1} = 10$, $IC_{50,2} = 1$, $m_1 = -1$, $m_2 = -2$, $\alpha = 0.5$.

The advantages of the isobogram by hand method include:

(a) the null reference model for no interaction is the Loewe additivity model, Eq. 6, which was given support in Section IV and is our preferred universal standard.

(b) the approach is simple, flexible, and to many users, intuitive.

(c) equipment to run the approach is inexpensive, and expert statistical advice and/or the learning of some modern statistical ideas are unnecessary.

(d) the approach is famous and widely accepted.

(e) variants of the basic method exist that add more statistical rigor (e.g., Gessner, 1974; Gennings et al., 1990) and that provide quantitative measures of interaction intensity (e.g., Hewlett, 1969; Eliot et al., 1954; Pöch, 1980).

(f) many newer, more rigorous methods have the basic isobogram approach as their underlying basis (e.g., the method of Berenbaum (1985), the nonparametric bivariate spline fitting approach of Sühnel (1990), and

the parametric response surface approach of Greco et al. (1990).

The disadvantages of the isobogram by hand method include:

(a) the method lacks many of the good characteristics of objective statistical procedures. It lacks the theoretical framework to allow inferences with a specified degree of certainty to be made from an experiment to the true situation. It lacks the option of objectively weighting more precise measurements greater than less precise ones.

(b) the basic isobogram method lacks a summary measure of the intensity of interaction.

(c) for the isobogram method, each concentration-effect curve should have data that encompasses the IC_X level. When this is not the case, such as with curves d-f, j-l in figure 13, for the 50% effect level, the data for those curves is wasted. If enough data is wasted, then the experiment may have to be rerun.

(d) in general, the basic isobogram method requires a relatively large amount of data. When data is expensive, combination experiments may become prohibitive.

(e) graphs of a measured dependent variable vs. an experimentally fixed independent variable, often fruitfully assumed to be recorded without error, are appealing, because they represent directly the actual experiment. Fitted curves can be superimposed upon actual observed data points to provide a good indication of the goodness of fit of the data by the curves. Isobograms are not such graphs; no observed data points appear on them. Both the X- and Y-variables in isobograms are subject to error of a complex, unknown distribution.

(f) the scatter of points in an isobogram may lead the researcher to a false conclusion of Loewe synergism in some regions and Loewe antagonism in other regions of the concentration-effect surface. Such a conclusion might be reached with the isobogram in the left panel of figure 14.

(g) it may take a relatively long time to plot by hand the required curves and to perform the required calculations.

(h) different data analysts are likely to plot the data differently and thus arrive at different answers.

B. Fractional Product Method of Webb (1963)

This method is a very simple one. Eq. 11, that for Bliss independence, is used to construct a set of predicted fractional responses, fu_{12} , as the product of the individual fractional effects, fu_1 and fu_2 , for specific concentration combinations. Then, optionally, the results can be re-expressed as responses on the original response scale by multiplying each fu_{12} by the control response, as was done to calculate the entries for column 5 of table 3 for the analysis of the 38-point common data set. For an inhibitory drug, when the predicted response exceeds the measured response, Bliss synergism is claimed; when the measured response exceeds the predicted re-

sponse, Bliss antagonism is claimed. Column 6 of table 3 lists the conclusions for each of the 25 combination points. There were 22 claims of Bliss antagonism and 3 claims of Bliss synergism. The overall conclusion is moderate Bliss antagonism, seemingly different from the conclusion of Loewe synergism from the isobogram analysis.

The advantages of the fractional product method include:

(a) it is the simplest of all methods; it is very intuitive. Calculations can be performed with pencil and paper; thus, equipment and personnel to run the method are inexpensive. The approach is famous and widely accepted.

(b) experimental designs can be very frugal; in principle, one can perform the experiment at single drug 1 and drug 2 concentrations, and thus one minimally needs only four data points to apply the method: (0, 0); (D_1 , 0); (0, D_2); and (D_1 , D_2).

(c) variants of the fractional product method exist that add some statistical rigor; e.g., the method of Steel and Peckham (1979) and the method of Prichard and Shipman (1990).

The disadvantages include:

(a) the no interaction null reference model for the fractional product method is the Bliss independence model, Eq. 11, which in our view, is slightly inferior to the Loewe additivity model, Eq. 6.

(b) the fractional product method is inconsistent with the isobogram method. It is possible to arrive at the opposite conclusion from that found with the isobogram method, as illustrated by the respective analyses of our common data set.

(c) there is no objective quantitative summary measure of the intensity of synergism or antagonism. It is not obvious how to combine results from several sets of measurements.

(d) a frugal design may give a misleading result if the pattern of interaction is different at different regions of the concentration-effect surface.

C. Method of Valeriote and Lin (1975)

This method is very similar to the fractional product method of Webb (1963). A predicted response is calculated from the Bliss independence null reference model; e.g., column 5 in table 3. Then, just as with Webb's method, the observed and predicted responses are compared. However, Valeriote and Lin (1975) further subdivide the less-than-additive region into subadditive, interference, and antagonism subregions. For an inhibitory drug, an interaction for a combination point is called (a) subadditive, if the surviving fraction is between predicted additivity and the surviving fraction for the more active drug, (b) interference, if the surviving fraction for the combination is between the observed surviving fractions of the two individual drugs, and (c)

antagonism, if the surviving fraction for the combination is more than for the least potent drug.

The results from the application of the Valeriote and Lin (1975) approach to the common data set are: 3 combination points showed Bliss synergism, 21 points showed subadditivity, and 1 point showed interference. The conclusion is subadditivity.

The advantages and disadvantages of the Valeriote and Lin (1975) method are essentially the same as of the fractional product method of Webb (1963). The extra subdivision of the less-than-additive region into three regions may have merit.

D. Method of Drewinko et al. (1976)

This approach is also similar to the fractional product method of Webb (1963). The predicted surviving fraction is calculated from the Bliss independence model and listed as in column 5 of table 3. Then, the predicted surviving fraction is subtracted from the measured surviving fraction for the combination points, and the difference scores are listed, such as in column 8 of table 3. The scores are then used as data for a Student's t-test for the hypothesis that the true mean is equal to zero. For the 25 combination points for the common data set, the mean Drewinko score was 2.59, with a standard error of 1.02. There was significant Bliss antagonism, $P < 0.05$.

The advantages and disadvantages of the method of Drewinko et al. (1976) are essentially the same as those of the last two approaches. A difference is that this method offers a summary measure of the intensity of interaction, with an associated statistical indication of the uncertainty in the measure. A disadvantage of the mean Drewinko score is that it is not the statistical expectation of any specific true parameter. In other words, the mean Drewinko score will very much depend upon which regions of the concentration-effect surface are sampled. A statistic, such as the mean Drewinko score, that depends heavily upon the design of the experiment is not ideal.

E. Interaction Index Calculation of Berenbaum (1977)

This method is the algebraic analog of the isobogram by hand method. The general formula for the interaction index, I , is Eq. 22, in which D_1 and D_2 are concentrations of drug 1 and drug 2 in the combination, and $ID_{X,1}$, $ID_{X,2}$, are the predicted inhibitory concentrations of each drug individually to give the observed effect of the combination. The specific method of estimating $ID_{X,1}$ and $ID_{X,2}$ is left to the researcher but is often done by hand with pencil, graph paper, and possibly, French curve.

$$I = \frac{D_1}{ID_{X,1}} + \frac{D_2}{ID_{X,2}} \quad [22]$$

We applied the interaction index method to the common data set by first fitting the first 13 data points with Eq. 13, that for Loewe additivity for two inhibitory drugs

that both individually follow Eq. 2. The first 13 data points include the control points plus the drug 1 alone and drug 2 alone points. The data were fit with nonlinear regression, weighted by the reciprocal of the square of the predicted effect. (This weighting factor is appropriate for continuous data that have errors that are normally distributed and proportional to the true response. This error structure is common in biological systems and was used to generate the common data set, as described in the legend of table 3.) The 5 parameter estimates were: $Econ = 99.2 \pm 5.2$; $IC_{50,1} = 9.52 \pm 1.7$; $IC_{50,2} = 0.966 \pm 0.094$; $m_1 = -0.989 \pm 0.11$; $m_2 = -1.93 \pm 0.13$. Then, using Eq. 8, the specific form of Eq. 22 for drugs that follow Eq. 2, and these 5 parameter estimates, the interaction indices were calculated for the 25 combination points and listed in the tenth column of table 3. When $I > 1$, Loewe antagonism is claimed; when $I < 1$, Loewe synergism is claimed. The results of this analysis are listed in column 11 of table 3. There were 21 cases of Loewe synergism and 4 cases of Loewe antagonism. The overall conclusion is Loewe synergism, in agreement with the isobogram by hand method, but in apparent disagreement with the fractional product method of Webb (1963), the method of Valeriote and Lin (1975), and the method of Drewinko et al. (1976).

The advantages and disadvantages of the interaction index method of Berenbaum (1977) are similar to the isobogram by hand method. The key advantages include:

(a) the null reference model is the Loewe additivity model, Eq. 6.

(b) if the individual concentration-effect curves for both drugs can be well characterized, then all of the combination data can be used. This eliminates some of the potential waste of data of the isobogram by hand method. Also, in principle, the experimental designs can be parsimonious.

The key disadvantages include:

(a) it is not obvious how to derive a good summary measure of the intensity of interaction. If one merely calculates a mean for all of the I s and then performs a Student's t-test with the null hypothesis that the true interaction index is equal to 1, then the same criticisms directed against the mean Drewinko score would apply here.

(b) the analysis results are not as visually informative as with the isobogram by hand method.

F. Method of Steel and Peckham (1979)

This approach has many similarities to the isobogram by hand approach but also several fundamental differences. In addition to the original reference, the approach is described well by Streffer and Müller (1984) and by Calabrese (1991). A variant of the original approach developed by Deen and Williams (1979) has been used extensively by Teicher and coworkers (e.g., Teicher et al. 1991). First, reference curves for the Bliss inde-

pendence model, Eq. 11 (called Mode I additivity) and for Mode II additivity, Eq. 20, are constructed for a particular effect level. An alternative equation for Mode II is provided by Kodell and Pounds (1991), although it is more common to describe the Mode II calculation with a diagram (e.g., Steel and Peckham, 1979; Streffer and Müller, 1984). Mode I and Mode II isobols for the 20% survival level are shown for the analysis of the common data set in figure 15. All calculations and graphs were made with pencil, graph paper, and French curve. However, automated curve fitting computer programs for the approach have been developed (Teicher et al., 1985). The data points are the ID_{80} values estimated from families of log-linear concentration-effect curves (not shown), not from the linear-log curves in figure 12. The positions of the ID_{80} points in figure 15 differ a little from the positions in figure 14 because of the differences in how the concentration-effect curves were drawn. Note that there are two Mode II isobols. Especially note that the Mode II isobols are not the same as the "classical" isobol simulated from the Loewe additivity model, Eq. 6. This is in direct contradiction to claims that the Mode II model and Loewe additivity are the same (Teicher et al., 1991). [This contradiction is the result of Steel and Peckham's (1979) misinterpretation of the first paper on isobograms in English by Loewe (1953). Unfortunately, this key paper, Loewe (1953), was written with a cryptic mathematical notation and is difficult to interpret. It is a dramatic contrast to his lucid original paper on the subject, Loewe and Muischnek (1926), written in German.] The area between the Mode I and Mode II isobols is called the "envelope of additivity."

Because most of the ID_{80} points fall between the borders of the envelope of additivity, using either Mode II isobol for the upper boundary, the conclusion for the common data set would be additivity.

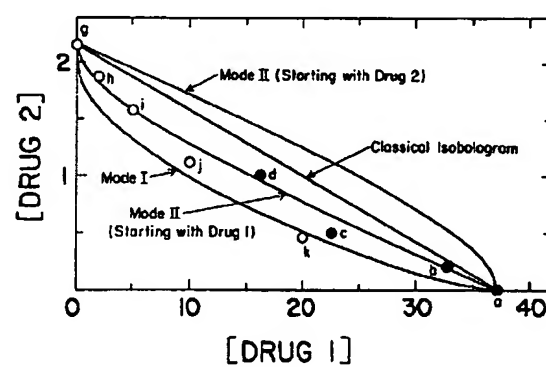


FIG. 15. Isobogram from the Method of Steel and Peckham (1979) for the 20% survival level (IC_{80}). Note that the isobol for the Mode I assumption, each of the two isobols for the Mode II assumption, and the isobol for the classical Loewe additivity assumption are all different. The data points are IC_{80} s taken from log-linear plots of %survival vs. drug concentration. The letters next to the points correspond to the legend of the linear-log survival plots in figure 13.

The advantages of the method of Steel and Peckham (1979) include:

(a) a region, the envelope of additivity, is provided to facilitate judgments about departures from no interaction, rather than a line. The envelope of additivity provides a standard, with a reasonable theoretical justification, to aid in the decision of whether a departure from additivity is great enough to warrant further consideration.

(b) the automated variant of the approach (Teicher et al., 1985) provides a degree of objectivity and some statistical rigor.

(c) the approach is widely accepted.

The disadvantages of the method include:

(a) neither of the two no interaction null reference models, that for Mode I or that for Mode II, are the preferred Loewe additivity model. The Mode II reference model is not part of other common approaches; in addition, it results in two predictions.

(b) the envelope of additivity does not take into account the precision of the data; it is not larger for data with more experimental error. It is not a statistical interval.

(c) the method lacks a summary measure of the intensity of interaction.

(d) the method is insensitive to small but real and potentially important interactions. It lacks good statistical power. This was seen for the analysis of the common data set.

G. Median-effect Method of Chou and Talalay (1984)

Of all of the methods examined in this paper, the median-effect approach received the most thorough review. This is because, of all of the methods to assess agent interaction introduced since 1970, the method of Chou and Talalay (1984) has been the most influential and controversial. Probably the key element of the approach that has led to its widespread use is the availability of an implementation in inexpensive microcomputer software (Chou and Chou, 1987). Chou (1991a) lists 79 recent publications that applied the median-effect approach to real laboratory data; 39 centered on anticancer agents, 25 centered on antiviral agents, and 15 centered on other miscellaneous agents. Our own literature survey located 3 application papers in 1985, 5 in 1986, 13 in 1987, 16 in 1988, 28 in 1989, 31 in 1990, and 11 in an incomplete survey of 1991 for a total of 107. It is clear that the approach has many advocates and that its use has continued to grow. The article, Chou and Talalay (1984), may become one of the most often-referenced scientific papers in the history of biomedicine.

The median-effect approach is the culmination of a long series of very technical papers centered on describing a wide variety of complex enzyme kinetic mechanisms with a general framework (see Chou, 1991a for a summary). Many useful concepts and equations were introduced by this series of papers, including several

used by our group in the development of our own response surface approach for assessing agent combinations (Greco et al., 1990). In fact, our original motivation in developing our approach was merely to add small improvements to the median-effect method. For instance, our first goal was to show (via Monte-Carlo simulation) that using weighted nonlinear regression to fit a nonlinear form of the median-effect equation, Eq. 1, to single drug data was superior to using unweighted linear regression to fit a linearized form of the median-effect model, Eq. 23, to single drug data (Syracuse and Greco, 1986). Even though the weighted nonlinear regression approach was consistently more precise and less biased than the unweighted linear regression approach, for the estimation of both D_m and m , the differences were usually not striking, and the simpler method performed very well for most cases. However, as we examined the method of Chou and Talalay (1984) more closely, we found several disturbing problems, which will be described below. In addition, our own approach developed along very different lines, most notably with the incorporation of some ideas of Berenbaum (1985). Today, our approach for assessing agent interaction (Greco et al., 1990) bears only a faint resemblance to the median-effect method.

The analysis of the common data set by the approach of Chou and Talalay (1984) is shown in figure 16. Only a

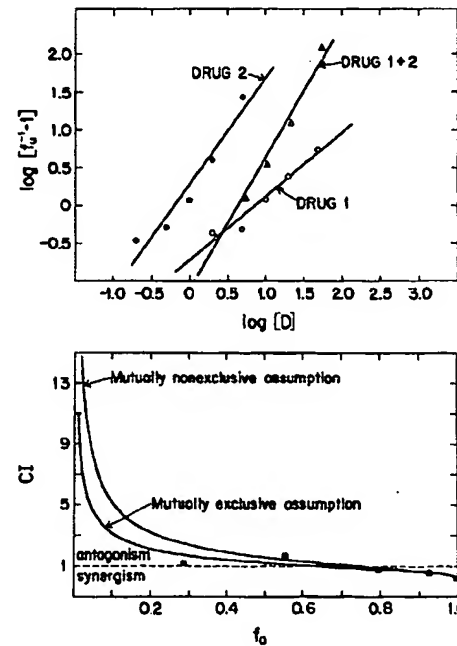


FIG. 16. Median-effect (upper panel) and CI vs. f_0 plot (lower panel) for the analysis of data from table 3, columns 2 through 4, for drug 1 alone (points 4 through 8), drug 2 alone (points 9 through 13) and for the combination at a fixed ratio of $D_1:D_2$ of 10:1 (points 14, 20, 26, 32, and 38). The solid square data points in the lower panel represent the five combination points and were calculated as described in the text.

brief description of the approach is included here; there have been many detailed recipes of the approach previously published (e.g., Chou and Talalay, 1984; Chou and Chou, 1987; Chou, 1991b; Calabresi, 1991). The easiest way to apply the approach to a data set is to use the software program by Chou and Chou (1987), which is available for both the Apple II and IBM-compatible personal computers. Eq. 23 is fit to data from drug 1 alone, drug 2 alone, and the combination of drug 1 and drug 2 in a fixed ratio. [Eq. 23 is a linearized form of Eq. 24, essentially equivalent to the Hill equation, Eq. 2, and was derived by Chou and Talalay (1981).]

$$\begin{aligned} \log[fu^{-1} - 1] &= \log[fa^{-1} - 1]^{-1} \\ &= m \log(D) - m \log(Dm) \end{aligned} \quad [23]$$

$$\frac{fa}{fu} = \left(\frac{D}{Dm} \right)^m \quad [24]$$

An average control effect was first calculated (the average of the 3 $D_1 = D_2 = 0$ points, 106, 99.2, and 115 from column 4 of table 3) to be 107. Then, each fu value was calculated by dividing the measured effect in column 4 by 107. For drug 1 alone, points 4 to 8 were used, for drug 2 alone, points 9 to 13 were used, and for the combination at a fixed ratio of 10:1, points 14, 20, 26, 32, and 38 were used. (In principle, more sets of points from other fixed ratios from the data set in table 2 could have been used for the analysis; however, it is very common to apply the approach to a single fixed ratio.) Additional calculations were performed on the 15 data points to construct the transformed y -values of $\log(fu^{-1} - 1)$ and the transformed x -values of $\log(D)$. Unweighted linear regression was applied separately to the three sets of five points each, and the slopes and y -intercepts were estimated, m and $-m \log(Dm)$, respectively. The transformed data and fitted curves are in the upper panel of figure 16. The Dm values were calculated from the y -intercepts and slopes. The six estimated parameters were: for drug 1, $Dm_1 = 7.40$, $m_1 = 0.845$; for drug 2, $Dm_2 = 0.631$, $m_2 = 1.37$; for drug 1 + 2 in a fixed ratio, $Dm_{12} = 4.48$ and $m_{12} = 1.77$. [Note that the signs of the m s have been made positive to correspond to the standard implementation of the approach of Chou and Talalay (1984); this is the opposite of the convention usually used by our group.] According to Chou and Talalay (1984), if $m_1 = m_2 = m_{12}$, then the two drugs are claimed to be mutually exclusive; if $m_1 = m_2 \neq m_{12}$, then the two drugs are claimed to be mutually nonexclusive; if $m_1 \neq m_2$, the mutual exclusivity of the drugs is unclear. Chou and Talalay (1984) do not explicitly state how the equivalencies of m_1 , m_2 , and m_{12} should be determined. However, we will make the conclusion that 0.845, 1.37, and 1.77 are sufficiently different from each other that the mutual exclusivity is unclear for the common data set.

In the lower panel of figure 16 are the CI vs. fa plots for both the mutually exclusive and mutually nonexclusive assumptions. These plots were generated by inserting the six estimated parameters from the median effect plots into Eq. 25 for the mutually exclusive case and into Eq. 26 for the mutually nonexclusive case (Chou and Chou, 1987; Chou, 1991b), and calculating CI for the range of fa from 0.01 to 0.99. (Here, R is the ratio of concentrations of D_1, D_2). The area above the $CI = 1$ line represents antagonism; below, synergism. The five data points in the lower panel represent the five combination points that have been transformed with Eq. 27 and directly plotted, without relying on the estimation of Dm_{12} and m_{12} . This addendum to the approach, suggested mainly for nonconstant combination ratios (Chou, 1991a), is also applicable to fixed combination ratios, as shown by our example. To the best of our knowledge, it is not yet available in the commercial software (as of August, 1992). This is essentially the same approach as described in Section V.E., the calculation of Berenbaum's (1977) interaction index.

$$CI = \frac{Dm_{12} \left[\frac{R}{R+1} \right] \left[\frac{fa}{1-fa} \right]^{1/m_{12}}}{Dm_1 \left[\frac{fa}{1-fa} \right]^{1/m_1}} + \frac{Dm_{12} \left[\frac{1}{R+1} \right] \left[\frac{fa}{1-fa} \right]^{1/m_{12}}}{Dm_2 \left[\frac{fa}{1-fa} \right]^{1/m_2}} \quad [25]$$

$$CI = \frac{Dm_{12} \left[\frac{R}{R+1} \right] \left[\frac{fa}{1-fa} \right]^{1/m_{12}}}{Dm_1 \left[\frac{fa}{1-fa} \right]^{1/m_1}} + \frac{Dm_{12} \left[\frac{1}{R+1} \right] \left[\frac{fa}{1-fa} \right]^{1/m_{12}}}{Dm_2 \left[\frac{fa}{1-fa} \right]^{1/m_2}} + \frac{Dm_{12}^2 \left[\frac{R}{(R+1)^2} \right] \left[\frac{fa}{1-fa} \right]^{2/m_{12}}}{Dm_1 Dm_2 \left[\frac{fa}{1-fa} \right]^{1/m_1} \left[\frac{fa}{1-fa} \right]^{1/m_2}} \quad [26]$$

$$CI = \frac{D_1}{Dm_1 \left[\frac{fa}{1-fa} \right]^{1/m_1}} + \frac{D_2}{Dm_2 \left[\frac{fa}{1-fa} \right]^{1/m_2}} \quad [27]$$

Overall, the conclusion is strong antagonism at low fas , slight synergism at $fa > 0.8$, with the assumption of mutual nonexclusivity; strong Loewe antagonism at low fas , slight Loewe synergism at $fa > 0.8$, with the assumption of mutual exclusivity. Note that the extreme antagonism occurs to the left of the combination data points. If one would just examine the five combination points calculated with Eq. 27, then one might conclude Loewe additivity; or slight Loewe antagonism at low fas and slight Loewe synergism at high fas .

The advantages and good features of the median-effect approach of Chou and Talalay (1984) include:

(a) the fundamental equations for the approach were derived from basic mass action enzyme kinetics, and thus, the estimable parameters have the potential to be biologically meaningful. However, the approach has most often been applied to much more complex systems, such as biochemical networks, viruses, bacterial cells, mammalian cells, intact mammals, or populations of mammals. Therefore, the biochemical origin of the median-effect approach, a relatively simple system of multiple inhibitors of a single enzyme, will usually not facilitate mechanistic insights into the more complex systems to which the approach is applied. The mechanistic models of the approach are used essentially in an empirical manner.

(b) many useful equations, combined-action concepts, and specific applications of the approach have been published that have inspired others to create newer approaches (e.g., Greco et al. 1990).

(c) part of the method involves the fitting of models to data with an objective, well accepted statistical approach, namely linear regression.

(d) the experimental design requires fewer data points than a typical design to be analyzed by the isobogram technique and other methods. However, the common sparse design with one fixed ratio of $D_1:D_2$ may miss some interesting regions of the full 3-D concentration-effect surface (Prichard and Shipman, 1990).

(e) the mutually exclusive model is consistent with the Loewe additivity null reference model.

(f) for many analyses of real data, when artifacts inherent in the approach do not make a major contribution, the overall general conclusions will be consistent with more rigorous methods. However, conversely, when artifacts do make a major contribution, the final conclusions will not be consistent with more rigorous methods. For example, in an informal survey of 37 application papers that used the Chou and Talalay (1984) approach, we re-analyzed 136 data sets with the parametric model fitting approach, using Eq. 5, described in Section V.L.1. For only 38 of the 136 data sets (28%) was there close agreement in the final conclusions for the two approaches.

(g) the method is available in microcomputer software for the popular Apple II (Apple Computer Inc., Cupertino, CA) and IBM PC (IBM Corporation, Boca Raton, FL) (and compatible) microcomputers. This last advantage is the most crucial: for any sophisticated data analysis technique to be used routinely by biomedical scientists, especially by those with little mathematical and statistical training, the method must be readily available in the form of inexpensive, user-friendly software.

The disadvantages of the method of Chou and Talalay (1984) include:

(a) the mutually nonexclusive model was not adequately derived. Appendix A includes an extensive discussion of this point, provides a derivation from basic enzyme kinetic arguments for Eq. 12, a model that can

also be derived directly from the concept of Bliss independence, and provides support for Eq. 12 being a more appropriate model for mutual nonexclusivity for two inhibitors against a single enzyme, than Chou and Talalay's model 18 (or an alternate form, Eq. 19). It must be noted that, as shown in Appendix A, the mutually nonexclusive model of Chou and Talalay (1984) for two inhibitors of a single enzyme can be derived from enzyme kinetic arguments by making some additional assumptions. However, it is unlikely that an equation derived from a set of unusual assumptions, for a rare experimental system, would have general utility for modeling concentration-effect phenomena from a wide spectrum of complex agent interaction systems. Another implication of this discussion is the weakness of Chou and Talalay's (1984) argument that the fractional product method of Webb (1963) is not valid for higher order systems with sigmoidal concentration-effect curves ($|m| > 1$). In fact, from a theoretical basis, any approach based upon Loewe additivity or Bliss independence is "valid" for most types of concentration-effect functions over a wide range of parameter values.

(b) as shown in Appendix B, Nonlinear Nature of the Median Effect Plot for Mutual Nonexclusivity section, the median-effect plot for mutually nonexclusive inhibitors is not linear; this leads to inaccuracies in the estimation of Dm_{12} and especially of m_{12} via linear regression, and then to artifacts in the CI vs. fa plot, including large antagonism at low fas . Interestingly, this nonlinearity in the median-effect plot for their mutually nonexclusive model was first shown by Chou and Talalay (1981) in their figure 2 (not shown here).

(c) the CI formula for the mutually nonexclusive case is not correct. This is shown in Appendix B, Incorrect Combination Index Calculations for the Mutually Nonexclusive Case section. This also leads to artifacts in the CI vs. fa plot.

(d) even for the mutually exclusive case, one effect of Loewe synergism or Loewe antagonism is to make the median-effect plot nonlinear, leading to artifacts in the CI vs. fa plot. This is shown in Appendix B, Nonlinear Nature of the Median Effect Plot for Mutual Exclusivity with Interaction section.

(e) The median-effect equations for both the mutually exclusive and nonexclusive cases were originally derived by Chou and Talalay (1981) with the assumption that $m_1 = m_2$. When $m_1 \neq m_2$, which is usually the case, both models are only approximately valid. The approximation becomes worse as the difference between the ms becomes larger. This problem and several others are illustrated in figure 17. Eight simulations were conducted using Eq. 5 as a model (not the model) for Loewe synergism or Loewe antagonism, using the values for m_1 , m_2 and α listed in the insets of the figure. The simulated data were plotted in panel A after the median-effect transformation. The CI vs. fa plots were simulated directly with Eq. 8, thus avoiding many of the calculation

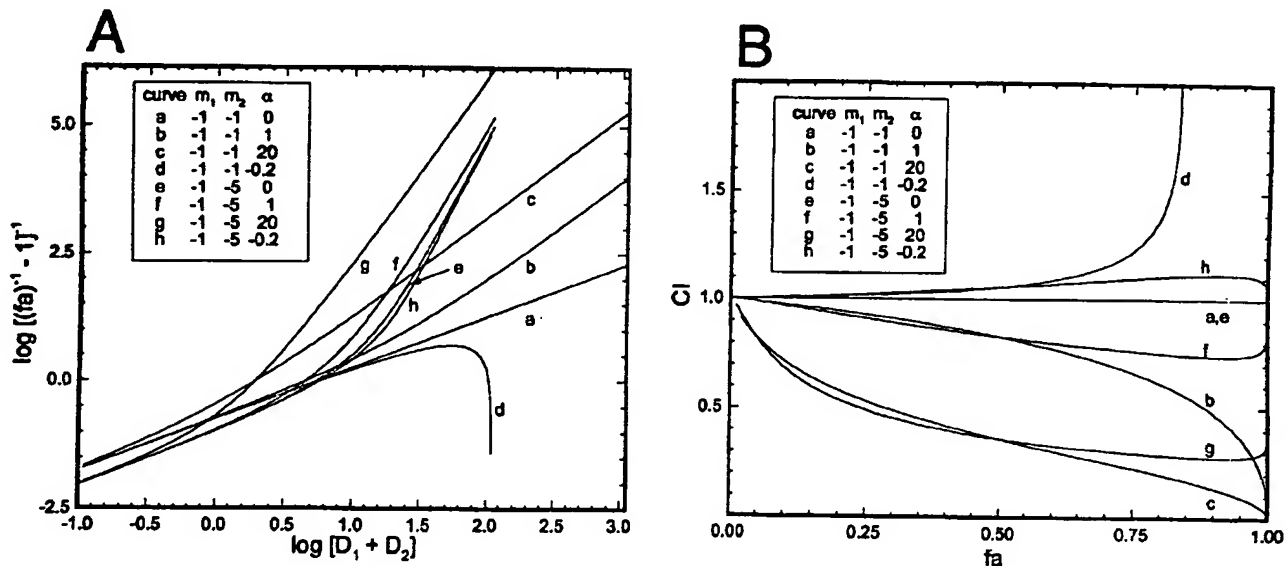


FIG. 17. Median-effect plots (A) and CI vs. fa plots (B) for data simulated with Eq. 5, with parameters: $Econ = 100$, $IC_{50,1} = 10$, $IC_{50,2} = 1$ and m_1, m_2, α as listed in the inset boxes in each panel. CI was calculated from Eq. 8. Note that the median-effect plot is a straight line only for the case in which $m_1 = m_2$ and $\alpha = 0$. Thus, both $m_1 \neq m_2$ and $\alpha \neq 0$ will result in a curved median-effect plot. Also note that the shape of the CI vs. fa plots are influenced by both the slope parameters and the interaction parameter.

artifacts discussed in points (b) through (d) of this section. Note that the median-effect plot is a straight line only for the case a., in which $m_1 = m_2 = -1$, and $\alpha = 0$. Thus, either $m_1 \neq m_2$, or $\alpha \neq 0$, or both conditions will result in a curved median-effect plot. Note that large differences in slope parameters (e.g., curve e., $m_1 = -1$, $m_2 = -5$, $\alpha = 0$) seem to have a more profound effect on the curvature than does a high α value (e.g., curve c., $m_1 = -1$, $m_2 = -1$, $\alpha = 20$). Because only pure Loewe additivity, pure Loewe synergism, or pure Loewe antagonism were simulated, none of the CI vs. fa plots cross the $CI = 1$ line. Note that all of the plots, for both Loewe synergism and Loewe antagonism, start at $CI = 1$ ($fa = 0$). This implies that all reported CI vs. fa plots that show large antagonism in the region near $fa = 0$, contain calculation artifacts. Indeed, the $CI = 1$ at $fa = 0$ point should be the anchor for all CI vs. fa plots, no matter what kind of combined-action is present. Also note that CI vs. fa curves b. and c. ($m_1 = m_2 = -1$) curve downward near $fa = 1$, whereas, curves f. and g. ($m_1 = -1$, $m_2 = -5$) curve upward near $fa = 1$. Finally, note that increasing degrees of Loewe synergism, for the same set of slope parameters, order the curves from bottom to top for the median-effect plot, but from top to bottom for the CI vs. fa plot. It is clear that in the vast majority of cases, the median-effect linearization of combination data at a fixed ratio will result in a true nonlinear curve. The nonlinearity may be small, and data variation may mask the nonlinearity, but the fitting of a median-effect straight line to such data will almost always be, at best, only approximately correct.

(f) the method of Chou and Talalay (1984) lacks many aspects of modern statistical approaches. First, the fit-

ting of the median-effect line to data with linear regression does not have the option of weighting. However, proper weighting only offers a slight improvement to the unweighted linear regression (Syracuse and Greco, 1986). Second, the only goodness of fit statistics offered are Pearson correlation coefficients, r , for each separate unweighted linear regression of the transformed data for each median-effect plot. It would be useful to have some overall goodness of fit statistic for the fit of the overall model simultaneously to all of the data. There is no uncertainty measure provided with the estimates of m_1, m_2 , and m_{12} to aid in making the decision between mutual exclusivity vs. mutual nonexclusivity. Most importantly, there is no uncertainty measure associated with the final result, the CI vs. fa plot. Objective decisions regarding the occurrence of moderate degrees of Loewe synergism or Loewe antagonism are therefore difficult. However, newer variants of the approach include more extensive statistical procedures, such as confidence intervals for the combination index (Belen'kii and Schinazi, 1994).

(g) the relationship between the CI vs. fa plot, the original raw data, and the original concentration-effect curves is somewhat hard to visualize. The experimenter may "lose touch" with his data. However, a good understanding of the relationship between the CI vs. fa plot and the 3-D concentration-effect surface for a two drug combination, figure 7, may assist in this visualization.

(h) the Chou and Talalay (1984) approach first involves a decision on mutual exclusivity vs. mutual nonexclusivity, and then a decision on synergism, additivity, or antagonism, for a total of six different cases. There is a conceptual difficulty in differentiating between mutual

exclusivity with synergism and mutual nonexclusivity with synergism, additivity, and especially with antagonism. The regions overlap. This can be seen in isobols of figure 6, in which curve E represents pure mutual exclusivity ($\alpha = 0$), curve C represents pure mutual nonexclusivity ($\alpha = 1$), and curve D ($\alpha = 0.5$) would be an example of Loewe synergism with reference to the mutually exclusive model and of Loewe antagonism with reference to the mutually nonexclusive model. In line with this reasoning, the figure legend of figure 2 from Chou and Talalay (1981) states that the curve for mutual nonexclusivity "clearly shows synergistic effects at high concentrations. . . ." In fact, one can see that the nonlinear form of the mutually nonexclusive model, Eq. 19, is the same as our flagship model for Loewe synergism, Eq. 5, with $m = m_1 = m_2$ and $\alpha = 1$.

(i) the available software (Chou and Chou, 1987) that implements the approach is relatively unsophisticated. Future changes in the computer software should include improvements in graphics, datafile editing, saving and retrieving, and the prevention of the program from "bombing" under certain conditions.

(j) if the concentration-effect curve for either agent in a combination does not follow the Hill model, Eq. 1 (or the equivalent median-effect model, Eq. 24), then the Chou and Talalay (1984) approach is not valid.

(k) there are three practical decisions that users of the Chou and Talalay (1984) approach must make that critically affect the final results: (1) what to do with data points in which % survival equals or exceeds 100%, or equals or is less than 0%; such data will lead to computational difficulties; (2) how to decide whether a specific two-agent interaction is mutually exclusive or mutually nonexclusive, especially when $m_1 \neq m_2$; and (3) how to conclude synergism, additivity, or antagonism from the CI vs. fa plot. There is a wide variety of different tactics used by different groups to make these three critical decisions. Therefore, the objectivity of the approach is lessened. For example, for decision (1), some groups either censor any extreme points ($fa \geq 1$, $fa \leq 0$) or change any $fa \geq 1$ to a usable fa such as 0.96 (e.g., Schinazi et al., 1986), whereas, most groups do not specify their procedure (e.g., Hartshorn et al., 1986). For decision (2), as recommended by Chou and Talalay (1984), some assume mutual exclusivity when the median-effect plots for both single drugs and the combination are parallel (e.g., Koshida et al., 1989), assume mutual nonexclusivity when the slope parameters for the single drugs are similar but the slope for the combination is much different (e.g., Nocentini et al., 1990), and report both exclusivities when the median-effect plots for both single drugs are not parallel (e.g., Eriksson and Schinazi, 1989). However, some groups report the mutual exclusivity results, because they feel that the mutually nonexclusive results would not be much different (e.g., Vogt et al., 1987; Kuebler et al., 1990). Some report mutual exclusivity, because it corresponds to the classi-

cal isobogram approach (e.g., Johnson et al., 1992); some groups assume mutual nonexclusivity, because it yields a more conservative estimate of CI (e.g., Vathsala et al., 1990). Some assume mutual nonexclusivity, because the two agents are known to act at different sites (e.g., Jackson, 1992), and some assume some exclusivity, but don't state which one or why (e.g., Richman et al., 1991). For decision (3), some groups stress the CI at high fas , such as 0.50, 0.75, 0.90 and 0.95 (e.g., Kong et al., 1991). Some show the whole CI vs. fa plot, from 0.01 to 0.99 and describe many of the nuances of the curve, including the point at which the $CI = 1$ line is crossed (e.g., Wadler et al., 1990). Some report an average CI for the 50% effect point from several replicate experiments, along with a standard deviation (e.g., Katz et al., 1990). Some use several other additional approaches to analyze the data, such as the isobogram approach, or the method of Steel and Peckham (1979) and then report a consensus (e.g., Nocentini et al., 1990). There are no firm guidelines for assessing the importance of small consistent differences between the CI vs. fa plot and the $CI = 1$ line. For example, in Chou and Chou (1987), the CI vs. fa plot on page 42 follows a path slightly above the $CI = 1$ line, with a conclusion of additivity; whereas, the CI vs. fa plot on page 61 follows a path slightly below the $CI = 1$ line, with a conclusion of strong synergism.

H. Method of Berenbaum (1985)

In one sense, the method of Berenbaum (1985) is merely a graphical version of the interaction index approach of Berenbaum (1977). However, interpreted differently, the method of Berenbaum (1985) is the basis of all modern nonparametric and parametric response surface approaches to be described in Sections V.K. and V.L. The approach consists of fitting concentration-effect models to data for each agent alone, deriving a model for Loewe additivity consistent with these single agent models, simulating the Loewe additivity model, superimposing this simulated Loewe additivity surface upon the raw data points, and then deciding whether points are above or below the surface, which will indicate Loewe synergism or Loewe antagonism, depending upon whether the 3-D concentration-effect surface rises or falls with increasing agent concentrations. The derived Loewe additivity models can accommodate different slope parameters for each agent when each agent's concentration-effect curve follows a Hill model, Eq. 2, 3. The Loewe additivity models can even accommodate different functional forms for the concentration-effect curve for each agent. Unfortunately, these models are often in unclosed form. A formal parametric model for Loewe additivity is useful, but optional: Berenbaum (1985) shows an example of fitting complex single agent data by hand. Sühnel (1992c) has derived and listed many parametric Loewe additivity models and emphasizes the use of 3-D interaction plots, such as figure 9, and 3-D difference surfaces such as in figure 10. The functional form of

the derived Loewe additivity response surfaces, e.g., Eq. 13, can easily be extended to include interaction terms, leading to a full combined-action model, such as Eq. 5. In fact, the guidelines from Berenbaum (1985) for deriving general Loewe additivity models led us directly to the derivation of Eq. 5, which was first published in Syracuse and Greco (1986). Interestingly, essentially the same logic for deriving Loewe additivity and combined-action models was part of a review paper by Hewlett (1969), who provides examples of combined-action models from Finney (1952), Plackett and Hewlett (1952), Landahl (1958), and Plackett and Hewlett (1967). However, Berenbaum's (1985) hallmark paper is much clearer and was published at a time when the necessary computer hardware and software were sufficiently available to enable the routine application of his paradigm and logical variants to real data.

We applied the method of Berenbaum (1985) to the common data set by first fitting the first 13 data points

in columns 2 to 4 of table 3 with Eq. 13, that for Loewe additivity for two inhibitory drugs that both individually follow Eq. 2, just as described for the interaction index approach of Berenbaum (1977) in Section V.E. The first 13 data points include the control points plus the drug 1 alone and drug 2 alone points. Just as in Section V.E., data were fit with nonlinear regression, weighted by the reciprocal of the square of the predicted effect. The five parameter estimates were: $E_{\text{con}} = 99.2 \pm 5.2$; $IC_{50,1} = 9.52 \pm 1.7$; $IC_{50,2} = 0.966 \pm 0.094$; $m_1 = -0.989 \pm 0.11$; $m_2 = -1.93 \pm 0.13$. Then, instead of calculating an interaction index using Eq. 8, the fitted curve is shown in figure 18(A), along with the raw data. For the 25 combination points, a solid point (above the surface) indicates Loewe antagonism, and an open point indicates Loewe synergism. The results are identical (as they must be) to the results from the interaction index approach of Berenbaum (1977) shown in columns 9 to 11 of table 3. There were 21 cases of Loewe synergism and 4

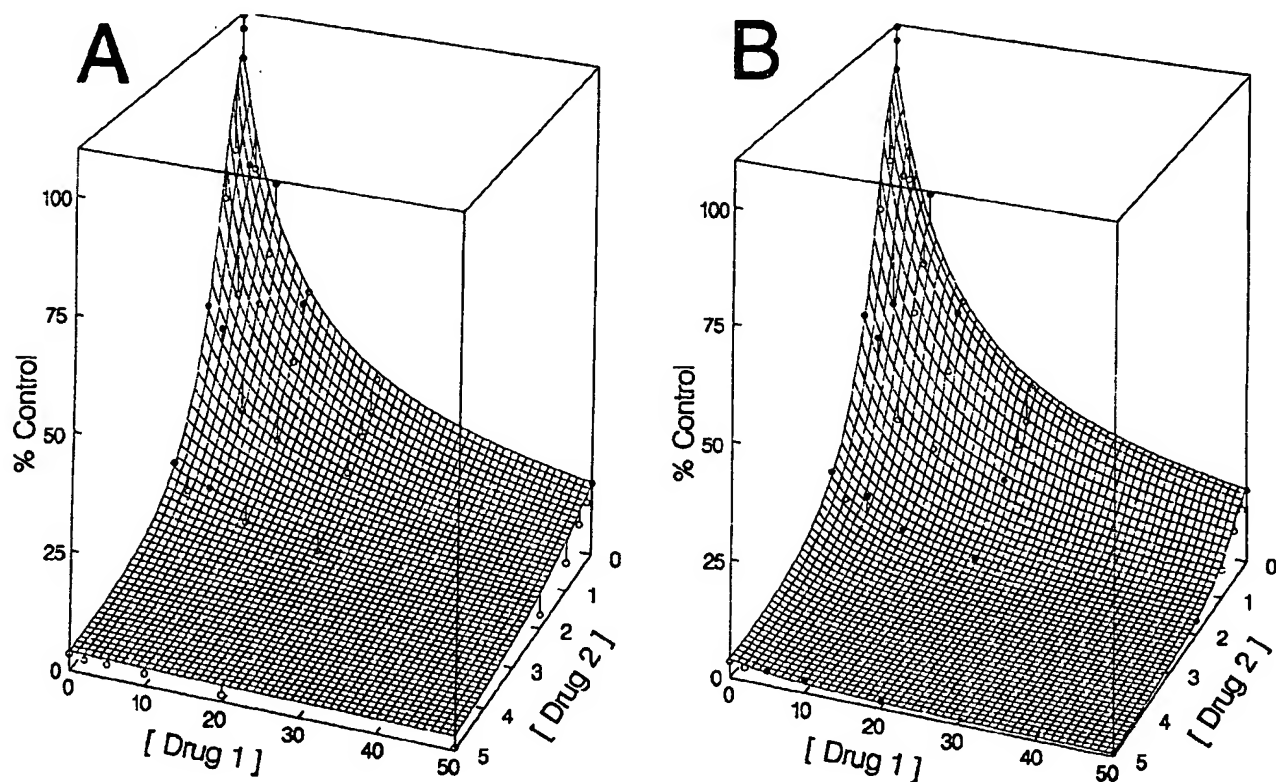


FIG. 18. Analyses of data from table 3, columns 2 through 4. (A) Approach interpreted from Berenbaum (1985). Data for drug 1 alone and drug 2 alone were fit by a Loewe additivity model, Eq. 13, with nonlinear regression as explained in the text. The 3-D fishnet is the best fit Loewe additivity surface. The full 38-point data set is plotted on the same graph, with vertical lines indicating the distance between the data points and the surface. Solid points are above the surface, and open points are below. For the 25 combination points, a solid point indicates Loewe antagonism, and an open point, Loewe synergism. There is an exact correspondence between this 3-D graph and columns 9 through 11 of table 3. (B) Graphical Bliss independence comparison. The best fit parameters from the fit of the Loewe additivity model, Eq. 13, were estimated as for panel (A), but these parameters were used with the Bliss independence model, Eq. 12 to simulate the 3-D surface. The full 38-point data set is again plotted on the same graph. There are 11 points above the surface (Bliss antagonism), and 14 points below the surface (Bliss synergism).

cases of Loewe antagonism. The overall conclusion is Loewe synergism.

The key advantages include:

(a) the null reference model is the Loewe additivity model, Eq. 6.

(b) if the individual concentration-effect curves for both drugs can be well characterized, then all of the combination data can be used.

(c) the experimental designs can be parsimonious.

(d) the single agent data are fit with a logical response surface model, possibly with modern curve fitting techniques.

(e) it is not necessary to derive or use some arbitrary combined-action model for fitting the combination data. Mosaics of regions of Loewe synergism and Loewe antagonism are thus easily accommodated.

(f) the approach led to the creation and use of full combined-action models (e.g., Greco et al., 1990).

(g) the approach can be used to characterize very complex mixtures of three or more agents. If one is chiefly interested in the assessment of combined-action at a specific combination of doses of the agents and not in characterizing the whole response surface, then experimental designs can be very frugal.

The key disadvantages include:

(a) just as with the interaction index calculation approach (Berenbaum, 1977), it is not obvious how to derive a good summary measure of the intensity of interaction, with an accompanying measure of uncertainty. However, Gennings (1995) recently proposed some extensions to Berenbaum's (1985) method that include some excellent statistical summary measures of departures from Loewe additivity.

(b) the derivation and application of complex Loewe additivity models may require considerable mathematical, statistical, and computing resources.

I. Bliss (1939) Independence Response Surface Approach

We did not find this specific method in the literature, but it is included because it is a logical cross between the Webb (1963) and Berenbaum (1985) approaches. This approach is a graphical version of the fractional product method of Webb (1963) and is similar, but not identical, to the method of Prichard and Shipman (1990) described in Section V.J. The results are shown in figure 18(B), which was made in the same way as described in Section V.H. for the Berenbaum (1985) approach, except that the Bliss independence model, Eq. 12, was used to simulate the 3-D surface. There are 11 points above the surface (Bliss antagonism) and 14 points below the surface (Bliss synergism). The overall conclusion would be Bliss independence. Interestingly, the results differ from those previously found with the fractional product approach (Webb, 1963) (column 6 of table 2; 4 cases of Bliss synergism and 21 cases of Bliss antagonism). This difference is caused by the use of fitted individual concen-

tration-effect curves for making the Bliss independence predictions for the surface approach, vs. the raw data for the individual drugs for making the Bliss independence predictions for the fractional product method.

This approach shares advantages (b) through (e) of the Berenbaum (1985) approach. It is possible that full combined-action models can be derived and applied, as suggested by Unkelbach (1992).

The key disadvantages include:

(a) the basis of the approach is Bliss independence, not our Loewe additivity preference.

(b) it is not obvious how to derive a good summary measure of the intensity of interaction, with an accompanying measure of uncertainty. However, variants of the recently proposed extensions by Gennings (1995) to Berenbaum's (1985) approach may solve this problem.

(c) the derivation and application of complex Bliss independence models may require considerable mathematical, statistical, and computing resources.

J. Method of Prichard and Shipman (1990)

This approach (e.g., Prichard et al., 1990) is a graphical, 3-D version of the fractional product method of Webb (1963). Figure 19 shows the result of the analysis of the common data set, columns 2 through 4 of table 3. A checkerboard (factorial) experimental design, like that provided by the common data set, is necessary for the optimal use of the approach. We used the MacSynergy II program (Prichard et al., 1992), which is a set of MicroSoft Excel (Microsoft Corporation, Redmond, WA) spreadsheets and macros, kindly provided by M. Prichard, which was run with Excel to perform the necessary calculations. We used the Tecplot graphics package (Amtec Engineering, Inc., 1988) to prepare figures 19 and 20.

First, the % inhibition for every data point is calculated ($100\% - \text{column 3 of table 3 divided by the average control, } 106.7$). (Note that 107 was the average control value used to generate columns 5 and 8 in table 3.) The points, connected with straight lines, are plotted on a 3-D graph in figure 19(A). The predictions, based upon Bliss independence, are calculated on a point-by-point basis, just as with the Webb (1963) approach and are plotted in figure 19(B). Figure 19(C) is the difference plot of the % inhibition above predicted. These differences are equivalent to the Drewinko et al. (1976) Scores in column 8 of table 3, after reversing the signs, and dividing the Drewinko Scores by the average control. There are 22 combination points below the zero plane, representing Bliss antagonism, and 3 points above the zero plane, representing Bliss synergism. These 3 data points are the same ones that showed Bliss synergism in table 3, data points 21, 26, and 36. The Bliss synergy differences were added up to yield a summary measure, 7.19, and the Bliss antagonism differences were added up to yield a Bliss antagonism summary measure, -65.27.

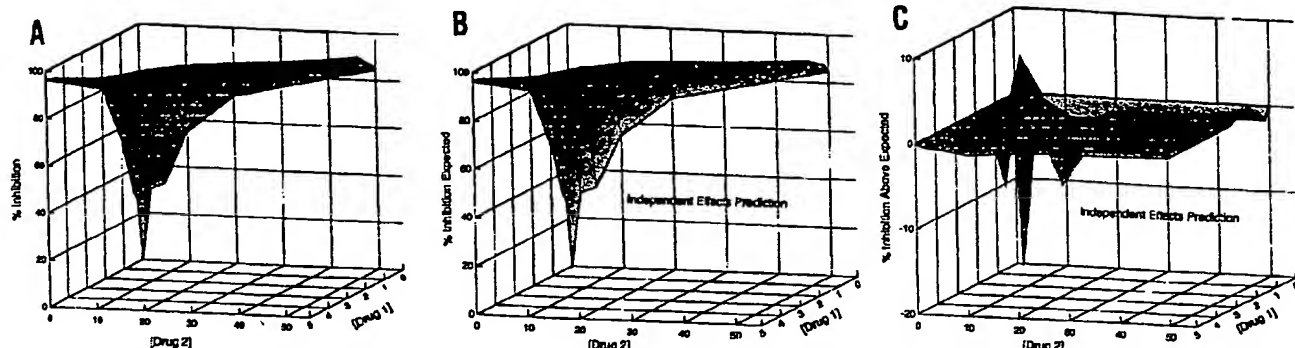


FIG. 19. Method of Prichard and Shipman (1990) applied to the data from table 3, columns 2 through 4. (A) Raw data, 36 data points (the 3 control points were averaged into 1 point), expressed as %inhibition, connected by straight lines, in a 3-D plot. (B) combination points are predicted directly from the raw data for drug 1 alone and drug 2 alone, with Eq. 11, that for Bliss independence, expressed as %inhibition, and connected with straight lines, in a 3-D plot. (C) The set of points from panel (B) are subtracted from the set of points from panel (A) and shown in a 3-D plot. Sections of the difference surface above 0 indicate Bliss synergism, below 0, Bliss antagonism. Both Bliss synergism and Bliss antagonism are seen.

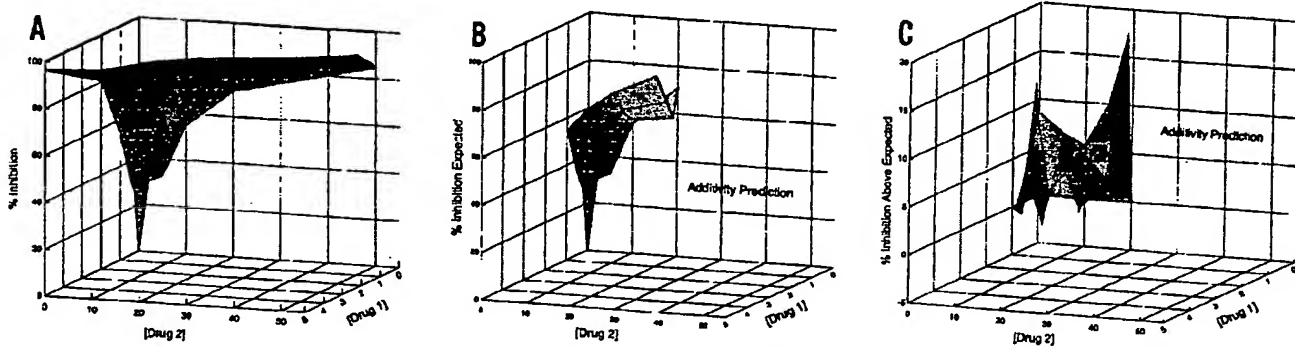


FIG. 20. An alternate approach provided by Prichard et al. (1992) that integrates the Loewe additivity reference concept of Berenbaum (1985), applied to the data from table 3, columns 2 through 4. (A) Same as panel (A), figure 19. (B) Predicted Loewe additivity surface analogous to panel (B) of figure 19. (C) Difference surface analogous to panel (C) of figure 19. Mostly, Loewe synergism is seen. The algorithm used by Prichard et al. (1992) does not make Loewe additivity predictions for points along the outer edge, and thus the predicted and difference surfaces appear to be smaller than those of figure 19.

Although we were able to successfully apply the Prichard and Shipman (1990) method to our common data set, the ideal data set for this approach will contain replicates. Replicates allow the calculation of point-by-point 95%, 99%, and 99.9% confidence intervals for the experimental data. If the lower confidence limit for a point is greater than the predicted Bliss independence, the observed Bliss synergy is considered to be significant. Similarly, if the upper confidence limit for a point is less than the predicted Bliss independence, the observed Bliss antagonism is considered to be significant. The significant Bliss synergism and antagonism differences are totaled separately for additional summary measures. The overall conclusion for the results of the analysis of our common data set is Bliss antagonism. However, as stated above, replicates are needed in order to make firm conclusions with this approach.

The main advantages of the approach are:

(a) the approach emphasizes the 3-D nature of combined-action concentration-effect surfaces; it is very visually oriented.

(b) the software, MacSynergy II, is inexpensive and straightforward to use, provided that one already is proficient with Excel (or possibly some other spreadsheet software) and a suitable graphics package.

(c) the approach is very flexible and does not require a parametric model for either the single agent concentration-effect curves or for combined-action. The approach is, essentially, a very simple nonparametric multivariate curve fitting procedure. The approach can easily accommodate mosaics of interspersed regions of Bliss synergism and Bliss antagonism.

(d) there are some summary and uncertainty measures associated with claims of Bliss synergism and Bliss antagonism.

(e) mathematical, statistical, and computing complexities associated with the fitting of full combined-action response surface models are avoided.

(f) when compared with all of the simpler approaches examined in this review, Sections V. A-V. G, the method of Prichard and Shipman (1990) stands out as having

the best combination of automation, accessibility, intuitiveness, and visualization.

The disadvantages include:

(a) Bliss independence is the main no interaction reference model. However, a new feature added to MacSynergy II, but not necessarily recommended by Prichard et al. (1992), is the ability to use Loewe additivity as the null reference model. The results of the analysis of the common data set are displayed in figure 20. Note that the algorithm used by Prichard et al. (1992) does not make Loewe additivity predictions for points along the outer edge, and thus the predicted and difference surfaces appear to be smaller than those of figure 19. The conclusion for the analysis in figure 20 is Loewe synergism.

(b) the ideal experimental design, a full checkerboard of drug dilutions with replicates, may be prohibitive for many applications. However, for many *in vitro* studies of antiviral or anticancer agents, experimental systems use 96-well culture plates, which facilitates the requirement of a large experimental design.

(c) similar methods described in Sections V.H. and V.I., in which the data for drug 1 alone and drug 2 alone are fit by specific parametric models, but in which the combination points are not fit by specific combined-action models, may offer a cost-effective advantage over the Prichard and Shipman (1990) approach.

(d) the approach is essentially, an exploratory approach. It may be ideal as a front-end for further parametric 3-D response surface approaches for most data sets, or possibly a reasonable final method for very complex data sets with numerous regions of true Bliss synergism and Bliss antagonism. However, it might be of interest to test whether some of the mosaics of Bliss synergism and Bliss antagonism disappear after substituting Loewe additivity for Bliss independence as the no interaction null reference model. Data sets generated with a full replicated checkerboard design likely contain much more useful information than can be revealed by a simple exploratory approach. It would be cost-effective to further analyze such data sets with powerful multivariate parametric response surface approaches, such as described in Section V.L.

The paper that introduced the method of Prichard and Shipman (1990) also provided an extensive review of other older rival approaches. There were many confusing arguments included in this review, and because it may have had a large impact on workers in the antiviral chemotherapy field, and many of their arguments are at odds with our own views, some of Prichard and Shipman's (1990) assertions will be disputed:

(a) they claim that Chou and Talalay's (1984) mutually exclusive model is not equivalent to the Loewe additivity model. As shown in discussions of figures 7 and 8, and elsewhere in our review, they are indeed equivalent. Prichard and Shipman's (1990) assertion was based upon the unreasonable assumption of linear single agent

concentration-effect curves, rather than sigmoidal curves following the Hill equation, Eq. 1.

(b) they claim that Loewe additivity is equivalent to fractional effect addition, Eq. 17, and to Steel and Peckham's (1979) Mode II model. All three models are different, as discussed in Section IV of our review. The cryptic paper of Loewe (1953) may be responsible for this confusion.

(c) they imply that Chou and Talalay's (1984) mutually nonexclusive model is, in general, equivalent to Bliss independence (Webb's 1963 model). This was shown not to be true in Appendix A and not to be true originally by Chou and Talalay (1984). Prichard and Shipman (1990) only examine the case of a first order system, an exceptional case in which the models are equivalent, as first demonstrated by Chou and Talalay (1984).

(d) Prichard and Shipman (1992) assert that the methods proposed by Sühnel (1990) and Greco et al. (1990) are not quantitative and that the method of Prichard and Shipman (1990) is "uniquely suited as it is the only one that quantitates statistically significant interactions." As we hope we demonstrated in our review, their conclusion is overstated.

K. Nonparametric Response Surface Approaches

There are many response surface approaches available that do not require an *a priori* assumption of a specific functional form containing estimable parameters. The method of Prichard and Shipman (1990) is a particularly simple nonparametric technique, which connects data points with straight lines. More sophisticated nonparametric approaches that have been applied to concentration-effect data include: kernel estimation (Staniswalis, 1989), spline-based procedures for monotone curve smoothing (Kelly and Rice, 1990), and a more traditional spline-based procedure introduced by Sühnel (1990) and later applied by Baumgart et al. (1991).

Laska et al. (1994) published an approach to detect Loewe synergism or Loewe antagonism, which uses some geometrical principles derived from Loewe additivity response surfaces, but which does not require assumptions regarding the specific functional form of the individual dose-response curves or the combined-action surface. Thus, the approach uses a nonparametric structural model. The random model used to describe data variation can be either parametric or nonparametric. A minimum of only three design points are needed to apply this method; it should be classified as an hypothesis-testing rather a response surface approach.

Only the traditional spline-based response surface approach will be reviewed here.

1. *Bivariate spline fitting* (Sühnel, 1990). Essentially, Sühnel (1990) proposed to fit data from combination experiments with bivariate splines, without and with smoothing, and then to display the resulting 3-D surface and contours at various levels of the surface. Bivariate

splines are sets of piecewise polynomials running in two dimensions that flexibly follow the points of a surface. The raw data from the common data set is shown in figure 21(A) with a bivariate spline (Harder and Desmarais, 1972; Meinguet, 1979), with no smoothing, fit to the data with the procedure, G3GRID from the SAS statistical package (SAS Institute, 1987). Figure 21(B) shows contours drawn from the raw data at 10% effect intervals (from 90% to 0% Control, from left to right), using the SAS procedure, GCONTOUR, using an algorithm from Snyder (1978). Sühnel emphasizes that the shape of the contours can be interpreted directly without the need of fitting a parametric function to the data. A straight diagonal NW-SE isobol would be consistent with Loewe additivity. Because the isobols in figure 21(B) are mostly slightly bowed downward, the conclusion is slight Loewe synergism. The approach is a more sophisticated version of the Prichard and Shipman (1990) approach, but with the null reference model being Loewe additivity, not Bliss independence. The Sühnel (1990) approach shares many of the advantages and disadvantages of the Prichard and Shipman (1990) approach.

The main advantages include:

(a) Loewe additivity is the null reference model.
 (b) the approach is very flexible and does not require a parametric model for either the single agent concentration-effect curves, or for combined-action. Mosaics of interspersed regions of varying degrees of both Loewe synergism and Bliss antagonism are easily accommodated. Sühnel (1992a, 1992b) considers this characteristic so important that he has questioned the routine use of 3-D combined-action models, such as Eq. 5, which include only a single interaction parameter.

The disadvantages include:

(a) like many nonparametric response surface approaches, the required experimental design must include a large number of regularly dispersed points.
 (b) the approach is essentially only an exploratory approach.
 (c) no summary measures of interaction intensity or conclusion uncertainty are provided.
 (d) the approach is more complex to implement and to use than the Prichard and Shipman (1990) approach.
 (e) the potential user is required to find his own software implementation of the approach.

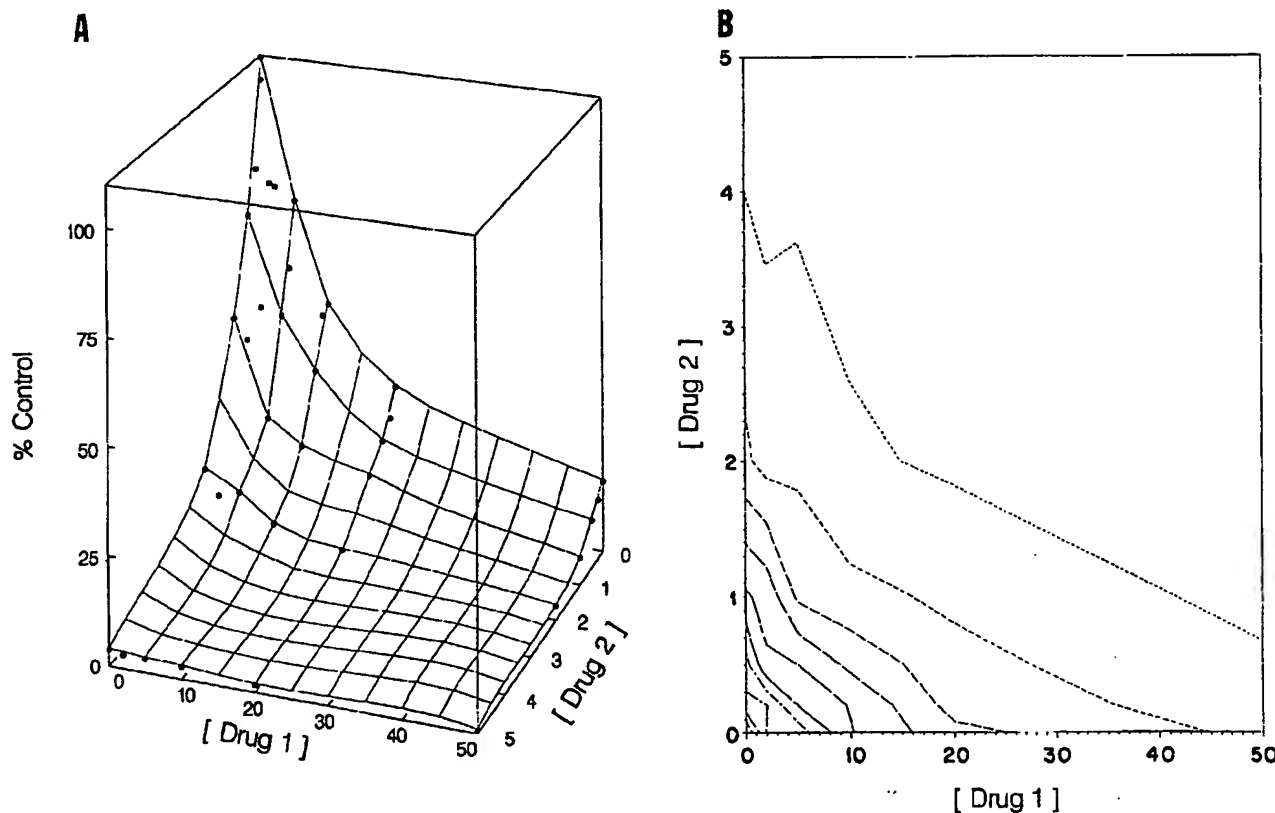


FIG. 21. Analysis of data from table 3, columns 2 through 4 by a nonparametric approach interpreted from Sühnel (1990). (A) The surface is a fit of the data with a bivariate spline (Harder and Desmarais, 1972; Meinguet, 1979), no smoothing, with the procedure, G3GRID, from SAS (SAS Institute, 1987). All 38 data points, whether they fall above or below the surface, are shown as solid circles. (B) Contours drawn from the raw data at 10% effect intervals (from 90% to 0% Control, from left to right), using the SAS procedure, GCONTOUR, using an algorithm from Snyder (1978). The general shape of the contours is in the direction of Loewe synergism.

L. Parametric Response Surface Approaches

In many senses, parametric response surface approaches are the most complex and difficult to apply to the problem of the joint action of agents. They may require the scientist-user to be facile with terminology and concepts that were not part of his formal education, may require the consultative advice of a statistician or other quantitative professional, and will require computing facilities and expertise. However, in a broader sense, these approaches may be the simplest of all of the methods discussed so far. In general, to apply the approaches, (a) logical models are fit to data with automated computer programs, (b) parameter estimates, other statistics, and graphs (3-D and 2-D) are generated and interpreted, (c) conclusions are made.

1. *Models of Greco et al. (1990).* Eq. 5 and close variants have been successfully applied to laboratory data from several studies (e.g., Greco et al., 1990; Gaumont et al., 1992; Greco and Dembinski, 1992; Greco and Rustum, 1992; Guimarães et al., 1994). Eq. 5 was fit to the common data set with nonlinear regression, weighted by the reciprocal of the square of the predicted effect. [Metzler (1981) provides a good description of nonlinear regression intended for biomedical scientists.] The Nash (1979) version of the Marquardt (1968) algorithm for nonlinear regression was coded by our group in MicroSoft FORTRAN, and run on MSDOS-compatible microcomputers.

The six best-fit parameter estimates (\pm standard error) were: $Econ = 95.1 \pm 4.5$; $IC_{50,1} = 11.1 \pm 1.3$; $IC_{50,2} = 1.07 \pm 0.068$; $m_1 = -1.05 \pm 0.078$; $m_2 = -2.04 \pm 0.080$; $\alpha = 0.519 \pm 0.11$. The 95% confidence intervals for each parameter can be calculated by multiplying each standard error by the appropriate value of the Student's t-test distribution and then adding and subtracting this value from the parameter estimate. The appropriate value of the $t_{0.025}$ distribution for two-sided 95% confidence intervals and 32 degrees of freedom (38 data points, 6 parameters) is 2.04. The 95% confidence intervals were: $Econ$, 86.0 to 104; $IC_{50,1}$, 8.40 to 13.9; $IC_{50,2}$, 0.934 to 1.21; m_1 , -1.21 to -0.892; m_2 , -2.20 to -1.88; α , 0.300 to 0.738. None of the 95% confidence intervals encompass zero; all of the parameters were well estimated. This is a positive indication of the model fitting the data well.

The raw data and best fit 3-D curve are shown in figure 22(A). A 2-D representation of the same concentration-effect surface is shown in the isobogram of figure 23, which was formed by the intersection of the surface with planes at 10, 50, 90, and 99% inhibition. Figure 24 includes concentration-effect curves (logarithmic concentration scales) for drug 1 at different drug 2 concentrations (left panel) and for drug 2 at different drug 1 concentrations (right panel). The curves are simulations of Eq. 5 with the best-fit estimated parameters. The curves are intersections of the surface shown in

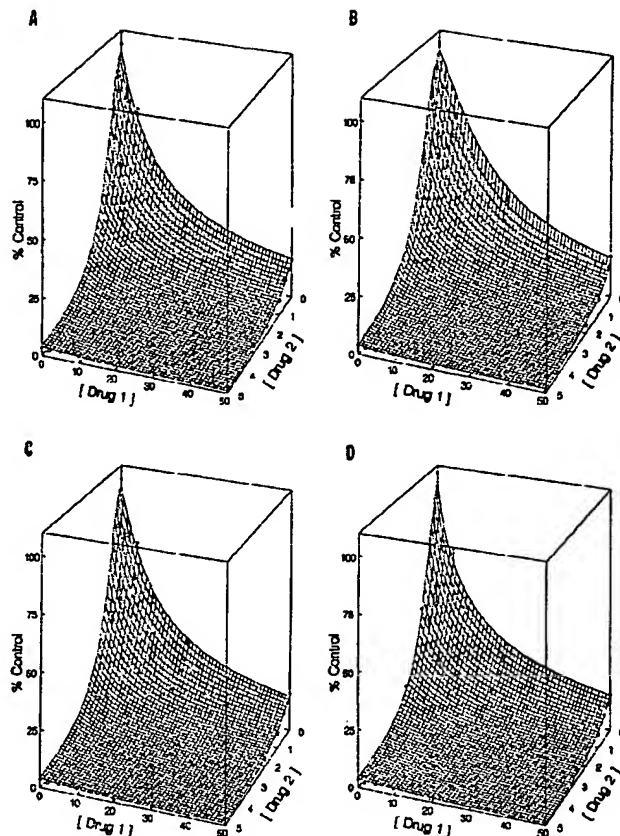


FIG. 22. 3-D concentration-effect surfaces estimated from the best fit of four different models, with weighted nonlinear regression as described in the text, to the data from table 3, columns 2 through 4. Both fitted and raw data are expressed as a percentage of the estimated Econ parameter. Solid points are above the surface; open points fall below the surface. (A) Eq. 5; (B) Eq. 28; (C) Eq. 29; (D) Eq. 29.

figure 22(A) with vertical planes at the concentrations of drug 2 and drug 1 listed in the figure. These curves, along with the actual data points, provide a visual analysis of the goodness of fit. Note the differences between the set of best-fit simulated curves in figure 24 and the analogous hand-drawn curves in figure 13. Figure 25 shows concentration-effect curves simulated with the best-fit parameters for drug 1, drug 2, a 10:1 mixture of drug 1 to drug 2, and a 10:1 mixture with the assumption of Loewe additivity ($\alpha = 0$). This 2-D representation of the full 3-D surface in figure 22(A) provides a visual assessment of the magnitude of the shift of the concentration-effect curves, because of Loewe synergism, for fixed ratio mixtures. The IC_{50} value for the 10:1 mixture of the Loewe synergistic combination was 1.015-fold (5.45/5.37) lower than the expected value for the Loewe additive combination. This is close to the ratio of 1.012-fold (5.00/4.94) for ideal data containing no error. It is apparent that an α value of 0.5 leads to only subtle shifts in mixture concentration-effect curves. Because the α estimate is positive and the 95% confidence interval,

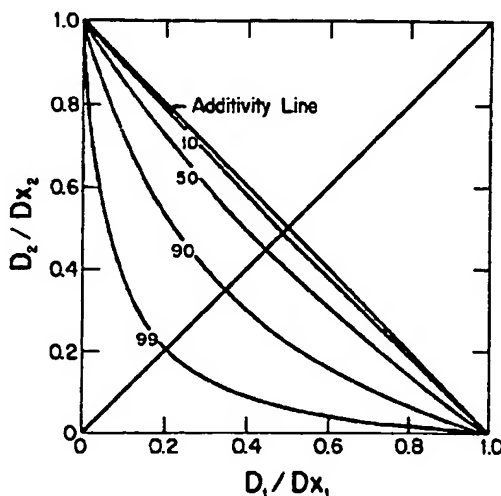


FIG. 23. Families of 2-D isobols for the best fit of Eq. 5 to the data from table 3, columns 2 through 4. The set of contours is a 2-D representation of the 3-D response surface in figure 22, panel (A). Note that the X- and Y-axes are the concentrations of each drug transformed by division by the appropriate value of the dose (or concentration) of drug that inhibits survival by X% (D_X). The numbers on the isobols indicate the % inhibitory level.

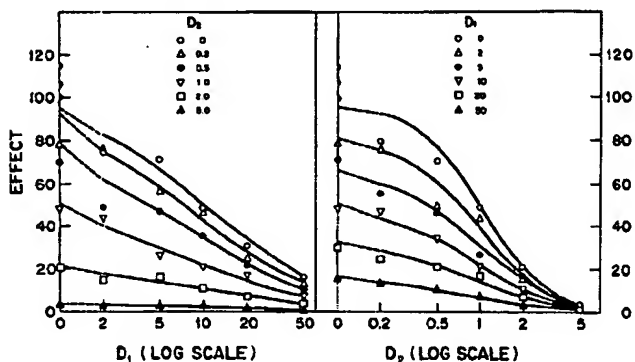


FIG. 24. Families of 2-D concentration-effect curves for the best fit of Eq. 5 to the data from table 3, columns 2 through 4. This is another 2-D representation of the 3-D response surface in figure 22, panel (A). Note that drug concentrations are on logarithmic scales.

0.300 to 0.738, does not encompass zero, a claim of small but significant synergism is made.

As was stated previously several times in this paper, Eq. 5, our flagship model, is a model for combined-action, not the model. Eq. 5 has a questionable property: for negative values of the interaction parameter, α , the 3-D concentration-effect surface has a saddle point and rises back to $Econ$ at simultaneous high concentrations of both agents. This is illustrated in figure 26, a simulation of Eq. 5 with $\alpha = -1$ (Loewe antagonism). Like the fit of second order polynomial models to data sets that show slight curvature, the fit of Eq. 5 to experimental data demonstrating Loewe antagonism may be valid for only a restricted region. The fit of Eq. 5 with negative α

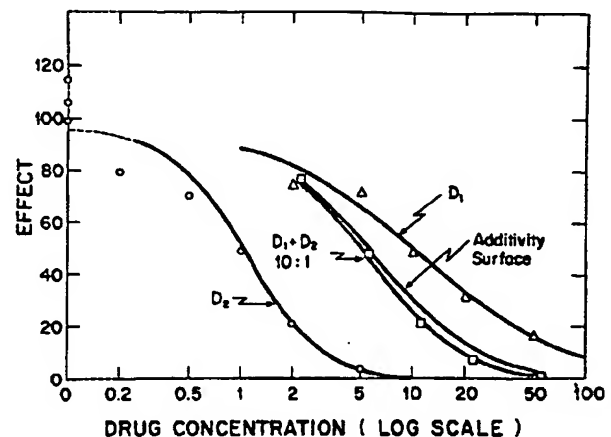


FIG. 25. Predicted 2-D concentration-effect curves for drug 1 alone, drug 2 alone, and the combination of drug 1 and 2 in a fixed 10:1 ratio for the best fit of Eq. 5 to the full data set from table 3, columns 2 through 4. The predicted Loewe additivity curve for the same combination at a fixed ratio of 10:1, simulated by setting $\alpha = 0$, is also shown. The X-axis is the sum of concentrations of drug 1 and drug 2 (logarithmic scale). The raw data points are the same ones shown in figure 16.

estimates to experimental data has been shown to be satisfactory (e.g., Greco and Dembinski, 1992). However, we have systematically searched for a logical model that would not rise up at mixtures of high agent concentrations.

Such an experimental model is Eq. 28, whose general form was first suggested by Finney (1952) and later included in a list of plausible interaction models by Hewlett (1969). (Eq. 28 rises back toward $Econ$ only at very high agent concentrations and large negative α values.) Eq. 28 is a specific example of the general Loewe combined-action model, Eq. 9. Eq. 28 differs from Eq. 5 by having all of the right-hand expression, except for α , raised to the $1/2$ power. For simulations of Eq. 28, the extent of bowing will be the same for isobols at different effect levels determined from plots of $D_2/ID_{X,2}$ vs. $D_1/ID_{X,1}$. This is in contrast to the greater bowing of isobols at higher levels of inhibition for Eq. 5, as seen in figures 4(E), 5(A), 8(C), and 23.

$$1 = \frac{D_1}{IC_{50,1} \left(\frac{E}{Econ - E} \right)^{1/m_1}} + \frac{D_2}{IC_{50,2} \left(\frac{E}{Econ - E} \right)^{1/m_2}} + \alpha \left(\frac{D_1 D_2}{IC_{50,1} IC_{50,2} \left(\frac{E}{Econ - E} \right)^{(1/m_1 + 1/m_2)}} \right)^{1/2} \quad [28]$$

Eq. 28 was fit to the common data set in the same way as described for Eq. 5. Figure 22(B) shows the best-fit 3-D surface and the raw data points. The six estimated parameters were: $Econ = 88.9 \pm 5.5$; $IC_{50,1} = 15.6 \pm 2.2$;

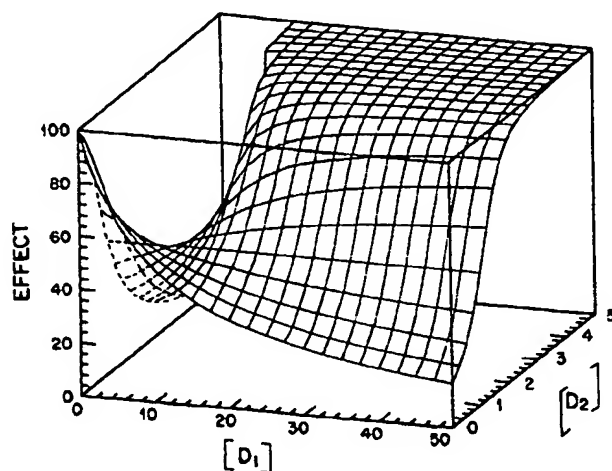


FIG. 26. Simulation of Eq. 5, with $Econ = 100$, $IC_{50,1} = 10$, $IC_{50,2} = 1$, $m_1 = -1$, $m_2 = -2$, $\alpha = -1$, an example of Loewe antagonism.

$IC_{50,2} = 1.27 \pm 0.11$; $m_1 = -1.34 \pm 0.11$; $m_2 = -2.28 \pm 0.13$; $\alpha = 0.643 \pm 0.18$. As seen in Figure 22(B) and in other 2-D plots not shown, the goodness of fit was adequate. Because α was positive and its 95% confidence interval did not encompass zero (0.270 to 1.02), Loewe synergism is claimed. [Note however, that for some negative values of α (from -1.414 to 0), the isobols simulated with Eq. 28 lie outside the limits of the graph of $D_2/ID_{X,2}$ vs. $D_1/ID_{X,1}$ shown in figure 5(A); i.e., they lie outside the unit square. This inadequacy of the general form of this model was first pointed out by Machado and Robinson (1994) and further explored by Khinkis and Greco (1994).]

2. *Models of Weinstein et al. (1990)*. Eq. 29 was introduced by Weinstein et al. (1990) and Bunow and Weinstein (1990); a reparameterization has been used more recently (Kageyama et al. (1992). Eq. 29 is called the robust potentiation model. Loewe additivity is its null reference model. PC_1 , PC_2 , are the concentrations of agents 1, 2 required to increase the apparent potency of the other drug by a factor of 2. The parameters, bp_1 , bp_2 , govern the slope of the potentiative effect of agents 1 and 2, respectively. Loewe synergism, but not Loewe antagonism, can be modeled with Eq. 29, because a negative PC parameter cannot be used with a corresponding non-integral bp parameter. Eq. 29 and several other models are integrated into the software package COMBO, which runs in the MLAB (Civilized Software Inc, 1991) environment on MSDOS-compatible microcomputers. We fit Eq. 29 to data with nonlinear regression with our FORTRAN program as described for Eqs. 5 and 28, with weights equal to the reciprocal of the square of the predicted response; we did not implement the interesting weighting scheme described by Bunow and Weinstein (1990), a Gaussian kernel windowing technique based on estimated responses.

We were unsuccessful in fitting the full nine-parameter model, Eq. 29 to the common data set. There was not

enough information in the data set to allow the estimation of four separate interaction parameters, PC_1 , PC_2 , bp_1 , and bp_2 . However we were successful in fitting two different reduced seven-parameter models to the common data set. Figure 22(C) shows the fit of Eq. 29, with the expression containing PC_1 and bp_1 eliminated, and figure 22(D) shows the fit of Eq. 29, with the expression containing PC_2 and bp_2 eliminated. The need to use only one of the two pairs of interaction parameters was also reported by Weinstein et al. (1990). The estimated parameters for the best fit shown in figure 22(C) were: $Econ = 95.3 \pm 4.8$; $IC_{50,1} = 11.0 \pm 1.4$; $IC_{50,2} = 1.02 \pm 0.084$; $m_1 = -1.13 \pm 0.077$; $m_2 = -1.94 \pm 0.10$; $PC_2 = 1.65 \pm 0.31$; $bp_2 = 1.55 \pm 0.21$. The estimated parameters for the best fit shown in figure 22(D) were: $Econ = 98.9 \pm 4.5$; $IC_{50,1} = 9.49 \pm 1.2$; $IC_{50,2} = 0.947 \pm 0.059$; $m_1 = -1.00 \pm 0.064$; $m_2 = -1.92 \pm 0.066$; $PC_1 = 44.8 \pm 5.0$; $bp_1 = 1.18 \pm 0.16$. Because the fit was good for both reduced models, the interaction parameters, PC_1 , PC_2 , were both positive, and their 95% confidence intervals did not encompass zero, the conclusion is Loewe synergism.

$$1 = \frac{D_1 \left(1 + \left(\frac{D_2}{PC_2} \right)^{bp_2} \right)}{IC_{50,1} \left(\frac{E}{Econ - E} \right)^{1/m_1}} + \frac{D_2 \left(1 + \left(\frac{D_1}{PC_1} \right)^{bp_1} \right)}{IC_{50,2} \left(\frac{E}{Econ - E} \right)^{1/m_2}} \quad [29]$$

There are many other parametric response surface models that could be applied to the common data set. Hewlett (1969) provides a general framework for deriving many specific, potentially useful, multivariate concentration-effect combined-action models. More recently, Machado and Robinson (1994) have reviewed this set of combined-action models, plus the general forms of Eqs. 5, 29, and an original model, Eq. 30. Eq. 30 has a single interaction parameter, which is called η . Unfortunately, like Eq. 28, Eq. 30 has the disadvantage of having isobols lie outside the unit square of the graph of $D_2/ID_{X,2}$ vs. $D_1/ID_{X,1}$ for values of η from $-\infty$ to -0.333 and from 1 to ∞ (Khinkis and Greco, 1994).

$$1 = (1 + \eta) \left[\frac{D_1}{IC_{50,1} \left(\frac{E}{Econ - E} \right)^{1/m_1}} + \frac{D_2}{IC_{50,2} \left(\frac{E}{Econ - E} \right)^{1/m_2}} \right] - \eta \left[\frac{D_1}{IC_{50,1} \left(\frac{E}{Econ - E} \right)^{1/m_1}} - \frac{D_2}{IC_{50,2} \left(\frac{E}{Econ - E} \right)^{1/m_2}} \right]^2 \quad [30]$$

The response surface approaches have the following advantages:

(a) they provide a quantitative measure of the intensity of interaction, along with a measure of its uncertainty.

(b) they reduce the full data set from an experiment to a smaller set of parameters, along with uncertainty estimates.

(c) they facilitate prediction of the response under new conditions.

(d) they are appropriate for complex situations, such as three-, four-, and five-drug combinations.

(e) they aid in experimental design, including the design of complex experiments. Also, they tend to be tolerant of a wide spectrum of designs.

(f) they have the potential to explain, in intimate detail, all of the characteristics of a complex system, and thereby facilitate a deep understanding of the system.

(g) they are objective (relatively), rigorous, and consistent with modern statistical theory. In addition to the brief statistical summary provided for the fits of Eq. 5, 28, and 29 to the common data set, there are other useful statistical diagnostics available, including overall goodness of fit statistics, confidence envelopes around the fitted surface, and residual (functions of the difference between the actual and fitted data) analyses (e.g., McCullagh and Nelder 1989; Seber and Wild, 1989; Bates and Watts, 1988; Carter et al., 1986; Machado and Robinson, 1994).

(h) parametric 3-D concentration-effect models may be used as the pharmacodynamic component of composite pharmacokinetic-pharmacodynamic models, to be used for the clinical study of the disposition and effect of drug combinations.

(i) finally, as described in Section III, response surface approaches are useful in explaining the similarities and differences among other rival approaches to the assessment of combined-action.

The four panels of figure 22 look very similar. From the statistics provided for the fit of Eqs. 5, 28 and 29 to the common data set, it would be difficult to choose the best structural model. To a great extent, the exact form of combined-action models is arbitrary, and considerations other than the goodness of fit of a model to a specific data set, must be used to decide upon a modeling framework. These criteria include:

(a) a model should allow the "slope" for each agent's individual concentration-effect curve to be different; this is allowed by Eqs. 5, 28, 29, 30.

(b) it is desirable to allow each agent's individual concentration-effect curve to have a different functional form; however, the need for such a model seldom arises.

(c) the model should be one from a hierarchical set, which allows expansion and reduction of models by inclusion and deletion of expressions and parameters, in a logical, hierarchical manner. For example, a model might be expanded to accommodate more than two agents, or to describe simultaneous Loewe synergism and Loewe antagonism in different regions of the concentration-effect surface, and reduced to describe an agent that increases the pharmacological effect of a second agent, but which has no effect by itself (synergism, see table 1).

(d) the simulation of the model should present no unsolvable numerical problems. For example, Eqs. 5, 28–30 all require appropriate one-dimensional root finders (e.g., Thisted, 1988), but these are easily programmed, and have been found to be reliable.

(e) if normalized isobols [e.g., fig. 8(C)] for typical data increase in bowing at higher levels of inhibition, then this characteristic should be intrinsic to the model.

(f) a model should have the fewest parameters possible to adequately describe combined-action data.

(g) it is desirable for the parameters to have some geometrical meaning; i.e., upon hearing of the values of a model's parameters, an experienced researcher should be able to mentally picture 2-D and 3-D concentration-effect curves. This would be true for Eqs. 5 and 28 through 30.

(h) it is desirable for the model to follow the correct course, even in regions for which there is no data. In other words, cautious extrapolation should be possible.

(i) the modeling paradigm should allow the combining of a 3-D concentration-effect structural model, such as Eqs. 5 and 28 through 30, with an appropriate random model, for fitting data with modern statistical approaches, such as maximum likelihood estimation.

(j) in general, the structural model should closely follow the overall average data, without following random fluctuations.

(k) the isobols for the model should lie within the unit square of the graph of $D_2/ID_{X,2}$ vs. $D_1/ID_{X,1}$ for all values of the interaction parameter(s). This last criteria is not met by Eqs. 28 and 30.

A critical area of future research will be the derivation, collection, and comparison of rival multivariate parametric concentration-effect combined-action models. A comprehensive critical comparison of rival models (e.g., Eqs. 5 and 28 through 30) is beyond the scope of this review. Machado and Robinson (1994) present one of the first such critical reviews; our group is also currently working in this area (Khinkis and Greco, 1994). Although the field of response surface modeling of agent interactions has old roots (e.g., Finney, 1952), only in recent years has the availability of computer hardware and software made it into a practical, universally important discipline.

The disadvantages of fitting 3-D parametric concentration-effect models to data include:

(a) there are an infinite number of plausible parametric models; it may be difficult to choose among rival models. Different rival models may lead to different conclusions. The parametric modeling paradigm is still evolving; an analysis of data with a current model might be proven to be suboptimal at a later time.

(b) the proper fitting of these models to data requires statistical and computing expertise and adequate computer hardware and software. However, the acquisition of these skills and tools is increasing among laboratory scientists, and, in our view, is very cost-effective. In addition, as an alternate solution, both initial and long-

term collaborations between laboratory and quantitative scientists can be very Loewe synergistic.

(c) the links between empirical models of combined-action, such as Eqs. 5 and 28 through 30, and theoretical mechanistic models of molecular, biochemical, and physiological systems have not been systematically made. In other words, after one makes a rigorous claim of, let's say, Loewe synergism, it is in no way obvious what this implies regarding the mechanistic interaction of two agents. Some work has been done in this field (e.g., Werkheiser et al., 1973; Jackson, 1980, 1984, 1991, 1992, 1993; Bravo et al., 1992). However, this critical research area is in its infancy.

VI. Comparison of Rival Approaches for Discrete Success/Failure Data

This section will discuss approaches to the assessment of the combined-action of agents, in which the measured or observed response is binary (quantal); i.e., it is success or failure, yes or no, dead or alive, on or off, 0 or 1. The data is often grouped by treatment and is expressed as a proportion of successes; e.g., five successes of eight trials, or 0.625. Most of the material in this section is from Greco (1989). A random model that describes the statistical variation in success/failure data is the Bernoulli distribution, and one that describes the variation in proportion data is the binomial distribution (Larson, 1982). Figure 3 showed a concentration-effect structural curve with binomial variation about one point on the curve. A formula for the binomial model is Eq. 31, in which n is the number of attempts in a binomial trial, k is the number of successes, Y is the proportion of successes ($Y = k/n$), y is a particular value of Y ($y = 0, 1/n, 2/n, \dots, 1$), μ is the mean or expected value of Y , $P(Y = y)$ is the probability that the general Y variable will equal the particular value y , and (\cdot) is the combination of n things taken ny at a time. [Note: Eq. 31 is different from but equivalent to the more common form of the binomial distribution equation (e.g., Larson, 1982) not shown here. We reparameterized the more common form into Eq. 31 to facilitate the combining of structural with random models.] Because the overall mean or expected value of Y is merely the value of the structural model, structural models for success/failure concentration-effect phenomena can be generated by simply substituting μ for E in any of the structural concentration-effect models previously described in this paper for continuous data. For example, the Hill model can be expressed as Eq. 32, and our flagship combined-action model can be expressed as Eq. 33. Note that the *Econ* parameter has been constrained to be the constant, 1, in Eqs. 32 and 33. In order to make a composite structural-random model for data fitting, the structural expression for μ is inserted into the binomial model, Eq. 31, either directly or

indirectly with a numerical procedure.

$$P(Y = y) = \binom{n}{ny} \mu^{ny} (1 - \mu)^{n(1-y)} \quad [31]$$

$$\mu = \frac{\left[\frac{D}{Dm} \right]^m}{1 + \left[\frac{D}{Dm} \right]^m} \quad [32]$$

$$1 = \frac{D_1}{Dm_1 \left[\frac{\mu}{1 - \mu} \right]^{1/m_1}} + \frac{D_2}{Dm_2 \left[\frac{\mu}{1 - \mu} \right]^{1/m_2}} \quad [33]$$

$$+ \frac{\alpha D_1 D_2}{Dm_1 Dm_2 \left[\frac{\mu}{1 - \mu} \right]^{(1/2m_1 + 1/2m_2)}}$$

Rival approaches for the assessment of combined-action when the response is quantal (proportions of success/failure) will be compared in a manner similar to the comparison in Section V of rival approaches for combined-action when the response is a continuous measure. A simulated data set for a pair of inhibitory drugs, listed in table 4, was generated by first calculating μ with Eq. 33 with parameters, $IC_{50,1} = 10$, $IC_{50,2} = 1$, $m_1 = -1$, $m_2 = -2$, $\alpha = 1$; and then entering μ , along with n into a binomial random number generator from the Statgraphics Software Package (STSC Inc., 1988). This data set will be analyzed with three different approaches, the approach of Gessner (1974), the fitting of the parametric response surface model, Eq. 33 (Greco and Lawrence, 1988) to the full data set, and the fitting of the multivariate linear logistic model (Cox, 1970), Eq. 34, to the full data set (e.g., Carter et al., 1983, 1988; Brunden et al., 1988).

$$\mu = \frac{\exp(\beta_0 + \beta_1 D_1 + \beta_2 D_2 + \beta_{12} D_1 D_2)}{1 + \exp(\beta_0 + \beta_1 D_1 + \beta_2 D_2 + \beta_{12} D_1 D_2)} \quad [34]$$

Many of the methods for analyzing continuous combined-action data, described in Section V, could be used, and have been previously used, for analyzing proportion data. If one merely calculates the proportions of survivors from table 4 as decimal numbers and then treats these numbers as continuous data, then methods E.1 through E.11 could be directly applied without any additional complications. However, the variation pattern (probability distribution) of proportion data is fundamentally different from that for typical continuous biological data. For proportion data, usually the numbers of survivors and the total numbers of organisms undergoing a treatment is known without error. The variation in responses is usually caused by the fundamental nature of discrete binary responses; the variation is usually wider in the ID_{50} range of the concentration-effect curve

TABLE 4
Data set, with a binary (proportion) response variable, used for comparison of rival data analysis approaches

D_1	D_2	Number of survivors*	Total number of organisms
0.1	0	100	100
0.3	0	97	100
0.5	0	96	100
1	0	96	100
3	0	72	100
5	0	59	100
10	0	57	100
30	0	32	100
50	0	13	100
100	0	13	100
0	0.01	100	100
0	0.03	100	100
0	0.05	99	100
0	0.1	98	100
0	0.3	95	100
0	0.5	72	100
0	1	46	100
0	3	6	100
0	5	3	100
0	10	2	100
0.1	0.01	99	100
0.3	0.03	97	100
0.5	0.05	94	100
1	0.1	87	100
3	0.3	59	100
5	0.5	53	100
10	1	24	100
30	3	7	100
50	5	2	100
100	10	0	100

* The number of survivors in column 3 was generated by (a) calculating μ with Eq. 33 with parameters, $IC_{50,1} = 10$, $IC_{50,2} = 1$, $m_1 = -1$, $m_2 = -2$, $\alpha = 1$; then entering μ , along with n (the total number of organisms, equal to 100) into a binomial random number generator from the Statgraphics Software Package (STSC Inc., 1986).

and smaller near the two ends of the curve. Proportions above 1 and below 0 do not exist. In contrast, continuous biological data often follow bell-shaped normal distributions, with larger variances associated with larger measurements (proportional error, constant coefficient of variation). Individual measurements (% control) both above 100% and below 0% often occur. Proportions will tend to become normally distributed as n becomes large, and as the true proportion tends away from the ends of the range, 0 and 1. Methods, E.1 through E.11, which ignore the true random component of the data, will only be, at best, approximately correct for binary data. However, they can provide very useful preliminary exploratory procedures. Nonetheless, only approaches that fully exploit the binary nature of the data will be compared in this section.

Much of the early work on the problem of combined-action of agents was focused on biological systems with quantal responses (e.g., Bliss, 1939; Finney, 1952, 1971; Hewlett and Plackett, 1959, 1979; Hewlett, 1969; Plack-

ett and Hewlett, 1948, 1952, 1967). (It seems that systems with quantal responses were of more interest to statisticians, whereas systems with continuous responses have been of more interest to pharmacologists.) Specific approaches and models of these pioneers in the field of combined-action assessment will not be reviewed in this paper. However, many of their concepts, approaches and models form the basis of the three approaches that will be compared.

A. Approach of Gessner (1974)

Our interpretation of the method of Gessner (1974) first consists of fitting appropriate single agent models to the data for agent 1 alone, agent 2 alone, and fixed ratios of $D_1:D_2$. Gessner (1974) recommends the probit model (e.g., Finney, 1952), Eq. 35, for this purpose; however, we also explored the use of the univariate linear logistic model with $\ln(D)$ as the input, Eq. 36, and the univariate linear logistic model with D as the input, Eq. 37. Note that Eq. 32 and 36 are different parameterizations of the same fundamental model, in which $\beta_0 = -m\ln(D_m)$ and $\beta_1 = m$. These three models were fit to the data for drug 1 alone, drug 2 alone, and the 10:1 mixture from table 4, with maximum likelihood estimation via nonlinear least squares (Jennrich and Moore, 1975), with the software package, PCNONLIN (Statistical Consultants, Inc., 1986), on an MSDOS-compatible microcomputer. The best fit of Eq. 32, and the equivalent model, Eq. 36, to the three sets of data points from the common 30-point data set, is shown in figure 27(A). The best fits of Eqs. 35 and 37 are shown in figures 27(B) and 27(C), respectively. The fits look good for Eqs. 32, 36, and 35, but not for Eq. 37. The parameter estimates \pm standard errors for the fits of these four models were: (for Eq. 32, drug 1, $D_m = 10.7 \pm 0.99$, $m = -0.982 \pm 0.060$; drug 2, $D_m = 0.895 \pm 0.056$, $m = -1.99 \pm 0.14$; drug 1+2, $D_m = 4.36 \pm 0.30$, $m = -1.59 \pm 0.10$). (For Eq. 36, drug 1, $\beta_0 = 2.33 \pm 0.16$, $\beta_1 = -0.982 \pm 0.060$; drug 2, $\beta_0 = -0.220 \pm 0.13$, $\beta_1 = -1.99 \pm 0.14$; drug 1+2, $\beta_0 = 2.34 \pm 0.19$, $\beta_1 = -1.59 \pm 0.10$). (For Eq. 35, drug 1, $\beta_0 = 6.36 \pm 0.084$, $\beta_1 = -1.32 \pm 0.072$; drug 2, $\beta_0 = 4.90 \pm 0.072$, $\beta_1 = -2.72 \pm 0.17$; drug 1+2, $\beta_0 = 6.35 \pm 0.10$, $\beta_1 = -2.12 \pm 0.12$). (For Eq. 37, drug 1, $\beta_0 = 1.61 \pm 0.10$, $\beta_1 = -0.0577 \pm 0.0043$; drug 2, $\beta_0 = 2.55 \pm 0.14$, $\beta_1 = -1.67 \pm 0.13$; drug 1+2, $\beta_0 = 2.52 \pm 0.16$, $\beta_1 = -0.403 \pm 0.032$). None of the 95% confidence intervals for any of the parameters for any of the models encompassed zero.

$$\text{Probit}(\mu) = \beta_0 + \beta_1 \ln(D) \quad [35]$$

$$\mu = \frac{\exp(\beta_0 + \beta_1 \ln(D))}{1 + \exp(\beta_0 + \beta_1 \ln(D))} \quad [36]$$

$$\mu = \frac{\exp(\beta_0 + \beta_1 D)}{1 + \exp(\beta_0 + \beta_1 D)} \quad [37]$$

The second stage of the method of Gessner (1974) is to plot the estimated D_m (ID_{50}) values, along with their

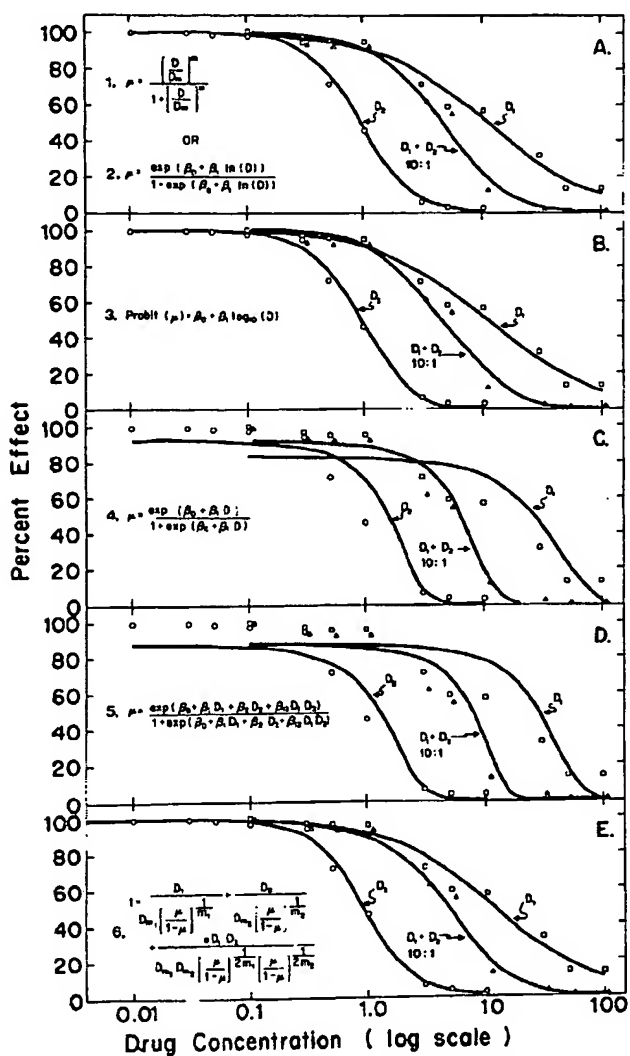


FIG. 27. Fitted curves of various models to the simulated data from table 4. See details in the text.

95% confidence intervals, for drug 1 alone, drug 2 alone, and for the mixture, on isobolograms. Figure 28 shows the isobolograms for the fits of Eqs. 32, 35 and 36, which all coincide, and figure 29 shows the isobogram for the fit of Eq. 37. The dashed lines connecting the ends of the 95% confidence intervals for the ID_{50} 's of drug 1 alone and drug 2 alone define a Loewe additivity region. Because the 95% confidence interval for the 10:1 mixture of drug 1+2 intersects the Loewe additivity region, a conclusion of Loewe additivity is made. In contrast, the isobogram replot for the fit of Eq. 37, figure 29, indicates Loewe synergism. Interestingly, the poor fit of Eq. 37 to the data resulted in poor estimates of the ID_{50} 's for each drug alone, and this lead to the "correct" claim of Loewe synergism. The overall conclusion for the method of Gessner (1974), based upon the fits of Eqs. 32, 35 or 36, and the isobogram replot in figure 28, is Loewe additivity.

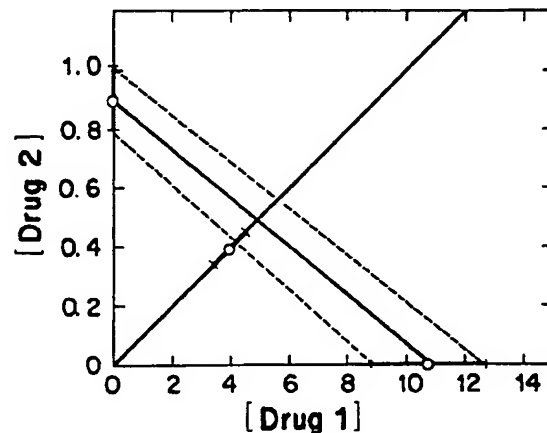


FIG. 28. Further isobographic analysis of data from figure 27, panels (A), (B), using an interpretation of the approach of Gessner (1974).

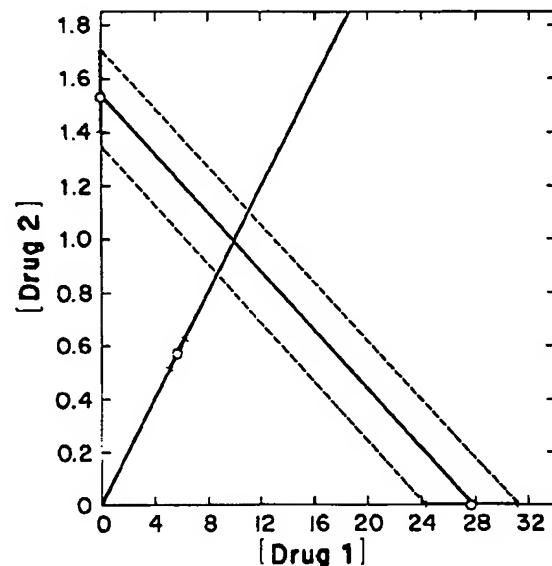


FIG. 29. Further isobographic analysis of data from figure 27, panel (C), using an interpretation of the approach of Gessner (1974).

It is also clear that the linear logistic model without the logarithmic transformation of the dose, Eq. 37, does not seem to have the ideal shape for typical concentration-effect data. It seems to miss points near 100% survival, and misses points for concentration-effect curves with relatively shallow slopes (around $m = -1$).

The advantages of the method of Gessner (1974) include:

- (a) the underlying null reference model is Loewe additivity.
- (b) the approach takes into account in an appropriate manner, the binomial variation of proportion data.
- (c) the approach allows the slopes of the individual concentration-effect curves to be different.

- (d) the derivation and application of complex full combined-action models are not necessary.
- (e) the isobologram replot is visual and intuitive.
- (f) uncertainty measures, the 95% confidence intervals about the ID_{50} s, are included in the analysis.
- (g) the approach can accommodate interspersed regions of Loewe synergism and antagonism.
- (h) the general concepts of estimating ID_{50} s, along with 95% confidence intervals, and making a replot isobologram, are very general, and could be applied to continuous data.
- (i) the approach is relatively easy to implement with standard software.

(j) the approach is an excellent front-end for more advanced model-fitting approaches and may provide the best final analysis for complex situations in which the degree of Loewe synergism and Loewe antagonism varies across the 3-D concentration-effect surface.

The disadvantages include:

(a) the additivity region bounded by the dashed lines connecting the ends of the 95% confidence intervals of the individual agent ID_{50} s was not created with a rigorous statistical derivation. The additivity region will tend to be too wide, too conservative, resulting in rejection of true Loewe synergism and Loewe antagonism too often. More realistic confidence bounds, based upon modern statistical theory, have been derived by Carter's group (Carter et al., 1986, 1988; Gennings et al., 1990).

(b) it is likely that the fitting of data for a fixed ratio of $D_1:D_2$ by concentration-effect models appropriate for single agents, such as Eqs. 32, 35, or 36, will result in biases, similar to the problems described for fitting the median-effect model to fixed ratio data, described in Appendix B, and in figure 17. We predict that the misfits will become more severe as the difference in slope parameters increases and as the intensity of interaction increases, as shown for the median-effect model, in figure 17. However, we predict, as indicated for the median-effect model in Appendix B, that the problems will tend to be minor if one focuses mainly on the ID_{50} s.

(c) maximum use is not made of the data, as compared with approaches centered on the fitting of full combined-action concentration-effect surfaces to all of the data simultaneously.

(d) summary measures of the intensity of interaction, along with uncertainty measures, are not provided.

An additional criticism—with which we take issue—leveled at the method of Gessner (1974) is that the approach does not adjust the 95% Loewe additivity region to take into account the problem of making multiple comparisons of ID_{50} s from several separate fixed ratio concentration-effect curves (Carter et al., 1988). Carter's group argues: "The procedure described suffers from the same problem associated with making multiple [Student's] t-tests to compare the means of a number of treatment groups. In such cases, the probability of incorrectly rejecting the null hypothesis of equality of

treatment means is inflated. Here, the null hypothesis is one of additivity. Hence, the probability of incorrectly rejecting additivity and thereby concluding synergism is inflated."

We respond to this criticism by pointing out that, when applying Gessner's (1974) approach to datasets with several fixed ratios of $D_1:D_2$, the pattern of ID_{50} confidence intervals is taken into account; albeit, in an ad hoc manner, when making a conclusion. Each ID_{50} confidence interval is not meant to be interpreted in isolation. For example, if there were 10 different fixed ratios for our common data set, and if their ID_{50} confidence intervals were plotted in figure 29, and if a random assortment of significant Loewe synergism and Loewe antagonism were demonstrated, one would conclude either that the combined-action was very complex or that some errors were made in conducting the experiment. The experiment would probably be repeated. If only 1 of 10 fixed ratios showed significant Loewe synergism, with no apparent trend in the ID_{50} estimates, then the Loewe synergism would be considered suggestive at best, possibly a random artifact, and, if possible, the experiment would be repeated with larger sample sizes, especially in the region of suspected Loewe synergism. However, with the more probable result of consistent patterns of Loewe synergism or Loewe antagonism, (e.g., Gessner, 1988), the clusters of Loewe synergistic and/or Loewe antagonistic ID_{50} intervals will reinforce each other, leading to a more conservative, not to a more liberal, conclusion. The use of improperly inflated P-values, and conversely, improperly deflated 95% confidence intervals, caused by the making of multiple statistical comparisons, is certainly an important general problem in biostatistics (Miller, 1981). However, the problem is not relevant to the application of Gessner's approach when rationally applied to agent combination data.

B. Parametric Response Surface Approaches

Just as for continuous data, full 3-D combined-action concentration-effect models can be fit to proportion data, to assess the nature and intensity of agent interaction. The use of two different structural models will be demonstrated: our flagship combined-action model, Eq. 33, and the multivariate linear logistic model, Eq. 34. In principle, the general form of Eq. 28, Eq. 29 (Weinstein et al., 1990), Eq. 30 (Machado and Robinson, 1994), and any of the models reviewed by Hewlett (1969) could also be tried, but these are not included in this part of the review.

1. Model of Greco and Lawrence (1988). Eq. 33 was fit to the full common data set in table 4 with maximum likelihood estimation in the same manner as described in Section VI.A. The best fit surface is shown as three curves in figure 27(E). The fitted surface hugs the raw data, with a random distribution of points about the

surface. The parameter estimates \pm standard errors were: $Dm_1 = 11.2 \pm 0.99$, $m_1 = -0.995 \pm 0.052$, $Dm_2 = 0.905 \pm 0.056$, $m_2 = -2.05 \pm 0.14$, $\alpha = 0.903 \pm 0.46$. The 95% confidence interval for α was from 0.001 to 1.80. Therefore, Loewe synergism is claimed.

2. Multivariate linear logistic model. The use of the multivariate linear logistic model (Cox, 1970) is very popular in the analysis of clinical trial data and in Epidemiology, in cases in which the response variable is binary (Hosmer and Lemeshow, 1989). It is the most popular response surface model that has been routinely applied to quantal combined-action data (e.g., Carter et al., 1983, 1988; Brunden et al., 1988). Eq. 34, the multivariate linear logistic model for two agents, includes one interaction parameter, β_{12} . When β_{12} is positive, Loewe synergism is indicated; when β_{12} is negative, Loewe antagonism is indicated, and when β_{12} is zero, Loewe additivity is indicated. Eq. 34 was fit to the common data set in table 4 with the maximum likelihood approach described in Section VI.A. The fitted surface is shown in figure 27(D). The parameter estimates were: $\beta_0 = 2.03 \pm 0.071$, $\beta_1 = -0.0713 \pm 0.0043$, $\beta_2 = -1.54 \pm 0.11$, $\beta_{12} = -0.0837 \pm 0.025$. Because the 95% confidence interval for β_{12} is from -0.133 to -0.0347, Loewe antagonism might be concluded. However, the best fit of Eq. 34 to the data, shown in figure 27(D), does not look very good. First, the surface misses the points near 100% survival. Second, because the linear logistic model constrains agent 1 alone, agent 2 alone, and the 10:1 mixture all to have the same dose-effect slope (on a logarithmic dose scale), the data points are not randomly scattered about the curves; the surface systematically misses most of the data. These two characteristics make the multivariate linear logistic model suboptimal for assessing the combined-action of agents in many systems.

This second problem with the use of the linear logistic model, the constraining of the slopes of the concentration-effect curves, may have profound implications for the use of the multiple linear logistic model in other fields. Therefore, a cleaner, simpler example of the problem, illustrated in figure 30, is presented here. The four curves, *a*, *b*, *c* and *d* for both panels, A and B, were simulated with the simple linear logistic model, Eq. 37. For curve *a*, $\beta_0 = 1.5$, $\beta_1 = -2.0$; for curve *b*, $\beta_0 = 3.0$, $\beta_1 = -2.0$; for curve *c*, $\beta_0 = 1.5$, $\beta_1 = -0.1$; for curve *d*, $\beta_0 = 3.0$, $\beta_1 = -0.1$. In panel A, μ is plotted against agent dose on a common logarithmic scale; whereas, in panel B, the logit of μ is plotted against agent dose on a linear scale. For each of these curves, 45 points, indicated by symbols, were simulated, and then the points connected via the spline option in SigmaPlot 2.0 (Jandel Scientific, 1994). The combined data for curves *b* and *c* ($n = 90$) were assumed to represent the proportion of organisms remaining after treatment with agent 1 and agent 2, respectively. A sample size of 1000 was assumed for each of the 90 treatment groups. No binomial variation was

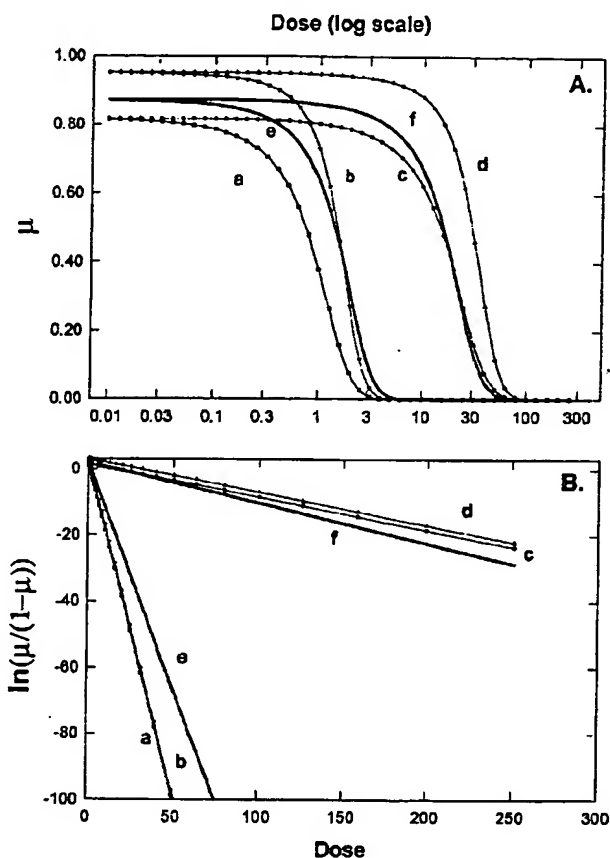


FIG. 30. Problems with use of logistic function for representing dose-response phenomena.

introduced. This set of data was then fit with Eq. 38, a multiple linear logistic model with three estimable parameters, β_0 , β_1 , and β_2 , but no β_{12} interaction parameter, with the LR program in BMDP (Dixon et al., 1990). This model assumes a common β_0 term, a β_1 term for agent 1, and a β_2 term for agent 2. The best fit estimates (\pm standard error) were: $\beta_0 = 1.93 \pm 0.013$; $\beta_1 = -1.36 \pm 0.016$; and $\beta_2 = -0.122 \pm 0.0015$. These parameter estimates were then used to simulate curves *e* and *f* in both panels (A) and (B).

$$\mu = \frac{\exp(\beta_0 + \beta_1 D_1 + \beta_2 D_2)}{1 + \exp(\beta_0 + \beta_1 D_1 + \beta_2 D_2)} \quad [38]$$

Note that in panel (A), the two members of each curve pair, *a* and *c*, *b* and *d*, and *e* and *f* share the same shape; they are parallel; they have the same dose-effect slope (on a logarithmic dose scale). For example, at every effect level (except $\mu = 1$ and $\mu = 0$), the dose for curve *c* is 20-fold higher than the corresponding dose on curve *a* (the ratio of their ID_{50} s). This is caused by the same β_0 term for each respective pair. The lateral separation of the curves for each pair is because of different β_1 terms. Because the ID_{50} is equal to $-\beta_0/\beta_1$, it is clear that a larger β_0 term will shift the concentration-effect curve to

the right, and a larger-in-magnitude β_1 term will shift the curve to the left. Note that in panel B, that curve pairs *a* and *b*, and *c* and *d* consist of parallel lines. This is caused by the same β_1 terms for each respective pair. There are common y-intercepts for curve pairs *a* and *c*, *b* and *d*, and *e* and *f*, in panel B, but this cannot be visually detected on the scale with which the graph is drawn.

When Eq. 38 is fit to the combined data from curves *b* and *c*, there are only three parameters available to represent the information that was originally contained in four parameters, so compromises were necessary. Note that the estimated β_0 for the combined data, 1.93, is a compromise between the β_0 terms for the individual concentration-effect curves, 1.5 and 3.0. Also note that the concentration-effect slopes in panel (A) for curves *e* and *f* appear to be the same, but these curves are different from those of *a* and *c*, and of *b* and *d*. The estimated β_1 term for curve *f*, -0.122, is somewhat different from the β_1 term of curve *c*, -0.1; the estimated β_2 term for curve *e*, -1.36, is somewhat different from the β_1 term of curve *b*, -2.0. The LD_{50} s for curves *e* and *f*, 1.42 and 15.8, respectively, are close to those of curves, *b* and *c*, 1.5 and 15, respectively. Curves *e* and *f* seem to attempt to closely follow the data from curves *b* and *c*, but fail, because the information contained in four parameters cannot be expressed completely by three parameters.

The advantages and disadvantages of fitting 3-D combined-action concentration-effect surfaces to proportion data are essentially the same as listed for continuous data. However, as seen with the experience of the multivariate linear logistic model, one must be very careful about choosing an appropriate combined-action model.

VII. Overall Conclusions on Rival Approaches

Tables 5 and 6 summarize the characteristics of the 13 rival approaches for assessing combined-action for continuous data, and the three rival approaches for assessing combined-action for quantal data, respectively. In addition, they also provide a condensed summary of the conclusions of each analysis. For the originators of the 13 approaches for continuous data, there is about an equal division between those who have Loewe additivity as their null reference model and those that have Bliss independence as their null reference model. Only the method of Steel and Peckham (1979) and the method of Chou and Talalay (1984) use additional models, Eq. 20 and Eq. 18, respectively, as integral null reference models for their approaches.

With today's universal accessibility to powerful, inexpensive computers with useful software, there is no good reason for an analysis of combined-action data to lack a graphical component. All of the methods that require graphics and advanced statistical procedures have either already been implemented into stand-alone software packages or are "easily" implemented with standard general statistical and graphical software.

At first glance, the conclusions of the authors of the 13 different approaches seem to be quite varied. However, the common continuous data set was simulated with Eq. 5 to contain a small degree of Loewe synergism (true $\alpha = 0.5$), which corresponds in most regions of the 3-D concentration-effect surface to a small degree of Bliss antagonism. Methods 1, 2, 4, 5, 8, and 10 through 12b yielded conclusions consistent with their respective "no interaction" reference models. This was also true for method 3, the method of Valeriote and Lin (1975), which further divides Bliss antagonism into three subcategories, including "subadditivity." In addition, because the true combined-action was between Loewe additivity and Bliss independence, ideal data would fall into the additivity envelope of method 6, that of Steel and Peckham (1979), and thus the conclusion of "additivity" for this approach is also consistent. The Bliss independence surface approach failed to detect the small amount of Bliss antagonism. Of the 13 different approaches, only the method of Chou and Talalay (1984) gave a conclusion opposite to the one expected, based on its respective null reference model(s). This is because of artifacts inherent in the calculation of the CI vs. fa plot.

The three approaches to the analysis of combined-action for quantal data listed in table 6 all share Loewe additivity as the null reference model. The method of Gessner (1974) is somewhat conservative and just missed the correct conclusion of a small degree of Loewe synergism. Not surprisingly, our flagship model that was used in the simulation of the common proportion data set, table 4, fit the data well, but just barely detected the small degree of synergism (true $\alpha = 1$), just above the noise level of the data. The multivariate linear logistic model arrived at the wrong conclusion, because it could not mold itself well to the data.

VIII. Experimental Design

The main decisions that must be made regarding experimental design are: (a) where to choose the concentrations, (b) numbers of replicates, and (c) numbers of experiments. These seemingly simple questions have spawned many full careers for statisticians, who have delved deeply into them to reveal their inherent complexity. The adoption of a response surface paradigm for the assessment of combined-action of agents facilitates the understanding of formal statistical experimental design. First, the experimenter must decide whether he is in an exploratory or a confirmatory mode. Screening experiments (exploratory mode) should first include, for each agent individually, agent concentrations that span the anticipated response region. Logarithmic spacing of the concentrations over a thousand-fold to a million-fold range is probably necessary, depending upon the previ-

TABLE 5
Comparison of conclusions from the application to the same simulated data set (representative example of continuous data from pure small synergism with 10% relative error), columns 2 through 4 of Table 3, of 13 rival approaches for assessing the nature and intensity of agent combined-action

Approach	Null "no" interaction* reference model*	Software availability†	Graphical approach?‡	"Advanced" statistical approach?‡	Long conclusion	Short conclusion§
1. Isobologram by hand	LADD	NN	N	N	No conclusion if IC_{50} values are used. Loewe synergism if IC_{50} values are used.	LSYN
2. Fractional Product method (Weibb, 1963)	BIND	NN	N	N	Overall Bliss antagonism, possible Bliss synergism at high concentrations.	BANT
3. Method of (Valeriote and Lin, 1975)	BIND	NN	N	N	Overall subadditivity, possible Bliss synergism at high concentrations.	SUB
4. Method of (Drewinko et al., 1976)	BIND	NN	N	N	Significant Bliss antagonism ($P < 0.05$).	BANT
5. Interaction index calculation (Berenbaum, 1978)	LADD	NN, YG	N	N	Overall Loewe synergism, possibly some Loewe antagonism.	LSYN
6. Method of Steel and Peckham (1979)	BIND, Eq. 20	YS	Y	N	Most of the combination points lie within the additivity envelope.	ADD
7. Median-effect method (Chou and Talalay, 1984)	LADD, Eq. 18	YS	Y	N	No conclusion on exclusivity. Strong Loewe antagonism, $f_A < 0.2$. Weak Loewe synergism, $f_A > 0.8$.	LANT and LSYN
8. Loewe Additivity surface method (Berenbaum, 1985)	LADD	YG	Y	Y	Overall Loewe synergism, with the intensity increasing at higher concentrations.	LSYN
9. Bliss independence surface method	BIND	YG	Y	Y	Overall Bliss independence.	BIND
10. MacSynergy (Prichard and Shipman, 1990)	BIND	YS	Y	N	Overall Bliss antagonism, possible small Bliss synergism at $D_1 = 5-10, D_2 = 1$.	BANT
11. 3-D Spline fitting, contours (Sühnel, 1990)	LADD	YG	Y	Y	Overall small Loewe synergism, possible Loewe antagonism at a few effect levels.	LSYN
12a. Parametric response surface approach (Greco et al., 1990)	LADD	YG	Y	Y	Small, but significant ($P < 0.05$) overall Loewe synergism, $\alpha = 0.518 \pm 0.11$.	LSYN
12b. Parametric response surface approach (Weinstein et al., 1990)	LADD	YS	Y	Y	Significant ($P < 0.05$) overall Loewe synergism.	LSYN

* The null reference abbreviations are: LADD (Loewe additivity), BIND (Bliss independence).

† The abbreviations are: NN (not needed), YS (yes, a specific software package is available), YG (yes, in general, the user must implement the approach with common statistical and/or graphical software packages).

‡ Advanced statistical approaches, which all require sophisticated numerical algorithms, include spline-fitting, nonlinear regression and maximum likelihood estimation.

§ The short conclusion abbreviations are: LSYN (Loewe synergism), BANT (Bliss antagonism), ADD (additivity) defined by Sicci and Peckham (1979), and SUB (subadditivity) defined by Valeriote and Lin (1975).

TABLE 6

Comparison of conclusions from the application to the same simulated data set (representative example of data from pure small synergism with binomial variation, Table 4), of three rival approaches for assessing the nature and intensity of agent combined-action

Approach	Null "no interaction" reference model*	Software availability	Graphical approach?	"Advanced" statistical approach	Long conclusion	Short conclusion
1. Method of (Gessner, 1974)	LADD	YS, YG	Y	N	Loewe additivity is claimed, but with a hint of small Loewe synergism.	LADD
2a. Parametric response surface approach (Greco and Lawrence, 1988)	LADD	YG	Y	Y	Small, borderline significant Loewe synergism ($P < 0.05$). $\alpha = 0.903 \pm 0.46$	LSYN
2b. Parametric response surface approach, multivariate logistic model (e.g., Carter et al, 1988)	LADD	YS	Y	Y	Significant Loewe antagonism ($P < 0.05$).	LANT

* The abbreviations used throughout Table 6 are the same as used in Table 5.

ous knowledge of the researcher about the concentration-effect behavior of the compound. After the individual agent concentration-effect curves are well characterized, a combination experiment should be conducted that repeats the single agent data points and which includes a set of combination points. Either a full factorial (checkerboard) design as suggested by Prichard and Shipman (1990), or a single ray (fixed-ratio) design, or a multiple ray design, all with logarithmically spaced concentrations, might be appropriate. If a complex 3-D concentration-effect surface is anticipated, then the entire interesting region of agent 1 and agent 2 concentrations should be sampled, either with a checkerboard or multiple ray design. However, if a well behaved 3-D concentration-effect surface is anticipated, and the specific combination being studied is only one of many candidates being screened, then a single ray may be sufficient. Composite designs consisting of a checkerboard and some rays might also be used. Of course, if the intended data analysis approach is firmly tied to a particular design, then that design will have to be used.

After the researcher has completed the analysis of the first mixture experiment in exploratory mode, he/she may want to switch to confirmatory mode. The repeat of the combination experiment may use the same design as in the exploratory experiment, but probably the knowledge gained from the first run will help to refine the design for the second run. If a complex 3-D concentration-effect surface was found in the exploratory experiment, then agent concentrations in the interesting regions of the surface should be accented in the confirmatory experiment. Increasing the numbers of replicates probably also will be necessary. If a simple 3-D concentration-effect surface was found in the exploratory experiment, i.e., one with pure Loewe synergism or Loewe antagonism, then a design that facilitates the estimation of parameters with the smallest variance might be appropriate. A single ray or a D-optimal design (Box and Lucas, 1959; Atkinson and Hunter, 1968; Silvey, 1980; Fedorov, 1972; Greco and Tung, 1991) might be indicated with many replicates.

There are many lettered-optimality criteria for experimental design. Atkinson and Donev (1992) present a recent comprehensive review. The D-optimality criterion has become popular for biological applications (e.g., Bezeau and Endrenyi, 1986; Greco et al., 1994). Reasons for its popularity include: (a) ease of application; (b) intuitiveness of its theoretical basis (For models nonlinear in the parameters, D-optimality minimizes the linear approximation of the volume of the joint confidence region of the parameters); (c) transformation of model parameters does not alter designs (Fedorov, 1972).

Interestingly, the number of design points in a D-optimal design is generally equal to the number of estimable parameters (Atkinson and Hunter, 1968). For example, if one assumes that Eq. 5, which contains 6 parameters, will adequately describe the 3-D combined-action concentration-effect curve, then a D-optimal design will include only six design points, with or without replicates. A description of our algorithms for calculating D-optimal designs for agent combination studies is included in Greco and Tung (1991) and Greco et al. (1993).

The D-optimal designs may, at first, seem to be very strange and potentially noninformative. For example, for the continuous common data set listed in table 2, which contains proportional error, the approximate D-optimal design based upon the ideal parameters ($Econ = 100$, $IC_{50,1} = 10$, $IC_{50,2} = 1$, $m_1 = -1$, $m_2 = -2$, $\alpha = 0.5$) is (point 1, $D_1 = 0$, $D_2 = 0$; point 2, $D_1 = 1,000$, $D_2 = 0$; point 3, $D_1 = 95$, $D_2 = 0$; point 4, $D_1 = 0$, $D_2 = 1,000$; point 5, $D_1 = 0$, $D_2 = 3.08$, point 6, $D_1 = 86.4$, $D_2 = 8.73$). This D-optimal design is only approximate because the assumption of pure proportional error (constant coefficient of variation) will drive many of the design points to unrealistic infinite concentrations (Bezeau and Endrenyi, 1986). We have reduced unrealistically large concentrations to 1000. Even with this adjustment, the D-optimal design still seems to be uninformative. (By visually plotting the six D-optimal design points in figure 25, the reader will note that one point is at the very top of the concentration-effect surface and that the other

five are at the bottom! None of the points lie in the middle region of the surface.) However, we have conducted Monte-Carlo simulations to verify that this type of D-optimal design results in the smallest variance for the six model parameters when compared with factorial and ray designs (Greco et al., 1994). We have also shown that the variance of the parameter estimates is approximately proportional to the reciprocal of the number of replicates. This type of frugal experimental design may have great potential for animal and human experiments, in which the experimental units are very dear.

The point at which the Loewe additivity model and the combined-action model are furthest apart in the vertical direction may be an important design point; this point may offer the maximum potential for discriminating between the two models (Mannervick, 1982). From figure 10(C), it was shown for our flagship model, with parameters ($E_{con} = 100$, $IC_{50,1} = 1$, $IC_{50,2} = 1$, $m_1 = -1$, $m_2 = -2$, $\alpha = 5$), that the largest vertical difference was near the point, ($IC_{50,1}$, $IC_{50,2}$). In contrast, figure 9 indicates that the largest horizontal difference between Loewe additivity and our combined-action model is at infinite concentrations of both agents. This implies that a pair of very large concentrations may be useful. These two design points, based upon maximum model differences, may be added to other designs discussed above.

Formal statistical experimental design often includes an interesting paradox: in order to design an experiment well, you have to know the final answer well. However, if you knew the final answer well, then you would not have to conduct the experiment. This paradox is solved with sequential experimentation; each experiment in a sequence provides better information for the planning of the subsequent experiment.

IX. General Proposed Paradigm

Readers of this review may not be particularly happy at this point. They may have become enlightened on the subject of combined-action after following the discussion of the different 3-D and 2-D representations of this phenomena. They may have carefully read the descriptions of the application of 13 rival approaches for assessing combined-action for continuous data, and of 3 rival approaches for quantal data. They may have digested and evaluated the long list of advantages and disadvantages of each approach. They may now have a greater appreciation of the similarities and differences among the rival approaches reviewed in this paper. Finally, they may have developed an understanding of the fundamental importance of mathematical models in the description and evaluation of complex systems. However, it is probably not at all clear how to actually proceed with the practical analysis of a data set from an experiment of combined-action.

We recommend the following general approach. Before the combined-action experiment is conducted, the

concentration-effect curves for the individual agents should be characterized well. Data for a combination experiment can then be generated from either a factorial design, from a fixed-ratio (ray) design, from a D-optimal design, from a model discrimination design, or some combination of the four. The numbers and distribution of different rows and columns in the factorial design, the numbers and distributions of rays in the fixed-ratio design, and the numbers of replicates, will depend upon the importance of the anticipated result, the cost of each experimental unit, and the degree of ignorance of the shape of the full 3-D concentration-effect surface.

The overall best initial data analysis, which will work with almost any conceivable, reasonable design, should include a combination of approaches V.H., the method of Berenbaum (1985), and V.I., the Bliss independence response surface approach. First, a logical Loewe additivity model should be fit, with an appropriate curve-fitting technique, to the data for agent 1 alone and agent 2 alone. Nonlinear regression should be used to fit models to continuous data, and maximum likelihood procedures used to fit models to quantal data. The 3-D Loewe additivity predicted surface should be shown in 3-D. Then sprinkle the raw data points on the same graph, and note the position of the points relative to the surface, such as was done in figure 18(A). Then construct the Bliss independence surface and sprinkle the raw data points, such as was done in figure 18(B). Combining Loewe additivity and Bliss independence surfaces on the same 3-D graph may be useful. Also, various 2-D representations of the 3-D surfaces, such as isobolograms, and families of 2-D concentration-effect curves, with accompanying data points, may be useful. A confidence envelope, adapted from suggestions of Carter et al. (1986, 1988), around the two surfaces might be used to discriminate between true departures from the null reference models and random variation. Note that our suggested approach has the flavor of the "additivity envelope" method of Steel and Peckham (1979), but the correct model for Loewe additivity is used to define one of the boundaries, instead of Eq. 20. Only in rare cases will it be difficult to find appropriate concentration-effect models to fit the concentration-effect data for the individual agents.

After this initial analysis, a decision should be made whether to derive and fit a full appropriate combined-action concentration-effect model to all of the experimental data simultaneously or to accept the initial analysis as the final answer. In many cases, it will be fruitful to complete this last step. The final summary statistics should include uncertainty measures around the final parameter estimates, confidence envelopes around the fitted surface, overall goodness of fit statistics, residual analyses, and sets of 3-D and 2-D graphs. These sets of graphs may include the 3-D combined-action concentration-effect surface along with the raw data, such as figure 22, 3-D difference plots such as figure 10, 3-D

combination index plots such as figure 9, 2-D isobolograms such as figure 23, 2-D families of concentration-effect curves, such as figures 24 and 25, plus any other informative graphical representations. Physical 3-D models of combined-action concentration-effect surfaces made with LEGO bricks (LEGO Systems Inc., Enfield, CT) (Greco, 1991) or other materials can accent important results.

To the best of our knowledge, a software package dedicated exclusively to this whole composite approach does not as yet exist. However, many general nonlinear regression packages, which allow the coding of a one-dimensional root finder for dealing with models in unclosed form, and with accompanying graphics capabilities, could be used to implement this approach. Such packages available for microcomputers include: PC-NONLIN (Statistical Consultants Inc., 1986), SAS (SAS Institute Inc., 1987), MLAB (Civilized Software, Inc., 1991), GAUSS (Aptech Systems Inc., 1991), and IMSL (IMSL, 1989). There are many more packages available for UNIX workstations, minicomputers, and mainframe computers with adequate capabilities to implement this full approach. Our group is currently developing an implementation of the full approach, which has been designed to work under the MicroSoft Windows operating system.

Several critical areas for future research and development in the field of the assessment of combined-action were pointed out in this review article:

(a) the relationship between empirical models of combined-action, and mechanistic theoretical models of biochemical and physiological systems should be explored.

(b) a library of combined-action models should be derived, collected, evaluated, and critically compared.

(c) the impact of using different experimental designs, especially D-optimal designs, should be evaluated, both from theoretical and practical perspectives.

(d) user-friendly, inexpensive computer software should be developed to facilitate the paradigm of experimental design and data analysis approaches described above.

X. Appendix A. Derivation of a Model for Two Mutually Nonexclusive Noncompetitive Inhibitors for a Second Order System

A. Motivation

The concepts of Bliss independence and mutual non-exclusivity, at first glance, seem to be the same. Equivalent general forms for the classical Bliss independence model are Eqs. 11 and 14, in which fu_1 , fu_2 , and fu_{12} are the fractions of possible response for drug 1, drug 2, and the combination (e.g., % survival, %control) unaffected (Chou and Talalay, 1981, 1984), and fa_1 , fa_2 , and fa_{12} are the fractions of possible response affected (e.g., % dead, % inhibition) [$fa(= 1 - fu)$]. For the common case in which each drug individually follows the Hill concentra-

tion-effect model, Eq. 2, (equivalent to the median-effect equation of Chou and Talalay, Eq. 24) the appropriate specific Bliss independence model would be Eq. 12 ($fu = E/Econ$).

$$fu_{12} = fu_1 fu_2 \quad [11]$$

$$fa_{12} = fa_1 + fa_2 - fa_1 fa_2 \quad [14]$$

$$E = \frac{Econ \left(\frac{D}{IC_{50}} \right)^m}{1 + \left(\frac{D}{IC_{50}} \right)^m} \quad [2]$$

$$\frac{fa}{fu} = \left(\frac{D}{Dm} \right)^m \quad [24]$$

$$E = \frac{Econ \left(\frac{D_1}{IC_{50,1}} \right)^{m_1} \left(\frac{D_2}{IC_{50,2}} \right)^{m_2}}{\left(1 + \left(\frac{D_1}{IC_{50,1}} \right)^{m_1} \right) \left(1 + \left(\frac{D_2}{IC_{50,2}} \right)^{m_2} \right)} \quad [12]$$

However, the mutually nonexclusive model of Chou and Talalay (1981, 1984), Eq. 18, is not equivalent to the Bliss independence model, except under the restrictive condition that the slope parameter, m , is equal to 1 (or to -1 by our convention of monotonically decreasing concentration-effect curves). Eq. 19 is a specific nonlinear form of Eq. 18. (Note that Eq. 19 is equivalent to our flagship interaction model, Eq. 5, with $m_1 = m_2 = m$, and $\alpha = 1$.) Chou and Talalay (1984) stressed this difference between the Bliss independence model and their mutually nonexclusive model and concluded that the Bliss independence model is not appropriate for higher order systems ($m > 1$).

$$\begin{aligned} \left(\frac{fa_{12}}{fu_{12}} \right)^{1/m} &= \left(\frac{fa_1}{fu_1} \right)^{1/m} + \left(\frac{fa_2}{fu_2} \right)^{1/m} + \left(\frac{fa_1 fa_2}{fu_1 fu_2} \right)^{1/m} \\ &= \frac{D_1}{Dm_1} + \frac{D_2}{Dm_2} + \frac{D_1 D_2}{Dm_1 Dm_2} \end{aligned} \quad [18]$$

$$E = \frac{Econ \left(\frac{D_1}{IC_{50,1}} + \frac{D_2}{IC_{50,2}} + \frac{D_1 D_2}{IC_{50,1} IC_{50,2}} \right)^m}{1 + \left(\frac{D_1}{IC_{50,1}} + \frac{D_2}{IC_{50,2}} + \frac{D_1 D_2}{IC_{50,1} IC_{50,2}} \right)^m} \quad [19]$$

We certainly agree that Eqs. 12 and 19 are not equivalent. It should be noted that the derivation of the mutually nonexclusive model (Chou and Talalay, 1981) was for multiple mutually nonexclusive reversible inhibitors of a single enzyme, in which the slope parameter, m , is the integral number of binding sites on the enzyme for each inhibitor, yet the application of the model has been mainly to much more complex systems, such as cell

cultures and batches of whole organisms, in which the nonintegral slope parameter, m , is related to the width of the tolerance distribution of the sensitivities of the cells or organisms to the agent. It might be argued that the difference between Eqs. 12 and 19 is caused by their differences in origin. However, we will show below that the primary reason that Bliss independence and mutually nonexclusivity are not equivalent is that the mutually nonexclusive model of Chou and Talalay (1981) was not properly derived.

B. Elements of the Derivation of the Mutually Nonexclusive Model for Higher Order Systems from Chou and Talalay (1981)

To keep confusion to a minimum, we will use \bar{f}_i and $\bar{f}v$ for the fractional inhibition and fractional velocity, respectively, which are slightly different from the variable symbols included in Chou and Talalay (1981). Also, instead of using Chou and Talalay's exact general equations for any number of enzyme inhibitors, we will list specific equations for sets of two inhibitors. We will designate Chou and Talalay's equations with a CT prefix, and use the equation number from Chou and Talalay (1981).

The key suspicious step in the derivation of the mutually nonexclusive model, Eq. CT22, appears on page 211 of Chou and Talalay (1981). It is stated:

Let us assume that m molecules of each of two mutually nonexclusive inhibitors bind to one molecule of enzyme. By analogy to Eqn (CT17) and addition of the term for nonexclusivity [Eqn(CT21)] we obtain:

$$\left[\frac{\bar{f}_{12}}{\bar{f}v_{12}} \right]^{1/m} = \left[\frac{\bar{f}_1}{\bar{f}v_1} \right]^{1/m} + \left[\frac{\bar{f}_2}{\bar{f}v_2} \right]^{1/m} + \left[\frac{\bar{f}_1 \bar{f}_2}{\bar{f}v_1 \bar{f}v_2} \right]^{1/m}$$

or

$$\bar{f}v_{12} = \frac{1}{1 + \left\{ \left[\frac{\bar{f}_1}{\bar{f}v_1} \right]^{1/m} + \left[\frac{\bar{f}_2}{\bar{f}v_2} \right]^{1/m} + \left[\frac{\bar{f}_1 \bar{f}_2}{\bar{f}v_1 \bar{f}v_2} \right]^{1/m} \right\}^m} \quad [\text{CT22}]$$

$$= \frac{1}{1 + \left[\frac{I_1}{I_{50,1}} + \frac{I_2}{I_{50,2}} + \frac{I_1 I_2}{I_{50,1} I_{50,2}} \right]^m}$$

It is our view that merely stating, "by analogy to Eqn(CT17) and addition of the term for nonexclusivity [Eqn(CT21)], we obtain" does not constitute a convincing derivation. Eq. CT17, or the equivalent, Eq. CT18, that for a mutually exclusive system was derived by combining Eq. CT11, the general equation for mutual exclusivity for multiple inhibitors in a first order system with Eq. CT12, the general median-effect or Hill equa-

tion for inhibition of higher order kinetic systems by a single inhibitor.

$$\frac{\bar{f}_{12}}{\bar{f}v_{12}} = \frac{\bar{f}_1}{\bar{f}v_1} + \frac{\bar{f}_2}{\bar{f}v_2} = \frac{I_1}{I_{50,1}} + \frac{I_2}{I_{50,2}} \quad [\text{CT11}]$$

$$\frac{\bar{f}_i}{\bar{f}v} = \left[\frac{I}{I_{50}} \right]^m \quad [\text{CT12}]$$

$$\frac{\bar{f}_{12}}{\bar{f}v_{12}} = \left[\frac{I_1}{I_{50,1}} + \frac{I_2}{I_{50,2}} \right]^m \quad [\text{CT17}]$$

which can be rewritten:

$$\bar{f}v_{12} = \frac{1}{1 + \left[\frac{I_1}{I_{50,1}} + \frac{I_2}{I_{50,2}} \right]^m} \quad [\text{CT18}]$$

Even for the derivation of Eq. CT17, that for mutual exclusivity, it is not entirely apparent to us how to properly combine Eqs. CT11 and CT12. However, via two other derivations not provided here, one based on enzyme kinetics and another based on the ideas of Benrenbaum (1985) and provided in Appendix A of Greco et al. (1990), we verified that Eq. CT17, that for mutual exclusivity, is correct.

Thus, the derivation of the mutually nonexclusive model for two enzyme inhibitors provided by Chou and Talalay (1981) is weak, incomplete, and suspicious. In order to settle the matter, we provide below a complete derivation for the case of two mutually nonexclusive, noncompetitive inhibitors of a single enzyme. We use the same restrictive assumption used by Chou and Talalay (1981) and also used in the derivation by Hill (1910) that, for each inhibitor, which has two identical binding sites on the enzyme, both of the two inhibitor molecules bind to the enzyme in one step. It should be emphasized that our goal is not to derive an alternate model for mutual nonexclusivity to be used by the biomedical community but rather to show that the Chou and Talalay model was not derived correctly. We therefore provide this one counterexample, for two mutually nonexclusive, noncompetitive inhibitors, to refute the general model for mutual nonexclusivity of Chou and Talalay (1981).

C. Assumptions of the Derivation of the Model for Mutual Nonexclusivity for Two Noncompetitive Higher Order Inhibitors

1. The enzyme (E) has one active site where one substrate molecule (S) may bind.
2. In addition to the active site for the substrate, there are two binding sites for inhibitor 1 and two other binding sites for inhibitor 2. Any occupation of an inhibitor site will prevent the substrate from being converted to product.

3. Both inhibitor 1 and 2 are noncompetitive with the substrate; 2 molecules of inhibitor 1 plus two molecules of inhibitor 2 may simultaneously bind to the enzyme, whether the substrate has occupied the active site or not.

4. The affinity of inhibitor 1 for the enzyme, and the affinity of inhibitor 2 for the enzyme, is unaffected by occupation of the active site by the substrate; thus, we have classical or pure noncompetitive inhibition.

5. The binding of inhibitor 1, I_1 , to its binding sites does not influence the binding of inhibitor 2, I_2 , to its binding sites, and vice versa.

6. When I_1 binds, two molecules bind at once; the same for I_2 . [This is the critical controversial Hill assumption, which was also made by Chou and Talalay (1981) in the derivation of the median effect equation for a single inhibitor.] In other words, the concentrations of enzyme species, E, ES, EI_1I_1 , EI_2I_2 , $EI_1I_1I_2I_2$, ESI_1I_1 , ESI_2I_2 , $ESI_1I_1I_2I_2$, exist; but EI_1 , EI_2 , ESI_1 , ESI_2 , EI_1I_2 , $EI_1I_2I_2$, $EI_1I_1I_2$, ESI_1I_2 , $ESI_1I_2I_2$, $ESI_1I_1I_2$ are negligible and will be assumed to not exist.

D. Derivation

1. The general rules for deriving enzyme kinetic rate equations from Segel (1975) are used.

2. The enzyme velocity (v) rate equation is written in terms of the rate constant for the formation of product (k_p) and the enzyme-substrate complex concentration ([ES]):

$$v = k_p[ES] \quad [A1]$$

3. The left side of the velocity equation is divided by the concentration of total enzyme, $[E_t]$, and the right side is divided by the equivalent sum of the concentrations of all non-negligible enzyme species: (Note: The denominators of Equations A2, A3 and A7 are too wide to fit easily into an equation in one column of a journal page. Therefore, each denominator has been defined by the terms, $DENOMA2$, $DENOMA3$, $DENOMA7$, respectively):

$$\begin{aligned} DENOMA2 = & [E] + [ES] + [EI_1I_1] + [EI_2I_2] + [EI_1I_1I_2I_2] \\ & + [ESI_1I_1] + [ESI_2I_2] + [ESI_1I_1I_2I_2] \end{aligned}$$

$$\frac{v}{[E_t]} = \frac{k_p[ES]}{DENOMA2} \quad [A2]$$

4. Concentrations of each species are expressed in terms of $[E]$. The term for any given complex is composed of a numerator and a denominator. The numerator is the product of the concentrations of all ligands in the complex. The denominator is the product of all dissociation constants between the complex and free enzyme, E.

Also, let the maximum enzyme velocity, $V_{max} = k_p [E_t]$.

$$\begin{aligned} DENOMA3 = & 1 + \left[\frac{S}{K_s} \right] + \left[\frac{I_1}{K_{I_1}} \right]^2 + \left[\frac{I_2}{K_{I_2}} \right]^2 + \left[\frac{I_1}{K_{I_1}} \right]^2 \left[\frac{I_2}{K_{I_2}} \right]^2 \\ & + \left[\frac{S}{K_s} \right] \left[\frac{I_1}{K_{I_1}} \right]^2 + \left[\frac{S}{K_s} \right] \left[\frac{I_2}{K_{I_2}} \right]^2 + \left[\frac{S}{K_s} \right] \left[\frac{I_1}{K_{I_1}} \right]^2 \left[\frac{I_2}{K_{I_2}} \right]^2 \end{aligned}$$

$$\frac{v}{V_{max}} = \frac{S/K_s}{DENOMA3} \quad [A3]$$

5. For a noncompetitive inhibitor, $I_{50} = K_i$ (Chou, 1974). Therefore, all K_i s are replaced with I_{50} s. In addition, Eq. A3 is simplified to Eq. A4.

$$v = \frac{V_{max}[S/K_s]/[1 + S/K_s]}{1 + \left[\frac{I_1}{I_{50,1}} \right]^2 + \left[\frac{I_2}{I_{50,2}} \right]^2 + \left[\frac{I_1}{I_{50,1}} \right]^2 \left[\frac{I_2}{I_{50,2}} \right]^2} \quad [A4]$$

6. The fractional velocity, fv , is equal to the ratio of the inhibited velocity, Eq. A4, divided by the uninhibited velocity, equal to $[V_{max} S]/[K_s + S]$. After this operation and some simplification, Eq. A5 is the result.

$$fv = \frac{1}{1 + \left[\frac{I_1}{I_{50,1}} \right]^2 + \left[\frac{I_2}{I_{50,2}} \right]^2 + \left[\frac{I_1}{I_{50,1}} \right]^2 \left[\frac{I_2}{I_{50,2}} \right]^2} \quad [A5]$$

Eq. A5 can be written in an equivalent form, Eq. A6.

$$fv = \left\{ \frac{1}{1 + \left[\frac{I_1}{I_{50,1}} \right]^2} \right\} \left\{ \frac{1}{1 + \left[\frac{I_2}{I_{50,2}} \right]^2} \right\} \quad [A6]$$

7. Note that Eq. A5 is not equivalent to the mutually nonexclusive model of Chou and Talalay (1981) for the case of second order inhibitors ($m = 2$). Rather, Eq. A5 and its equivalent, Eq. A6 is exactly equivalent to the Bliss independence model, Eq. 11, for two second order inhibitors. Thus, a complete specific derivation for the case of two mutually nonexclusive, second order, non-competitive enzyme inhibitors, which follows the general but incomplete derivation provided by Chou and Talalay (1981), yields an equation inconsistent with their final model, Eq. CT22, but consistent with the Bliss independence model, Eq. 11.

E. Possible Rationalization of the Mutually Nonexclusive Model of Chou and Talalay (1981)

1. The expansion of the mutually nonexclusive model of Chou and Talalay (1981), Eq. CT22, for the case of

$m = 2$, yields Eq. A7.

$$DENOMA7 = 1 + \left[\frac{I_1}{I_{50,1}} \right]^2 + \left[\frac{I_2}{I_{50,2}} \right]^2 + \left[\frac{I_1}{I_{50,1}} \right]^2 \left[\frac{I_2}{I_{50,2}} \right]^2 + 2 \left[\frac{I_1}{I_{50,1}} \right] \left[\frac{I_2}{I_{50,2}} \right] + 2 \left[\frac{I_1}{I_{50,1}} \right]^2 \left[\frac{I_2}{I_{50,2}} \right] + 2 \left[\frac{I_1}{I_{50,1}} \right] \left[\frac{I_2}{I_{50,2}} \right]^2$$

$$fu = \frac{1}{DENOMA7} \quad [A7]$$

2. The difference between this expansion of the mutually nonexclusive model of Chou and Talalay (1981), Eq. A7, and the mutually nonexclusive model derived above, Eq. A5, which is equivalent to Bliss independence, is the additional three right-hand terms in the denominator. These three terms imply the existence of six additional enzyme species— $2 EI_1I_2$, $2 EI_1I_2I_2$, $2 EI_1I_1I_2$, $2 ESI_1I_2$, $2 ESI_1I_2I_2$, and $2 ESI_1I_1I_2$ —that we initially assumed were negligible and did not exist. This stems from the key Hill assumption that when and if an inhibitor binds, either I_1 or I_2 , two molecules of that inhibitor bind at once. Possibly, one might be willing to get rid of this assumption, and replace it with a less restrictive assumption such as:

EI_1 , EI_2 , ESI_1 , ESI_2 are all negligible, but enzyme forms that contain at least two inhibitor molecules, possibly a mixture of the two inhibitors, including EI_1I_2 , $EI_1I_2I_2$, $EI_1I_1I_2$, ESI_1I_2 , $ESI_1I_2I_2$, and $ESI_1I_1I_2$, are not negligible.

If so, then the mutually nonexclusive model of Chou and Talalay (1981) would have a firmer theoretical basis. However, it is unlikely that an equation derived from a set of very unusual assumptions, for the rare case of two mutually nonexclusive higher order inhibitors of a single enzyme, would have general utility for modeling concentration-effect phenomena from a wide spectrum of complex agent interaction systems.

XI. Appendix B: Problems with the Use of the Median Effect Plot and Combination Index Calculations to Assess Drug Interactions

Both the inherent nonlinear nature of the median effect plot and the incorrect calculation of the combination index (CI), for the case of mutual nonexclusivity, contribute to incorrect artifactual conclusions concerning synergism and antagonism, when applying the method of Chou and Talalay (1984) to real laboratory data. In addition, the median effect plot for drug combination data for mutually exclusive drugs showing synergism or antagonism will also be nonlinear. The extent, origins, and impact of these problems are illustrated by the simulation shown in figures B1, B2, B3, in table B1, and the following narrative.

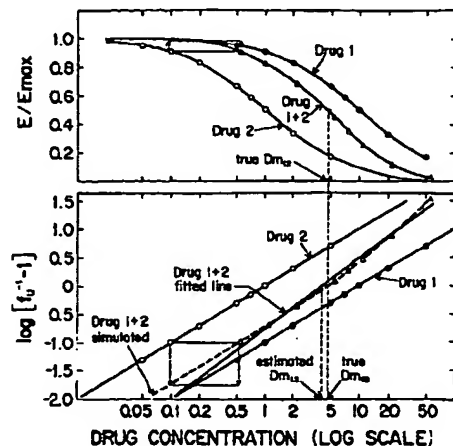


FIG. B1. Upper panel: Data points plotted from table B1. The data points and the curves connecting the points were simulated using Eq. B1, that for mutual nonexclusivity, with $Dm_1 = 10$, $Dm_2 = 1$, $m_1 = 1$, and $R = 10$. The Y-axis is $E/Emax$ or fu ; the X-axis is the sum of drug 1 and drug 2 concentrations on a logarithmic scale. Lower panel: The three median-effect lines were made by separately fitting each of the three subsets of data with unweighted linear regression. The curved, dashed line is the median-effect curve for the combination of drug 1 + 2 simulated from Eq. B1. The rectangular boxes in each panel represent equivalent ranges of fractional effect. The arrows on the side of the boxes indicate the direction of decreasing fu (increasing fu).

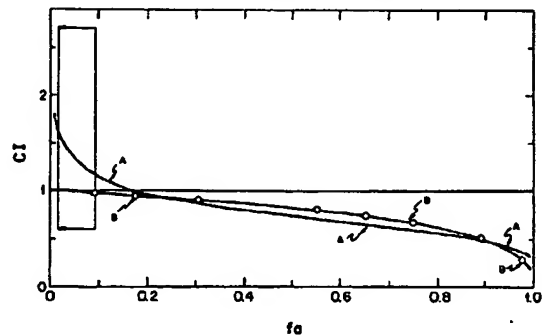


FIG. B3. Mutually exclusive CI vs. fu plots for the data from table B1 and figure B1. Curve A was generated in the exact way suggested by Chou and Talalay (1984) and included in the commercially available program (Chou and Chou, 1987), i.e., by estimating Dm_1 , m_1 , Dm_2 , m_2 , Dm_{12} , m_{12} with unweighted linear regression as in the lower panel of figure B1, and then plugging these values into Eq. 25 to calculate CI for a range of fu values. Curve B was generated by calculating Dm_{12} and m_{12} with Eqs. B2 through B4, from the original (same as estimated) values, $Dm_1 = 10$, $Dm_2 = 1$, $m_1 = m_2 = 1$, and then plugging these values into Eq. 25. The box represents a range of fractional effects equivalent to the boxes in figure B1, with the arrows of the box indicating the direction of decreasing fu . The open data points represent the eight combination points, each calculated with the CI formula for the mutually exclusive assumption for the raw data itself, Eq. 27.

A. Nonlinear Nature of the Median Effect Plot for Mutual Nonexclusivity

The median effect plot for mutually nonexclusive drugs is inherently nonlinear. This was shown originally by Chou and Talalay (1981) in figure 2 of their paper. Therefore, the estimation of Dm_{12} and m_{12} via simple linear regression can never be correct. The data points in

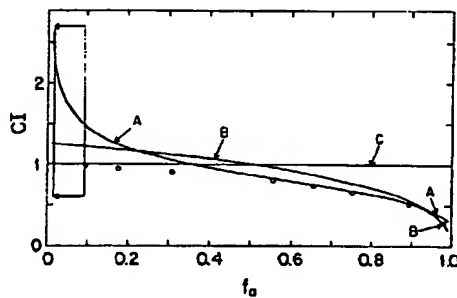


FIG. B2. Mutually nonexclusive CI vs. fa plots for the data from table B1 and figure B1. Curve A was generated in the exact way suggested by Chou and Talalay (1984) and included in the commercially available program (Chou and Chou, 1987); i.e., by estimating Dm_1 , m_1 , Dm_2 , m_2 , Dm_{12} , m_{12} with unweighted linear regression as in the lower panel of figure B1, and then plugging these values into Eq. 26 to calculate CI for a range of fa values. Curve B was generated by calculating Dm_{12} and m_{12} with Eqs. B2 through B4, from the original (same as estimated) values, $Dm_1 = 10$, $Dm_2 = 1$, $m_1 = m_2 = 1$, and then plugging these values into Eq. 26. Curve C, $CI = 1$, was generated by calculating Dm_{12} and m_{12} with Eqs. B2 through B4, but then using Eq. B5 for the CI calculation. The box represents a range of fractional effects equivalent to the boxes in figure B1, with the arrows of the box indicating the direction of decreasing fa . The open data points represent the eight combination points, each calculated with the CI formula for the mutually exclusive assumption for the raw data itself, Eq. 27.

figure B1 and table B1 were simulated by using Eq. B1, that for mutual nonexclusivity, and using $Dm_1 = 10$, $Dm_2 = 1$, $m = 1$, and $R = 10$. (Here, R is the ratio of concentrations of D_1 : D_2). The data consists of 24 simulated data points, 8 for drug 1 alone, 8 for drug 2 alone, and 8 for the combination of drug 1+2 in a 10:1 constant ratio. Four significant figures were retained through all calculations to eliminate any appreciable errors in the simulated data.

$$\left[\frac{fa_{12}}{fa_{12}} \right]^{1/m} = \left[\frac{1}{fa_{12}} - 1 \right]^{1/m} = \frac{D_1}{Dm_1} + \frac{D_2}{Dm_2} + \frac{D_1 D_2}{Dm_1 Dm_2} \quad [B1]$$

In the upper panel of figure B1, the three concentration-effect curves were simulated directly with Eq. B1. The data points in figure B1 correspond to the 24 simulated points in table B1. In the lower panel, the three median effect straight lines were made by separately fitting each of the three sets of data with unweighted linear regression. The curved, dashed line is the nonlinear median effect curve for the combination of drug 1+2 simulated from Eq. B1. The rectangular boxes in each panel represent equivalent ranges of effect. The arrows on the sides of the boxes indicate the direction of decreasing fa (from $fa = 0.091$ to 0.017). The parameters estimated from the three linear regression lines were: $Dm_1 = 10.0$, $m_1 = 1.00$, $Dm_2 = 1.00$, $m_2 = 1.00$, $Dm_{12} = 4.04$, $m_{12} = 1.24$. The correct Dm_{12} calculated from Eq. B2 was 4.56. The correct m_{12} calculated from Eqs. B3 and B4, which are fa -dependent, increased from 1.04 at $fa = 0.01$ to 1.49 at $fa = 0.99$. (The derivations of Eqs. B2 through

B4, for the restricted case of $m_1 = m_2 = m$, are not included here but can be requested from W. R. Greco.) Note the vertical dashed line in figure B1, which shows the alignment of the true Dm_{12} value. Also note the small displacement of the estimated Dm_{12} value from the true Dm_{12} . It is the approximation of the varying m_{12} by a constant m_{12} estimated from the median effect linear regression, which is responsible for most of the mismatch between the true median effect nonlinear curve and the approximate straight line. (Note: The numerators of Equations B2 and B4 are too wide to fit easily into an equation in one column of a journal page. Therefore, each numerator has been defined by the terms $NUMB2$ and $NUMB4$, respectively):

$$NUMB2 = - \left[\frac{RDm_2 + Dm_1}{(1+R)Dm_1 Dm_2} \right] + \sqrt{\left[\frac{RDm_2 + Dm_1}{(1+R)Dm_1 Dm_2} \right]^2 + \left[\frac{4R}{(1+R)^2 Dm_1 Dm_2} \right]}$$

$$Dm_{12} = \frac{NUMB2}{\frac{2R}{(1+R)^2 Dm_1 Dm_2}} \quad [B2]$$

$$m_{12} = \frac{m \log \left[\frac{[RDm_2 + Dm_1]Z + RZ^2}{Dm_1 Dm_2} \right]}{\log \left[\frac{Z(1+R)}{Dm_{12}} \right]} \quad [B3]$$

where:

$$NUMB4 = \left[\frac{RDm_2 + Dm_1}{Dm_1 Dm_2} \right] + \sqrt{\left[\frac{RDm_2 + Dm_1}{Dm_1 Dm_2} \right]^2 + \left[\frac{4R}{Dm_1 Dm_2} \right] \left[\frac{fa_{12}}{1-fa_{12}} \right]^{1/m}}$$

$$Z = \frac{NUMB4}{-2 \left[\frac{R}{Dm_1 Dm_2} \right]} \quad [B4]$$

Figure B2 is a mutually nonexclusive CI vs. fa plot for the data in table B1 and figure B1. Curve A in figure B2 was calculated as suggested by Chou and Talalay (1984), from the three straight median effect lines in figure B1, using the formula, Eq. 26, incorporated into the commercial software package, Dose-Effect Analysis with Microcomputers (Chou and Chou, 1987). The interested reader should be able to reproduce this curve by plugging the 24 data points listed in table B1 into the commercial software package. Like many real examples from the literature, the standard CI vs. fa plot, curve A, crosses the additivity, $CI = 1$ line. The conclusion from

TABLE B1
Simulated data for mutual nonexclusivity examination*

D_1	D_2	fu	fa	$\log(fu^{-1} - 1)$
0.5	0	0.9524	0.04762	-1.301
1	0	0.9091	0.09091	-1.000
2	0	0.8333	0.1667	-0.6989
5	0	0.6667	0.3333	-0.3011
7	0	0.5882	0.4118	-0.1548
10	0	0.5000	0.5000	0.0000
20	0	0.3333	0.6667	0.3011
50	0	0.1667	0.8333	0.6989
0	0.05	0.9524	0.04762	-1.301
0	0.1	0.9091	0.09091	-1.000
0	0.2	0.8333	0.1667	-0.6989
0	0.5	0.6667	0.3333	-0.3011
0	0.7	0.5882	0.4118	-0.1548
0	1	0.5000	0.5000	0.0000
0	2	0.3333	0.6667	0.3011
0	5	0.1667	0.8333	0.6989
0.5	0.05	0.9070	0.0930	-0.9891
1	0.1	0.8264	0.1736	-0.6776
2	0.2	0.6944	0.3056	-0.3565
5	0.5	0.4444	0.5556	0.09699
7	0.7	0.3460	0.6540	0.2765
10	1	0.2500	0.7500	0.4771
20	2	0.1111	0.8889	0.9031
50	5	0.02778	0.9722	1.544

* The data was simulated using Eq. B1, that for mutual nonexclusivity, with $Dm_1 = 10$, $Dm_2 = 1$, $m = 1$, and $R = 10$. This is an ideal data set with no random errors added; any inexactness is caused by roundoff errors in the fourth significant figure.

Curve A is appreciable antagonism at low fractional effects and appreciable synergism at high fractional effects. However, the data in table B1 was simulated for pure, unadulterated, mutual nonexclusivity! The final CI vs. fa plot should be a straight, horizontal line at $CI = 1$! Note the large box on the left-hand side of figure B2. This is the same box as was shown in figure B1, upper and lower panel, for a range of concentration-effect, except that its height has been magnified in the CI vs. fa plot. Thus, the difference between the true nonlinear median effect curve, and the approximate median effect straight line, has been magnified in the CI vs. fa plot.

$$CI = \frac{Dm_{12} \left[\frac{R}{R+1} \left[\frac{fa}{1-fa} \right]^{1/m_{12}} \right]}{Dm_1 \left[\frac{fa}{1-fa} \right]^{1/m_1}} + \frac{Dm_{12} \left[\frac{1}{R+1} \left[\frac{fa}{1-fa} \right]^{1/m_{12}} \right]}{Dm_2 \left[\frac{fa}{1-fa} \right]^{1/m_2}} \quad [26]$$

$$+ \frac{Dm_{12}^2 \left[\frac{R}{(R+1)^2} \left[\frac{fa}{1-fa} \right]^{2/m_{12}} \right]}{Dm_1 Dm_2 \left[\frac{fa}{1-fa} \right]^{1/m_1} \left[\frac{fa}{1-fa} \right]^{1/m_2}}$$

Curve B in figure B2 was generated with Eq. B5, but with the correct values for Dm_{12} and m_{12} as calculated from Eqs. B2 through B4. Curve B is closer to the target, $CI = 1$ line, but there remains a problem.

B. Incorrect Combination Index Calculations for the Mutually Nonexclusive Case

Eq. 26, that suggested by Chou and Talalay (1984) and incorporated into the commercial software (Chou and Chou, 1987), is slightly wrong. This is shown by the difference between curve B in figure B2 and the $CI = 1$ line. By using a rational trial-and-error strategy, we discovered the correct form of the CI vs. fa equation for the mutually nonexclusive case for the restricted case of $m = m_1 = m_2$, Eq. B5 (Syracuse and Greco, 1986). An equivalent form of Eq. B5 has also been recently published by Lam et al. (1991). When Eq. B5 is used with the correct values of Dm_{12} and m_{12} , curve C results, the correct $CI = 1$ line.

$$CI = \frac{Dm_{12} \left[\frac{R}{R+1} \left[\frac{fa}{1-fa} \right]^{1/m_{12}} \right]}{Dm_1 \left[\frac{fa}{1-fa} \right]^{1/m_1}} + \frac{Dm_{12} \left[\frac{1}{R+1} \left[\frac{fa}{1-fa} \right]^{1/m_{12}} \right]}{Dm_2 \left[\frac{fa}{1-fa} \right]^{1/m_2}} \quad [B5]$$

$$+ \frac{Dm_{12}^2 \left[\frac{R}{(R+1)^2} \left[\frac{fa}{1-fa} \right]^{2/m_{12}} \right]}{Dm_1 Dm_2 \left[\frac{fa}{1-fa} \right]^{1/m}}$$

C. Nonlinear Nature of the Median Effect Plot for Mutual Exclusivity with Interaction

Because of the many problems inherent with assuming a mutually nonexclusive model, one might prefer to assume a mutually exclusive model for all experimental data, including cases in which a median effect analysis shows that $m_1 = m_2 \neq m_{12}$. Combination plots generated with Eq. 25, that for mutual exclusivity (Chou and Talalay, 1984), are presented in figure B3.

$$CI = \frac{Dm_{12} \left[\frac{R}{R+1} \left[\frac{fa}{1-fa} \right]^{1/m_{12}} \right]}{Dm_1 \left[\frac{fa}{1-fa} \right]^{1/m_1}} + \frac{Dm_{12} \left[\frac{1}{R+1} \left[\frac{fa}{1-fa} \right]^{1/m_{12}} \right]}{Dm_2 \left[\frac{fa}{1-fa} \right]^{1/m_2}} \quad [25]$$

Curve A is the CI calculated exactly as suggested by Chou and Talalay (1984), and is the result that one would find using the commercial software (Chou and Chou, 1987) with the data in table B1. To generate curve A, Eq. 25 was used with the six parameter estimates derived from the three median effect lines of figure B1. As with the mutually nonexclusive assumption, the mutually exclusive assumption still shows an initial incorrect antagonism because of the incorrect linear extrapolation of the inherently nonlinear median effect curve for the drug combination. Curve B was also generated with Eq. 25, but with the correct values for Dm_{12} ($= 4.56$) and m_{12} (1.04 to 1.49). Curve B does portray the correct situation; i.e., synergism along the entire range

of *fa* (with reference to the mutually exclusive model). However, because the method of Chou and Talalay (1984) does not include a reliable method to estimate Dm_{12} and m_{12} from the inherently nonlinear median effect plot for drug combinations, a useful *CI* vs. *fa* plot, such as curve B, is not readily generated.

The eight open points in figure B3 (and in figure B2) are the eight combination data points from table B1, directly plotted without the estimation of Dm_{12} and m_{12} . Instead, the raw data were plugged into Eq. 27, which depends only on the individual drug parameters, Dm_1 , m_1 , Dm_2 , and m_2 , to calculate *CI*. This approach has been discussed (Chou, 1991a), but to the best of our knowledge, is not as yet available in the commercial software (as of January, 1994).

$$CI = \frac{D_1}{Dm_1 \left[\frac{fa}{1-fa} \right]^{1/m_1}} + \frac{D_2}{Dm_2 \left[\frac{fa}{1-fa} \right]^{1/m_2}} \quad [27]$$

Acknowledgements. We wish to thank many scientists for stimulating discussions and arguments that eventually led to this review. These scientists include: Morris Berenbaum, Ting-Chao Chou, Mark Prichard, Stella Machado, Peter Gessner, Jürgen Sühnel, Hans-Dieter Unkelbach, Gerald Pöch, John Weinstein, W. Hans Carter, Chris Gennings, Wolfgang Bödeker, Michael Kundi, Robert Jackson, and Leonid Khinkis.

REFERENCES

AMTEC ENGINEERING, INC.: (1989). Tecplot, Version 5, User's Manual [computer program manual]. Bellevue, WA: Amtec Engineering, Inc.

AMTEC SYSTEMS, INC.: (1991). The GAUSS System, version 3.0 [computer program]. Maple Valley, WA: Aptech Systems, Inc.

ASHFORD, J. R.: General models for the joint action of mixtures of drugs. *Biometrics* 37: 457-474, 1981.

ASHFORD, J. R., AND SMITH, C. S.: General models for quantal response to the joint action of a mixture of drugs. *Biometrika* 51: 413-428, 1964.

ATKINSON, A. C., AND DONEV, A. N.: Optimum Experimental Designs, Oxford University Press, Oxford, UK, 1992.

ATKINSON, A. C., AND HUNTER, W. G.: Optimal design: experiments for parameter estimation. *Technometrics* 10: 271-289, 1968.

BATES, D. M., AND WATTS, D. G.: Nonlinear Regression Analysis and Its Applications, John Wiley & Sons, New York, 1988.

BAUMGART, J., SCHLÖTT, B., SURHNEL, J., VATER, W., SCHULZE, W., AND BEHNKE, D.: Synergistic cytotoxicity of human recombinant tumour necrosis factor α combined with microtubule effectors. *J. Cancer Res. Clin. Oncol.* 117: 239-243, 1991.

BELENKII, M. S., AND SCHINAZI, R. F.: Multiple drug effect analysis with confidence interval. *Antiviral Res.* 25: 1-11, 1994.

BERENBAUM, M. C.: Synergy, additivity and antagonism in immunosuppression. *Clin. Exp. Immunol.* 28: 1-18, 1977.

BERENBAUM, M. C.: A method for testing for synergy with any number of agents. *J. Infect. Dis.* 137: 122-130, 1978.

BERENBAUM, M. C.: Criteria for analysing interactions between biologically active agents. *Adv. Cancer Res.* 35: 269-335, 1981.

BERENBAUM, M. C.: The expected effect of a combination of agents: the general solution. *J. Theor. Biol.* 114: 413-431, 1985.

BERENBAUM, M. C.: Isobolographic, algebraic, and search methods in the analysis of multagent synergy. *J. Am. Coll. Toxicol.* 7: 927-938, 1988.

BERENBAUM, M. C.: What is synergy? *Pharmacol. Rev.* 41: 93-141, 1989.

BEZEAU, M., AND ENDRENYI, L.: Design of experiments for the precise estimation of dose-response parameters: the Hill equation. *J. Theor. Biol.* 123: 415-430, 1986.

BLISS, C. I.: The toxicity of poisons applied jointly. *Ann. Appl. Biol.* 26: 585-615, 1939.

BOX, G. E. P., AND DRAPER, N. R.: Empirical Model-Building and Response Surfaces, p. 1, John Wiley & Sons, New York, 1987.

BOX, G. E. P., AND LUCAS, H. L.: Design of experiments in nonlinear situations. *Biometrika* 46: 77-90, 1959.

BOX, G. E. P., AND MÜLLER, M. E.: A note on the generation of normal deviates. *Annals of Mathematical Statistics* 29: 610-611, 1958.

BRAVO, G., JACKSON, R. C., PLURAD, D. A., AND GRECO, W. R.: Comparison of theoretical and empirical mathematical models of the biochemical effects of combinations of anticancer agents. *Proc. Am. Assoc. Cancer Res.* 33: 439-439, 1992.

BRUNDEN, M. N., VIDMAR, T. J., AND MCKEAN, J. W.: Drug Interaction and Lethality Analysis, CRC Press, Boca Raton, FL, 1988.

BUNOW, B., AND WEINSTEIN, J. N.: COMBO: A new approach to the analysis of drug combinations in vitro. *Annals of the New York Academy of Sciences* 616: 490-494, 1990.

CALABRESE, E. J.: Multiple Chemical Interactions, Lewis Publishers, Chelsea, MI, 1991.

CARTER, W. H., JR., CHINCHILLI, V. M., WILSON, J. D., CAMPBELL, E. D., KESSLER, F. K., AND CARCHMAN, R. A.: An asymptotic confidence region for the ED100p from the logistic response surface for a combination of agents. *American Statistician* 40: 124-128, 1986.

CARTER, W. H., JR., GENNINGS, C., STANISWALIS, J. G., CAMPBELL, E. D., AND WHITE, K. L., JR.: A statistical approach to the construction and analysis of isobolograms. *J. Am. Coll. Toxicol.* 7: 963-973, 1988.

CARTER, W. H., JR., WAMPLER, G. L., AND STABLEIN, D. M.: Regression Analysis of Survival Data in Cancer Chemotherapy, Marcel Dekker, New York, 1983.

CHOU, J., AND CHOU, T. C.: Dose-Effect Analysis with Microcomputers, Elsevier Science Publishers BV, Amsterdam, 1987.

CHOU, J. H.: Quantitation of synergism and antagonism of two or more drugs by computerized analysis. In *Synergism and Antagonism in Chemotherapy*, ed. by T.-C. Chou and D. C. Rideout, pp. 223-241, Academic Press, New York, 1991b.

CHOU, T.-C.: Relationships between inhibition constants and fractional inhibitions in enzyme-catalyzed reactions with different numbers of reactants, different reaction mechanisms, and different types of mechanisms of inhibition. *Mol. Pharmacol.* 10: 235-247, 1974.

CHOU, T.-C.: The median-effect principle and the combination index for quantitation of synergism and antagonism. In *Synergism and Antagonism in Chemotherapy*, ed. by T.-C. Chou and D. C. Rideout, pp. 61-102, Academic Press, New York, 1991a.

CHOU, T.-C., AND RIDEOUT, D. C.: Synergism and Antagonism in Chemotherapy, Academic Press, New York, 1991.

CHOU, T. C., AND TALALAY, P.: Generalized equations for the analysis of inhibitions of Michaelis-Menten and higher order kinetic systems with two or more mutually exclusive and nonexclusive inhibitors. *Eur. J. Biochem.* 115: 207-216, 1981.

CHOU, T. C., AND TALALAY, P.: Analysis of combined drug effects: a new look at a very old problem. *Trends Pharmacol. Sci.* 4: 450-454, 1983.

CHOU, T. C., AND TALALAY, P.: Quantitative analysis of dose-effect relationships: the combined effects of multiple drugs or enzyme inhibitors. *Adv. Enzyme Regul.* 22: 27-55, 1984.

CIVILIZED SOFTWARE, INC.: (1991). MATLAB: Mathematical Modeling System User's Manual [computer program manual]. Bethesda, MD: Civilized Software, Inc.

COPENHAVER, T. W., LIN, T.-L., AND GOLDBERG, K. M.: Joint drug action: a review. American Statistical Association, Proceedings of the Biopharmaceutical Section 160-164, 1987.

COX, D. R.: The Analysis of Binary Data, Methuen, London, 1970.

DEEN, D. F., AND WILLIAMS, M. E.: Isobogram analysis of X-ray-BCNU interactions in vitro. *Radiat. Res.* 79: 483-491, 1979.

DEVITA, V. T., JR.: Principles of chemotherapy. In *Cancer Principles and Practice of Oncology*, ed. by V. T. DeVita, Jr., S. Hellman, and S. A. Rosenberg, pp. 276-300, J. B. Lippincott, Philadelphia, 1989.

DIXON, W. J., BROWN, M. B., ENGELMAN, L., AND JENNICH, R. I.: (1990). BMDP Statistical Software Manual, vol. 2, pp. 1013-1046 [computer program manual]. Berkeley, CA: University of California Press.

DRYWINKO, B., LOO, T. L., BROWN, B., GOTTLIEB, J. A., AND FREIREICH, E. J.: Combination chemotherapy in vitro with adriamycin. Observations of additive, antagonistic, and synergistic effects when used in two-drug combinations on cultured human lymphoma cells. *Cancer Biochem. Biophys.* 1: 187-195, 1976.

ELION, G. B., SINGER, S., AND HITCHINGS, G. H.: Antagonists of nucleic acid derivatives: Part VIII. Synergism in combinations of biochemically related antimetabolites. *J. Biol. Chem.* 208: 477-488, 1954.

ERIKSSON, B. F. H., AND SCHINAZI, R. F.: Combinations of 3'-azido-3'-deoxythymidine (zidovudine) and phosphonofomate (foscarnet) against human immunodeficiency virus type 1 and cytomegalovirus replication in vitro. *Antimicrob. Agents Chemother.* 33: 663-669, 1989.

FEDOROV, V. V.: Theory of Optimal Experiments, Academic Press, New York, 1972.

FINNEY, D. J.: Probit Analysis, 2nd ed., pp. 122-159, Cambridge University Press, Cambridge, UK, 1952.

FINNEY, D. J.: Probit Analysis, 3rd ed., pp. 230-268, Cambridge University Press, Cambridge, UK, 1971.

FRASER, T. R.: An experimental research on the antagonism between the actions of physostigmine and atropine. *Proc. R. Soc. Edinb.* 7: 506-511, 1870-1871.

FRASER, T. R.: The antagonism between the actions of active substances. *Br. Med. J.* 2: 485-487, 1872.

FREI, W.: Versuche über Kombination von Desinfektionsmitteln. *Z. Hyg. Infektionskr.* 75: 433-496, 1913.

GAUMONT, Y., KISLIUK, R. L., PARSONS, J. C., AND GRECO, W. R.: Quantitation of folic acid enhancement of antifolate synergism. *Cancer Res.* 52: 2228-2235, 1992.

GENNINGS, C.: An efficient experimental design for detecting departure from additivity in mixtures of many chemicals. (accepted) *Toxicology*, 1996.

GENNINGS, C., CARTER, W. H., JR., CAMPBELL, E. D., STANISWALIS, J. G., MARTIN, T. J., MARTIN, B. R., AND WHITE, K. L., JR.: Isobolographic characterization of drug interactions incorporating biological variability. *J. Pharmacol. Exp. Ther.* 252: 208-217, 1990.

GESNER, P. K.: The isobolographic method applied to drug interactions. In *Drug Interactions*, ed. by P. L. Morselli, S. Garattini, and S. N. Cohen, pp. 349-362, Raven Press, New York, 1974.

GESNER, P. K.: A straightforward method for the study of drug interactions: an isobolographic analysis primer. *J. Am. Coll. Toxicol.* 7: 987-1012, 1988.

GRECO, W. R.: Importance of the structural component of generalized nonlinear models for joint drug action. American Statistical Association, Proceedings of the Biopharmaceutical Section 183-188, 1989.

GRECO, W. R.: The use of LEGO bricks to construct solid 3-dimensional dose-response surfaces. In *Proceedings of the 23rd Symposium on the Interface of Computing Science and Statistics: Interface '91*, 326-331, 1991.

GRECO, W. R., AND DEMBINSKI, W. E.: Fundamental concepts in the assessment of the joint interaction of biological response modifiers with other agents. *Can. J. Infectious Dis.* 3 (suppl B): 60B-68B, 1992.

GRECO, W. R., AND LAWRENCE, D. L.: Assessment of the degree of drug interaction where the response is discrete. American Statistical Association, Proceedings of the Biopharmaceutical Section 226-231, 1988.

GRECO, W. R., PARK, H. S., AND RUSTUM, Y. M.: An application of a new approach for the quantitation of drug synergism to the combination of cis-diamminedichloroplatinum and 1-β-D-arabinofuranosylcytosine. *Cancer Res.* 50: 5318-5327, 1990.

GRECO, W. R., AND RUSTUM, Y. M.: Reply to letters by Berenbaum and Sühnel concerning Greco et al. (1990), in *Cancer Res.* 50: 5318-5327, 1990. *Cancer Res.* 52: 4561-4565, 1992.

GRECO, W. R., SUTOR, D. C., PARSONS, J. C., KHINKIS, L. A., HSIEH, L., RAO, S. R., TUNG, Y., CURRIE, C. C., AND SUSICE, R.: Monte Carlo comparison of rival experimental designs for two-agent combined action studies. *Can. J. Infectious Dis.* 3 (suppl): 51A-59A, 1994.

GRECO, W. R., AND TUNG, Y.: D-optimal experimental designs for quantifying synergy in drug combination studies. American Statistical Association, Proceedings of the Biopharmaceutical Section 244-249, 1991.

GRECO, W. R., UNKELBACH H. D., PÖCH, G., SÜHNL, J., KUNDI, M., AND BÖDEKER, W.: Consensus on concepts and terminology for interaction assessment: the Saareikü Agreement. *Arch. Complex Environmental Studies* 4: 65-69, 1992.

GRINDEY, G. B., MORAN, R. G., AND WERKHEISER, W. C.: Approaches to the rational combination of antimetabolites for cancer chemotherapy. In *Drug Design*, vol 5, pp. 170-249, Academic Press, New York, 1975.

GUMARAES, M. A., GRECO, W. R., SLOCUM, H. K., HUBEN, R. P., AND RUSTUM, Y. M.: The combined-action of ICI-D1694, 5-fluoro-2'-deoxyuridine and 5-fluorouracil in inhibiting the growth of a human renal cell carcinoma cell line (RPMI-SE) in vitro. *Int. J. Oncol.* 4: 137-141, 1994.

HALI, M. J., AND DUNCAN, I. B.: Antiviral drug and interferon combinations. In *Antiviral Agents: The Development and Assessment of Antiviral Chemotherapy*, ed. by H. J. Field, pp. 29-84, CRC Press, Boca Raton, FL, 1988.

HARDER, R. L., AND DESMARais, R. N.: Interpolation using surface splines. *J. Aircraft* 9: 189-191, 1972.

HARTSHORN, K. L., SANDSTROM, E. G., NEUMAYER, D., PARADIS, T. J., CHOU, T.-C., SCHOOLEY, R. T., AND HIRSCH, M. S.: Synergistic inhibition of human T-cell lymphotropic virus type III replication in vitro by phosphonoformate and recombinant α - λ interferon. *Antimicrob. Agents Chemother.* 30: 189-191, 1996.

HEWLETT, P. S.: Measurement of the potencies of drug mixtures. *Biometrics* 25: 477-487, 1969.

HEWLETT, P. S., AND PLACKETT, R. L.: A unified approach for quantal responses to mixtures of drugs: non-interactive action. *Biometrics* 15: 591-610, 1959.

HEWLETT, P. S., AND PLACKETT, R. L.: The Interpretation of Quantal Responses in Biology, pp. 1-81, University Park Press, Baltimore, MD, 1979.

HILL, A. V.: The possible effects of the aggregation of the molecules of haemoglobin on its dissociation curves. *J. Physiol.* 40: iv-vii, 1910.

HOLFORD, N. H. G., AND SCHEINER, L. B.: Understanding the dose-effect relationship: clinical applications of pharmacokinetic-pharmacodynamic models. *Clin. Pharmacokinet.* 6: 429-453, 1981.

HOSMER, D. H., AND LEMESHOW, S. L.: *Applied Logistic Regression*, John Wiley & Sons, New York, 1989.

IMSL: (1989). *IMSL User's Manual, Version 1.1* [computer program manual]. Houston, TX: IMSL.

JACKSON, R. C.: Kinetic simulation of anticancer drug interactions. *Int. J. Biomed. Computing* 11: 197-224, 1980.

JACKSON, R. C.: A kinetic model of regulation of the deoxyribonucleoside triphosphate pool composition. *Pharmacol. & Ther.* 24: 297-301, 1984.

JACKSON, R. C.: Synergistic and antagonistic drug interactions resulting from multiple inhibition of metabolic pathways. In *Synergism and Antagonism in Chemistry*, ed. by T.-C. Chou and D. C. Rideout, pp. 363-408, Academic Press, New York, 1991.

JACKSON, R. C.: The Theoretical Foundations of Cancer Chemotherapy Intro-duced by Computer Models, Academic Press, New York, 1992.

JACKSON, R. C.: Amphibolic drug combinations: the design of selective antimetabolite protocols based upon the kinetic properties of multienzyme systems. *Cancer Res.* 53: 3998-4003, 1993.

JANDEL SCIENTIFIC: (1994). *Sigma Plot User's Manual*. San Rafael, CA: Jandel Scientific.

JENNICH, R. I., AND MOORE, R. H.: Maximum likelihood estimation by means of nonlinear least squares. American Statistical Association, Proceedings of the Statistical Computing Section 57-65, 1975.

JOHNSON, V. A., MERRILL, D. P., CHOU, T.-C., AND HIRSCH, M. S.: Human immunodeficiency virus type 1 (HIV-1) inhibitory interactions between protease inhibitor Ro 31-8959 and zidovudine, 2',3'-dideoxyctidine, or recombinant interferon- α against zidovudine-sensitive or -resistant HIV-1 in vitro. *J. Infect. Dis.* 168: 1143-1146, 1992.

KAGEYAMA, S., WEINSTEIN, J. N., SHIRASAKA, T., KEMPF, D. J., NORBECK, D. W., PLATTNER, J. J., ERICKSON, J., AND MITSUYA, H.: Antimicrob. Agents Chemother. 36: 926-933, 1992.

KATZ, E. J., ANDREWES, P. A., AND HOWELL, S. B.: The effect of DNA polymerase inhibitor on the cytotoxicity of cisplatin in human ovarian carcinoma cells. *Cancer Commun.* 2: 159-164, 1990.

KELLY, C., AND RICE, J.: Monotone smoothing with application to dose-response curves and the assessment of synergism. *Biometrics* 46: 1071-1085, 1990.

KHINKIS, L. A., AND GRECO, W. R.: Analytical solution of the D-optimal design problem for studies of drug synergy. American Statistical Association, Proceedings of the Biopharmaceutical Section 323-327, 1993.

KHINKIS, L. A., AND GRECO, W. R.: Critical review of response-surface models of synergy. American Statistical Association, Proceedings of the Biopharmaceutical Section in press, 1994.

KODELL, R. L., AND POUNDS, J. G.: Characterization of the joint action of two chemicals in an in vitro test system. American Statistical Association, Proceedings of the Biopharmaceutical Section 48-53, 1985.

KODELL, R. L., AND POUNDS, J. G.: Assessing the toxicity of mixtures of chemicals. In *Statistics in Toxicology*, ed. by D. Krewski and C. Franklin, pp. 559-591, Gordon and Breach, New York, 1991.

KONG, X.-B., ZHU, Q.-Y., RUPRECHT, R. M., WATANABE, K. A., ZEIDLER, J. M., GOLD, J. W. M., POLSKY, B., ARMSTRONG, D., AND CHOU, T.-C.: Synergistic inhibition of human immunodeficiency virus type 1 replication in vitro by two-drug and three-drug combinations of 3'-azido-3'-deoxythymidine, phosphonoformate, and 2',3'-dideoxythymidine. *Antimicrob. Agents Chemother.* 36: 2003-2011, 1991.

KOSHIDA, R., VRANG, I., GILLJAM, G., HARMENBERG, J., OBERG, B., AND WAHREN, B.: Inhibition of human immunodeficiency virus in vitro by combinations of 3'-azido-3'-deoxythymidine and foscarnet. *Antimicrob. Agents Chemother.* 33: 778-780, 1989.

KUEBLER, J. P., GODETTE, G. A., BOCK, D. J., AND EPSTEIN, R. B.: Synergistic effects of vinblastine and recombinant interferon- β on renal tumor cell lines. *J. Interferon Res.* 10: 281-291, 1990.

LAM, Y. M., PTM, J., AND CAMPING, B. G.: Statistical models for assessing drug interactions. *Proc. Am. Stat. Assoc. Biopharm. Sect.* 214-219, 1991.

LANDAHL, H. D.: Theoretical considerations on potentiation in drug interaction. *Bull. Math. Biophys.* 20: 1-23, 1958.

LARSON, H. J.: *Introduction to Probability Theory and Statistical Inference*, 3rd ed., John Wiley & Sons, New York, 1982.

LASKA, E. M., MEISNER, M., AND SIEGEL, C.: Simple designs and model-free tests for synergy. *Biometrika* 50: 834-841, 1994.

LOEWE, S.: Die Quantitativen Probleme der Pharmakologie. *Ergeb. Physiol. Biol. Chem. Exp. Pharmakol.* 27: 47-187, 1928.

LOEWE, S.: Die problem of synergism and antagonism of combined drugs. *Arzneim. Forsch.* 3: 285-290, 1953.

LOEWE, S.: Antagonism and antagonists. *Pharmacol. Rev.* 9: 237-242, 1957.

LOEWE, S., AND MÜNSCHNEK, H.: Effect of combinations: mathematical basis of problem. *Arch. Exp. Pathol. Pharmakol.* 114: 313-326, 1926.

MACHADO, S. G., AND ROBINSON, G. A.: A direct, general approach based on isobolograms for assessing the joint action of drugs in preclinical experiments. *Stat. Med.* 13: 2289-2309, 1994.

MANNERVICK, B.: Regression analysis, experimental error, and statistical criteria in the design and analysis of experiments for discrimination between rival kinetic models. *Methods Enzymol.* 87: 370-390, 1982.

MARQUARDT, D. W.: An algorithm for least squares estimation of nonlinear parameters. *J. Soc. Industrial Applied Math.* 11: 431-441, 1963.

MCCULLAGH, P., AND NELDER, J. A.: *Generalized Linear Models*, 2nd ed., Chapman and Hall, London, 1989.

MEINGUET, J.: Multivariate interpolation at arbitrary points made simple. *J. Applied Math. Physics* 30: 292-304, 1979.

METZLER, C. M.: Estimation of pharmacokinetic parameters: statistical considerations. *Pharmacol. Ther.* 13: 543-556, 1981.

MILLER, R. G., JR.: *Simultaneous Statistical Inference*, 2nd ed., Springer, New York, 1981.

NASH, J. C.: *Compact Numerical Methods for Computers: Linear Algebra and Function Minimization*, John Wiley & Sons, New York, 1979.

NATIONAL RESEARCH COUNCIL: *Complex Mixtures: Methods for In Vivo Toxicity Testing*, National Academy Press, Washington, DC, 1988.

NOCENTINI, G., BARZI, A., AND FRANCHETTI, P.: Implications and problems in analysing cytotoxic activity of hydroxyurea in combination with a potential

inhibitor of ribonucleotide reductase. *Cancer Chemother. Pharmacol.* 26: 345-351, 1990.

PLACKETT, R. L., AND HEWLETT, P. S.: Statistical aspects of the independent joint action of poisons, particularly insecticides: I. The toxicity of a mixture of poisons. *Ann. Appl. Biol.* 35: 347-358, 1948.

PLACKETT, R. L., AND HEWLETT, P. S.: Quantal responses to mixtures of poisons. *J. R. Statistical Soc. B14*: 141-163, 1952.

PLACKETT, R. L., AND HEWLETT, P. S.: A comparison of two approaches to the construction of models for quantal responses to mixture of drugs. *Biometrics* 23: 27-44, 1967.

POCH, G.: Dose factor of potentiation derived from isoboles. *Arzneim. Forsch.* 30: 2195-2196, 1980.

POCH, G.: Application of the isobologram technique for the analysis of combined effects with respect to additivity as well as independence. *Can. J. Pharmacol.* 68: 682-688, 1990.

POCH, G.: Evaluation of combined effects with respect to independent action. *Arch. Complex Environmental Studies* 3: 65-74, 1991.

POCH, G.: *Modern Evaluation of Combined Effects in Theory and Practice*, Springer, Berlin, 1993.

POCH, G., DITTRICH, P., AND HOLZMAN, S.: Evaluation of combined effects in dose-response studies by statistical comparison with additive and independent interactions. *J. Pharmacol. Methods* 24: 311-325, 1990a.

POCH, G., DITTRICH, P., REIFFENSTEIN, R. J., LENK, W., AND SCHUSTEK, A.: Evaluation of experimental combined cytotoxicity by use of dose-frequency curves: comparison with theoretical additivity as well as independence. *Can. J. Physiol. Pharmacol.* 68: 1338-1345, 1990b.

POCH, G., REIFFENSTEIN, R. J., AND UNKELBACH, H.-D.: Application of the isobologram technique for the analysis of combined effects with respect to additivity as well as independence. *Can. J. Physiol. Pharmacol.* 68: 682-688, 1990c.

PRICHARD, M. N., ASELTINE, K. R., AND SHIPMAN, C. JR.: (1992). MacSynergy II, version 1.0 [computer program]. Ann Arbor, MI: University of Michigan.

PRICHARD, M. N., PRICHARD, L. E., BAGULEY, W. A., NASSIRI, M. R., AND SHIPMAN, C. JR.: Three dimensional analysis of the synergistic cytotoxicity of ganciclovir and zidovudine. *Antimicrob. Agents Chemother.* 36: 1060-1065, 1990.

PRICHARD, M. N., AND SHIPMAN, C. JR.: A three dimensional model to analyze drug-drug interactions (review). *Antiviral Res.* 14: 181-208, 1990.

PRICHARD, M. N., AND SHIPMAN, C. JR.: Response to J. Sühnel's comment on the paper: A three-dimensional model to analyze drug-drug interactions, by Prichard, M. N., and Shipman, C. Jr., in *Antiviral Res.* 14: 181-208, 1990 (letter to the editor). *Antiviral Res.* 17: 95-98, 1992.

RICHMAN, D., ROSENTHAL, A. S., SKOOG, M., ECKNER, R. J., CHOU, T.-C., SABO, J. P., AND MERLUZZI, V. J.: BI-RG-587 is active against zidovudine-resistant human immunodeficiency virus type 1 and synergistic with zidovudine. *Antimicrob. Agents Chemother.* 35: 305-308, 1991.

RIDEOUT, D. C., AND CHOU, T.-C.: Synergism, antagonism, and potentiation in chemotherapy: an overview. In *Synergism and Antagonism in Chemotherapy*, ed. by T.-C. Chou and D. C. Rideout, pp. 3-60, Academic Press, New York, 1991.

SAS INSTITUTE, INC.: (1987). *SAS/STAT Guide for Personal Computers*, Version 6 Edition [computer program manual]. Cary, NC: SAS Institute, Inc.

SCHINAZI, R. F.: Combined chemotherapeutic modalities for viral infections: rationale and clinical potential. In *Synergism and Antagonism in Chemotherapy*, ed. by T.-C. Chou and D. C. Rideout, pp. 109-181, Academic Press, New York, 1991.

SCHINAZI, R. F., CHOU, T.-C., SCOTT, R. T., YAO, X. J., AND NAHMIAS, A. J.: Delayed treatment with combinations of antiviral drugs in mice infected with herpes simplex virus and application of the median-effect method of analysis. *Antimicrob. Agents Chemother.* 30: 491-498, 1986.

SEBER, G. A. F., AND WILD, C. J.: *Nonlinear Regression*, John Wiley & Sons, New York, 1989.

SEGEL, I. H.: *Enzyme Kinetics: Behavior and Analysis of Rapid Equilibrium and Steady-State Enzyme Systems*, John Wiley & Sons, New York, 1975.

SHELTON, D. W., AND WEBER, L. J.: Quantification of the joint effects of mixtures of hepatotoxic agents: evaluation of a theoretical model in mice. *Environ. Res.* 28: 33-41, 1981.

SILVEY, S. D.: *Optimal Design*, Chapman and Hall, New York, 1980.

SNYDER, W. V.: Algorithm 531 contour plotting [J6]. *Association of Computing Machinery Transactions on Mathematical Software* 4: 290-294, 1978.

STANISWALIS, J. G.: The kernel estimate of a regression function in likelihood-based models. *J. Am. Stat. Assoc.* 84: 276-283, 1989.

STATISTICAL CONSULTANTS, INC.: PCNONLIN and NONLIN84 software for the statistical analysis of nonlinear models. *Am. Statist.* 40: 52-52, 1986.

STEELE, G. G., AND PECKHAM, M. J.: Exploitable mechanisms in combined radiotherapy-chemotherapy: the concept of additivity. *Int. J. Radiat. Oncol. Biol. Phys.* 5: 85-91, 1979.

STREFFER, C., AND MÜLLER, W.-U.: Radiation risk from combined exposures to ionizing radiations and chemicals. *Adv. Radiat. Biol.* 11: 173-210, 1984.

STSC, INC.: (1988). *Statgraphics User's Guide*. Rockville, Maryland: STSC.

SÜHNEL, J.: Evaluation of synergism and antagonism for the combined action of antiviral agents. *Antiviral Res.* 13: 23-40, 1990.

SÜHNEL, J.: Comment on the paper: A three-dimensional model to analyze drug-drug interactions, by Prichard, M. N., and Shipman, C. Jr., in *Antiviral Res.* 14: 181-186, 1990. *Antiviral Res.* 17: 91-93, 1992a.

SÜHNEL, J.: Correspondence regarding W. R. Greco et al: Application of a new approach for the quantitation of drug synergism to the combination of cis-diamminedichloroplatinum and 1-β-D-arabinofuranosylcytosine. *(Cancer Res.* 50: 5318-5327, 1990) *Cancer Res.* 52: 4560-4561, 1992b.

SÜHNEL, J.: Zero interaction response surfaces, interaction functions and difference response surfaces for combinations of biologically active agents. *Arzneim. Forsch.* 42: 1251-1258, 1992c.

SYRACUSE, K. C., AND GRECO, W. R.: Comparison between the method of Chou and Talalay and a new method for the assessment of the combined effects of drugs: a Monte-Carlo simulation study. *American Statistical Association Proceedings of the Biopharmaceutical Section* 127-132, 1986.

TALLARIDA, R. J.: Statistical analysis of drug combinations for synergism. *Pain* 49: 93-97, 1992.

TALLARIDA, R. J., PORRECA, F., AND COWAN, A.: Statistical analysis of drug-drug and site-site interactions with isobolograms. *Life Sci.* 45: 947-961, 1989.

TEICHER, B. A., GUNNER, L. J., AND ROACH, J. A.: Chemospotentiation of mitomycin C cytotoxicity in vitro by platinum complexes. *Br. J. Cancer* 52: 833-839, 1985.

TEICHER, B. A., HERMAN T. S., AND EIDER J. P.: Chemosynthetic potentiation through interaction at the level of DNA. In *Synergism and Antagonism in Chemotherapy*, ed. by T.-C. Chou and D. C. Rideout, pp. 541-583, Academic Press, New York, 1991.

THISTED, R. A.: *Elements of Statistical Computing*, p. 170, algorithm 4.2.5, Chapman and Hall, New York, 1988.

UNKELBACH, H. D.: What does the term "non-interactive" mean? *Arch. Complex Environmental Studies* 4: 29-34, 1992.

UNKELBACH, H. D., AND WOLF T.: Drug combinations: concepts and terminology. *Arzneim. Forsch.* 34: 935-938, 1984.

VALERIOTE, F., AND LIN, H.: Synergistic interaction of anticancer agents: a cellular perspective. *Cancer Chemother. Rep.* 69: 895-900, 1975.

VATHSALA, A., CHOU, T.-C., AND KAHAN, B. D.: Analysis of the interactions of immunosuppressive drugs with cyclosporine in inhibiting DNA proliferation. *Transplantation* 49: 463-472, 1990.

VOGT, M. W., HARTSHORN, K. L., FURMAN, P. A., CHOU, T.-C., FVPR, J. A., COLEMAN, L. A., CRUMPACKER, C., SCHOOLEY, R. T., AND HIRSCH, M. S.: Ribavirin antagonizes the effect of azidothymidine on HIV replication. *Science (Wash. DC)* 235: 1376-1379, 1987.

VOLLMAR, H. J., AND UNKELBACH, H. D.: *Biometrie in der Chemisch-pharmazeutischen Industrie 2: Biometrische Analyse von Kombinationswirkungen*, Gustav Fischer Verlag, Stuttgart, Germany, 1985.

WADLER, S., WERSTO, R., WEINBERG, V., THOMPSON, D., AND SCHWARTZ, E. L.: Interaction of fluorouracil and interferon in human colon cancer cell lines: cytotoxic and cytokinetic effects. *Cancer Res.* 50: 5735-5739, 1990.

WAMPLER, G. L., CARTER, W. H., JR., CAMPBELL, E. D., AND KEEFE, P. A.: Relationships between various uses of antineoplastic drug-interaction terms. *Cancer Chemother. Pharmacol.* 31: 111-117, 1992.

WAUD, D. R., LEESON, S., AND WAUD, B. E.: Kinetic and empirical analysis of dose-response curves illustrated with a cardiac example. *Life Sci.* 22: 1275-1286, 1978.

WAUD, D. R., AND PARKER, R. B.: Pharmacological estimation of drug-receptor dissociation constants, statistical evaluation: II. Competitive antagonists. *J. Pharmacol. Exp. Ther.* 117: 13-24, 1971.

WEBB, J. L.: Effect of more than one inhibitor. In *Enzymes and Metabolic Inhibitors*, vol. 1, pp. 66-79 & 487-512, Academic Press, New York, 1963.

WEINSTEIN, J. N., BUNOW, B., WEISLOW, O. S., SCHINAZI, F., WAHL, S. M., WAHL, L. M., AND SZEBENI, J.: Synergistic drug combinations in AIDS therapy. *Ann. NY Acad. Sci.* 616: 367-384, 1990.

WERKHEISER, W. C., GRINDEY, G. B., AND MORAN, R. G.: Mathematical simulation of the interaction of drugs that inhibit deoxyribonucleic acid biosynthesis. *Mol. Pharmacol.* 9: 320-329, 1973.